



E-ISSN 2667-5846

EXPERIMED

Volume **12** Issue **3** December 2022

experimed.istanbul.edu.tr



ISTANBUL
UNIVERSITY
PRESS

EXPERIMED

INDEXING AND ABSTRACTING

ULAKBIM TR Index

Chemical Abstracts Service (CAS)

EBSCO - Central & Eastern European Academic Source

SOBIAD

EXPERIMED

OWNER

Prof. Dr. Günnur DENİZ

Department of Immunology, Istanbul University, Aziz Sancar Institute of Experimental Medicine, Istanbul, Türkiye

RESPONSIBLE MANAGER

Prof. Dr. Bedia ÇAKMAKOĞLU

Department of Molecular Medicine, Istanbul University, Aziz Sancar Institute of Experimental Medicine, Istanbul, Türkiye

CORRESPONDENCE ADDRESS

Istanbul University, Aziz Sancar Institute of Experimental Medicine,

Vakıf Gureba Avenue, 34093, Çapa, Fatih, Istanbul, Türkiye

Phone: +90 (212) 414 22 29

E-mail: experimed@istanbul.edu.tr

PUBLISHER

Istanbul Üniversitesi Yayınevi / Istanbul University Press

Istanbul University Central Campus,

34452 Beyazıt, Fatih / Istanbul, Türkiye

Phone: +90 (212) 440 00 00

Authors bear responsibility for the content of their published articles.

The publication language of the journal is English.

This is a scholarly, international, peer-reviewed and open-access journal published triannually in April, August and December.

Publication Type: Periodical

EXPERIMED

EDITORIAL MANAGEMENT BOARD

Editor-in-Chief

Prof. Dr. Bedia ÇAKMAKOĞLU

Department of Molecular Medicine, Istanbul University, Aziz Sancar Institute of Experimental Medicine, Istanbul, Türkiye – bedia@istanbul.edu.tr

Co-Editors-in-Chief

Assoc. Prof. Umut Can KÜÇÜKSEZER

Department of Immunology, Istanbul University, Aziz Sancar Institute of Experimental Medicine, Istanbul, Türkiye – uksezer@istanbul.edu.tr

Assoc. Prof. Vuslat YILMAZ

Department of Neuroscience, Istanbul University, Aziz Sancar Institute of Experimental Medicine, Istanbul, Türkiye – vuslat.yilmaz@istanbul.edu.tr

Managing Editor

Prof. Dr. Sema Sırma EKMEKÇİ

Department of Genetics, Istanbul University, Aziz Sancar Institute of Experimental Medicine, Istanbul, Türkiye – sirmasem@istanbul.edu.tr

Editorial Management Board Members

Dr. Canan Aysel ULUSOY

Department of Neuroscience, Istanbul University, Aziz Sancar Institute of Experimental Medicine, Istanbul, Türkiye – canan.ulusoy@istanbul.edu.tr

MSc. Barış ERTUĞRUL

Department of Molecular Medicine, Istanbul University, Aziz Sancar Institute of Experimental Medicine, Istanbul, Türkiye – baris.ertugrul@istanbul.edu.tr

Section Editors

Prof. Dr. Elif ÖZKÖK

Department of Neuroscience, Istanbul University, Aziz Sancar Institute of Experimental Medicine, Istanbul, Türkiye – eozkok@istanbul.edu.tr

Assoc. Prof. Elif Sinem İPLİK

Department of Biochemistry, Faculty of Pharmacy, Acıbadem Mehmet Ali Aydınlar University, Istanbul, Türkiye – sinem.iplik@acibadem.edu.tr

Assoc. Prof. Ferda PAÇAL

Department of Genetics, Istanbul University, Aziz Sancar Institute of Experimental Medicine, Istanbul, Türkiye – ferda.pacal@istanbul.edu.tr

Assit. Prof. Ali Cihan TAŞKIN

Department of Lab Animal Science, Istanbul University, Aziz Sancar Institute of Experimental Medicine, Istanbul, Türkiye – ataskin@istanbul.edu.tr

Language Editors

Elizabeth Mary EARL

Istanbul University, Department of Foreign Languages, Istanbul, Türkiye – elizabeth.earl@istanbul.edu.tr

Alan James NEWSON

Istanbul University, Department of Foreign Languages, Istanbul, Türkiye – alan.newson@istanbul.edu.tr

Statistics Editor

Sevda ÖZEL YILDIZ

Department of Biostatistic, Istanbul Medical Faculty, Istanbul University, Istanbul, Türkiye – sevda@istanbul.edu.tr

EXPERIMED

EDITORIAL BOARD

Aziz SANCAR (Honorary Member)

Department of Biochemistry and Biophysics, University of North Carolina School of Medicine, Chapel Hill, North Carolina, USA – aziz_sancar@med.unc.edu

Abid HUSSAINI

Department of Pathology and Cell Biology, Columbia University, Taub Institute, New York, USA – abid.hussaini@columbia.edu

Ahmet GÜL

Department of Internal Medicine, Istanbul University School of Medicine, Istanbul, Türkiye – agul@istanbul.edu.tr

Ali Önder YILDIRIM

Department of Lung Biology and Diseases, Helmholtz Zentrum München, München, Germany – oender.yildirim@helmholtz-muenchen.de

Batu ERMAN

Department of Molecular Biology, Genetics and Bioengineering, Sabanci University, Istanbul, Türkiye – batu.erman@boun.edu.tr

Çağla EROĞLU

Department of Cell Biology, Duke University, North Carolina, USA – cagla.eroglu@duke.edu

Ebba LOHMANN

Department of Neurodegenerative Diseases, Tübingen University, Tübingen, Germany – ebba.lohmann@uni-tuebingen.de

Elif APOHAN

Department of Biology, İnönü University, Malatya, Türkiye – elif.apohan@inonu.edu.tr

Erdem TÜZÜN

Department of Neuroscience, Istanbul University, Aziz Sancar Institute of Experimental Medicine, Istanbul, Türkiye – erdem.tuzun@istanbul.edu.tr

Gökçe TORUNER

Department of Hematology, MD Anderson Cancer Center, Houston, Texas, USA – gatoruner@mdanderson.org

Günnur DENİZ

Department of Immunology, Istanbul University, Aziz Sancar Institute of Experimental Medicine, Istanbul, Türkiye – gdeniz@istanbul.edu.tr

Gürol TUNÇMAN

Department of Genetics and Complex Diseases, Harvard University, Massachusetts, USA – gtuncman@hsph.harvard.edu

Hannes STOCKINGER

Molecular Immunology Unit, Vienna School of Medicine, Pathophysiology Center, Vienna, Austria – hannes.stockinger@medunivien.ac.at

Hülya YILMAZ

Department of Molecular Medicine, Istanbul University, Aziz Sancar Institute of Experimental Medicine, Istanbul, Türkiye – yilmazh@istanbul.edu.tr

İhsan GÜRSEL

Department of Molecular Biology and Genetics, Bilkent University, Ankara, Türkiye – ihsangursel@bilkent.edu.tr

Melih ACAR

Texas University Pediatric Research Institute, Dallas, Texas, USA – melihacar@gmail.com

Numan ÖZGEN

Department of Pathology and Immunology, Baylor University School of Medicine, Texas, USA – numan.oezguen@bcm.edu

Serhat PABUÇÇUOĞLU

Department of Reproduction & Artificial Insemination, Istanbul University-Cerrahpaşa School of Veterinary, Istanbul, Türkiye – serpab@iuc.edu.tr

Sühendan EKMEKÇİOĞLU

MD Anderson Cancer Center, Texas University, Houston, Texas, USA – sekmekcioglu@mdanderson.org

Yusuf BARAN

Department of Molecular Biology and Genetics, İzmir Institute of Technology, İzmir, Türkiye – yusufbaran@iyte.edu.tr

EXPERIMED

CONTENTS

ORIGINAL ARTICLES

- 103** **Do *Lactobacillus rhamnosus*-Originated Probiotic and Parabiotic Have Inhibitory Effects on Intraocular Lens Biofilm?**
Sertac Argun Kivanc, Berna Akova, Merih Kivanc
- 108** **Caspase-9 rs1052576 Polymorphism is not Associated with Glioblastoma in Turkish Patients**
Deryanaz Billur, Fatma Tuba Akdeniz, Seda Gulec-Yilmaz, Zerrin Barut, Cumhur Kaan Yaltirik, Turgay Isbir
- 113** **The Effect of Whey Proteins on the Brain and Small Intestine Nitric Oxide Levels: Protein Profiles in Methotrexate-Induced Oxidative Stress**
Sumeyye Yilmaz, Elif Tufan, Guzin Goksun Sivas, Begum Gurel Gokmen, Ercan Dursun, Dilek Ozbeyli, Goksel Sener, Tugba Tunali-Akbay
- 119** **Assessing E-Cadherin and Connexin 43 Gene Expressions in Colorectal Cancer**
Saime Surmen, Soykan Arikan, Ozlem Timirci Kahraman, Mustafa Gani Surmen, Canan Cacina, Ilhan Yaylim
- 125** **A Histological Evaluation of the Effect of Ghrelin on Wound Healing in Rats**
Esin Ak, Kerime Ulusoy-Dag, Feriha Ercan, Ahmet Corak
- 130** **Preoperative Screening for COVID-19: Results from a Clinical Diagnostic Laboratory**
Okan Aydogan, Ezgi Gozun Saylan, Ozlem Guven, Akif Ayaz, Turkan Yigitbasi
- 134** **Determination of Bisphenol A and Phthalate Levels in Wastewater Samples**
Mansur Akcay, Perihan Seda Ates-Kalkan, Unsal Veli Ustundag, Ismail Unal, Derya Cansiz, Ebru Emekli-Alturfan, Ahmet Ata Alturfan
- 139** **The Mitochondrial Origins of the Hellenistic Individuals of Ayasuluk Hill**
Fatih Tepgec, Mehmet Gorgulu
- 149** **Fetal Hand Anomalies: 18 Cases Diagnosed Between 2020-2022 from a Single Tertiary Care Center**
Ayca Dilruba Aslanger, Tugba Sarac Sivrikoz, Tugba Kalayci, Seher Basaran, Oya Uyguner
- 155** **Activation-Induced Cytidine Deaminase Expression in Patients with Chronic Myeloid Leukemia**
Emin Oguz, Aynur Daglar Aday, Akif Selim Yavuz
- 160** **Evaluating the Long-Term Outcomes of Medical and Surgical Treatments in Fibrostenotic Crohn's Disease Patients Treated with Anti-TNF/Biologic Therapy**
Cagatay Ak, Suleyman Sayar, Resul Kahraman, Kamil Ozdil
- 168** **Comparing the VDR Gene *BsmI* and *CDX2* Polymorphisms in Healthy Turks and Healthy Somalians Living in Turkiye**
Ender Coskunpinar, Betul Nilgun Engin
- 174** **Self-Discontinuation of Antiseizure Medication During Pregnancy Increases Postpartum Seizure Frequency**
Miray Atacan Yasguclukal, Zeynep Acar, Birgul Bastan, Aytul Mutlu, Ozlem Cokar
- 181** **Germline Screening of Cancer-Related Genes in Turkish Ovarian Cancer Patients**
Esra Arslan Ates, Ceren Alavanda, Bilgen Bilge Geckinli, Ahmet Ilter Guney, Tuba Gunel
- 188** **Differential Cytotoxic Activity of a New Cationic Pd(II) Coordination Compound with N₄-Tetradentate Hybrid Ligand in Cancer Cell Lines**
Merve Erkisa Genel, Selin Selvi, Ismail Yilmaz, Remzi Okan Akar, Ilhan Yaylim, Abdurrahman Sengul, Engin Ulukaya

EXPERIMED

CONTENTS

ORIGINAL ARTICLES

- 202** Cytotoxic and Cytostatic Effects of Targeting mTOR and Hedgehog Pathways in Acute Myeloid Leukemia
Enes Cicek, Fulya Mina Kucuktas, Munevver Yenigul, Emel Basak Gencer Akcok
- 209** Shotgun Lipidomics Elucidates the Lipidome Alterations of the Mcl-1 Inhibitor S63845 in AML Cell Lines with a Focus on Sphingolipids
Melis Kartal Yandim, Mesut Bilgin
- 215** Cerrahpaşa Medical Faculty Hospital HIV-1/-2 Serological Test Data: 2019-2022 Retrospective Evaluation
Harika Oyku Dinc, Elif Keskin, Banu Tufan Kocak, Bekir Kocazeybek
- 219** Alcohol Withdrawal at Different Points in Time Distinctly Affects *Wistar* Rats' Spatial Reference Memory
Ilknur Dursun, Birsen Elibol, Ebru Haciosmanoglu, Ewa Jakubowska-Dogru
- 225** Increased Perforin- and IL-21-Expressing NK Cells in Patients with Early-Stage Chronic Lymphocytic Leukemia
Fatih Akboga, Fehmi Hindilerden, Emine Gulturk, Ipek Yönel-Hindilerden, Abdullah Yilmaz, Gunnur Deniz, Metin Yusuf Gelmez
- 232** Clues to the Harmful Effects of Aspartame on Liver Morphology and Function
E. Rumeysa Hekimoglu, Birsen Elibol, Ceyhun Toruntay, Seda Kirmizikan, Ozge Pasin, Ufuk Sarikaya, Damla Alkhalidi, Mukaddes Esrefoglu
- 238** The Antioxidant Effects of Sesamol on Bleomycin-Induced Oral Submucous Fibrosis
Sevilay Erimsah, Ayhan Cetinkaya, Ummugul Uyeturk, Ugur Uyeturk, Yusufhan Yazir

EXPERIMED

Experimed is very happy to announce that the last issue of 2022 shares twenty-two original research articles belonging to sixteen different universities from Turkiye to the literature.

Herein, I would like to present my special thanks and gratitude for,

Academicians who have preferred and supported Experimed with their valuable researches,

Reviewers who have worked on and evaluated the manuscripts,

Dear Institute Director Prof. Dr. Günnur Deniz who has supported and helped for all requests from Experimed to University's management platform,

Editorial Board Team who have labored with great devotion in all stages,

Dear Istanbul University Press employee Eda Kolukisa Doğru who has showed her support day and night with great positive energy,

Dear Adem Durmaz who worked with great efforts on each manuscript draft for publishing on time.

We wish to shed a light on the world of science with these marvelous Experimed Crew.

Prof. Dr. Bedia Çakmaköđlu

Do *Lactobacillus rhamnosus*-Originated Probiotic and Parabiotic Have Inhibitory Effects on Intraocular Lens Biofilm?

Sertac Argun Kivanc¹ , Berna Akova¹ , Merih Kivanc² 

¹Department of Ophthalmology, Faculty of Medicine, Bursa Uludag University, Bursa, Türkiye

²Department of Biology, Faculty of Science, Eskişehir Technical University, Eskişehir, Türkiye

ORCID ID: S.A.K. 0000-0002-0932-6977; B.A. 0000-0003-0995-5260; M.K. 0000-0002-8647-3428

Cite this article as: Kivanc SA, Akova B, Kivanc M. Do *Lactobacillus rhamnosus*-originated probiotic and parabiotic have inhibitory effects on intraocular lens biofilm? *Experimed* 2022; 12(3): 103-7.

ABSTRACT

Objective: Our aim was to investigate the formation of *Staphylococcus (S.) epidermidis* biofilm on hydrophobic acrylic lenses and whether the inhibition of the formed biofilm is possible with probiotic *Lactobacillus (L.) rhamnosus* 312 and parabiotic prepared from it.

Materials and Methods: The probiotic bacteria *L. rhamnosus* 312 and intercellular adhesion (ICA) gene-positive tested bacteria *S. epidermidis* KA15.8 were used in the study from stock. To obtain the parabiotic the cultures were developed in De Man Rogosa and Sharpe (MRS) broth for 48 hours and autoclaved at 121°C for 15 minutes. Biofilms on hydrophobic acrylic intraocular lenses and the antibiofilm effects of parabiotic and probiotic *L. rhamnosus* were evaluated. Scanning electron microscopy photos of biofilms produced on intraocular lenses (IOLs) were taken.

Results: Probiotic *L. rhamnosus* 312 and the parabiotic test showed antibacterial activity on test bacteria, ICA positive *S. epidermidis* KA15.8. However, the probiotic *L. rhamnosus* 312 zone diameter was found to be wider. After the biofilm was formed, the addition of parabiotic inhibited the biofilm formed by *S. epidermidis* KA15.8 by 58.29%. The number of *S. epidermidis* KA15.8 in the biofilm also decreased.

Conclusion: Parabiotic and probiotic *L. rhamnosus* 312 was found effective for its antibiofilm effect. However, further studies with different concentrations are needed.

Keywords: Probiotic, parabiotic, ophthalmology, cataract, intraocular lens, biofilm

INTRODUCTION

Staphylococcus (S.) epidermidis constitute the main flora of the ocular surface and eyelids together with *Corynebacterium* species and *Propionibacterium acnes*. Also, *S. epidermidis* is the most common bacteria that causes postoperative endophthalmitis. Biofilm formation ability on abiotic surfaces contribute to the virulence of *S. epidermidis* (1-5). It is mostly accepted that *S. epidermidis* enters the intraocular area during and/or after ocular surgeries and causes endophthalmitis (3). Postoperative endophthalmitis is a devastating complication of intraocular lens (IOL) implantation after cataract surgeries. Researchers have reported the incidence rates of postoperative endophthalmitis as 0.08-0.11% after surgery

(4, 6). The adhesion of bacteria and biofilm formation on IOL materials has been reported by investigators (4, 5, 7, 8).

Biofilm is a defense mechanism developed by microorganisms to avoid the bactericidal effect of an antimicrobial agent or to protect themselves against improper environmental conditions and the host's defense. The self-secreted extracellular polymeric substance (EPS) constitutes a protective environment. The formation of biofilm by ocular bacteria on intraocular lenses, contact lenses, suture material, valve implants, socket implants, orbital implants, and scleral buckles have been reported (9). It has been shown in studies that *S. epidermidis* with the intercellular adhesion (ICA) A gene adheres to intraocular

Corresponding Author: Merih Kivanc **E-mail:** mkivanc@eskisehir.edu.tr

Submitted: 08.09.2022 **Revision Requested:** 05.10.2022 **Last Revision Received:** 05.10.2022 **Accepted:** 12.10.2022 **Published Online:** 29.12.2022



Content of this journal is licensed under a Creative Commons Attribution-NonCommercial 4.0 International License.

lenses (10,11). According to the production of polysaccharide intercellular adhesion (PIA) molecules encoded by the ICA locus, biofilm formation ability may exist, especially in ICA A gene, ICA B gene, ICA C gene, and ICA D gene-positive strains (12-14).

Biofilm-producing bacteria are resistant to antibiotics. Studies on the search for new compounds to inhibit biofilms are increasing day by day. For this purpose, probiotics, postbiotics, and/or parabiotics have started to gain importance in recent years. Postbiotics and parabiotics are the terms that have begun to be used to identify non-vivid microorganisms or non-bacterial extracts that benefit the host by providing bioactivity (15). *In vitro* and *in vivo* studies have shown that some postbiotics and parabiotics exhibit bioactivities such as anti-inflammatory, anti-proliferative, antioxidant, antimicrobial and immunomodulatory (15,16).

In this study, it was aimed to investigate the formation of *S. epidermidis* biofilm on hydrophobic acrylic lenses and whether the inhibition of the formed biofilm is possible with probiotic *Lactobacillus (L.) rhamnosus 312* and parabiotic prepared from it.

MATERIALS AND METHODS

Bacteria

The probiotic bacteria *L. rhamnosus 312* and tested bacteria *S. epidermidis KA15.8* used in the study were obtained from Eskişehir Technical University Faculty of Science, Microbiology Department. *L. rhamnosus 312* is a probiotic bacteria of human origin. *S. epidermidis KA15.8* is a methicillin-resistant pathogen isolated from the ocular surface and has the ICA gene (8). *L. rhamnosus 312* and *S. epidermidis KA15.8* were removed from stock. *L. rhamnosus 312* was seeded in De Man Rogosa and Sharpe (MRS) broth (Merck, 110661) and *S. epidermidis KA 15.8* in brain-heart infusion (BHI) broth (Merck, 1104930500). The MRS broth tubes were incubated at 37 °C for 48 hours under 5% CO₂ conditions. BHI broth tubes were incubated at 37 °C for 24 hours. A line culture was incubated on MRS agar (Merck, 110660) and BHI agar (Merck, 1038700500) separately from the liquid media for purity control under appropriate conditions. After incubation, the purity of the cultures were checked morphologically and microscopically by Gram staining and then used in the studies.

Determination of the Antibacterial Effect of *L. rhamnosus 312* Live (probiotic) and Autoclaved Cultures (parabiotic) of the Cultures

The antibacterial activity of *L. rhamnosus 312* was determined by the well method. The *S. epidermidis* culture was transferred into sterile Mueller Hinton (MH) agar (Merck, 1038720500) at 10⁶ cfu/mL and mixed well. It was then transferred to a sterile petri dish. After the agar was solidified, a 0.8 mm diameter well was opened using a sterile cork borer. Then, 80 µL of the cultures that had been developed in MRS broth for 48 hours and autoclaved at 121°C for 15 minutes and live bacterial culture in MRS broth were transferred to the well and incubated at 37°C for 24 hours. Zone diameters formed at the end of the incubation period were measured and evaluated. Petri dishes containing pathogenic bacteria were used as control.

Determination of Antibiofilm Activity of Probiotic and Parabiotic *L. rhamnosus 312* Culture on Intraocular Lenses

The experiment was carried out in two ways. In the first group, 48-hours cultures containing 10¹⁰ cfu/mL *L. rhamnosus 312* were used directly. In the other group, 48-hour cultures of *L. rhamnosus 312*, whose cell density was adjusted to 10¹⁰ cfu/mL, were used after autoclaving (paraprobiotic) for 15 minutes at 121°C. Two separate experimental sets were set up for each group, one before biofilm formation and one after biofilm formation. *S. epidermidis* was inoculated in BHI broth and incubated at 37°C for 24 hours.

Intraocular acrylic lenses were taken out of their packages, placed in the falcon containing phosphate-buffered saline (PBS), and incubated at 37 °C for 15 minutes. Then, an acrylic lens was placed in each well in a 12-well ELISA petri dish. Next, 200 µL of medium was added to the lenses to be used as a control. In order to determine the biofilm of *S. epidermidis KA15.8*, 25 µL of *S. epidermidis KA15.8* culture was transferred onto the lenses and 975 µL of tryptic soy broth (TSB) (Merck, 1054590500) containing 2% glucose was added. To determine the biofilm formed by *L. rhamnosus 312* live cells, 25 µL of *L. rhamnosus 312* culture was added to the lenses, and 975 µL of TSB containing 2% glucose was added. To determine the antibiofilm activity of *L. rhamnosus 312*, 25 µL of *S. epidermidis KA15.8* culture was added to the lenses, and 475 µL of TSB containing 2% glucose was added to 500 µL of *L. rhamnosus 312* culture. Then the prepared petri dishes were incubated at 37°C for 24 hours. All tests were prepared in triplicate. The same procedures were repeated with the autoclave *L. rhamnosus 312*.

Determination of Biofilm

In order to determine the biofilm, the lenses were carefully washed with PBS, and the bacteria in planktonic form were removed and then transferred to Eppendorf tubes. Next, 200 µL of 96% methanol was added to them, kept for 10 minutes, and washed with sterile PBS, and 100 µL of crystal violet was transferred to each Eppendorf tube and kept for 5 minutes. After washing them with sterile PBS, they were placed on 12 plates and 1000 µL of 33% glacial acetic acid was transferred onto them to release the cells. Then, 200 µL was transferred to 96 plates and a reading was made in the spectrophotometer at 570 nm.

Determination of the Count of Bacteria in Biofilm

The same set of experiments set up for biofilm was prepared. In order to determine the biofilm, the lenses were carefully washed with sterile PBS, and the bacteria in planktonic form were removed, and then transferred to falcons containing 1 mL of sterile PBS. To separate the cells from the biofilm matrix, they were vortexed for 1.5 seconds and sonicated for 15 minutes. Then, bacteria counts were done by using the drop plate method. Lactic acid bacteria were incubated at 37°C for 48 hours in an environment containing 5% CO₂, and pathogens were incubated at 37°C for 24 hours. Bacteria counts were done after incubation. All studies were examined in triplicated.

Scanning Electron Microscope (SEM)

Bacterial adhesion was examined by SEM with some modifications according to Okajima et al. (17). The *S. epidermidis* isolate was incubated in TSB containing 0.25% glucose for 24 hours at 37°C. After incubation, IOLs were carefully removed and washed 3 times with PBS. The IOL was fixed with 2.5% (wt/vol) glutaraldehyde in 0.1 M phosphate buffer (pH 7.4) by keeping it for 2 hours at room temperature. It was then washed 3 times for 15 minutes in 0.1 M sodium cacodylate. After this process, the lenses were rinsed with distilled water and dehydration was performed with alcohol series (50%, 70%, 80% and 95%). After 7 minutes in each batch, they were kept in two pure alcohols for 15 minutes. Drying was carried out in a Critical Point Dryer immediately after the alcohol series. They were then covered with gold and examined in SEM.

RESULTS

Probiotic *L. rhamnosus* 312 and the parabiotic test showed antibacterial activity on the tested bacteria, ICA-positive *S. epidermidis* KA15.8. However, the probiotic *L. rhamnosus* 312 zone diameter was found to be wider. Zone diameters of probiotic *L. rhamnosus* 312 and parabiotic were measured as 13 mm and 11 mm, respectively. Both probiotic *L. rhamnosus* 312 and *S. epidermidis* KA15.8 formed a biofilm on the acrylic lens (Figure 1). The addition of probiotic bacteria before biofilm formation inhibited the biofilm formation of *S. epidermidis* KA15.8 by 57.55%. The viable bacteria count in the biofilm also supported this finding. The number of *S. epidermidis* KA15.8 in the biofilm decreased from 7.00 Log 10/mL to 5.22 Log 10/mL. In the case of autoclaved probiotic bacteria/parabiotic addition, biofilm formation decreased by 59.61%. Due to bacterial numbers, the number of *S. epidermidis* bacteria decreased from 7.10 Log 10/mL to 3.45 Log 10/mL (Figure 1). After biofilm formation, the addition of probiotic *L. rhamnosus*

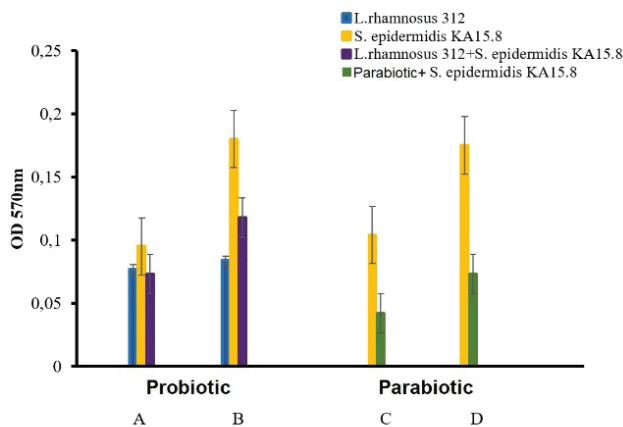


Figure 1. Antibiofilm activity of probiotic *L. rhamnosus* 312 and parabiotic.

A: Addition of the probiotic before biofilm formation; B: Addition of the probiotic after biofilm formation; C: Addition of the parabiotic before biofilm formation; D: Addition of parabiotic after biofilm formation.

312 inhibited the biofilm formation of *S. epidermidis* KA15.8 by 55.3%. Due to *S. epidermidis* KA15.8 numbers in the biofilm, it decreased from 8.40 Log 10/mL to 6.16 Log 10/mL. After the biofilm was formed, the addition of parabiotic inhibited the biofilm formed by *S. epidermidis* KA15.8 by 58.29%. The number of *S. epidermidis* KA15.8 in the biofilm also decreased from 8.20 Log 10/mL to Log 4.65 Log 10/mL (Figure 2). SEM images also confirm the findings (Figure 3).

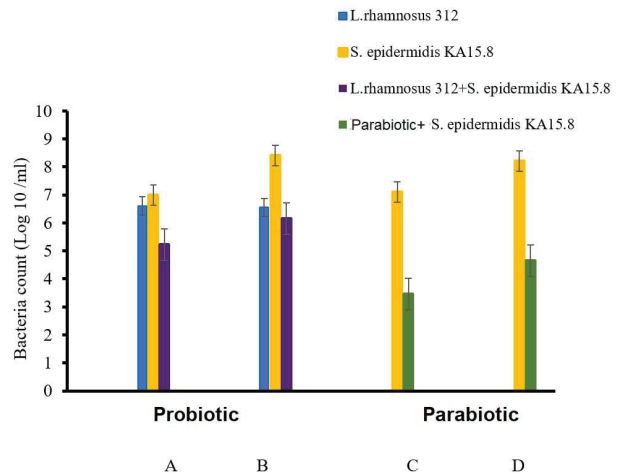


Figure 2. Bacteria counts in the biofilm.

A: The number of bacteria in the biofilm formed as a result of the addition of the probiotic before the biofilm formation; B: The number of bacteria in the biofilm when the probiotic is added after the biofilm has formed; C: The number of *S. epidermidis* in the biofilm formed as a result of the addition of the parabiotic before the biofilm is formed; D: The number of *S. epidermidis* with the addition of parabiotic after biofilm formation.

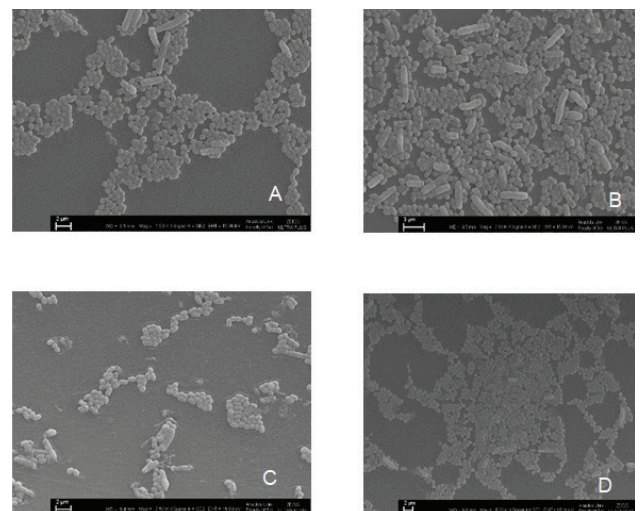


Figure 3. The effect of probiotic *L. rhamnosus* 312 and parabiotic on *S. epidermidis* 15.8 biofilm.

A: Probiotic applied before biofilm formation; B: Probiotic applied after biofilm formation; C: Parabiotic applied before biofilm formation; D: Parabiotic applied after biofilm formation.

DISCUSSION

The term paraprobiotics are used to refer to non-living or inactivated strains of probiotics, in their intact or fragmented form (18). However, there is no complete consensus on these definitions. It usually includes probiotic-derived metabolites or cell wall-derived materials without living microorganisms or cell structures (18). The preparations of *L. rhamnosus* 312, both alive and non-living, both prevented the biofilm formation of *S. epidermidis* and inhibited the formed biofilm on the acrylic lens.

Mohamed et al. reported that cell-free filtrates of *Lactobacillus* and *Bifidobacterium* inhibited the growth of *S. epidermidis* isolates originating from the conjunctiva (19). Researchers reported that probiotics could be alternative antimicrobials against pathogenic *Staphylococcus spp.* associated with conjunctivitis. Their findings support our results. It has been reported that the antimicrobial effect is associated with metabolic products of probiotic bacteria, such as bacteriocin, bacteriocin-like substances, hydrogen peroxide, acetic acid, and substances such as diacetyl, and lactic acid (20). Negi et al. found that the antimicrobial activity of cell-free supernatants of *Lactobacillus spp.* was dependent on the presence of an antimicrobial protein (21). Mazoteris et al. (22) reported that biofilm on IOLs can be found many years after uncomplicated cataract surgeries. Kivanc et al. (23) and Okajima et al. (17) reported that *S. epidermidis* formed a strong biofilm on acrylic lenses, as in our findings. El-Ganiny et al. (24) reported that, contrary to our findings, *S. epidermis* isolates, isolated from soft lenses formed weak biofilms. The fact that bacteria in biofilms are more resistant to antiseptics, antibiotics, and host defenses causes problems in their inhibition. Physiological heterogeneity, complex structure, high flow expression, and the relative anaerobicity in the deeper layers of the biofilm may be responsible for this high resistance. Studies for the prevention and inhibition of biofilm formation have intensified in recent years. One of the leading methods is probiotic lactic acid bacteria.

Studies on the application of postbiotics and parabiotics to foods are increasing day by day. There are also some studies in the field of health. Mantziari et al. presented a data about the usage of post-probiotics against pathogens that cause pediatric infectious diseases. However, a study on lenses were not encountered in the literature review (25). According to our knowledge, this study is the first study on the inhibition of *S. epidermidis* biofilm in acrylic lenses by probiotic lactic acid bacteria and parabiotic biofilm. A product has been prepared and patented for the use of the supernatant of *Lactobacillus paracasei* in the treatment of conjunctivitis, especially vernal keratoconjunctivitis (VKC) (26). There are some studies on the inhibition of biofilm in soft lenses and the antibiofilm activity of some disinfectants, herbs, and solutions (24, 27, 28). Kilvington and Lonnen evaluated the ability of contact lens solutions to remove the biofilm formed on silicone hydrogel lenses. Results have been reported to be unsatisfactory when the scrubbing and rinsing steps of the lenses are skipped (29).

In recent years, it has been shown that as an alternative to the antimicrobial and antibiofilm activities of probiotic bacteria, cell-free filtrates or substrates with inhibited cells also show antimicrobial and antibiofilm activities. Postbiotics include products of microbial action such as the fermentation of carbohydrates, vitamins, various peptides, and the synthesis of enzymes. Even some structural components of bacteria, such as teichoic acid, are considered postbiotics. It has been reported that postprobiotics have different functions such as immunomodulators, antioxidants, and antimicrobials (16, 30). From this perspective, postbiotics/parabiotics prepared from lactic acid bacteria contain many metabolites used as raw concentrate (extract) or semi-purified form (18).

In conclusion, the parabiotic of *L. rhamnosus* 312 was found effective for its antibiofilm effect. However, further studies are needed on this subject. Putatively, higher antibiofilm activity can be achieved with a concentration adjustment. In particular, the parabiotic product can have many advantages. *L. rhamnosus* 312 is a promising isolate considering that paraprobiotics and postbiotics have significant potential for the development of biotechnological products.

Acknowledgement: We would like to thank Associate Professor Volkan Kilic for his contribution in taking SEM photographs in the study.

Ethics Committee Approval: Ethics committee approval was not obtained because there was no use of human and animal data in this study.

Peer-review: Externally peer-reviewed.

Author Contribution: Conception - S.A.K., B.A., M.K.; Formal analysis- S.A.K., B.A., M.K.; Methodology S.A.K., B.A., M.K.; Investigation - S.A.K., B.A., M.K.; Writing - original draft - S.A.K., B.A., M.K.; Writing - Review & Editing - S.A.K., B.A., M.K.; Performing experiments- M.K.; Supervision - MK.; Final Approval and Accountability- S.A.K., B.A., M.K.

Conflict of Interest: The authors have no conflict of interest to declare.

Financial Disclosure: This project was supported by Anadolu University Scientific Research Projects Commission (1404F202).

REFERENCES

- Christensen GD, Simpson WA, Bisno AL, Beachey EH. Adherence of slime-producing *Staphylococcus epidermidis* to smooth surfaces. *Infect Immun* 1982; 37: 318-26. [CrossRef]
- Peters G, Locci R, Pulverer G. Adherence and growth of coagulase-negative staphylococci on surfaces of intravenous catheters. *J Infect Dis* 1982; 146: 479-82. [CrossRef]
- Kattan HM, Flynn HW Jr, Pflugfelder SC, Robertson C, Forster RK. Nosocomial endophthalmitis survey: current incidence of infection after intraocular surgery. *Ophthalmology* 1991; 98: 227-38. [CrossRef]
- Wong TY, Chee SP. The epidemiology of acute endophthalmitis after cataract surgery in an Asian population. *Ophthalmology* 2004; 111: 699-705. [CrossRef]
- Miller JJ, Scott IU, Flynn HW Jr, Smiddy WE, Newton J, Miller D. Acute-onset endophthalmitis after cataract surgery (2000-2004): Incidence, clinical settings, and visual acuity outcomes after treatment. *Am J Ophthalmol* 2005; 139: 983-7. [CrossRef]

6. Aaberg TM Jr, Flynn HW Jr, Schiffman J, Newton J. Nosocomial acute-onset postoperative endophthalmitis survey. A 10-year review of incidence and outcomes. *Ophthalmology* 1998; 105: 1004-10. [\[CrossRef\]](#)
7. Griffiths PG, Elliot TSJ, McTaggart L. Adherence of *Staphylococcus epidermidis* to intraocular lenses. *Br J Ophthalmol* 1989; 73: 402-6. [\[CrossRef\]](#)
8. Kivanç SA, Kivanç M, Kılıç V, Güllülü G, Özmen AT. Comparison of biofilm formation capacities of two clinical isolates of *Staphylococcus epidermidis* with and without *icaA* and *icaD* genes on intraocular lenses. *Turk J Ophthalmol* 2017; 47: 68-73. [\[CrossRef\]](#)
9. Zegans ME, Becker HI, Budzik J, O'Toole G. The role of bacterial biofilms in ocular infections. *DNA Cell Biol* 2002; 21: 415-20. [\[CrossRef\]](#)
10. Pinna A, Sechi LA, Zanetti S, Delogu D, Carta F. Adherence of ocular isolates of *Staphylococcus epidermidis* to AcrySof intraocular lenses: a scanning electron microscopy and molecular biology study. *Ophthalmology* 2000; 107: 2162-6. [\[CrossRef\]](#)
11. Kodjikian L, Burillon C, Roques C, Pellon G, Freney J, Renaud FN. Bacterial adherence of *Staphylococcus epidermidis* to intraocular lenses: a bioluminescence and scanning electron microscopy study. *Invest Ophthalmol Vis Sci* 2003; 44: 4382-7. [\[CrossRef\]](#)
12. McKenney D, Hubner J, Muller E, Wang Y, Goldmann DA, Pier GB. The *ica* locus of *Staphylococcus epidermidis* encodes production of the capsular polysaccharide/adhesion. *Infect Immun* 1998; 66: 4711-20. [\[CrossRef\]](#)
13. Cramton SE, Gerke C, Schnell NF, Nichols WW, Gotz F. The intercellular adhesion (*ica*) locus is present in *Staphylococcus aureus* and is required for biofilm formation. *Infect Immun* 1999; 67: 5427-33. [\[CrossRef\]](#)
14. von Eiff C, Heilmann C, Peters G. New aspects in the molecular basis of polymer-associated infections due to staphylococci. *Eur J Clin Microbiol Infect Dis* 1999; 18: 843-6. [\[CrossRef\]](#)
15. Cuevas-González PF, Liceaga AM, Aguilar-Toalá JE. Postbiotics and paraprobiotics: From concepts to applications. *Food Res Int* 2020; 136: 109502. [\[CrossRef\]](#)
16. Aguilar-Toalá JE, Garcia-Varela R, Garcia HS, Mata-Haro V, González Córdova AF, Vallejo-Cordoba B, et al. Postbiotics: an evolving term within the functional foods field. *Trends Food Sci Technol* 2018; 75: 105-14. [\[CrossRef\]](#)
17. Okajima Y, Kobayakawa S, Tsuji A, Tochikubo T. Biofilm formation by *Staphylococcus epidermidis* on intraocular lens material. *Invest Ophthalmol Vis Sci* 2006; 47: 2971-5. [\[CrossRef\]](#)
18. Moradi R, Molaei R, Guimaraes JT. A review on preparation and chemical analysis of postbiotics from lactic acid bacteria. *Enzyme Microb Technol* 2021; 143: 109722. [\[CrossRef\]](#)
19. Mohamed S, Elmohamady MN, Abdelrahman S, Amer MM, Abdelhamid AG. Antibacterial effects of antibiotics and cell-free preparations of probiotics against *Staphylococcus aureus* and *Staphylococcus epidermidis* associated with conjunctivitis. *Saudi Pharm J* 2020; 28: 1558-65. [\[CrossRef\]](#)
20. Hor YY, Liang MT. Use of extracellular extracts of lactic acid bacteria and bifidobacteria for the inhibition of dermatological pathogen *Staphylococcus aureus*. *Dermatol Sin* 2014; 32, 141-7. [\[CrossRef\]](#)
21. Negi YK, Pandey C, Saxena N, Sharma S, Garg FC, Garg SK. Isolation of antibacterial protein from *Lactobacillus* spp. and preparation of probiotic curd. *J Food Sci Technol* 2018; 55: 2011-20. [\[CrossRef\]](#)
22. Mazoterias P, Quiles MG, Martins Bispo PJ, Höfling-Lima AL, Pignatari AC, Casaroli-Marano RP. Analysis of intraocular lens biofilms and fluids after long-term uncomplicated cataract surgery. *Am J Ophthalmol* 2016; 169: 46-57. [\[CrossRef\]](#)
23. Kivanç SA, Kivanç M, Bayramlar H. Microbiology of corneal wounds after cataract surgery: biofilm formation and antibiotic resistance patterns. *J Wound Care* 2016; 25: 14-9. [\[CrossRef\]](#)
24. El-Ganiny AM, Shaker GH, Aboelazm AA, El-Dash HA. Prevention of bacterial biofilm formation on soft contact lenses using natural compounds. *J Ophthalmic Inflamm Infect* 2017; 7: 11. [\[CrossRef\]](#)
25. Mantziari A, Salminen S, Szajewska H, Malagón-Rojas JN. Postbiotics against pathogens commonly involved in pediatric infectious diseases. *Microorganisms* 2020; 8: 1510. [\[CrossRef\]](#)
26. Rescigno M, Penna, G. Postbiotic-based composition for treatment of ocular inflammation. Patent. 2019. Available from: URL: WO2018024833A1.pdf (storage.googleapis.com)
27. Leshem R, Maharshak I, Ben Jacob E, Ofek I, Kremer I. The effect of nondialyzable material (NDM) cranberry extract on formation of contact lens biofilm by *Staphylococcus epidermidis*. *Invest Ophthalmol Vis Sci* 2011; 52: 4929-34. [\[CrossRef\]](#)
28. Szczotka-Flynn LB, Imamura Y, Chandra J, Yu C, Mukherjee PK, Pearlman E, et al. Increased resistance of contact lens-related bacterial biofilms to antimicrobial activity of soft contact lens care solutions. *Cornea* 2009; 28: 918-26. [\[CrossRef\]](#)
29. Kilvington S, Lonnen J. A comparison of regimen methods for the removal and inactivation of bacteria, fungi and Acanthamoeba from two types of silicone hydrogel lenses. *Cont Lens Anterior Eye* 2009; 32: 73-7. [\[CrossRef\]](#)
30. Tsilingiri K, Rescigno M. Postbiotics: What else? *Benef Microbes* 2013; 4: 101-7. [\[CrossRef\]](#)

Caspase-9 rs1052576 Polymorphism is not Associated with Glioblastoma in Turkish Patients

Deryanaz Billur¹ , Fatma Tuba Akdeniz² , Seda Gulec-Yilmaz² , Zerrin Barut³ ,
Cumhur Kaan Yaltirik⁴ , Turgay Isbir² 

¹Department of Molecular Medicine, Institute of Health Sciences, Yeditepe University, Istanbul, Turkiye

²Department of Medical Biology, Faculty of Medicine, Yeditepe University, Istanbul, Turkiye.

³Department of Basic Medical Sciences, Faculty of Dentistry, Antalya Bilim University, Antalya, Turkiye

⁴Department of Neurosurgery, Umraniye Training and Research Hospital, Istanbul, Turkiye

ORCID ID: D.B. 0000-0002-6079-8224; F.T.A. 0000-0002-6076-0509; S.G.Y. 0000-0002-8119-2862; Z.B. 0000-0002-6289-5562; C.K.Y. 0000-0002-4312-5685; T.I. 0000-0002-7350-6032

Cite this article as: Billur D, Akdeniz FT, Gulec-Yilmaz S, Barut Z, Yaltirik CK, Isbir T. Caspase-9 rs1052576 polymorphism is not associated with glioblastoma in Turkish patients. *Experimed* 2022; 12(3): 108-12.

ABSTRACT

Objective: As an aggressive type of brain cancer, glioblastoma remains obscure with its short survival time and unclear molecular architecture. Single nucleotide polymorphisms (SNPs), such as those located in the regions of the caspase-9 gene (*CASP9*), have been reported to be associated with genetic susceptibility to glioblastoma. There is no exact result on the effect of *CASP9* SNP rs1052576 on glioblastoma and its biomarker candidacy for the Turkish population. Investigating the polymorphism of the exon 5 (+32 G/A) region of the *CASP9* in glioblastoma patients in the Turkish population was the aim of this study.

Materials and Methods: Real-time polymerase chain reaction (RT-PCR) method on blood samples of glioblastoma patients (n=33) and healthy controls (n=35) were used to analyze *CASP9* SNP rs1052576. Statistical data were obtained using SPSS v.23 software.

Results: For *CASP9* rs1052576, no evidence was found of its role in glioblastoma (p=0.594).

Conclusion: This study was designed to determine the association between glioblastoma and *CASP9* SNP rs1052576 within the Turkish population. Our results indicated that *CASP9* SNP rs1052576 is not related to glioblastoma in Turkish patients. To clarify these results, further studies with a larger sample size are needed.

Keywords: Caspase-9, glioblastoma, polymorphism, rs1052576

INTRODUCTION

As an aggressive type of adult primary brain tumor, glioblastoma is known for its poor survival rate (average survival of only 8 months) (1). It constitutes about 14.0 % of all primary (2) and at least 60 % of all brain tumors in adults (3). Necrosis, hypercellularity, microvascular proliferation, and nuclear atypia are some histological features of glioblastoma (4). Diverse genetic factors and epigenetic alterations are responsible for the development and progression of glioblastoma (5, 6). Decreased apoptosis, one of the reasons for the aggressive characteristics of the

disease, and intrinsic deregulation in apoptotic cell death are seen in this multifactorial disease (7).

In human cancers such as glioblastoma, evasion of apoptosis is accepted as a hallmark (8). Cell proliferation and cell death homeostasis is maintained by apoptotic mechanisms (7). There are two identified apoptotic pathways, namely: Extrinsic (triggered through membrane death receptors) and intrinsic (activated by cellular stresses) also called the mitochondrial pathway (9). A defect in apoptosis underpins the tumorigenesis and malignant progression of glioblastoma (10). Because of

Corresponding Author: Deryanaz Billur **E-mail:** deryanazbillur@gmail.com

Submitted: 04.10.2022 **Revision Requested:** 18.10.2022 **Last Revision Received:** 20.10.2022 **Accepted:** 01.11.2022 **Published Online:** 05.12.2022



Content of this journal is licensed under a Creative Commons Attribution-NonCommercial 4.0 International License.

their crucial roles in apoptosis, caspases are at the center of studies on carcinogenesis. Caspase-9, as a member of this conserved cysteine-aspartic proteases family, takes place in the regulation of intrinsic apoptosis as an initiator, and it is indispensable for efficient apoptosis. Activation of caspase-9 results in the induction of apoptotic cell death by cleavage of effector caspases. Cellular damage can also cause a response by triggering intrinsic apoptosis and tumor growth can be suppressed by caspase-9. However, as a consequence of the evasion of apoptosis, caspase-9 can be inhibited by some tumors. The apoptotic potential of caspase-9 is regulated by processes such as interference with its binding to the apoptosome. Further, some inactivating mutations and certain polymorphisms can affect the abundance or activity of caspases (11). Polymorphisms in genes regulating apoptosis can determine the efficiency of apoptosis (8). Not only at the gene level, but also at the single nucleotide polymorphism (SNP) level, alterations of caspase-9 gene (*CASP9*) have been associated with human cancers (11). The human *CASP9*, which encodes an apoptosis-related cysteine protease, caspase-9, is located on chromosome 1 region p36.2 (12). In databases, a few candidate *CASP9* SNPs have been listed (13). Some of these SNPs as potential biomarkers are found in the promoter (e.g. rs4645978, rs4645981) or exon sequence of *CASP9* (e.g. rs1052576).

Susceptibility to various cancers, including lung cancer, colorectal cancer, liver cancer, and prostate cancer, can occur through *CASP9* polymorphisms, such as the ones aforementioned, influencing caspase-9 expression (14). Among the *CASP9* polymorphisms, there are only a few studies that have examined whether the *CASP9* exon 5 (+32 G/A) SNP rs1052576 is a predisposing factor to human diseases or not (15). As a consequence of this exonic polymorphism at codon 221, glutamine amino acid is converted to arginine (Q221R). As a result of this substitution, a conformational change occurs in the caspase-9 molecule, and the apoptotic mechanism is influenced through modification of the binding of caspase-9 to Apaf-1 (16). Based on all this information, the role of *CASP9* SNP rs1052576 in glioblastoma was investigated in this study, which was performed in the Turkish population.

MATERIALS AND METHODS

Study Population and Clinical Procedures

In this study, 68 individuals were analyzed (including 35 controls and 33 glioblastoma cases). All participants were selected and recruited from Yeditepe University Neurosurgery Department (Istanbul, Turkiye) after detailed clinical examinations and

whole blood samples were taken. This study was performed per tenets of the Declaration of Helsinki. Ethical approval was obtained for this study from the Yeditepe University Medical Faculty Ethics Committee (Date: 24.10.2018 and No: 916). Data about the clinical and demographic characteristics of the study groups were registered before the experimental phase of the study. Also, all individuals signed an informed consent form.

CASP9 SNP rs1052576 Genotyping

Following ethical procedures, EDTA tubes were used to collect blood samples from all individuals. An iPrep Purification device (Invitrogen, Life Technologies, Carlsbad, California, USA), 350 µL of peripheral blood, and an Invitrogen iPrep PureLink gDNA blood isolation kit (Invitrogen, Life Technologies, Carlsbad, California, USA) were used in the DNA extraction procedure. NanoDrop 2000 (Thermo Scientific, Waltham, Massachusetts, USA) was chosen to measure the genomic DNA purity and its concentration. The dilution concentration of the DNA samples was 100 ng/µL. Genotyping for *CASP9* SNP rs1052576 was performed by an Applied Biosystems 7500 Fast Real-Time polymerase chain reaction (RT-PCR) device. The components of the PCR master-mix were 1 µL DNA template, 0.25 µL TaqMan Genotyping Assay, 5 µL TaqMan Genotyping Master Mix (TaqMan Reagents, Applied Biosystems, Foster City, CA, USA), and 3.75 µL DNase free water. The holding stage at 95°C for 10 min, the denaturation stage at 92°C for 15 sec (40 cycles), and the binding/elongation stage at 60°C for 1 min were the conditions of the PCR using sequence-specific primers (Table 1).

Statistical Analyses

Obtained data were analyzed using SPSS 23 program (SPSS Inc., Chicago, IL, USA). Student's t-test was conducted to compare the significance of the differences between groups. Chi-square and Fisher's exact tests were used to determine the difference in the existence of target polymorphism in the patient and control groups. Statistical significance was assessed by at least $p < 0.05$.

RESULTS

Table 2 shows the demographic characteristics of the study participants. Of the 68 individuals, 33 were patients (72.30% male, 27.70% female) with a mean age of 48.69 ± 18.34 years and 35 individuals were healthy controls (62.90% male, 37.10% female) with a mean age of 42.75 ± 11.70 years. The mean age ($p=0.108$) and gender ($p=0.386$) of the study populations were not significantly different.

Table 1. The polymorphism and experimental details

Gene, chromosome location, base change, SNP	Genotyping method	Primers
<i>CASP9</i> , 1p36.21 Ex5 +32G > A, rs1052576	PCR	5'-GGCTTTGCTGGAGCTGGCCC-3' (sense) 5'-AGTACCCAATGCCTGCCAGGG-3' (antisense)

Table 2. Demographic data of the study subjects

Characteristic	Patient (n=33)	Control (n=35)	p-value
Gender (%)	Male / Female 72.3 / 27.7 (n=24) / (n=9)	Male / Female 62.9 / 37.1 (n=22) / (n=13)	0.386
Age (year) (mean ± SD)	48.69 ± 18.34	42.75 ± 11.70	0.108

n: Number of the sample, SD: Standard deviation

Table 3. Distribution of *CASP9* SNP rs1052576 genotypes and alleles in cases and controls

Polymorphism rs1052576	Case (n=33) n (%)	Control (n=35) n (%)	p-value	Odds Ratio	95%-CI%
Exon 5 +32 Genotypes					
GG	11 (33.3)	16 (45.7)	0.493	1.3714	0.5559 - 3.3835
GA	18 (54.5)	14 (40.0)	0.471	0.7333	0.3150 - 1.7072
AA	4 (12.2)	5 (14.3)	0.817	1.1786	0.2912 - 4.7706
Alleles					
G	40 (60.6)	46 (65.71)	0.803	1.0843	0.5735 - 2.0501
A	26 (39.4)	24 (34.29)	0.709	0.8703	0.4191 - 1.8074

n= Number of the sample, CI: Confidence interval

Table 3 summarizes the information on genotype and allele frequencies for *CASP9* SNP rs1052576 in the study groups. According to the information in Table 3, it is seen that there is no statistical significance in the *CASP9* SNP rs1052576 genotype frequencies between groups ($p > 0.05$). Out of 33 glioblastoma patients, the frequencies of the GG:GA:AA genotypes were 11:18:4. Out of 35 healthy individuals, the frequencies of GG:GA:AA genotypes were 16:14:5. While the frequency of *CASP9* rs1052576 G-allele was 60.60% in those with glioblastoma, it was 65.71% in the control group. In 39.40% of patients and 34.29% of healthy individuals, the mutant A allele was present. The *CASP9* ancestral G allele and mutant A allele were not associated with glioblastoma ($p = 0.803$ and $p = 0.709$, respectively) (Table 3).

DISCUSSION

It is known how important apoptotic mechanisms are in diseases with genetically complex architecture such as glioblastoma. Examining molecules such as caspase-9, which has a key role in the regulation of intrinsic pathways, is important in elucidating the molecular mechanism of the disease. Though SNPs are not considered to be the only causative factors of glioblastoma, they are important genetic factors in disease susceptibility because of their impact on gene regulation and its products.

Hence, this study was initiated to analyze the place of *CASP9* SNP rs1052576 in glioblastoma.

This target SNP at codon 221 in exon 5 of the *CASP9* causes the substitution of glutamine by arginine (Q221R) (15). Some studies have suggested that this Q221R variant might influence carcinogenesis due to conformational changes in caspase-9. The conformational changes lead to alterations in the binding affinity of caspase-9 for Apaf-1 (14, 16). Despite previous studies reporting a significant relationship of this SNP with several human diseases (15), in our Turkish cohort of glioblastoma patients, a genetic link between the *CASP9* SNP rs1052576 and glioblastoma has not been detected.

In the literature, there are studies examining *CASP9* polymorphisms and their impact on cancer development and progression in different cancer types, including multiple myeloma (17), and non-Hodgkin's lymphoma (18). These studies showed that *CASP9* SNP rs1052576 decreased susceptibility to the diseases. Furthermore, three different comprehensive meta-analyses have shown that the A allele of rs1052576 is protective against cancer (16, 19, 20). The impact of *CASP9* polymorphisms (rs4645978, rs1052576, and rs4645981) on cancer susceptibility has been shown via investigations performed by Xu et al. They have reported that

carriers of the A allele of rs1052576 in the Asian subgroup have less risk for cancer (14). Mutations in the *CASP9* have been analyzed by Yan et al. in Chinese, American, Russian and Caucasian populations. According to the results of this study, while the A allele is protective against the risk of cancer in the Chinese and American populations, no relationship was found between this allele and disease susceptibility in the Russian and Caucasian populations, as in our study population (20). The association of rs1052576 with primary brain tumors has been investigated by another study in the Turkish population. Their results showed that the A allele of the Q221R variant decreased the risk for glioma development. In addition, they showed a protective role of *CASP9* SNP rs1052576 GG genotype against gliomas (21). However, Ozdogan et al. did not report the number of glioblastoma cases within the glioma group. In this respect, this study differs from our research. Although the same population and the same disease were studied, the clearest explanation for the different results may be that we examined only glioblastoma patients. Our study reveals more detailed information about whether the SNP is a distinctive genetic factor or not in glioblastoma, a high-grade glioma, in the Turkish population.

Though the link of rs1052576 polymorphism with cancer susceptibility has been documented in these studies, no significant relationship has been found between the *CASP9* SNP rs1052576 and glioblastoma in our study. This controversy with our results might depend on factors like population and ethnic differences.

Consequently, the present study ascertains that *CASP9* SNP rs1052576 is not associated with glioblastoma susceptibility in the Turkish population. However, our study is one of the few studies examining the *CASP9* SNP rs1052576 and glioblastoma susceptibility. The results need to be validated in other independent cohorts, with larger sample sizes.

CONCLUSION

As described earlier, *CASP9* SNP rs1052576 has not been found to be related to glioblastoma. Briefly, these results do not support the role of the *CASP9* rs1052576 variant in susceptibility to glioblastoma disease in the Turkish population.

Ethical Committee Approval: The ethical standards of the 1975 Declaration of Helsinki guidelines and its later amendments were adhered to in all procedures performed in studies involving human participants. The research on humans study protocol was approved by the Yeditepe University Medical Faculty Ethics Committee (file no: 24.10.2018/916).

Peer-review: Externally peer-reviewed.

Authors' Contributions: Conception/Design of Study – T.I., D.B.; Data Acquisition – C.K.Y.; Performing experiments – D.B.; Data Analysis/ Interpretation – S.G.Y., D.B., F.T.A., Z.B.; Drafting Manuscript – T.I., D.B.; Critical Revision of Manuscript – T.I.; Final Approval and Accountability – T.I., D.B.

Conflicts of Interest: The authors declare no conflict of interest.

Financial Disclosure: The authors declare that this study has received no financial support.

REFERENCES

- Ostrom QT, Patil N, Cioffi G, Waite K, Kruchko C, Barnholtz-Sloan JS. CBTRUS Statistical report: primary brain and other central nervous system tumors diagnosed in the United States in 2013-2017 Neuro Oncol 2020; 22(12 Suppl 2): iv1-iv96. [CrossRef]
- Ostrom QT, Gittleman H, Farah P, Ondracek A, Chen Y, Wolinsky Y, et al. CBTRUS statistical report: primary brain and central nervous system tumors diagnosed in the United States in 2012-2016. Neuro Oncol 2019; 25(5): 1-100. [CrossRef]
- Hanif F, Muzaffar K, Perveen K, Malhi SM, Simjee ShU. Glioblastoma multiforme. A review of its epidemiology and pathogenesis through clinical presentation and treatment. Asian Pac J Cancer Prev 1 2017; 18(1): 3-9.
- D'Alessio A, Proietti G, Sica G, Scicchitano BM. Pathological and molecular features of glioblastoma and its peritumoral tissue. Cancers (Basel) 2019; 11(4): 469. [CrossRef]
- Crespo I, Vital AL, Gonzalez-Tablas M, Patino Mdel C, Otero A, Lopes MC, de Oliveira C, Domingues P, et al. Molecular and genomic alterations in glioblastoma multiforme. Am J Pathol 2015; 185(7):1820-33. [CrossRef]
- Haque A, Banik NL, Ray SK. Molecular alterations in glioblastoma: Potential targets for immunotherapy. Prog Mol Biol Transl Sci 2011; 98: 187-234. [CrossRef]
- Valdés-Rives SA, Casique-Aguirre D, Germán-Castelán L, Velasco-Velázquez MA, González-Arenas A. Apoptotic signaling pathways in glioblastoma and therapeutic implications. Biomed Res Int 2017; 7403747. [CrossRef]
- Olsson M, Zhivotovsky B. Caspases and cancer. Cell Death Differ 2011; 18(9): 1441-9. [CrossRef]
- McIlwain DR, Berger T, Mak TW. Caspase functions in cell death and disease. Cold Spring Harb Perspect Biol 2013; 5(4): a008656. [CrossRef]
- Mohammad RM, Muqbil I, Lowe L, Yedjou C, Hsu HY, Lin LT, et al. Broad targeting of resistance to apoptosis in cancer. Semin Cancer Biol 2015; 35 Suppl(0): S78-S103. [CrossRef]
- Avrutsky MI, Troy CM. Caspase-9. A multimodal therapeutic target with diverse cellular expression in human disease. Front Pharmacol 2021; 12: 701301. [CrossRef]
- Abel F, Sjöberg RM, Ejeskär K, Krona C, Martinsson T. Analyses of apoptotic regulators *CASP9* and *DFFA* at 1P36.2, reveal rare allele variants in human neuroblastoma tumours. Br J Cancer 2002; 86(4): 596-604. [CrossRef]
- National Library of Medicine, NCBI Databases. Available from: URL://www.ncbi.nlm.nih.gov/pubmed/?term=caspase+9+polymorphism
- Xu W, Jiang S, Xu Y, Chen B, Li Y, Zong F, et al. A meta-analysis of caspase 9 polymorphisms in promoter and exon sequence on cancer susceptibility. PLoS One 2012; 7(5): e37443. [CrossRef]
- Hirano A, Nagai H, Harada H, Haga S, Kajiwara T, Emi M. Two novel single-nucleotide polymorphisms of the Caspase-9 (*CASP9*) gene in the Japanese population. Genes Immun 2001; 2(2): 117-8. [CrossRef]
- Andreoli V, Trecroci F, La Russa A, Valentino P, Condino F, Latorre V et al. *CASP-9*. A susceptibility locus for multiple sclerosis in Italy. J Neuroimmunol 2009; 210(1-2): 100-3. [CrossRef]
- Hosgood HD 3rd, Baris D, Zhang Y, Zhu Y, Zheng T, Yeager M, et al. Caspase polymorphisms and genetic susceptibility to multiple myeloma. Hematol Oncol 2008; 26(3): 148-51. [CrossRef]

18. Lan Q, Zheng T, Chanock S, Zhang Y, Shen M, Wang SS, et al. Genetic variants in caspase genes and susceptibility to non-Hodgkin lymphoma. *Carcinogenesis* 2007; 28(4): 823-7. [\[CrossRef\]](#)
19. Zhang ZY, Xuan Y, Jin XY, Tian X, Wu R. CASP-9 gene functional polymorphisms and cancer risk: a large-scale association study plus meta-analysis. *Genet Mol Res* 2013; 12(3): 3070-8. [\[CrossRef\]](#)
20. Yan S, Li YZ, Zhu XW, Liu CL, Wang P, Liu YL. Role of the CASP-9 Ex5+32 G>A polymorphism in susceptibility to cancer: A meta-analysis. *Exp Ther Med* 2013; 5(1): 175-80. [\[CrossRef\]](#)
21. Ozdogan S, Kafadar A, Yilmaz SG, Timirci-Kahraman O, Gormus U, Isbir T. Role of Caspase-9 Gene Ex5+32 G>A (rs1052576) variant in susceptibility to primary brain tumors. *Anticancer Res* 2017; 37(9): 4997-5000. [\[CrossRef\]](#)

The Effect of Whey Proteins on the Brain and Small Intestine Nitric Oxide Levels: Protein Profiles in Methotrexate-Induced Oxidative Stress

Sumeyye Yilmaz¹ , Elif Tufan² , Guzin Goksun Sivas² , Begum Gurel Gokmen² , Ercan Dursun² , Dilek Ozbeyli³ , Goksel Sener¹ , Tugba Tunali-Akbay² 

¹Vocational School of Health Services, Fenerbahçe University, Istanbul, Turkiye

²Department of Basic Medical Sciences, Faculty of Dentistry, Marmara University, Istanbul, Turkiye

³Vocational School of Health Services, Marmara University, Istanbul, Turkiye

ORCID ID: S.Y. 0000-0001-5529-7380; E.T. 0000-0003-0684-3693; G.G.S. 0000-0001-7347-490X; B.G.G. 0000-0002-3955-1948; E.D. 0000-0001-6025-9565; D.Ö. 0000-0002-4141-6913; G.Ş. 0000-0001-7444-6193; T.T.A. 0000-0002-2091-9298

Cite this article as: Yilmaz S, Tufan E, Goksun Sivas G, Gurel Gokmen B, Dursun E, Ozbeyli D, Sener G, Tunali-Akbay T. The effect of whey proteins on the brain and small intestine nitric oxide levels: Protein profiles in methotrexate-induced oxidative stress. *Experimed* 2022; 12(3): 113-8.

ABSTRACT

Objectives: The aim of this study was to determine the effects of whey proteins on methotrexate (MTX)-induced brain and small intestine damage.

Materials and Methods: 30 Sprague Dawley rats (200-300 g) were divided into four groups: Control, control + whey, MTX, and MTX+whey. MTX was administered at 20 mg/kg (single dose) intraperitoneally to the MTX group rats, and 2 mg/kg of whey protein were administered by oral gavage for 10 days to the whey groups. Lipid peroxidation, glutathione, and nitric oxide (NO) levels, as well as glutathione-S-transferase and superoxide dismutase activities were measured in the brain and small intestine. SDS-polyacrylamide gel electrophoresis of the brain and intestine tissues were also carried out.

Results: While MTX treatment caused oxidative damage in the brain and small intestine, whey protein administration ameliorated MTX-induced oxidative stress. MTX administration did not change the brain's NO level, while an increase in intestinal NO level was detected.

Conclusion: MTX induced oxidative stress in the brain and small intestine changed the protein metabolism in these tissues regardless of reduced food intake. Consecutive 10-day administration of whey proteins has shown its therapeutic effect on MTX-induced brain and small intestine oxidative damage.

Keywords: Methotrexate, whey protein, brain, small intestine, nitric oxide, oxidative stress

INTRODUCTION

As a folate anti-metabolite, methotrexate (MTX) is used to treat some malignancies and immunological disorders (1). It inhibits the mammalian dihydrofolate reductase (DHFR) enzyme, which is required to generate tetrahydrofolate (THF) from folic acid and synthesizes purines and pyrimidines for the progression of the cell cycle. The mechanism of action against the DHFR enzyme appears to be the same in both bacterial and mammalian cells, despite the different drug susceptibility between bacterial strains

(2). MTX causes gastrointestinal toxicity, including nausea, diarrhea, and signs of decreased nutrient absorption, while also inducing enteritis. The inhibition of DHFR is the first step in the process of MTX-induced gastrointestinal damage and is related to DNA synthesis. The mucosa's barrier function against intravascular pathogens is therefore impaired, leading to bacterial translocation and inflammation. Oxidative damage has also been detected in human intestinal cells during MTX treatment (3, 4). Miyazono and Horie (5) revealed oxidative damage to

Corresponding Author: Tugba Tunali-Akbay **E-mail:** ttunali@marmara.edu.tr

Submitted: 16.10.2022 **Revision Requested:** 31.10.2022 **Last Revision Received:** 03.11.2022 **Accepted:** 16.11.2022 **Published Online:** 27.12.2022



Content of this journal is licensed under a Creative Commons Attribution-NonCommercial 4.0 International License.

contribute the neutrophil infiltration into inflammatory areas in the intestine and also contribute to increased transendothelial and transepithelial permeability. Disturbances at any stage of digestion might promote dysregulation in various digestive and non-digestive diseases (3). MTX also increases the oxidative stress by raising the concentration of reactive oxygen species (ROS) generation, and resulting in neurotoxicity (6). A high dose of MTX has been shown to cause acute, subacute, and chronic neurotoxicity. Acute toxicity often causes temporary impairment. Subacute and chronic toxicity are linked to alterations in the brain that may result in coma and death. Furthermore, MTX interferes with the biochemical activities of folate, homocysteine, adenosine, S-adenosylmethionine/S-adenosylhomocysteine, and bipterin, resulting in biochemical alterations related to neurological symptoms (7). MTX inhibits the NADP malic enzyme and NAD (P)-dependent dehydrogenases, thus it appears to reduce NADPH availability in cells by inhibiting the enzymes for the pentose phosphate pathway. As a result of failure of the antioxidant defense system, cells may become more vulnerable to MTX-induced oxidative damage. In addition, glutathione-S-transferase (GST), a family of phase-II detoxification enzymes, has been shown to catalyze the binding of glutathione (GSH) to a variety of electrophilic compounds, including MTX, and preventing these drugs from reaching their intended cellular targets (8). Since GSH is used to detoxify MTX and is unable to show an antioxidant effect, it may not prevent the increase of lipid peroxidation.

Various antioxidants, plant extracts, and nutrients are currently being researched for reducing or eliminating the damage caused by MTX treatment. For example, melatonin (4), retinol (9), garlic extract (10), and sodium tungstate (5) have been demonstrated to protect against MTX-induced injuries. This study was concentrated on the possible antioxidant properties of whey proteins regarding MTX-induced brain and small intestine damage. Whey proteins form about 20% of all milk proteins and can be produced after the precipitation of casein at 20 °C and a pH of 4.6. Whey proteins are mostly composed of globular proteins such as lactoferrin, b-lactoglobulin, albumin, immunoglobulins, a-lactalbumin, lactoperoxidase, protease peptones, and bioactive peptides (11). Valin, leucine, and isoleucine (branched-chain amino acids) are abundant in the whey fraction that contribute to muscle growth, and the protective role of whey protein concentrate (WPC) on the intestinal barrier has also been shown (12). *In vitro*, bovine whey products and hydrolysates exhibit antioxidant activity by chelating metals; reducing lipid peroxidation; decreasing ferric ions; scavenging radicals, hydroxyls, and superoxides; and neutralizing synthetic radicals. Whey proteins have been shown to possess a protective role against cellular oxidation and an antioxidant effect by increasing antioxidant enzymes such as glutathione peroxidase, superoxide dismutase (SOD), and catalase (in lung fibroblasts, hepatocytes, and endothelial cells) (11, 13). As a result, the present study examined the potential antioxidant mechanism of whey proteins against MTX-induced brain and small intestine damage.

MATERIALS AND METHODS

Experimental Design and Animal Testing

The Marmara University School of Medicine Animal Care and Use Committee approved the study (Protocol Number: 55.2021.mar). Sprague-Dawley (male) rats weighing between 200–300 g were housed in standard conditions and fed with a regular diet. The rats were separated into four different groups: control (C), whey-treated control (C+W), methotrexate (MTX), and whey-treated methotrexate (MTX+W) groups. The dose of MTX was decided based on the study by Aykac et al. (14). MTX injections (in physiological saline, 20 mg/kg, single dose) were continued over the next 10 days using either the saline (MTX group, $n = 8$), or whey protein (2 g/kg, oral gavage, MTX + W group, $n = 8$). Other rats received either the saline (C group, $n = 6$) or whey protein (2 g/kg, oral gavage C+W group, $n = 8$) for 10 days after receiving a single injection of saline. The rats were decapitated under ether anesthesia on day 10, and brain and small intestine tissue samples were taken.

Whey Protein

Lyophilization was used to preserve the whey protein beverage (Tazelen) that had been purchased from Kaanlar Food Industry and Trade, Turkiye. The relevant groups received 2 g/kg (oral gavage) of the lyophilized whey protein beverage dissolved in tap water. The whey protein dosage was chosen based on Shimizu et al. study (15).

Biochemical Analysis

10% small intestine and brain tissue homogenates in physiological saline were prepared using a glass homogenizer. The cooling process during homogenization was done by immersing a glass homogenizer into a beaker containing ice. Tissue homogenates were then centrifuged at 3000xg for 10 minutes. The supernatant samples were used for biochemical analysis. Malondialdehyde (MDA) levels were used as a marker of lipid peroxidation (16), SOD activity (17), GST activity (18), nitric oxide (NO) levels (19), and GSH levels (20) were also determined.

SDS-Polyacrylamide Gel Electrophoresis

The basic concept of Laemmli SDS-polyacrylamide gel electrophoresis (SDS-PAGE) was used to examine small intestine tissue and brain in terms of electrophoresis (21). The BIO-RAD mini protean precast II dual slab gel apparatus was used for SDS-PAGE (BIO-RAD, USA). For protein electrophoresis, mini PAGE gels (Any kD precast polyacrylamide gel, 8.6 6.7 cm (W L), Catalog Number: 4569033, BIO-RAD, USA) were used.

Statistical Analyses

Graphpad Prism 6.0 was used to perform the statistical analyses (GraphPad Software, San Diego, CA, USA). The results were provided in terms of means and standard deviations (SD). To compare the groups, ANOVA (post hoc Tukey test) was performed, with $p < 0.05$ being considered significant. Statistical power analysis was performed on the small intestine and brain NO levels using Faul et al.'s (22) method.

RESULTS

Brain

MTX administration significantly increased MDA levels and significantly decreased the levels of GSH, SOD and GST activities compared to the control group ($p < 0.05$). NO levels did not significantly change in the MTX group compared to the control group ($p > 0.05$; Figure 1). Whey protein administration to the MTX group significantly decreased MDA levels and significantly increased GSH levels, SOD levels and GST activity ($p < 0.05$). Brain NO levels did not significantly alter with the whey protein administration to the MTX group ($p > 0.05$). Upon administering whey proteins to the control group, no significant change occurred in MDA or GSH levels, nor in SOD and GST activity ($p > 0.05$); moreover, brain NO levels did decrease significantly ($p < 0.05$; Figure 1). When considering specific effect size, level, and sampling methods, the power analysis of the brain NO levels was found to be 0.84, which indicates an 84% possibility of disproving the null hypothesis.

Small Intestine

MTX administration significantly increased MDA and NO levels and significantly decreased GSH, SOD levels and GST activity compared to the control groups ($p < 0.05$; Figure 2). Whey protein administration to the MTX group decreased

MDA and NO levels and significantly increased GSH levels, SOD levels and GST activity ($p < 0.05$). Upon administering the whey proteins to the control group, significant decreases in MDA and NO levels and significant increases in GSH levels and SOD activity occurred ($p < 0.05$), while no significant change occurred in GST levels ($p > 0.05$; Figure 2). Given a specific effect size, level, and sample size, the power analysis of the small intestine NO levels was found to be 0.86, which indicates an 86% possibility of disproving the null hypothesis.

SDS Polyacrylamide Gel Electrophoresis

Electrophoretic models of brain and small intestine tissue belonging to all groups were shown in Figure 3 and Figure 4. Some differences in the densities of the brain and small intestine protein bands were detected in the electrophoretic examination. MTX administration decreased some protein bands of brain tissue detected between 50 kDa and 37 kDa, while whey protein administration to the MTX group increased these decreased bands. The majority of small intestine proteins were located at about 14, 30, 66 and 70 kDa during the administration. MTX administration decreased the density of 14 kDa and 30 kDa protein bands, while whey protein administration was able to increase these bands. Whey protein administration to the control group also increased the small intestine 30 kDa protein.

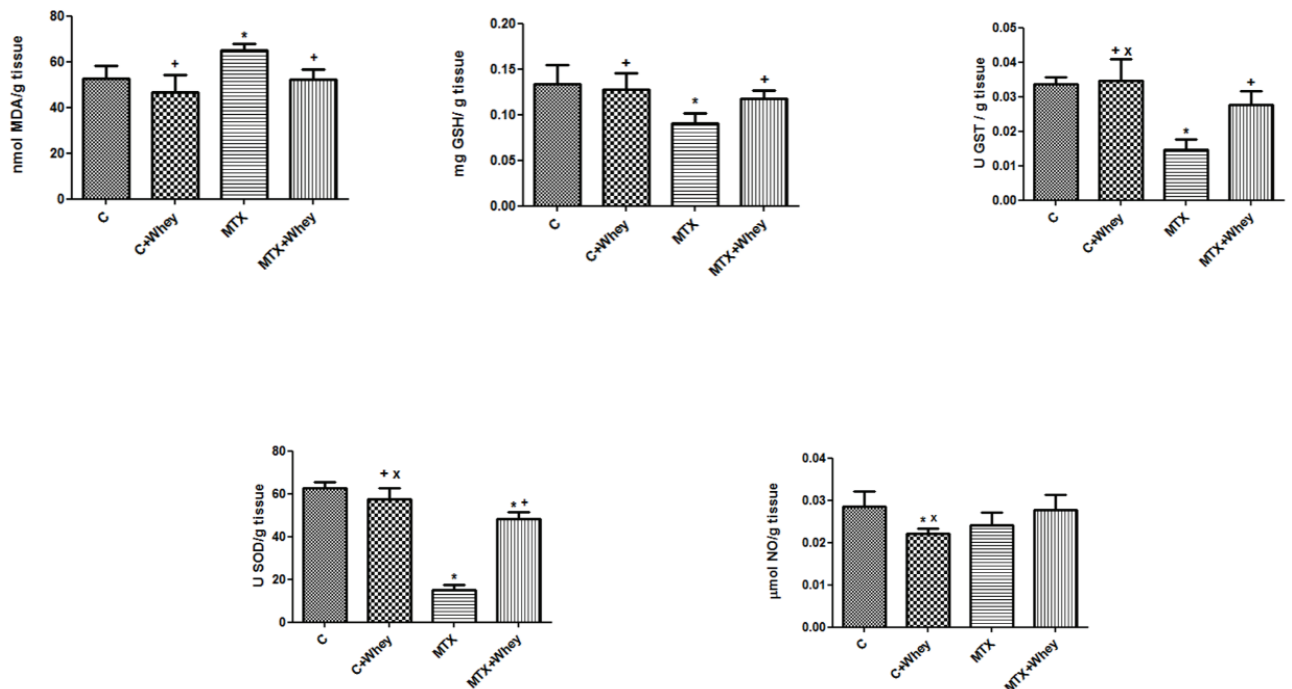


Figure 1. Biochemical analysis of brain tissue.

C: Control group, C+whey: Whey-administered control group, MTX: Methotrexate-administered group, MTX+whey: Methotrexate and whey protein -administered group, MDA: Malondialdehyde, GSH: Glutathione, SOD: Superoxide dismutase, GST: Glutathione-S-transferase, NO: Nitric oxide, * $p < 0.05$ compared to the control group, ** $p < 0.05$ compared to the MTX group, ** $p < 0.05$ compared to the C+whey group (n = 8).

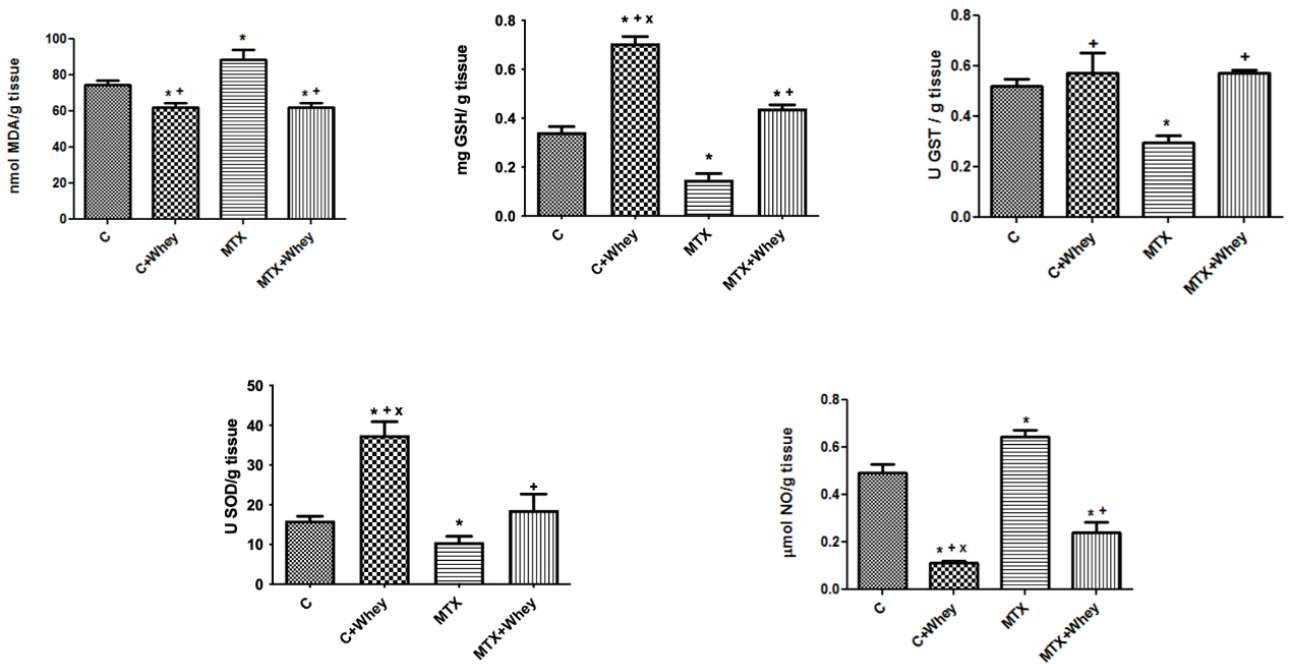


Figure 2. Biochemical analysis of small intestine tissue.

C: Control group, C+whey: Whey-administered control group, MTX: Methotrexate-administered group, MTX+whey: Methotrexate and whey protein -administered group, MDA: Malondialdehyde, GSH: Glutathione, SOD: Superoxide dismutase; GST: Glutathione-S-transferase, NO: Nitric oxide, *p<0.05 compared to the control group, *p<0.05 compared to the MTX group, +p<0.05 compared to the C+whey group (n=8).

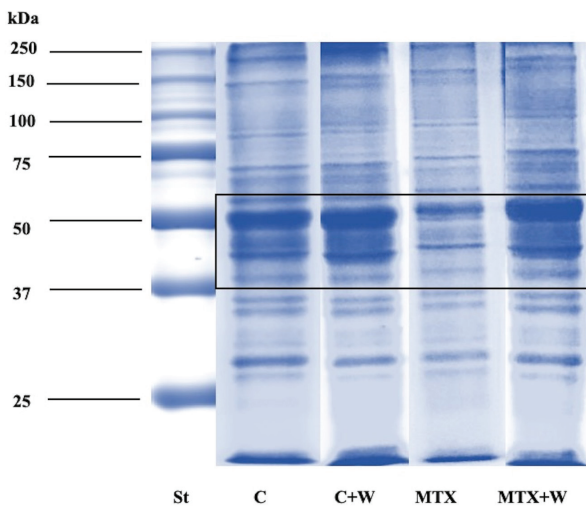


Figure 3. SDS- polyacrylamide gel electrophoresis of brain tissue.

St: Standard, C: Control group, C+W: Whey protein-administered control group, MTX: Methotrexate-administered group, MTX+W: Methotrexate and whey protein-administered group.

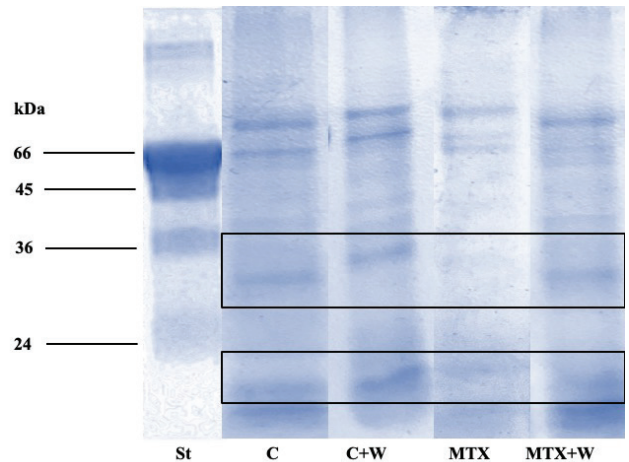


Figure 4. SDS- polyacrylamide gel electrophoresis of small intestine tissue.

St: Standard, C: Control group, C+W: Whey protein-administered control group, MTX: Methotrexate-administered group, MTX+W: Methotrexate and whey protein-administered group.

DISCUSSION

The gut-brain pathway is a network that links the central nervous system with the gastrointestinal tract and is made up

of a half billion neurons that innervate the gut and immune cells in gastrointestinal circulation (23). Any damage to the brain or small intestine might disrupt this connection and affect tissues. MTX treatment can also affect intestinal microbiota growth at physiologic concentrations (24).

Oxidative stress is one of the most important pathogenic processes for neurological disorders such as Parkinson's and Alzheimer's, as well as acute conditions like stroke and brain trauma. Meanwhile, brain lesions of different etiologies change gut characteristics and microbiota (2). These new concepts may lead the way to novel treatment methods for a variety of neurological diseases. This study has shown that MTX increased the oxidative stress in both the brain and the small intestine, as well as it lowers the activity of antioxidant enzymes. GST has been found to catalyze the conjugation of GSH to some electrophilic anticancer drugs, preventing drugs from reaching their cellular targets. One reason for this to use as an antioxidant is to reduce the increased lipid peroxidation due to the application of MTX, while another reason may be that GSH binds to MTX at which point it gets consumed; namely, GSH begins a detoxification reaction. MTX did not affect the brain NO levels, whereas the small intestine NO level was increased. The effects of MTX on the SDS/PAGE profiles of the brain and small intestinal tissues were reproducible. Whey protein administration, however, reduced oxidative stress, improved antioxidant defenses, and restored the disappeared protein bands in the brain and small intestinal tissues of rats that had been given MTX. The whey protein administration to the MTX group did not alter the brain NO levels either, although it lowered NO levels in the small intestine. Whey protein administration to the control group reduced NO levels in both brain and small intestine.

NO is a key signaling molecule that plays critical functions in the neuronal and intestinal tissues, as well as in inflammatory responses. Modifications to the biomolecules caused by oxidative stress may affect their physiological function and have serious repercussions for an organism (25). Furthermore, oxidative stress may result in the uncoupling of the endothelial nitric oxide synthase (eNOS), reducing NO synthesis/bioavailability and increasing NO-dependent oxidative stress. As a result, the prooxidative and antioxidative states of cells and tissues significantly influence NO production and bioactivity (25). Although NO is necessary for healthy gastrointestinal function, some evidence exists that an excessive amount of NO may impair the digestive system (26). An increase of NO in tissue may cause an increase in NO-dependent oxidative stress in that tissue. Our findings pointed out that MTX-induced brain oxidative damage did not affect brain NO levels. However, the increase in intestinal NO levels in parallel with the MTX-induced oxidative stress may have further increased the severity of oxidative damage. When exposing intestinal epithelial cells to high NO levels, their permeability increased. Apoptosis and intestinal secretion could both be stimulated by high levels of NO. However, NO may also prevent apoptosis and lessen inflammation by preventing NF- κ B activation (27). MTX also inhibits NF- κ B activity (28). This study used whey proteins to reverse these MTX-induced abnormalities to a healthy condition. Whey is a protein complex found in milk and is suggested as a food supplement with several health advantages. The biological contents of whey protein such as beta-lactoglobulin,

lactoferrin, alpha-lactalbumin, immunoglobulins, and glycomacropptide exhibit a range of immune-stimulating properties. Whey can also be used as an antihypertensive, anticancer, hypolipidemic, antibacterial, antiviral, antioxidant, and chelating agent. The principal mechanism by which whey protein is considered to exert its benefits is by intracellular conversion of the amino acid cysteine to GSH, a potent cellular antioxidant (29). Cysteine contains the sulfhydryl group, which acts as a reducing agent in the prevention of oxidative stress. GSH is more efficient as an antioxidant in its reduced form (30). In this study, whey administration to the MTX group decreased the MDA levels in the brain and small intestine tissue and increased the GSH levels as well as SOD and GST activity. While this cause no change in brain NO levels, it decreased NO levels in the small intestine tissue of the control groups. The brain had a more complex protein band profile than the small intestine, but the bands were more visible. The reason for the sharper protein band is related to the brain tissue's protein content. Although the protein bands in the small intestine were not clearly visible, the reductions in protein bands caused by MTX were demonstrated to have been restored through the administration of whey protein.

The limitation of this study is examining the effects of a single of a single dose of MTX determined in the experimental animal model. However, MTX is administered to patients in repeated doses, and the application time of whey proteins could also change in this case.

CONCLUSION

The study suggests that the whey proteins may have a therapeutic impact on the MTX-induced changes and oxidative stress in brain and small intestine tissues.

Ethics Committee Approval: This study was approved by the Clinical Research Ethics Committee of Marmara University Medical Faculty (26.05.2021-50.2021).

Peer-review: Externally peer-reviewed.

Author Contributions: Conception/Design of Study - T.T.A., G.S.; Data Acquisition - S.Y., E.T., G.G.S., B.G.G., E.D., D.O., G.S., T.T.A.; Performing experiments - S.Y., E.T., G.G.S., B.G.G., E.D., D.O., G.S., T.T.A.; Data Analysis/ Interpretation - S.Y., E.T., G.G.S., B.G.G., E.D., D.O., G.S., T.T.A.; Statistical Analyses - S.Y., E.T., G.G.S., B.G.G., E.D., D.O., G.S., T.T.A.; Drafting Manuscript - S.Y., E.T., G.G.S., B.G.G., E.D., D.O., G.S., T.T.A.; Critical Revision of Manuscript - S.Y., E.T., G.G.S., B.G.G., E.D., D.O., G.S., T.T.A.; Final Approval and Accountability - S.Y., E.T., G.G.S., B.G.G., E.D., D.O., G.S., T.T.A.

Conflicts of Interest: The authors declare no conflict of interest.

Financial Disclosure: The authors declare that this study has received no financial support.

REFERENCES

1. Hannoodee M, Mittal M. Methotrexate. StatPearls (Internet): StatPearls Publishing; 2021.

2. Letertre MP, Munjoma N, Wolfer K, Pechlivanis A, McDonald JA, Hardwick RN, et al. A two-way interaction between methotrexate and the gut microbiota of male sprague-dawley rats. *J Proteome Res* 2020; 19(8): 3326-39. [\[CrossRef\]](#)
3. Maeda T, Miyazono Y, Ito K, Hamada K, Sekine S, Horie T. Oxidative stress and enhanced paracellular permeability in the small intestine of methotrexate-treated rats. *Cancer Chemother Pharmacol* 2010; 65(6): 1117-23. [\[CrossRef\]](#)
4. Jahovic N, Şener G, Çevik H, Ersoy Y, Arbak S, Yeğen BÇ. Amelioration of methotrexate-induced enteritis by melatonin in rats. *Cell Biochem Funct.* 2004; 22(3): 169-78. [\[CrossRef\]](#)
5. Miyazono Y, Gao F, Horie T. Oxidative stress contributes to methotrexate-induced small intestinal toxicity in rats. *Scand J Gastroenterol* 2004; 39(11): 1119-27. [\[CrossRef\]](#)
6. Welbat JU, Naewla S, Pannangrong W, Sirichoat A, Arnanarochana A, Wigmore P. Neuroprotective effects of hesperidin against methotrexate-induced changes in neurogenesis and oxidative stress in the adult rat. *Biochem Pharmacol* 2020; 178: 114083. [\[CrossRef\]](#)
7. Vezmar S, Becker A, Bode U, Jaehde U. Biochemical and Clinical Aspects of Methotrexate Neurotoxicity. *Chemotherapy* 2003; 49(1-2): 92-104. [\[CrossRef\]](#)
8. Townsend DM, Tew KD. The role of glutathione-S-transferase in anti-cancer drug resistance. *Oncogene* 2003; 22(47): 7369-75. [\[CrossRef\]](#)
9. Tsurui K, Kosakai Y, Horie T, Awazu S. Vitamin A protects the small intestine from methotrexate-induced damage in rats. *J Pharmacol Exp Ther* 1990; 253(3): 1278-84.
10. Horie T, Matsumoto H, Kasagi M, Sugiyama A, Kikuchi M, Karasawa C, et al. Protective effect of aged garlic extract on the small intestinal damage of rats induced by methotrexate administration. *Planta Med* 1999; 65(06): 545-8. [\[CrossRef\]](#)
11. Corrochano AR, Arranz E, De Noni I, Stuknytė M, Ferraretto A, Kelly PM, et al. Intestinal health benefits of bovine whey proteins after simulated gastrointestinal digestion. *J Funct Foods* 2018; 49: 526-35. [\[CrossRef\]](#)
12. Sprong RC, Schonewille AJ, van der Meer R. Dietary cheese whey protein protects rats against mild dextran sulfate sodium-induced colitis: role of mucin and microbiota. *J Dairy Sci* 2010; 93(4): 1364-71. [\[CrossRef\]](#)
13. Akal C. Benefits of Whey Proteins on Human Health. Chapter 28; In: Watson RR, Collier RJ, Preedy VR, editors. *Dairy in Human Health and Disease Across the Lifespan*: Academic Press; 2017. p. 363-72. [\[CrossRef\]](#)
14. Aykaç A, Becer E, Özbeyli D, Şener G, Başer K. Protective effects of *Origanum onites* essential oil in the methotrexate-induced rat model: role on apoptosis and hepatotoxicity. *Rec Nat Prod* 2020; 14(6): 395-404. [\[CrossRef\]](#)
15. Shimizu Y, Hara H, Hira T. Glucagon-like peptide-1 response to whey protein is less diminished by dipeptidyl peptidase-4 in comparison with responses to dextrin, a lipid and casein in rats. *Br J Nutr* 2021; 125(4): 398-407. [\[CrossRef\]](#)
16. Ledwozyw A, Michalak J, Stepień A, Kadziolka A. The relationship between plasma triglycerides, cholesterol, total lipids and lipid peroxidation products during human atherosclerosis. *Clin Chim Acta* 1986; 155(3): 275-83. [\[CrossRef\]](#)
17. Mylroie AA, Collins H, Umbles C, Kyle J. Erythrocyte superoxide dismutase activity and other parameters of copper status in rats ingesting lead acetate. *Toxicol Appl Pharmacol* 1986; 82(3): 512-20. [\[CrossRef\]](#)
18. Habig WH, Jakoby WB. Assays for differentiation of glutathione S-transferases. *Methods Enzymol* 1981; 77: 398-405. [\[CrossRef\]](#)
19. Miranda KM, Espey MG, Wink DA. A rapid, simple spectrophotometric method for simultaneous detection of nitrate and nitrite. *Nitric Oxide* 2001; 5(1): 62-71. [\[CrossRef\]](#)
20. Beutler E. *Red cell metabolism: a manual of biochemical methods*. 3rd edition, New York, 1984.
21. Laemmli UK. Cleavage of structural proteins during the assembly of the head of bacteriophage T4. *Nature* 1970; 227(5259): 680-5. [\[CrossRef\]](#)
22. Faul F, Erdfelder E, Lang A-G, Buchner A. G* Power 3: A flexible statistical power analysis program for the social, behavioral, and biomedical sciences. *Behav Res Methods* 2007; 39(2): 175-91. [\[CrossRef\]](#)
23. Leeanantsaksiri P. Gut-Brain Axis Association to the Brain Function. *Inter J Formal Sci: Curr Future Res Trend* 2022; 13(1): 167-81.
24. Nayak RR, Alexander M, Deshpande I, Stapleton-Gray K, Rimal B, Patterson AD, et al. Methotrexate impacts conserved pathways in diverse human gut bacteria leading to decreased host immune activation. *Cell Host Microbe* 2021; 29(3): 362-77.e11. [\[CrossRef\]](#)
25. Modun D, Giustarini D, Tsikas D. Nitric oxide-related oxidative stress and redox status in health and disease. *Oxidative Medicine and Cellular Longevity*, Hindawi; 2014. [\[CrossRef\]](#)
26. Lanas A. Role of nitric oxide in the gastrointestinal tract. *Arthritis Res Ther* 2008; 10 Suppl 2(Suppl 2): S4. [\[CrossRef\]](#)
27. Dijkstra G, van Goor H, Jansen P, Moshage H. Targeting nitric oxide in the gastrointestinal tract. *Curr Opin Investig Drugs* 2004; 5: 529-36.
28. Cronstein BN, Aune TM. Methotrexate and its mechanisms of action in inflammatory arthritis. *Nat Rev Rheumatol* 2020; 16(3): 145-54. [\[CrossRef\]](#)
29. Keri Marshall N. Therapeutic applications of whey protein. *Altern Med Rev* 2004; 9(2): 136-56.
30. Walzem R, Dillard C, German JB. Whey components: millennia of evolution create functionalities for mammalian nutrition: What we know and what we may be overlooking. *Crit Rev Food Sci Nutr* 2002; 42(4): 353-75. [\[CrossRef\]](#)

Assessing E-Cadherin and Connexin 43 Gene Expressions in Colorectal Cancer

Saime Surmen¹ , Soykan Arikan^{2,3} , Ozlem Timirci Kahraman⁴ , Mustafa Gani Surmen¹ ,
Canan Cacina⁴ , Ilhan Yaylim⁴ 

¹Department of Molecular Medicine, Hamidiye Institute of Health Sciences, University of Health Sciences, Istanbul, Turkiye

²Department of General Surgery, Istanbul Training and Research Hospital, Istanbul, Turkiye

³General Surgery/Surgical Oncology Clinic, Cam and Sakura City Hospital, Istanbul, Turkiye

⁴Department of Molecular Medicine, Aziz Sançar Institute of Experimental Medicine, Istanbul University, Istanbul, Turkiye

ORCID ID: S.S. 0000-0002-7748-0757; S.A. 0000-0001-7132-6161; O.T.K. 0000-0002-2641-5613; M.G.S. 0000-0001-9084-7528; C.C. 0000-0001-7911-4390; I.Y. 0000-0003-2615-0202

Cite this article as: Surmen S, Arikan S, Timirci Kahraman O, Surmen MG, Cacina C, Yaylim I. Assessing E-cadherin and connexin 43 gene expressions in colorectal cancer. *Experimed* 2022; 12(3): 119-24.

ABSTRACT

Objective: Dysregulation of cellular adhesion is one of the main mechanisms responsible for tumor initiation, proliferation, and survival. E-cadherin is a cell adhesion molecule associated with tissue invasion and metastasis in most epithelial cancers. Gap junctions are known as small molecular channels that allow communication between neighboring cells and consist of connexin molecules. Connexin 43 (Cx43) is a gap junction protein that plays a central role in cell-cycle regulation and has an important function in carcinogenesis. The present study aimed to evaluate the expression levels of E-cadherin and Cx43 in colorectal cancer patients using clinical and prognostic parameters.

Materials and Methods: The quantitative real-time polymerase chain reaction (qRT-PCR) method was utilized to characterize the expression patterns of the E-cadherin and Cx43 genes in tumor and adjacent non-tumoral colon tissues from 32 colorectal cancer patients. Analysis of gene expression data was carried out using the delta-CT method.

Results: The results show the expression level of Cx43 to decrease 14-fold in tumor tissue compared to normal tissue ($p < 0.05$). However, the study could find no significant difference with regard to E-cadherin expression.

Conclusion: The research provides valuable clues to the elucidation of tumor development and metastatic processes for further studies.

Keywords: Colorectal cancer, cell adhesion, connexin 43, E-cadherin, qRT-PCR

INTRODUCTION

Colorectal cancer (CRC) is a multifaceted and therapeutically challenging disease. The development, progression, and metastatic spread of CRC have been comprehensively investigated in terms of characterizing the genomic and proteomic alterations of the disease in different populations. The different stages of tumor onset and progression involve irregularities in both intracellular and intercellular communication networks. The systematic literature review by Nalewajska et al. (1) emphasized targeting the connexins that connect the cytoplasm

of neighboring cells to possibly be an effective way for treating specific tumors.

Gap junction intercellular communication (GJIC) is defined as intercellular channels allowing small molecules (e.g., ions, metabolites and second messengers such as cAMP) to pass between cells and has an important role in apoptosis, cell growth, cell cycle control, tissue differentiation, and homeostasis. GJIC consists of the protein subunits of connexin, which has more than 20 isoforms. As the most commonly known isoform of the family member, connexin 43 (Cx43) has been named according to its molecular weight and is encoded by the GJA1 gene (1, 2).

Corresponding Author: Ilhan Yaylim **E-mail:** iyaylim@istanbul.edu.tr

Submitted: 16.10.2022 **Revision Requested:** 03.11.2022 **Last Revision Received:** 09.11.2022 **Accepted:** 21.11.2022 **Published Online:** 27.12.2022



Content of this journal is licensed under a Creative Commons Attribution-NonCommercial 4.0 International License.

Studies have shown a negative correlation to exist between Cx43 expression and tumor growth. Accordingly, both the cell surface and cytoplasmic Cx43 may have a suppressive role in tumor growth through their C-termini tails that bind to signaling molecules (3). However, some reports have stated increased Cx43 expression to appear to be associated with poor prognosis and poor patient survival (2). According to the STRING database, the GJA1 protein, which interacts with tight junction protein ZO-1, vinculin, and E-cadherin, is involved in the regulation of cell-cell junction assembly and cell migration (Figure 1). Decreased Cx43 and E-cadherin expression have been reported to contribute to the presence of primary gastric cancer, while concurrent elevated expression levels of these proteins can contribute to metastatic lymph nodes (4). The cytoplasmic domains of Cx43 may interact with cell adhesion molecules that play a pivotal role in invasion and metastatic processes. E-cadherin is a member of the calcium dependent cell adhesion molecules that are thought to have a crucial role in maintaining epithelial tissue integrity (5). Researchers have demonstrated a loss of the E-cadherin protein to be related to a decrease in intercellular adhesion. Accordingly, the aberrant E-cadherin expression triggers the invasion and metastasis abilities of cells (6, 7). Several alterations of regulation that have adverse impacts on E-cadherin can arise during the progression of cancer in ways such as decreased transcriptional activities, mutations, and promoter methylation (8). Previous reports have highlighted E-cadherin expression to be downregulated in certain cancers (e.g., gastric, colorectal, cervical, and breast) (9-11). In addition, decreased expressions of Cx43 and E-cadherin in lung cancer cells have been reported to be significantly correlated with one another (12).

When considering the relation between gap junctions and adhesion molecules, the expression patterns of these two genes may play a significant role in tissue homeostasis, differentiation, and proliferation and thereby contribute to carcinogenesis. The aberrant expression of Cx43 or E-cadherin has been reported in different cancer types (1, 6). However, the relationship between E-cadherin and Cx43 expressions in colon cancer has yet to be fully explained, with studies evaluating both genes together still being needed. This study aims to examine both the mRNA expression of Cx43 and E-cadherin in tissue samples from colorectal cancer patients and to evaluate their relationship with the patients' clinical and pathological features.

MATERIALS AND METHODS

Case Information

The study protocol was approved from the ethical committee of the Istanbul University Faculty of Medicine (16.04.2012/665). For expression analysis, 32 tumor and 32 non-tumor tissues were obtained from CRC patients at the surgery clinic of Istanbul Research and Education Hospital between 2012 and 2013. A written informed consent was obtained from each participant. These CRC patients had not undergone any chemotherapy, radiotherapy, or other treatment pre-operation.

RNA Isolation

All tissue samples were collected as fresh frozen within 30 min after tissue resection. PureLink RNA Mini Kit was used according to standard kit protocol for total RNA isolation (Ambion-Life Technologies™, USA). Tissue samples of approximately 100 mg in 1000 µL TRIzol Reagent (Ambion-Life Technologies™, USA) were homogenized with RNase-free mortars and pestles. The lysate (up to 0.6 mL) was transferred to the spin cartridge and the binding, washing, and elution steps were applied in that order. Following RNA purification, DNase I digestion procedure was performed to remove DNA contamination. The purity and concentration of all RNA products were detected by measuring the absorbance ratio at A260/A280 nm. Finally, the purified RNA yields were stored at -80 °C until further analysis.

cDNA Synthesis

High-capacity RNA to cDNA master mix was used for single-stranded cDNA synthesis (Applied Biosystems, Foster City, CA, USA). The cDNA conversion procedure was as follows: 20 µL of the reaction mix was added to the master mix and diluted to an RNA ratio of 1:5. The mix was run on a PCR thermal cycler under optimized conditions (Step 1: 25 °C for 10 min; Step 2: 42 °C for 2 h; Step 3: 85 °C for 5 min).

Quantitative Real-time Polymerase Chain Reaction (qRT-PCR)

The expression levels of Cx43 (UniGene ID Hs.700699) and E-cadherin (UniGene ID Hs.461086) were evaluated by qRT-PCR using the Stratagene Mx3005P System (Agilent Technologies, USA). cDNA products were amplified using TaqMan Gene Expression Master Mix (Applied Biosystem, CA, USA) and

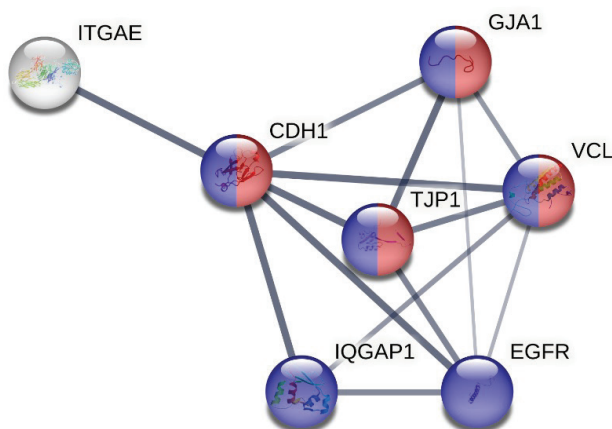


Figure 1. Protein interaction network. GJA1: Gap junction alpha-1 protein; CDH1: Cadherin-1; TJP1: Tight junction protein ZO-1; VCL: Vinculin. Purple and red colors indicate proteins involved in cell-cell junction assembly and the regulation of cell migration, respectively.

TaqMan gene expression assay, which includes the target gene-specific primer and probe sets (Applied Biosystems, Foster City, CA, USA). TaqMan assays with the following IDs were purchased: Assay ID Hs01023894_m1 for the E-cadherin and Assay ID Hs00748445_s1 for Cx43. As a result of the literature review, β -actin (Assay ID: Hs99999903_m1) was chosen as a housekeeping gene to normalize the levels of Cx43 and E-cadherin. The PCR mix was prepared in a final volume of 20 μ L, and the cycling conditions were as follows: hot start 10 min at 95 °C, next 40 cycles of 15 s at 95 °C, and lastly 1 min at 60 °C. All reactions were run in duplicate. The quantification results have been evaluated using the comparative CT method, in which $2^{-\Delta\Delta CT}$ values were calculated.

Statistical Analyses

Statistical analyses were examined using the program IBM SPSS version 20.0 for Windows (IBN Corp., Armonk, NY, USA). Data were given as means and standard deviations (\pm SD).

Statistical comparisons of the differences between the two groups were carried out with the Mann-Whitney U test, with a $p < 0.05$ being assumed to show statistical significance.

RESULTS

This study compared the obtained gene expression data from the tumor tissue and corresponding normal tissue of the same patients. Of the 32 patients, 24 (75%) were male and eight (25%) were female, with the mean age of all CRC patients being 63.19 ± 10.55 years (range= 36-80 years). The

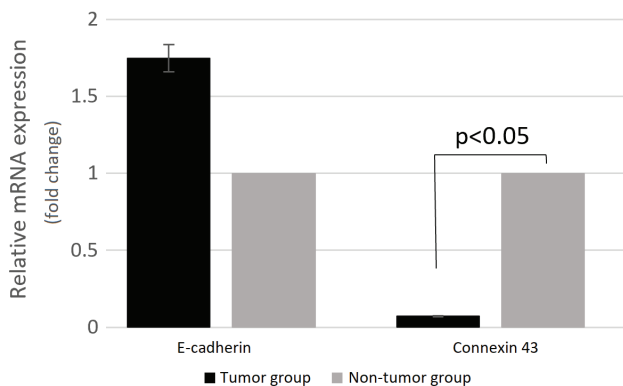


Figure 2. Comparison of E-cadherin and Cx43 mRNA levels in tumor and non-tumor tissues from CRC patients.

patients' clinicopathologic characteristics were determined according to the American Joint Committee on Cancer (AJCC) 7th TNM stage. The distribution of tumor stages I and II among all patients was 18.8%, with 81.3% having tumors in an advanced stage. The patients were equally distributed according to the presence of metastasis. A total of 43.8% of patients had no lymph node involvement, while 37.5% had N1, and 18.8% had N2. When evaluating the specimens histopathologically, 25.9% of the tumors were noticed to be poorly differentiated, 55.6% to be moderately differentiated, and 18.5% to be well differentiated. The majority of tumor was localized to the sigmoidal colon (44.8%), with other tumors being located in the right colon (24.1%), in the left colon (3.4%), in the transverse colon (10.3%), in the cecum (3.4%), and in the rectum (13.8%).

The mRNA expression levels of the Cx43 and E-cadherin genes were observed to change in tumor tissue compared to the normal tissue of patients diagnosed with CRC (Figure 2), with the expression of Cx43 having significantly decreased 14-fold in the tumor tissue ($p < 0.05$). Although the study has found no statistically significant difference in expression levels of the E-cadherin gene, a 1.75-fold increase was found in the expression of the E-cadherin gene within tumor tissue ($p > 0.05$). When comparing tumor stages, the study detected E-cadherin expression to have increased 1.33-fold in advanced-stage tumors ($p > 0.05$). The expression patterns of both genes are summarized in Table 1. In addition, when evaluating the expression of both Cx43 and E-cadherin in terms of clinical pathological features such as tumor stage, lymphatic invasion, differentiation grade, and metastasis, no significant differences were found ($p > 0.05$). The relations between the pathologic features of the tumor samples and expression patterns of two genes are given in Table 2.

DISCUSSION

The spread of cancer cells beyond the origin of the tumor to surrounding tissues and organs is tightly associated with molecules involved in cell-cell and cell-matrix adhesion (13). In this process, epithelial tissue cells acquire the mesenchymal phenotype through loss of adhesion and increased migration. To the best of the study's knowledge, epithelial mesenchymal transition (EMT) contributes to cancer progression and promotes cells to metastasize in removed regions. In many types of epithelial cancers, several steps are involved in

Table 1. Fold change value of E-cadherin and Cx43 genes in tumor tissue compared to normal tissue.

Gene	Log2 Fold Change	95%CI	Fold Change	95%CI	p Value	Fold Regulation
Cx43	-3.816	(-5.643- -3.058)	0.071	(0.02-0.12)	0.039*	-14.052
E-Cadherin	0.807	(0.88-1.56)	1.750	(0.54-2.96)	0.336	1.750

*p values less than 0.05 denoted statistical significance.

Table 2. Fold change value of Cx43 and E-cadherin genes according to clinical pathological features.

		Log2 Fold Change	95%CI	Fold Change	P-value
E-Cadherin Gene Expression	Distant Metastases	-0.049	(-2,556 - 0,81)	0.966	p>0.05
	Lymphatic Invasion	-0.125	(-2.058-0.669)	0.9171	
	Differentiation	0.177	(-5.058-0.97)	1.131	
	Grade	-0.418	(-4.321-0.536)	0.748	
Cx43 Gene Expression	Distant Metastases	1.658	(-0.64 - -2.503)	3.157	
	Lymphatic Invasion	1.183	(-0.971-2.014)	2.2726	
	Differentiation	-4.921	(-16.609- -0.234)	0.330	
	Grade	0.820	(-16.609-1.933)	1.766	

*p values less than 0.05 denoted statistical significance.

tumor metastasis, including the genetic reprogramming and transitioning of cancer cells (14). E-cadherin is a tumor suppressor gene and one of the crucial molecular markers that trigger EMT. In addition, E-cadherin expression has been associated with cell migration, poor differentiation, and metastasis (15,16). This study has investigated the mRNA levels of E-cadherin and Cx43 genes in 32 patients with CRC. Unlike most previous studies, this one has shown E-cadherin gene expression to be 1.75 times higher in tumor tissue compared to normal tissue. However, this difference detected in tumor tissue was not statistically significant. Two studies were published by El-Bahrawy et al. (17, 18) revealed the mRNA levels of E-cadherin and catenin (α, β, γ) to increase in colorectal carcinomas compared to non-neoplastic mucosa. The reason for the increased expression of E-cadherin has been attributed to its accumulation in the cytoplasm.

Furthermore, this study has also evaluated the relation between the E-cadherin expression levels and the pathological parameters of CRC patients. Although a negative correlation does exist between E-cadherin expression and pathological features (i.e., stage, distant metastasis and grade of differentiation) of colorectal carcinoma patients, it was not statistically significant ($p > 0.05$). The literature contains various results regarding the impact of E-cadherin expression on CRC progression. Mădălina Palaghia et al. (19) conducted a study on 65 patients who'd undergone a colectomy for CRC and concluded E-cadherin expression abnormalities to be an important marker of tumor aggressiveness and spread potential. Gao et al. (20) showed the expression of E-cadherin to be lower in colon cancerous tissues during metastasis. In addition, one meta-analysis showed the downregulation of E-cadherin to be significantly related to poor prognosis in Asian patients with CRC (21). Previous studies have led to the conclusion that decreased E-cadherin expression is associated with invasive colorectal cancer (16).

In addition to epithelial tissue integrity, E-cadherin also plays a pivotal role in ensuring communication between adherent cells by means of Cx43. E-cadherin facilitates the formation of gap junctions by playing a role in the cell membrane transport of Cx43 (22, 23). A positive correlation has been reported to exist between E-cadherin and Cx43 protein expression with regard to gastric, lung, and colorectal cancer (4, 12, 24). Xu et al. (12) showed the pattern of E-cadherin expression to be related to Cx43 expression levels and reported overexpression of Cx43 to induce E-cadherin expression in lung cancer cells. Their same study also found concurrent reduction of expressions in both genes to be associated with lymph node metastasis. Similarly, Tang et al. (4) showed the concurrent reduction of Cx43 and E-cadherin in primary gastric cancer using immunostaining. In addition, Zhao et al. (25) investigated E-cadherin and Cx43 with regard to both mRNA and protein levels in Chinese patients with non-small cell lung cancer (NSCLC). They found decreased E-cadherin and Cx43 protein levels to correlate to NSCLC progression, clinic stage, and lymph node metastasis. However, E-cadherin and Cx43 mRNA levels significantly increased with regard to advanced tumor stages, poor differentiation, and lymph node metastasis. These results reveal the need to explain the cause of variability in mRNA and protein levels.

According to the literature review, Cx43 acts as a tumor suppressor, with its low expression contributing to colon carcinogenesis. Sirnes et al. (26) examined the clinical significance of the irregular expression of Cx43 in CRC tissue and cell lining. They reported Cx43 to regulate cell growth negatively in HT29 colon cancer cells by inducing apoptosis. Decreased expression of Cx43 was related to overall survival for patients in the early stages. Furthermore, the study results implied that Cx43 may also cause different clinical effects according to its subcellular localization. The present study has found Cx43 expression to be reduced 14-fold in tumors compared to adjacent normal tissue, and this data

was statistically significant. Ismail et al. (27) examined Cx43 expression by immunohistochemical analysis and reported downregulation of Cx43 to be significantly related to the histological features of the colon cancer. The current study observed an increase in Cx43 expression for patients in advanced stage who were metastasis-positive; however, the differences were not significant. Kanczuga-Koda et al. (24) examined the correlation among the expressions of E-cadherin, β -catenin, and the three Cx proteins (i.e., Cx26, Cx32, and Cx43) in colorectal cancer tissues using immunohistochemistry. According to their study, a significant positive correlation was found between E-cadherin and Cx26 in the total patient group and between E-cadherin and Cx43 protein expression levels in patients with metastatic lymph nodes and tumors in advanced stages. Despite the decrease in Cx43 expression found in the current study, this was not correlated with E-cadherin expression. In addition, when examining the mRNA levels of Cx43 and E-cadherin in terms of tumor size, lymph node involvement, remote metastasis, and differentiation, the study found no significant differences.

CONCLUSION

Although a wide range of data is available about the linkage between E-cadherin and Cx43 protein levels, less is known about the mRNA levels for both E-cadherin and Cx43 genes with respect to colorectal cancer. Our study findings suggest that Cx43 may play a crucial role in the progression of colorectal cancer. However, the current study also has limitations. It evaluated only the mRNA expressions of these genes and not protein levels through the immunohistochemical method or western blotting. The cause of the malfunction of E-cadherin and Cx43 remains unclear. This is a preliminary study for CRC, which has a complex pathogenesis. Thus, a large-scale study that comprehensively investigates mRNA and protein levels is needed. In future studies in particular, revealing the relationship between E-cadherin and Cx43, which help maintain cell-to-cell communications, will contribute to the clear elucidation of tumor development and metastasis.

Ethics Committee Approval: The study protocol was approved from the ethical committee of the Istanbul University Faculty of Medicine (16.04.2012/665).

Peer-review: Externally peer-reviewed.

Author Contributions: Conception/Design of Study - I.Y., O.T.K., S.S.; Data Acquisition - S.S., S.A.; Performing experiments - O.T.K., S.S., M.G.S., C.C.; Data Analysis/Interpretation - S.S.; Drafting Manuscript - I.Y., C.C., M.G.S., O.T.K., S.A.; Critical Revision of Manuscript - I.Y., S.S., S.A., O.T.K., M.G.S., C.C.; Final Approval and Accountability - I.Y.

Conflicts of Interest: The authors declare no conflict of interest.

Financial Disclosure: This study was funded by The Scientific Research Projects Coordination Unit of Istanbul University (Project number:24522).

REFERENCES

1. Nalewajska M, Marchelek-Mysłiwiec M, Opara-Bajerowicz M, Dziedziejko V, Pawlik A. Connexins-therapeutic targets in cancers. *Int J Mol Sci* 2020; 21(23): 9119. [\[CrossRef\]](#)
2. Bonacquisti EE and Nguyen J. Connexin 43 (Cx43) in cancer: Implications for therapeutic approaches via gap junctions. *Cancer Lett* 2019; 442: 439-44. [\[CrossRef\]](#)
3. Wu JI and Wang LH. Emerging roles of gap junction proteins connexins in cancer metastasis, chemoresistance and clinical application. *J Biomed Sci* 2019; 26(1): 8. [\[CrossRef\]](#)
4. Tang B, Peng ZH, Yu PW, Yu G, Qian F. Expression and significance of Cx43 and E-cadherin in gastric cancer and metastatic lymph nodes. *Med Oncol* 2011; 28(2): 502-8. [\[CrossRef\]](#)
5. Gall TM, Frampton AE. Gene of the month: E-cadherin (CDH1). *J Clin Pathol* 2013; 66(11): 928-32. [\[CrossRef\]](#)
6. Kaszak I, Witkowska-Piłaszewicz O, Niewiadomska Z, Dworecka-Kaszak B, Ngosa Toka F, Jurka P. Role of cadherins in cancer-A review. *Int J Mol Sci* 2020; 20: 7624. [\[CrossRef\]](#)
7. Techasen A, Loilome W, Namwat N, Khuntikeo N, Puapairoj A, Jearanaikoon P, Saya H, Yongvanit P. Loss of E-cadherin promotes migration and invasion of cholangiocarcinoma cells and serves as a potential marker of metastasis. *Tumour Biol* 2014; 35(9): 8645-52. [\[CrossRef\]](#)
8. Bex G, van Roy F. Involvement of members of the cadherin superfamily in cancer. *Cold Spring Harb Perspect Biol* 2009; 1(6): a003129. [\[CrossRef\]](#)
9. He X, Chen Z, Jia M, Zhao X. Downregulated E-cadherin expression indicates worse prognosis in Asian patients with colorectal cancer: evidence from meta-analysis. *PLoS One* 2013; 8(7): e70858. [\[CrossRef\]](#)
10. Peng J, Qi S, Wang P, Li W, Song L, Liu C, et al. F. Meta-analysis of downregulated E-cadherin as a poor prognostic biomarker for cervical cancer. *Future Oncol* 2016; 12(5): 715-26. [\[CrossRef\]](#)
11. Shargh SA, Sakizli M, Khalaj V, Movafagh A, Yazdi H, Hagigatjou E, et al. Downregulation of E-cadherin expression in breast cancer by promoter hypermethylation and its relation with progression and prognosis of tumor. *Med Oncol* 2014; 31(11): 250. [\[CrossRef\]](#)
12. Xu HT, Li QC, Zhang YX, Zhao Y, Liu Y, Yang ZQ, et al. Connexin 43 recruits E-cadherin expression and inhibits the malignant behaviour of lung cancer cells. *Folia Histochem Cytobiol* 2008; 46(3): 315-21. [\[CrossRef\]](#)
13. Gassmann P, Haier J. The tumor cell-host organ interface in the early onset of metastatic organ colonisation. *Clin Exp Metastasis* 2008; 25(2): 171-81. [\[CrossRef\]](#)
14. Thiery JP, Acloque H, Huang RY, Nieto MA. Epithelial-mesenchymal transitions in development and disease. *Cell* 2009; 139(5): 871-90. [\[CrossRef\]](#)
15. Na TY, Schecterson L, Mendonsa AM, Gumbiner BM. The functional activity of E-cadherin controls tumor cell metastasis at multiple steps. *Proc Natl Acad Sci USA*. 2020; 117(11): 5931-37. [\[CrossRef\]](#)
16. Tzanou E, Peschos D, Batistatou A, Charalabopoulos A, Charalabopoulos K. The E-cadherin adhesion molecule and colorectal cancer. A global literature approach. *Anticancer Res* 2008; 28(6A): 3815-26.
17. El-Bahrawy MA, Poulson R, Jeffery R, Talbot I, Alison MR. The expression of E-cadherin and catenins in sporadic colorectal carcinoma. *Hum Pathol* 2001; 32(11): 1216-24. [\[CrossRef\]](#)
18. El-Bahrawy MA, Talbot IC, Poulson R, Jeffery R, Alison MR. The expression of E-cadherin and catenins in colorectal tumours from familial adenomatous polyposis patients. *J Pathol* 2002; 198(1): 69-76. [\[CrossRef\]](#)

19. Palaghia M, Mihai C, Lozneau L, Ciobanu D, Trofin AM, Rotariu A, et al. E-cadherin expression in primary colorectal cancer and metastatic lymph nodes. *Rom J Morphol Embryol* 2016; 57(1): 205-9.
20. Gao M, Zhang X, Li D, He P, Tian W, Zeng B. Expression analysis and clinical significance of eIF4E, VEGF-C, E-cadherin and MMP-2 in colorectal adenocarcinoma. *Oncotarget* 2016; 7(51): 85502-14. [\[CrossRef\]](#)
21. He X, Chen Z, Jia M, Zhao X. Downregulated E-cadherin expression indicates worse prognosis in Asian patients with colorectal cancer: evidence from meta-analysis. *PLoS One* 2013; 8(7): e70858. [\[CrossRef\]](#)
22. Chakraborty S, Mitra S, Falk MM, Caplan SH, Wheelock MJ, Johnson KR, et al. E-cadherin differentially regulates the assembly of Connexin43 and Connexin32 into gap junctions in human squamous carcinoma cells. *J Biol Chem* 2010; 285(14):10761-76. [\[CrossRef\]](#)
23. Govindarajan R, Chakraborty S, Johnson KE, Falk MM, Wheelock MJ, Johnson KR, et al. Assembly of connexin43 into gap junctions is regulated differentially by E-cadherin and N-cadherin in rat liver epithelial cells. *Mol Biol Cell* 2010; 21(23): 4089-107. [\[CrossRef\]](#)
24. Kanczuga-Koda L, Wincewicz A, Fudala A, Abrycki T, Famulski W, Baltaziak M, et al. E-cadherin and β -catenin adhesion proteins correlate positively with connexins in colorectal cancer. *Oncol Lett* 2014; 7(6): 1863-70. [\[CrossRef\]](#)
25. Zhao JQ, Sun FJ, Liu SS, Yang J, Wu YQ, Li GS, et al. Expression of connexin 43 and E-cadherin protein and mRNA in non-small cell lung cancers in Chinese patients. *Asian Pac J Cancer Prev* 2013; 14(2): 639-43. [\[CrossRef\]](#)
26. Sirnes S, Bruun J, Kolberg M, Kjenseth A, Lind GE, Svindland A, et al. Connexin43 acts as a colorectal cancer tumor suppressor and predicts disease outcome. *Int J Cancer* 2012; 131(3): 570-81. [\[CrossRef\]](#)
27. Ismail R, Rashid R, Andrabi K, Parray FQ, Besina S, Shah MA, et al. Pathological implications of Cx43 down-regulation in human colon cancer. *Asian Pac J Cancer Prev* 2014; 15(7): 2987-91. [\[CrossRef\]](#)

A Histological Evaluation of the Effect of Ghrelin on Wound Healing in Rats

Esin Ak¹ , Kerime Ulusoy-Dag¹ , Feriha Ercan² , Ahmet Corak¹ 

¹Department of Basic Medical Science, Faculty of Dentistry, Marmara University, Istanbul, Turkiye

²Department of Histology and Embryology, Faculty of Medicine, Marmara University, Istanbul, Turkiye

ORCID ID: E.A. 0000-0002-3467-7808; K.U.D. 0000-0002-6122-3019; F.E. 0000-0003-2339-5669; A.Ç. 0000-0003-3840-5145

Cite this article as: Ak E, Ulusoy Dag K, Ercan F, Corak A. A histological evaluation of the effect of ghrelin on wound healing in rats. *Experimed* 2022; 12(3): 125-9.

ABSTRACT

Objective: This study aimed to investigate the potential effects of ghrelin on wound healing.

Materials and Methods: Sprague-Dawley rats were divided into 3 groups: Control ($n = 8$), wound-saline (W+S, $n = 16$), and wound-ghrelin (W+Gr, $n = 16$). A wound was created on the cervical back region of rats using an 8 mm biopsy punch tool in the W+S and W+Gr groups. Either saline (1 mL/kg) or ghrelin (10 ng/kg) was administered intraperitoneally each day to the rats in the non-control groups after the onset of the wound. Rats from the W+S and W+Gr groups were euthanized on the 7th ($n = 8$ from each group) and 14th day ($n = 8$ from each group) of the experiment. The histopathological score was evaluated statistically using one-way analysis of variance and Tukey's multiple comparison tests.

Results: The rats euthanized from the W+S group on day 7 (subgroup W+S₇) showed degenerated epidermis, no hair follicles, presence of granulation tissue, inflammatory cell infiltration, vasocongestion, and increased collagen fibers in dermis. However, all these histopathological findings significantly decreased in the rats euthanized from the W+Gr group on day 7 (subgroup W+Gr₇) compared to the W+S₇ group ($p < 0.05$). The W+S₁₄ group showed thick epidermis, a few hair follicles, angiogenesis, and increased collagen fibers in the dermis. Additionally, the histopathological findings decreased significantly in the W+Gr₁₄ group compared to W+S₁₄ group ($p < 0.05$).

Conclusion: Based on the statistical analysis of the histological findings, the ghrelin treatment appears to have a beneficial effect on wound healing.

Keywords: Wound healing, ghrelin and histology

INTRODUCTION

Wound healing is a complicated process involving crosstalk between cells, growth factors, and inflammatory cytokines in three distinct phases: Inflammation, new tissue formation, and remodeling. The first step is inflammation and takes place within the first 3 days after the injury with the invasion of neutrophils and macrophages. The proliferative phase starts after the inflammatory phase with the formation of new blood vessels (neoangiogenesis), the production of connective tissue, and contraction of the wound at this stage. Lastly, the remodeling phase starts usually from day 21 up to 2 years after the injury, during which the collagen fibers

reorganize and the tissue remodels and matures, resulting an overall increase in tensile strength (1).

Improper wound healing is one of the most important factors affecting the convalescence of patients worldwide. Currently, the removal of necrotic tissue, changing of bandages, and local and systemic antibiotic therapies have been commonly used to treat patients with improper wound healing (2). The administration of topical growth factors coupled with several biomaterials have also been reported for overcoming this issue (3).

Ghrelin is a gastrointestinal peptide hormone and has a central function in balancing feeding, adiposity, body

Corresponding Author: Esin Ak **E-mail:** esinakdr@gmail.com

Submitted: 20.10.2022 **Revision Requested:** 15.11.2022 **Last Revision Received:** 20.11.2022 **Accepted:** 22.11.2022 **Published Online:** 30.12.2022



Content of this journal is licensed under a Creative Commons Attribution-NonCommercial 4.0 International License.

weight, and glucose metabolism (4). Ghrelin has been identified as the endogenous ligand for the growth hormone secretagogue receptor (GHSR) 1a and to stimulate the secretion of growth hormones from the pituitary gland (5). Ghrelin has also been shown to be able to prevent organ injury and to improve survival in irradiated rats with severe sepsis by decreasing the induction of inflammatory mediators (6, 7). This study aims to histologically examine the role of parenteral ghrelin treatment with regard to wound healing in rats.

MATERIALS AND METHODS

Animals

The study obtained 40 adult Sprague-Dawley rats (200-250 g) from Marmara University, School of Medicine's Animal Laboratory. The rats were kept under standard laboratory conditions, including a 12-h light/dark cycle and constant temperature ($22 \pm 2^\circ\text{C}$) and humidity (45–65%). They were also given Ad Lib standard pellet food and tap water. All procedures were carried out in accordance with the *Guide for the Care and Use of Laboratory Animals* (8). This study procedure was approved by the relevant animal experimental local ethics committee of Marmara University (protocol no. 10.2008.mar).

Experimental Design

The Sprague-Dawley rats were divided into 3 groups: Control (C; $n = 8$), wound+saline (W+S; $n = 16$), and wound-ghrelin (W+Gr; $n = 16$), with no treatment being applied to the control group. The W+S group was given saline (1 mL/kg, intraperitoneal (i.p.)) and the W+Gr group was given ghrelin (10 ng/kg, i.p., Sigma, G8903, St Louis, MO) once a day immediately after the wound was created (9). In both the W+S and W+Gr groups, rats were euthanized on the 7th (subgroups W+S₇ & W+Gr₇, $n = 8$ for each) and 14th (subgroups W+S₁₄ and W+Gr₁₄, $n = 8$ for each) days following the wound creation. At the end of the experiment, skin samples were removed for histological examination.

Wound Creation Protocol

After the application of general anesthesia of ketamine hydrochloride (100 mg/kg, i.p.) and xylazine hydrochloride (10 mg/kg, i.p.), the dorsal area of the animals was shaved and cleaned with 70% alcohol. The wound was created using an 8 mm biopsy punch tool on the shaved cervical back region (10).

Histological Analysis

Skin samples were fixed in a 10% formaldehyde solution and underwent a routine process for embedding in paraffin wax. To identify histological degeneration, 5–6 μm thick paraffin sections were stained with hematoxylin and eosin. Skin sections were also stained with Gomori's one-step trichrome for collagen distribution. All stained sections were evaluated under a light microscope (Olympus BX51, Tokyo, Japan) and photographed with a digital camera (Olympus DP72, Tokyo, Japan). Each sample was examined over at least five microscopic areas for histopathologic scoring. Epithelial and hair follicular degeneration, inflammatory cell infiltration, vasocongestion, and collagen density were assessed for scoring criteria (11). Each criterion was scored semi-quantitatively as

follows: 0 = none, 1 = mild, 2 = moderate, and 3 = severe, with the maximum total score being 12.

Statistical Analyses

Statistical analysis was performed using the program GraphPad Prism 9 (GraphPad Software, San Diego, USA). After confirming the normal distribution of the data using the Kolmogorov–Smirnov test, the one-way analysis of variance (ANOVA) test and Tukey's multiple comparison tests were applied, with the data being presented as mean \pm standard deviation (SD) and a $p < 0.05$ indicating a significant difference.

RESULTS

The histological investigation of skin samples taken from the control groups of rats showed regular epidermis and dermis with a distribution of collagen fibers and hair follicles. The W+S₇ subgroup was observed to have degenerated epidermis, no hair follicles, severe inflammatory cell infiltration and vasocongestion, the presence of granulation tissue, and increased collagen fibers in the dermis. The presence of granulation tissue in the sections from the saline-treated rats indicated the healing to have been impaired, albeit with no obvious retardation in wound healing. The W+S₁₄ subgroup was observed to have a thick epidermis, moderate inflammatory cell infiltration and vasocongestion, a small number of hair follicles, angiogenesis, and increased collagen fibers in the dermis. The W+Gr₇ subgroup showed degenerated epidermis, no hair follicles, moderate inflammatory cell infiltration and vasocongestion, the presence of granulation tissue, and increased collagen fibers in the dermis. The W+Gr₁₄ subgroup had a regular epidermis, a small number of hair follicles, angiogenesis, mild inflammatory cell infiltration and vasocongestion, and increased collagen fibers in the dermis (Figure 1).

In the semiquantitative analyses, significantly higher histopathological scores were observed for both the saline- and ghrelin-treated wound healing groups compared to the control group. However, the 7-day treatment with ghrelin showed a reduced total histopathological score in the W+Gr₇ subgroup (8.93 ± 0.90) compared to the W+S₇ group (10.19 ± 0.96 ; $p = 0.028$). Moreover, a similar benefit regarding the total histopathological score was also obtained for the 14-day treatment with ghrelin in the W+Gr₁₄ subgroup (4.31 ± 0.53) compared to the W+S₁₄ subgroup (5.50 ± 0.92 , $p = 0.04$; Figure 2).

DISCUSSION

The study's outcomes demonstrate the ghrelin treatment to have had a prominent impact on the healing process of the rats who'd had wounds induced with the biopsy punch. From a histological point of view, both the 7- and 14-day treatments with ghrelin resulted in significant improvements in the rats' histopathological score compared to the saline treatment. The histopathological findings of the study suggest the potential anti-inflammatory role of ghrelin treatment in the initial stage of wound healing.

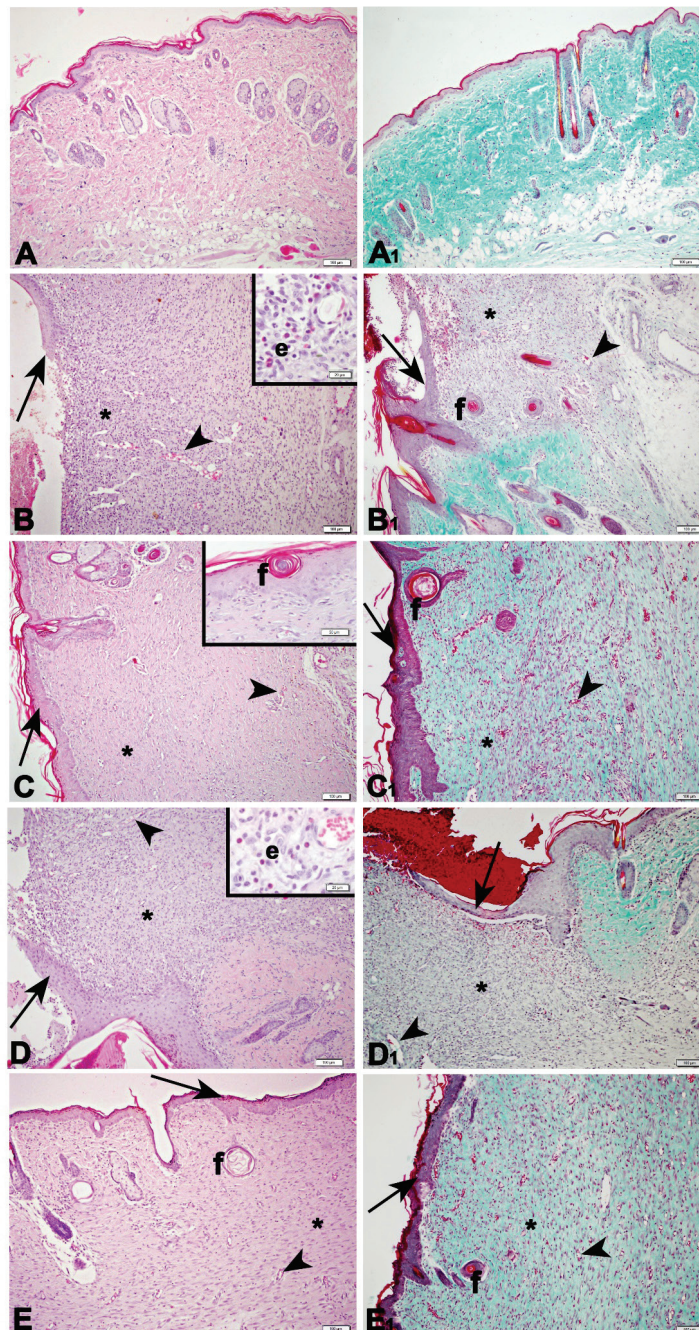


Figure 1. Representative photomicrographs of skin tissue samples from the experimental groups. The control group (A and A1) shows regular epidermis, collagen fibers and hair follicles in the dermis. The W+S₇ subgroup (B and B1) shows degenerated epidermis morphology (arrow), inflammatory cell infiltration (e, B), localized increase in collagen fibers (asterisks), hair follicles (f, B1), and the formation of blood vessels (arrowhead) in the dermis. The W+S₁₄ subgroup (C and C1) shows thick epidermis morphology (arrow), localized increase in collagen fibers (asterisks), hair follicles (f, C), formation of new blood vessels (arrowhead) in the dermis. The W+S₇ subgroup (D and D1) shows degenerated epidermis morphology (arrow), inflammatory cell infiltration (e, D), localized increase in collagen fibers (asterisks), formation of new blood vessels (arrowhead) in the dermis. The W+S₁₄ subgroup (E and E1) shows quite a regular epidermis morphology (arrow), localized increase in collagen fibers (asterisks), hair follicles (f), and formation of new blood vessels (arrowhead) in the dermis. A-E: Hematoxylin and eosin staining; A1-E1: Gomori's one-step trichrome staining. Original magnifications are x100 and x400 (inset).

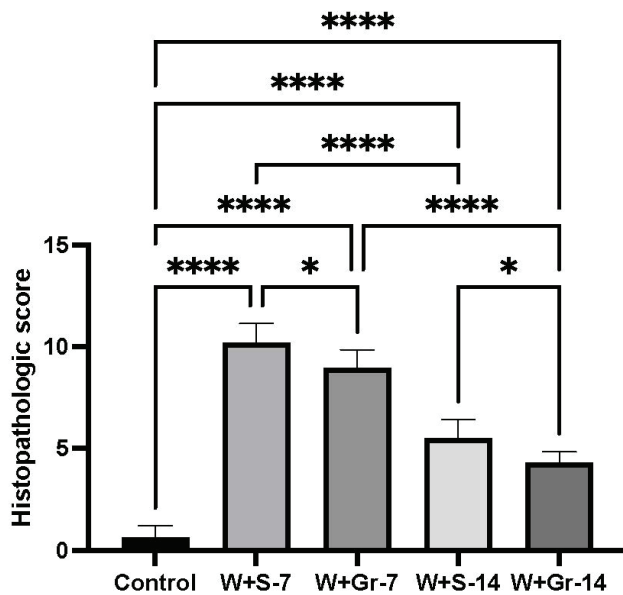


Figure 2. The histopathologic score of the experimental groups. * $p < 0.05$; **** $p < 0.0001$ shows a significant difference between the experimental groups. Each group consists of 8 rats.

Improper wound healing is an important health issue that affects patient convalescence and is known to occur under many clinical conditions such as surgical procedures, diabetes mellitus, and cancer. Apart from being a health problem, delayed wound healing also increases the cost of hospitalization. Moreover, it leads to social isolation, especially for patients with diabetes and obesity (12, 13). The inability to re-epithelialize has been known to dictate the development of improper healing and to lead to chronic non-healing wounds. The disturbance of re-epithelization paves the way for the impairment of the normal phases of wound healing in an orderly and timely manner (14). The current study found the ghrelin treatment in the W+Gr₁₄ subgroup to have improved epidermis and hair follicle formation in wound healing compared to the W+S₁₄ subgroup.

In addition to inducing the release of growth hormones, ghrelin has multiple functions such as modulating the secretion of several growth factors and affecting the mechanisms of cellular migration, proliferation, and angiogenesis (15). Moreover, recent evidence has suggested ghrelin as having anti-inflammatory and antioxidant effects, with its potential role in oxygen free radical homeostasis being claimed to facilitate the healing process in regard to several tissues (14-18). Sehrlı et al.'s study (19) showed ghrelin to have a prominent role in recovering from burn-induced skin and remote organ damage in rats due to its anti-inflammatory and antioxidant effects. The decreased histopathological score and decrease of inflammatory cell infiltration in the ghrelin-treated wound 7- and 14-day subgroups show ghrelin to possibly regulate wound healing by regulating inflammation through the inhibition of oxidative stress.

The impact of the ghrelin treatment on wound healing has been studied with regard to several tissue types. Cieszkowski et al.'s study (20) showed ghrelin treatment (i.p) to increase mucosal blood flow and decrease local inflammation by reducing mucosal interleukin-1 β concentrations in an experimental rat model with mucosal gingival damage. In addition to oral mucosa, ghrelin has been shown to also exert a positive effect on healing other parts of the gastrointestinal tract. Lyra, Jr. et al.'s study (21) studied the potential role of postoperative intraperitoneal ghrelin therapy (i.p, 23 μ g/kg/d) on healing colonic anastomosis. They concluded that, due to its anti-inflammatory and antioxidizing effects, ghrelin had increased both the resistance and the hydroxyproline content of colonic anastomosis postoperatively. The current study has found a 14-day ghrelin treatment (10 ng/kg, i.p.) on wound healing to have quite improved the epidermis and dermis injury through epithelial and hair follicle regeneration, collagen distribution, and a decrease of inflammatory cell infiltration.

Several studies have also examined the impact of ghrelin on skin wounds. Liu et al.'s study (22) investigated the protective role of ghrelin with regard to impaired wound healing from radiation exposure. Histologically, they found ghrelin (100 nmol/kg and 200 nmol/kg) to decrease the average wound healing time by about 3-5 days and ghrelin to also boost the expression of vascular endothelial growth factor (VEGF) and transforming growth factor β (TGF- β) through higher collagen content and enhanced neovascularization. The current study found both the 7- and 14-day application of ghrelin (10 ng/kg, i.p.) to improve the biopsy punch wound healing by modulating the inflammatory response.

This study has a few limitations. It did not biochemically examine the anti-inflammatory or antioxidant parameters regarding the skin samples, which may have helped to understand ghrelin's role in wound healing with detail.

CONCLUSION

Based on the statistical analysis of this study's histological findings, ghrelin may have a potential role in accelerating the healing of wounds through its potential anti-inflammatory effects.

Ethics Committee Approval: This study procedure was approved by the relevant animal experimental local ethics committee of Marmara University (protocol no. 10.2008.mar).

Peer-review: Externally peer-reviewed.

Author Contributions: Conception/Design of Study - A.C., K.U.D., E.A.; Data Acquisition - A.C., E.A.; Data Analysis/Interpretation - E.A., F.E.; Drafting Manuscript - E.A., F.E Critical Revision of Manuscript - F.E., A.C., K.U.D., E.A.; Final Approval and Accountability - E.A., F.E., K.U.D., A.C.

Conflicts of Interest: The authors declare no conflict of interest.

Financial Disclosure: The authors declare that this study has received no financial support.

REFERENCES

1. Gurtner GC, Werner S, Barrandon Y, Longaker MT. Wound repair and regeneration. *Nature* 2008; 453(7193): 314-21. [\[CrossRef\]](#)
2. Lipsky BA, Berendt AR, Cornia PB, Pile JC, Peters EJ, Armstrong DG, et al. 2012 Infectious Diseases Society of America clinical practice guideline for the diagnosis and treatment of diabetic foot infections. *Clin Infect Dis* 2012; 54(12): e132-73. [\[CrossRef\]](#)
3. Demidova-Rice TN, Hamblin MR, Herman IM. Acute and impaired wound healing: pathophysiology and current methods for drug delivery, part 2: Role of growth factors in normal and pathological wound healing: therapeutic potential and methods of delivery. *Adv Skin Wound Care* 2012; 25(8): 349-70. [\[CrossRef\]](#)
4. Tschop M., Smiley D.L., Heiman M.L. Ghrelin induces adiposity in rodents. *Nature* 2000; 407(6806): 908-13. [\[CrossRef\]](#)
5. Müller TD, Nogueiras R, Andermann ML, Andrews ZB, Anker SD, Argente J, et al. Ghrelin. *Mol Metab* 2015; 4(6): 437-60. [\[CrossRef\]](#)
6. Shah KG, Wu R, Jacob A, Blau SA, Ji Y, Dong W, et al. Human ghrelin ameliorates organ injury and improves survival after radiation injury combined with severe sepsis. *Mol Med* 2009; 15(11-12): 407-14. [\[CrossRef\]](#)
7. Liu C, Huang J, Li H, Yang Z, Zeng Y, Liu J, et al. Ghrelin accelerates wound healing through GHS-R1a-mediated MAPK-NF- κ B/GR signaling pathways in combined radiation and burn injury in rats. *Sci Rep* 2016; 6: 27499. [\[CrossRef\]](#)
8. National Research Council (US) Committee for the Update of the Guide for the Care and Use of Laboratory Animals. *Guide for the Care and Use of Laboratory Animals*. 8th ed. Washington (DC): National Academies Press (US); 2011.
9. Işeri SO, Sener G, Yüksel M, Contuk G, Cetinel S, Gedik N, et al. Ghrelin against alendronate-induced gastric damage in rats. *J Endocrinol* 2005; 187(3): 399-406. [\[CrossRef\]](#)
10. Sidhu GS, Thaloor D, Singh AK, Raghunath PN, Maheshwari RK. Enhanced biosynthesis of extracellular matrix proteins and TGF- β 1 by polyinosinic-polycytidylic acid during cutaneous wound healing in vivo. *J Cell Physiol* 1996; 169(1): 108-14. [\[CrossRef\]](#)
11. Aktop, S, Çaliskan Ak E, Emekli-Alturfan E, Gocmen G, Atali O, Ercan F, et al. Effects of ankaferd blood stopper on soft tissue healing in warfarin-treated rats. *Int J Med. Res Health Sci* 2016; 5(5): 200-9.
12. Zarchi K, Martinussen T, Jemec GB. Wound healing and all-cause mortality in 958 wound patients treated in-home care. *Wound Repair Regen* 2015; 23(5): 753-8. [\[CrossRef\]](#)
13. Sen CK. Human Wounds and Its Burden: An Updated Compendium of Estimates. *Adv Wound Care (New Rochelle)* 2019; 8(2): 39-48. [\[CrossRef\]](#)
14. Rousselle P, Braye F, Dayan G. Re-epithelialization of adult skin wounds: Cellular mechanisms and therapeutic strategies. *Adv Drug Deliv Rev* 2019; 146: 344-65. [\[CrossRef\]](#)
15. Kojima M, Hosoda H, Date Y, Nakazato M, Matsuo H, Kangawa K. Ghrelin is a growth-hormone-releasing acylated peptide from the stomach. *Nature* 1999; 402(6762): 656-60. [\[CrossRef\]](#)
16. Ersahin M, Toklu HZ, Erzik C, Cetinel S, Akakin D, Velioglu-Oğünç A, et al. The anti-inflammatory and neuroprotective effects of ghrelin in subarachnoid hemorrhage-induced oxidative brain damage in rats. *J Neurotrauma* 2010; 27(6): 1143-55. [\[CrossRef\]](#)
17. Warzecha Z, Ceranowicz D, Dembinski A, Ceranowicz P, Cieszkowski J, Kuwahara A, et al. Ghrelin accelerates the healing of cysteamine-induced duodenal ulcers in rats. *Med Sci Monit* 2012; 18(5): BR181-7. [\[CrossRef\]](#)
18. Ceranowicz P, Warzecha Z, Dembinski A, Sendur R, Cieszkowski J, Pawlik WW, et al. Treatment with ghrelin accelerates the healing of acetic acid-induced gastric and duodenal ulcers in rats. *J Physiol Pharmacol* 2009; 60(1): 87-98.
19. Sehirli O, Sener E, Sener G, Cetinel S, Erzik C, Yeğen BC. Ghrelin improves burn-induced multiple organ injury by depressing neutrophil infiltration and the release of pro-inflammatory cytokines. *Peptides* 2008; 29(7): 1231-40. [\[CrossRef\]](#)
20. Cieszkowski J, Warzecha Z, Ceranowicz P, Ceranowicz D, Kusnierz-Cabala B, Pedziwiatr M, et al. Therapeutic effect of exogenous ghrelin in the healing of gingival ulcers is mediated by the release of endogenous growth hormone and insulin-like growth factor-1. *J Physiol Pharmacol* 2017; 68(4): 609-17.
21. Lyra Junior HF, de Lucca Schiavon L, Rodrigues IK, Couto Vieira DS, de Paula Martins R, Turnes BL, et al. Effects of ghrelin on the oxidative stress and healing of the colonic anastomosis in rats. *J Surg Res* 2019; 234: 167-77. [\[CrossRef\]](#)
22. Liu C, Hao Y, Huang J, Li H, Yang Z, Zeng Y, et al. Ghrelin accelerates wound healing in combined radiation and wound injury in mice. *Exp Dermatol* 2017; 26(2): 186-93. [\[CrossRef\]](#)

Preoperative Screening for COVID-19: Results from a Clinical Diagnostic Laboratory

Okan Aydogan¹ , Ezgi Gozun Saylan² , Ozlem Guven³ , Akif Ayaz² , Turkan Yigitbasi² 

¹Department of Medical Microbiology, Istanbul Medipol University School of Medicine, Istanbul, Turkiye

²Istanbul Medipol University Genetic Diseases Assessment Center, Istanbul, Turkiye

³Department of Medical Microbiology, Istanbul Medipol University International School of Medicine, Istanbul, Turkiye

ORCID ID: O.A. 0000-0001-7275-8724; E.G.S. 0000-0001-8964-7131; O.G. 0000-0003-0394-8772; A.A. 0000-0001-6930-7148; T.Y. 0000-0002-0675-1839

Cite this article as: Aydogan O, Gozun Saylan E, Guven O, Ayaz A, Yigitbasi T. Preoperative screening for COVID-19: Results from a clinical diagnostic laboratory. *Experimed* 2022; 12(3): 130-3.

ABSTRACT

Objective: The study aimed to determine what proportion of Turkiye's preoperative patient population has tested positive for COVID-19 and to ascertain whether the increasing or decreasing trend in the numbers of positive preoperative patients resembles the general population of Turkiye during the same period.

Materials and Methods: The study cohort involved of the 14,776 patients from various services between January 1-December 31, 2021 who needed preoperative COVID-19 test reports. The patient's SARS-CoV-2 RNA's were detected with real-time polymerase chain reaction (RT-PCR) technique.

Results: SARS-CoV-2 RT-PCR positivity was detected in 422 (2.86%) patients, of which 59.72% ($n = 252$) were female and 40.28% ($n = 170$) were male; their mean age was 40.2 years. Of the 422 positive cases, 84.12% were young adults (18-65 years), and 9% were middle-aged (66-79 years). Positive cases involving those under the age of 18 were found to account for 5.22% ($n = 22$) of the total. The highest positivity rate was observed in April 2021 at 8.28% of all test requests, while the lowest positivity rate was observed in June 2021, at 0.36% of all test requests. The highest positivity rate of April was followed by March (5.07%), October (4.74%), and August (3.13%).

Conclusion: In conclusion, the COVID-19 RT-PCR positivity rate in the series was detected as 2.85% in preoperative patients over the one-year period. Monthly positivity rates in screening results are consistent with the number of cases seen in the general population.

Keywords: COVID-19, preoperative screening, SARS-CoV-2, RT-PCR

INTRODUCTION

An ongoing outbreak of the Coronavirus Disease 2019 (COVID-19) was first identified in Wuhan, China at the end of 2019. As the spread of the novel coronavirus accelerated, person-to-person transmission in homes and hospitals as well as the intercity spread of the severe acute respiratory syndrome-Coronavirus-2 (SARS-CoV-2) also occurred. COVID-19 was named by the World Health Organization (WHO), which also declared it as a pandemic on March 11, 2020. On that same date, Turkiye reported its first confirmed COVID-19 case. As of October 2022, more than 620 million cases and more than 6.55 million deaths have

been reported worldwide, with COVID-19 having caused more than 16.5 million cases and more than 101,000 deaths in Turkiye (1, 2). Due to the lack of information about the prognosis of the disease in the early days of the pandemic, all operations and surgical interventions that were not life-threatening were postponed indefinitely. Although the widespread use of vaccines that largely prevent the disease and the necessary medical precautions being taken in hospitals bring comfort that operations can be performed safely, determining which of the patients will undergo surgery are SARS-CoV-2 carriers is essential. According to the Royal Australasian College of Surgeons, the common opinion is that each patient should be tested with real-time polymerase chain reaction (RT-PCR) before surgery,

Corresponding Author: Ozlem Guven **E-mail:** oguven@medipol.edu.tr

Submitted: 18.10.2022 **Revision Requested:** 04.11.2022 **Last Revision Received:** 18.11.2022 **Accepted:** 23.11.2022 **Published Online:** 30.12.2022



Content of this journal is licensed under a Creative Commons Attribution-NonCommercial 4.0 International License.

due to the prevalence of asymptomatic and presymptomatic patients being unknown (3, 4). The COVID-19 RT-PCR test is performed approximately 48 hours before the operation date on preoperative patients, as suspected COVID-19 patients may pose a risk to healthcare workers and other patients. In Turkiye, RT-PCR tests for COVID-19 and chest computed tomography (CT) are requested when deemed necessary before even planning the operation. During the pandemic, treating all patients as if they were COVID-19 positive and using personal protective equipment that would limit contact with patients has been important (5).

The aims of this study were to determine the SARS-CoV-2 positivity rates of preoperative patients and whether the increasing and decreasing trends in the numbers of positive preoperative patients resembled the overall general population of Turkiye during the same period.

MATERIALS AND METHODS

The study included 14,776 patients whose clinical cases had been sent with a preoperative COVID-19 RT-PCR test request from various services between January 1-December 31, 2021.

Viral nucleic acid isolation was performed by treating the nasopharyngeal swab, bronchoalveolar lavage, and tracheal aspirate samples with the viral nucleic acid buffer (vNAT). SARS-CoV-2 RNAs were isolated from the Bio-Speedy® SARS-CoV-2 Double Gene RT-qPCR and Bio-Speedy® SARS-CoV-2 Triple Gene RT-qPCR kits (Bioeksen R&D Technologies Ltd., Istanbul, Turkiye) and performed in Bio-Rad CFX96 and Bio-Rad DX RT-PCR systems (Hercules, CA, USA).

This study was carried out with the approval of the Istanbul Medipol University Clinical Research Ethics Committee (Decision No. 156 dated February 17, 2022), and permission for the study was obtained from the Scientific Study Platform of the Ministry of Health (Application No: 2022-02-04T12_58_42 dated February 5, 2022). Next, the study retrospectively reviewed the results of the preoperative screening tests (all specialties & services) performed between January 1-December 31, 2021 at the Laboratory of Istanbul Medipol University Genetic Diseases Assessment Center. Because many patients have undergone multiple tests, having the study clearly make the unit of analysis the number of patients tested for COVID-19 instead of the number of tests performed is important.

RESULTS

The study includes $n = 14,776$ patients, of whom 9,933 (67.2%) are female and 4,843 (32.8%) are male. Of these, 422 (2.86%) patients tested positive with the RT-PCR test, 252 (59.72%) female, and 170 (40.28%) male, with an overall mean age of 40.2 years. According to age classification, 84.12% of patients were young adults (18-65 years), and 9% were middle-aged (66-79). The positivity rate for those under 18 years was 5.22% ($n = 22$; Table 1).

Table 1. Demographic features of the patients.

	ALL CASES n = 14,776	RT-PCR (+) n = 422 (%)
Gender		
Female	9,933 (67.2%)	170 (40.28%)
Male	4,843 (32.8%)	252 (59.72%)
Age		
0-2	69 (0.47%)	4 (0.95%)
3-11	360 (2.44%)	8 (1.9%)
12-17	175 (1.18%)	10 (2.37%)
18-65	12,544 (84.89%)	355 (84.12%)
18-30	4,406 (29.82%)	104 (24.64%)
31-40	3,647 (24.68%)	113 (26.78%)
41-50	2,346 (15.87%)	78 (18.48%)
51-65	2,145 (14.52%)	60 (14.22%)
66-79	1,338 (9%)	38 (9%)
80+	290 (%1.66)	7 (%1.66)

The highest percentage of positivity was found to be 8.28% in April 2021, while the lowest was found to be 0.36% in June. The positivity rates for 2021 by month are shown in Figure 1.

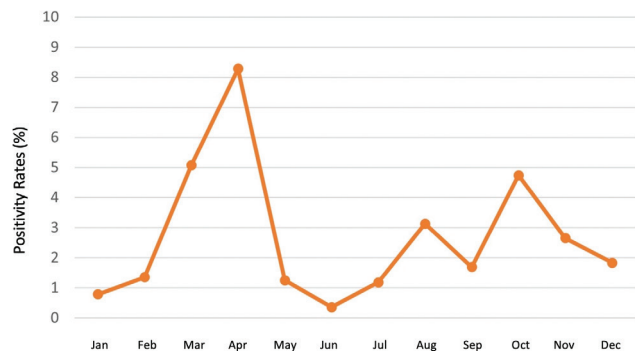


Figure 1. The positivity rates by month.

DISCUSSION

Preoperative risk assessment of patients has always been critical for safe surgical practice and has become even more important for the safety of patients and healthcare workers during the COVID-19 pandemic. Routine preoperative testing for COVID-19 helps distinguish patients with asymptomatic infections. This study detected a 2.85% SARS-CoV-2 RT-PCR positivity rate for 14,776 preoperative patients. Studies have shown surgical procedures to be associated with worse clinical outcomes, increased postoperative complications, and mortality with regard to SARS-CoV-2 positive patients (6-9). Current knowledge of SARS-CoV-2 and COVID-19 during the pandemic is rapidly being renewed and is based on limited available data. Therefore, local and global data,

protocols, and guidelines should be updated and published frequently (10).

Due to the low sensitivity of detecting SARS-CoV-2 during the incubation period using RT-PCR test, preoperative self-isolation and quarantining patients 14 days before the planned surgery date has been reported to be able to possibly eliminate the risk of it going undetected (11). However, the general opinion is that RT-PCR test screening should be performed to manage patients' pre-surgery (3, 4). Although the use of serological tests are frequently used for screening in the diagnosis of infectious agents, their use for SARS-CoV-2 infections is a controversial point, with complementary and epidemiological studies thought to be needed regarding the diagnosis of COVID-19 (12). In the report from 11 health institutions in the USA state of North Carolina, all patients were reported to have been preoperatively screened for SARS-CoV-2, with the opinion being that serological tests are unnecessary for asymptomatic patients. Of the tests that were run, these 11 institutions reported that 53,745 tests came back positive at rates ranging from 0.31% to 1.35% of the overall tests. Similarly, in the USA state of Florida, 85 (1.2%) RT-PCR tests were found to be positive out of 7,213 preoperative patients (7,13). Hendrickson et al. (14) performed SARS-CoV-2 screening with RT-PCR on 3,794 preoperative patients with a reported positivity rate of 0.69%. A study conducted in the USA state of Texas during the peak era of positive cases (May-June 2020) found positive RT-PCR results in 51 (1.4%) of the 3,563 preoperative patients (15).

SARS-CoV-2 RT-PCR positivity rates for preoperative patients are closely related to their treatment service, comorbidities, age, case rates in their region, and date. A study conducted in England reported the frequency of false negatives before orthopedic surgery to have been quite low (1:1,400) and the risk of death after infection to have been even lower (1:7,000). In addition, positive test rates were found to be higher in younger patients. Singer et al. showed asymptomatic COVID-19 positivity to have been detected in 0.13% of 4,739 preoperative patients, with the positive tested patients being under 60 years of age and the rate tends to increase as age decreases (16). Other studies have also reported higher positivity rates among younger patients (17-19). Similarly, the two groups with the highest positivity rates among the patients included in our study were the 31-40 (26.8%) and 18-30 (24.6%) age groups.

The present study should be viewed in light of several limitations. Firstly, despite having a large number of patients ($n = 14,776$), the hospital department information and clinical features of the patients are inaccessible, and secondly, this is a retrospective study.

In conclusion, the average rate of SARS-CoV-2 RT-PCR positivity among the preoperative patients studied here over a one-year period was not found to be high based on the course of the outbreak among the general population. However, peak periods were shown to be able to occur among preoperative patients.

Scientific Presentation: The study was presented as a poster presentation at the 22nd Turkish Society of Clinical Microbiology and Infectious Diseases Congress on March 9-12, 2022.

Ethics Committee Approval: This study was approved by the Clinical Research Ethics Committee of Istanbul Medipol University (Date: 17.02.2022, Decision Number: 156).

Peer-review: Externally peer-reviewed.

Author Contributions: Conception/Design of Study - O.A., E.G.Ş., Ö.G., A.A., T.Y.; Data Acquisition - O.A., E.G.Ş.; Data Analysis/Interpretation - O.A., E.G.Ş., Ö.G., A.A., T.Y.; Writing Manuscript - O.A., E.G.Ş., Ö.G., A.A., T.Y.; Critical Review: O.A., E.G.Ş., Ö.G., A.A., T.Y.

Conflicts of Interest: The authors declare no conflict of interest.

Financial Disclosure: The authors have no conflict of interest to declare.

REFERENCES

1. World Health Organization Coronavirus (COVID-19) Dashboard. Available from: URL: <https://covid19.who.int/> Access Date: October 2022.
2. T.C. Sağlık Bakanlığı. Türkiye'deki Güncel Durum. Available from: URL: <https://covid19.saglik.gov.tr/> Access Date: October 2022.
3. Guidelines on the Preoperative Diagnostic Workup for COVID-19. A rapid review commissioned by Royal Australasian College of Surgeons. Available from URL: www.surgeons.org/-/media/Project/RACS/surgeons-org/files/news/covid19-information-hub/Guidelines-on-the-Preoperative-Diagnostic-Workup-forCOVID-19.pdf
4. Çimen C, Keske Ş, Ergönül E. What is the 'new normal' in surgical procedures in the era of COVID-19? *Clin Microbiol Infect* 2021; 27: 16-8. [CrossRef]
5. Alkaya Solmaz F, Özcan MS, Özden ES, Balık O, Kırdemir P. operating room management and anesthetic approach in COVID-19 pandemic. *Med J SDU* 2021; 51: 125-31.
6. Bui N, Coetzer M, Schenning KJ, O'Glasser AY. Preparing previously COVID-19-positive patients for elective surgery: a framework for preoperative evaluation. *Perioper Med* 2021; 10: 1. [CrossRef]
7. Villa J, Pannu T, McWilliams C, Kizer C, Rosenthal R, Higuera C, et al. Results of preoperative screening for COVID-19 correlate with the incidence of infection in the general population -a tertiary care experience. *Hosp Pract* 2021; 49: 216-20. [CrossRef]
8. Nepogodiev D, Bhangu A, Glasbey JC, Li E, Omar OM, Simoes JF, et al. Mortality and pulmonary complications in patients undergoing surgery with perioperative SARS-CoV-2 infection: an international cohort study. *Lancet* 2020; 396: 27-38. [CrossRef]
9. Doglietto F, Vezzoli M, Gheza F, Lussardi GL, Domenicucci M, Vecchiarelli L, et al. Factors associated with surgical mortality and complications among patients with and without coronavirus disease 2019 (COVID-19) in Italy. *JAMA Surg* 2020; 155: 691-702. [CrossRef]
10. Heffernan DS, Evans HL, Huston JM, Claridge JA, Blake DP, May AK, et al. Surgical Infection Society Guidance for Operative and Peri-Operative Care of Adult Patients Infected by the Severe Acute Respiratory Syndrome Coronavirus-2 (SARS-CoV-2). *Surg Infect* 2020; 21: 301-8. [CrossRef]
11. Lother SA. Preoperative SARS-CoV-2 screening: Can it really rule out COVID-19? *Can J Anaesth* 2020; 67: 1321-6. [CrossRef]

12. Dinç HÖ, Özdemir YE, Alkan S, Güngördü Dalar Z, Gareayaghi N, Sirekbasan S, et al. SARS-CoV-2 ile ilgili farklı prensipli ticari antikor testlerinin COVID-19 hastalarındaki tanısal performanslarının değerlendirilmesi. Mikrobiyol Bul 2021; 55: 207-22. [\[CrossRef\]](#)
13. Weissler EH, Kibbe MR, Mann JWF, Caulfield H, Harr C, Hildreth AN, et al. Preoperative Screening for COVID-19. NC Med J 2021; 82: 85-6.
14. Hendrickson NR, Kesler K, DeMik DE, Glass NA, Watson MK, Ford BA, et al. Asymptomatic pre-operative COVID-19 screening for essential and elective surgeries: early results of universal screening at a midwestern academic medical center. Iowa Orthop J 2021; 41: 33-8.
15. Kothari AN, Trans AT, Caudle AS, Clemens MW, Katz MHG, Woodman SE, et al. Universal preoperative SARS-CoV-2 testing can facilitate safe surgical treatment during local COVID-19 surges. Br J Surg 2021; 27(108): e24-e26. [\[CrossRef\]](#)
16. Singer JS, Cheng EM, Murad DA, de St Maurice A, Hines OJ, Uslan DZ, et al. Low prevalence (0.13%) of COVID-19 infection in asymptomatic pre-operative/pre-procedure patients at a large, academic medical center informs approaches to perioperative care. Surgery 2020; 168: 980-6. [\[CrossRef\]](#)
17. Gutman MJ, Patel MS, Vannello C, Lazarus MD, Parvizi J, Vaccaro AR, et al. What was the prevalence of COVID-19 in asymptomatic patients undergoing orthopaedic surgery in one large united states city mid-pandemic? Clin Orthop Relat Res 2021; 479: 1691-9. [\[CrossRef\]](#)
18. Kader N, Clement ND, Patel VR, Caplan N, Banaszkiwicz P, Kader D. The theoretical mortality risk of an asymptomatic patient with a negative SARS-CoV-2 test developing COVID-19 following elective orthopaedic surgery. Bone Joint J 2020; 102-B: 1256-60. [\[CrossRef\]](#)
19. Aydoğan O, Gözün Şaylan E, Güven Ö, Ayaz A, Yiğitbaşı T. Prevalence of SARS-CoV-2 variants in COVID-19 positive patients. Klimik Derg 2022; 35(4): 220-3.

Determination of Bisphenol A and Phthalate Levels in Wastewater Samples

Mansur Akcay¹ , Perihan Seda Ates-Kalkan² , Unsal Veli Ustundag³ , Ismail Unal⁴ , Derya Cansiz³ , Ebru Emekli-Alturfan⁵ , Ahmet Ata Alturfan⁶ 

¹Institute of Forensic Sciences, Istanbul University-Cerrahpaşa, Istanbul, Turkiye

²Department of Biochemistry, Istanbul Health and Technology University, Istanbul, Turkiye

³Department of Medical Biochemistry, Faculty of Medicine, Medipol University, Istanbul, Turkiye

⁴Institute of Health Sciences, Marmara University, Istanbul, Turkiye

⁵Department of Basic Medical Sciences, Faculty of Dentistry, Marmara University, Istanbul, Turkiye

⁶Department of Medical Biochemistry, Faculty of Medicine, Istanbul University-Cerrahpaşa, Istanbul, Turkiye

ORCID ID: M.A. 0000-0002-0529-017x; P.S.A.K. 0000-0002-4905-1912; Ü.V.Ü. 0000-0003-0804-1475; I.U. 0000-0002-8664-3298; D.C. 0000-0002-6274-801X; E.E.A. 0000-0003-2419-8587; A.AA. 0000-0003-0528-9002

Cite this article as: Akcay M, Ates-Kalkan PS, Ustundag UV, Unal I, Cansiz D, Emekli-Alturfan E, Alturfan A. Determination of bisphenol a and phthalate levels in wastewater samples. *Experimed* 2022; 12(3): 134-8.

ABSTRACT

Objective: The use of endocrine-disrupting chemicals (EDCs) such as bisphenol A (BPA) in plastics manufacturing, agriculture, livestock, and paint manufacturing increases daily. The water treated in wastewater treatment plants is used in many areas such as irrigation of parks and gardens, and reinforcement of underground water resources. However, whether the treatment process eliminates EDCs in wastewater is not exactly known, and determining this as well as the amounts of these chemicals in treated water are important in terms of protecting the environment and human health. The aim of the study was to determine BPA and phthalate concentrations in the influent and effluent flow samples obtained from wastewater treatment plants.

Materials and Methods: BPA and phthalate concentrations were measured in influent and effluent flow samples using the enzyme-linked immunosorbent assay (ELISA) method. BPA and phthalate measurements were performed as competitive measurements of BPA and total phthalates in samples using specific monoclonal antibodies.

Results: BPA and phthalate levels were measured respectively as 7.69 µg/L and 78.27 µg/L in the influent water samples and 3.17 µg/L and 25.56 µg/L in the effluent water samples. The concentration of BPA and phthalates in the effluent samples decreased significantly compared to the influent water samples.

Conclusion: This study is believed to shed light on the importance of monitoring BPA and phthalate concentrations in wastewater treatment plants and inspections for detecting other EDCs in wastewater.

Keywords: Wastewater, bisphenol A, phthalate, endocrine-disrupting chemical

INTRODUCTION

Although water is the most abundant molecule on Earth, humans are able to use only 0.3% of this water for drinking purposes. In addition, the need for potable water and utility water have increased daily due to rapid population growth, environmental pollution, global warming, and limited

fresh water resources. Therefore, urgent measures should be taken against environmental and water pollution, and new water sources should be sought. In this regard, being able to effectively remove toxic chemicals from wastewater is important for reuse in homes, agriculture, and industry (1-3). Around the globe, domestic water and safe water resources are rapidly diminishing and heading toward a

Corresponding Author: Ahmet Ata Alturfan **E-mail:** ataalturfan@gmail.com

Submitted: 21.10.2022 **Revision Requested:** 09.11.2022 **Last Revision Received:** 09.11.2022 **Accepted:** 23.11.2022 **Published Online:** 29.12.2022



Content of this journal is licensed under a Creative Commons Attribution-NonCommercial 4.0 International License.

point of depletion. Wastewater needs to be treated in order to minimize the possibility of contaminating drinking and utility water and using water resources more efficiently. Wastewater treatment is an applied physical, chemical, and biological recycling process for regaining some or all of the physical, chemical, and bacteriological properties of water that have been lost as a result of various uses (4, 5). After being subjected to appropriate treatment processes in wastewater treatment plants, water that registers non-toxic values by considering its biological characteristics can be used for irrigating agricultural areas, recreation areas, urban green spaces, car washes, toilets, heating pipes, concrete construction works, firefighting, and drinking water and can be assessed as an alternative to domestic water supplies (3, 6).

Endocrine-disrupting chemicals (EDCs) are exogenous agents that can mimic hormones and are responsible for maintaining homeostasis and regulating developmental processes; EDCs can also cause the production, release, transport, binding, and elimination of natural hormones in the body (7).

Agriculture, animal husbandry, industrial production, and technological developments have increased alongside the rapid human population growth around the world. These increases have caused rising for the use of EDCs such as bisphenol A (BPA), phthalates, atrazine, dioxins, diethylstilbesterol, and genistein in pesticides, herbicides, the manufacture of plastics, pharmaceuticals, the textile industry, livestock, the dye industry, and sewage systems.

EDCs cannot be completely removed through conventional wastewater treatment methods in treatment plants and thus spread to the environment. The literature has reported these EDCs to largely be fully non-degradable in treatment plants, to be detected in effluent flows, and to contaminate groundwater, potable water, and utility water supplies (7).

The aim of this study was to evaluate BPA and phthalate concentrations in the influent and effluent water samples from wastewater treatment plants. For this aim, BPA and total phthalate concentrations were measured using the enzyme-linked immunosorbent assay (ELISA) method in the influent and effluent water samples obtained from wastewater treatment plants. The BPA and phthalate levels were measured competitively with regard to BPA and total phthalate levels in specimens using specific monoclonal antibodies.

MATERIALS AND METHODS

The study has been carried out over seven influent and seven effluent water samples obtained from the Ataköy Advanced Biological Wastewater Treatment Plant at various times over a six-month period during the spring and summer. Influent water samples were obtained from the post-screen, pre-sand and grease trap sections by means of a sample collection device, while the effluent samples were obtained from a part of the facility close to the discharge point using a composite sampling device and then transferred to sterile 250 mL plastic

containers. These influent and effluent water samples were then delivered to the laboratory through a light-proof black bag. The samples were transferred to 50 mL centrifuge tubes and centrifuged at 3,000 rpm for 2 minutes to separate the supernatants. Next, the wastewater and treated wastewater samples were transferred to prewashed glass containers that had been autoclaved and rinsed with methanol. The wastewater samples were filtered through a 0.45 micrometer Sartorius Minisart® NML injector filter containing cellulose acetate. Subsequently, the glass containers were wrapped with aluminum foil and stored in a deep freezer at -80°C. One day prior to the day of the study, the samples were transferred to a refrigerator at +4°C (8).

BPA Measurement

The assay is based on the principle that BPA is directly recognized and bound by monoclonal antibodies (Ecologiena Supersensitive BPA ELISA Kit; Tokiwa Chemical Industries, Tokyo, Japan). Samples containing BPA and the BPA-enzyme mixture were added to each well of the microplate and competed for the binding sites of specific antibodies fixed on the surface of these wells.

BPA and the excess BPA-enzyme mixtures that didn't bind after the first treatment were washed away. The presence of BPA is detected by addition of a color solution. Enzyme-labeled BPA bound to the BPA antibody on the plate triggers the substrate to turn a specific color. After a certain incubation time, the reaction is stopped by addition of a diluted acid. The absorbance measured by the intensity of the color that formed varied inversely with the amount of BPA present in the samples. In this way, the BPA concentrations in the examined samples were determined.

The standard curve was obtained according to the absorbance value at 450 nm based on the BPA standards of known concentrations. The BPA concentration for each sample has been calculated using the absorbance values obtained from the standard curve.

Di-(2-ethylhexyl) Phthalate (DEHP) Measurement

Direct competitive ELISA (Abraxis Phthalates ELISA, Railroad Drive, Warminster, PA) method was used based on the detection of test phthalates with specific antibodies. Samples containing DEHP and a phthalate-enzyme mixture were added to the wells of the microplate. The phthalates present in the samples and the phthalate-enzyme mixture competed for the binding sites of the anti-phthalate antibodies in solution. The phthalate antibodies then bind with a second antibody (goat anti-rabbit) fixed to the surface of the wells.

After the washing step and the addition of the substrate solution, a blue color developed. The color reaction was stopped after 30 minutes by addition of a diluted acid. The intensity of the blue color was inversely proportional to the phthalate concentration in the sample.

A standard curve was obtained with respect to absorbance at 450 nm based on DEHP standards of known concentrations.

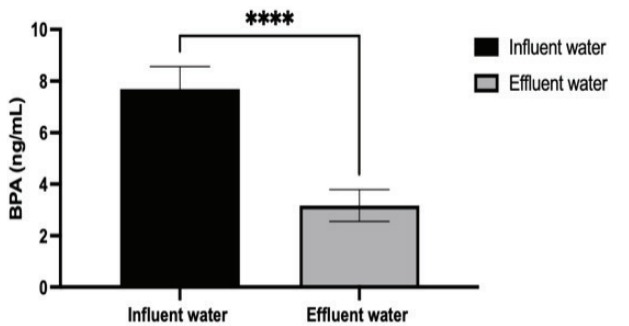
The DEHP concentration in each sample was calculated using the absorbance values obtained from the standard curve.

Statistical Analyses

GraphPad Prism 9.0 (GraphPad Software, San Diego, USA) was used for all statistical analyses. All data are expressed as a mean ± the standard deviation (SD). Unpaired t-test was used to evaluate the differences between the groups. The correlation between BPA and DEHP levels in the water samples were determined using the Pearson correlation analysis, with a value of $p < 0.05$ being considered statistically significant.

RESULTS

Figure 1 provides the BPA levels (ng/mL) in the influent and effluent water samples from the wastewater treatment plant. BPA levels decreased significantly in the effluent water samples when compared to the influent water samples ($p < 0.0001$). Figure 2 provides the DEHP levels in the influent and effluent water samples of the wastewater treatment plant. Significantly decreased DEHP levels were found in the effluent water samples when compared to the influent water samples ($p < 0.0001$).



	Influent Water	Effluent Water
BPA (ng/mL)	7.69±0.87	3.17±0.62****

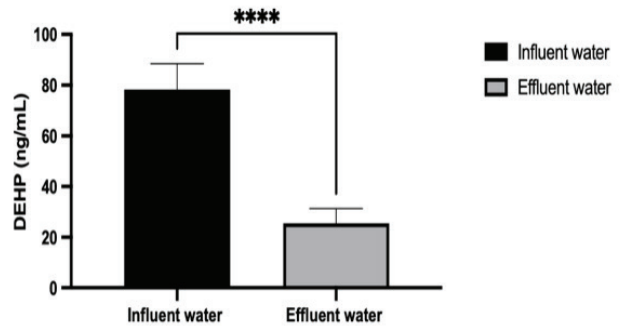
Figure 1. BPA (ng/mL) levels in the influent and effluent water samples of the wastewater treatment plant.

Table 1 presents the findings from the correlation analysis of the BPA and DEHP levels in the influent and effluent water samples from the wastewater treatment plant. Accordingly, BPA levels in the influent water and effluent water samples were found to be positively correlated.

Table 1. Correlation of BPA and DEHP levels in the influent and effluent water samples of the wastewater treatment plant.

	BPA in influent water samples	BPA in effluent water samples	DEHP in influent water samples	DEHP in effluent water samples
BPA in influent water samples		$r=0.921$ $p=0.026^*$	$r=0.109$ $p=0.861$	$r=-0.547$ $p=0.340$
BPA in effluent water samples	$r=0.921$ $p=0.026^*$		$r=0.091$ $p=0.884$	$r=-0.382$ $p=0.526$
DEHP in influent water samples	$r=0.109$ $p=0.861$	$r=0.091$ $p=0.884$		$r=0.670$ $p=0.216$
DEHP in effluent water samples	$r=-0.547$ $p=0.340$	$r=-0.382$ $p=0.526$	$r=0.670$ $p=0.216$	

*: $p < 0.05$



	Influent Water	Effluent Water
DEHP (ng/mL)	78.27±10.15	25.56±5.75****

Figure 2. DEHP levels in the influent and effluent water samples of the wastewater treatment plant.

DISCUSSION

Endocrine disruptors such as BPA and phthalates that come to wastewater treatment plants through plastics cannot be completely eliminated during treatment processes. Such chemicals cause environmental pollution by being discharged to environments such as rivers, lakes, and seas through the effluent flows of the treatment plant. However, some studies have reported BFA to be degradable within 2 days after being discharged into a receiving environment (9, 10). The concentrations of BPA and similar chemicals in rivers and streams under hydrological and climatic conditions have been shown to occur in the range of 0.5-16 ng/L in Germany and 90-12.000 ng/L in the United States (11, 12). Another study conducted in Germany determined BPA levels to be 1927 ng/L at the point where the wastewater treatment plant discharged into a river (13). The presence of BPA has been detected even in wastewater sediments in China, Korea, and Japan (14-16).

Phthalates are distributed over a wide range of concentrations in streams where wastewater is discharged based on their physicochemical characteristics. Among these phthalates, DEHP is the most common, with a concentration range of 0.05-4.95 µg/L (17). Phthalates are found in wastewater sediments as high molecular-weight compounds such as di-n-butyl phthalate, butyl benzyl phthalate, di-isobutyl phthalate, and diethyl-hexyl phthalate (18, 19).

At the beginning of the 2000s, the European Water Framework Directive identified DEHP as one of 33 hazardous materials. According to the Environmental Quality Standards (EQS), the recommended annual average concentration value for surface waters is 1.3 µg/L, with a maximum of 4.720 µg/kg dry weight for sediments. The discharge values for DEHP in receiving waters such as the lakes, rivers, and streams where wastewater is discharged in Europe are 3.2 µg/L, with a 30 mg/kg dry weight for sediments (20). Wastewaters host quite a few chemicals that cause various pathologies in humans. Due to the reusable properties of these waters, determining the presence and amount of EDCs in treated wastewater in terms of protecting public health and preventing environmental pollution has gained importance. In accordance with this argument, the current study aimed to determine the concentrations of BPA and phthalates in the inlet and outlet waters of wastewater treatment plants, with both phthalate and BPA being found in all the wastewater samples that were taken. According to the obtained data, the overall BPA and phthalate levels in the influent flow to the facility that underwent advanced biological wastewater treatment were found to be 7.69 µg/L and 78.27 µg/L, respectively, with the respective levels in the effluent water being 3.17 µg/L and 25.56 µg/L. The study found the concentrations of BPA and phthalates in the effluent water samples to have significantly decreased compared to the influent water samples.

Because some endocrine disruptors are not fully biologically degradable due to their physicochemical structures, they spread rapidly from one environment to another. For example, the percentage of BPA purified from wastewater treatment plants varies between 30-90%. As can be seen, not all of these chemicals can be eliminated. On the other hand, the removal efficiency for phthalates is higher than for BPA at a range of 68-95% (21, 22). Most of the research in the literature has been based on the removal efficiency of EDCs in wastewater treatment plants. Tran et al. found the BPA and DEHP levels in the influent wastewater coming to the wastewater treatment plants near the Seine River to be 4 µg/L and 33 µg/L, respectively, and to reduce respectively to 0.4 µg/L and 2 µg/L in the effluent water samples. According to the treatment techniques used in their study, they reported a BPA removal in the range of 30-90% and phthalate removal in the range of 68-95% (20).

Significant numerical differences are found worldwide in studies determining the phthalate concentrations in untreated wastewater. The minimum and maximum concentrations of DEHP (13-101 µg/L) as measured by Vethaak et al. (23) for the inlet water of a treatment plant in the Netherlands in 2005 prior to the implementation of the European Wastewater Regulation Decisions (DCE2008) resemble the numerical values found in the current study. Similarly, Mattinen et al. (24) measured the minimum and maximum value ranges of DEHP concentrations to be 28-122 µg/L in Finland in 2003, which is also consistent with the current study. As a result of the research, this study has observed the BPA data regarding the treatment plant effluent flow to average 3.17 µg/L, which matches the values of 0.47-

12 µg/L as found by Höhne and Püttmann (25) in Germany. Sousa et al.'s study (26) in Portugal stated effluent BPA levels of 3-316 ng/L after decantation and biological treatment applications. Considering the physicochemical properties of endocrine disruptors, the most effective treatment methods are suggested as decantation, biodegradation, ultrafiltration, volatilization, advanced oxidation, and ozonation applications.

In our study we found the BPA and phthalate concentrations in the effluent flow of the treatment plant to be significantly lower compared to the influent water samples. By using advanced biological wastewater treatment methods on untreated wastewater, BPA was seen to be removed at a rate of 58.8% and phthalates at a rate of 67.4%. These data also reveal the efficiency with which EDCs are purified from the wastewater of the treatment plant. These data also overlap with the data from the study of Sanchez-Avila (21) in Spain, in which the percentage of phthalates removed was reported as 68%. When analyzing the wastewater characteristics, the inlet waters of the treatment plant where the study was conducted mainly pertain to industrial areas and domestic wastewater.

According to the data this study obtained, BPA and phthalate levels in wastewater treatment plants were observed to be significantly lower in the effluent samples compared to the influent water samples. While these data reveal the treatment performance of the facility, they also reveal the treatment performance, which can be further improved by using advanced treatment technologies.

In order to protect public health, the environment, and natural life, BPA and phthalate concentrations in the influent and effluent water samples of the wastewater treatment plants need to be constantly monitored. Further research on this area would shed light on the enactment of new laws and regulations, the inclusion of heavy penal sanctions on businesses that discharge illegal wastewater into the receiving aquatic environment, the intensification and dissemination of inspections, and the application of proper treatment technologies.

Ethics Committee Approval: Ethics committee approval is not required because of no material or experimental animal that would require permission.

Peer-review: Externally peer-reviewed.

Author Contributions: Conception/Design of Study - A.A.A.; Data Acquisition - M.A., U.V.U., I.U., P.S.A.K., D.C.; Performing experiments - A.A.A., E.E.A.; Data Analysis/Interpretation - A.A.A., E.E.A.; Statistical Analyses - A.A.A., E.E.A.; Drafting Manuscript - A.A.A., E.E.A.; Critical Revision of Manuscript - A.A.A., E.E.A.; Final Approval and Accountability - A.A.A., E.E.A.

Conflicts of Interest: The authors declare no conflict of interest.

Financial Disclosure: This study is funded by Scientific Research Projects Coordination Unit of Istanbul University-Cerrahpaşa. Project number: FYL-2017-24111.

REFERENCES

- Dağlı H. İçmesuyu kalitesi ve insan sağlığına etkileri. Bizim İller. İller Bankası Aylık Yayın Organı 2005; 3: 16-21.
- Atalık A. Küresel ısınmanın su kaynakları ve tarım üzerine etkileri. Bilim ve Ütopya 2006; 139: 18-21.
- Toze S. Reuse of effluent water-benefits and risks. J Agricultural Manage 2006; 80: 147-59. [CrossRef]
- Haviland WA. Kültürel Antropoloji: Hüsamettin İnaç, Seda Çiftçi, editors. Kaktüs Yayınları: Sosyoloji Serisi No:3. İstanbul 2002; 143.
- Nasr FA, Doma HS, Abdel Halim HS, El-Shafai SA. Chemical industry wastewater treatment. Environmentalist 2007; 27: 275-86. [CrossRef]
- Kukul YS, Ünal Çalışkan AD, Anaç S. Artırılmış atıksuların tarımda kullanılması ve insan sağlığı yönünden riskler. Ege Üniversitesi Ziraat Fakültesi Dergisi 2007; 44(3): 101-16.
- Gultekin I, Ince NH. Synthetic endocrine disruptors in the environment and water remediation by advanced oxidation processes. J Environ Manage 2007; 85: 816-32. [CrossRef]
- Wu Q, Lam JCW, Kwok KY, Tsui MMP, Lam PKS. Occurrence and fate of endogenous steroid hormones, alkylphenol ethoxylates, bisphenol A and phthalates in municipal sewage treatment Systems. J Environ Sci 2017; 61: 49-58. [CrossRef]
- Klecka GM, Gonsior SJ, West RJ, Goodwin PA, Markham DA. Biodegradation of bisphenol A in aquatic environments: River die-away. Environ Toxicol Chem 2001; 20: 2725-35. [CrossRef]
- Flint S, Markle T, Thompson S, Wallace E. Bisphenol A Exposure, effects, and policy: A wildlife perspective. J Environ Manage 2012; 104: 19-34. [CrossRef]
- Kuch HM, Ballschmiter K. Determination of endocrine-disrupting phenolic compounds and estrogens in surface and drinking water by Hrgc-(Nci)-Ms in the picogram per liter range. Environ Sci Technol 2001; 35: 3201-06. [CrossRef]
- Kolpin DW, Furlong ET, Meyer MT, Thurman EM, Zaugg SD, Barber LB, et al. Pharmaceuticals, hormones and other organic wastewater contaminants in U.S. Streams 1999-2000: A national reconnaissance. Environ Sci Technol 2002; 36: 1202-11. [CrossRef]
- Quednow K, Püttmann W. Endocrine Disruptors in freshwater streams of Hesse, Germany: Changes in concentration levels in the time span from 2003 to 2005. Environ Pollut 2008; 152: 476-83. [CrossRef]
- Khim JS, Lee KT, Villeneuve DL, Giesy JP, Koh CH. Trace organic contaminants in sediment and water from Ulsan Bay and its vicinity, Korea. Arch. Environ Contam Toxicol 2001; 40: 141-50. [CrossRef]
- Kitada Y, Kawahata H, Suzuki A, Omori T. Distribution of pesticides and BPA in sediments collected from rivers adjacent to coral reefs. Chemosphere 2008; 71: 2082-2090. [CrossRef]
- Lui Y, Guan Y, Tam NFY, Tsuno H, Zhu W. Influence of rainfall and basic water quality parameters on the distribution of endocrine-disrupting chemicals in coastal area. Water Air Soil Pollut 2010; 209: 333-43. [CrossRef]
- Dargnat C, Blanchard M, Chevreuil M, Teil MJ. Occurrence of phthalate esters in the Seine River Estuary (France). Hydrol Process 2009; 23: 1192-201. [CrossRef]
- Huang PC, Tien CJ, Sun YM, Hsieh CY, Lee CC. Occurrence of phthalates in sediment and biota: Relationship to aquatic factors and the biota-sediment accumulation factor. Chemosphere 2008; 73: 539-44. [CrossRef]
- Fatoki OS, Bornman M, Ravandhalala L, Chimuka L, Genthe B, Adeniyi A. Phthalate ester plasticizers in freshwater systems of Venda, South Africa and potential health effects. Water Sa 2010; 36: 1. [CrossRef]
- Tran BC, Teil MJ, Blanchard M, Alliot F, Chevreuil M. BPA and phthalate fate in a sewage network and an elementary river of France. Influence of hydroclimatic conditions. Chemosphere 2015; 119: 43-51. [CrossRef]
- Sánchez-Avila J, Tauler R, Lacorte S. Determination and occurrence of phthalates, alkylphenols, BPA, PBDEs, PCBs and PHAs in an industrial sewage grid discharging to a municipal wastewater treatment. Plant Sci Total Environ 2009; 407: 4157-67. [CrossRef]
- Clara M, Windhofer G, Hartl W, Braun K, Simon M, Gans O, et al. Occurrence of phthalates in surface runoff, untreated and treated wastewater and fate during wastewater treatment. Chemosphere 2010; 78: 1078-84. [CrossRef]
- Marttinen S, Kettunen R, Rintala J. Occurrence and removal of organic pollutants in sewages and landfill leachates. Sci Total Environ 2003; 301: 1-12. [CrossRef]
- Vethaak AD, Lahr J, Schrap SM, Belfroid AG, Rij GBJ, et al. An integrated assessment of estrogenic contamination and biological effects in the aquatic environment of the Netherlands. Chemosphere 2005; 59: 511-24. [CrossRef]
- Höhne C, Püttmann W. Occurrence and temporal variations of xenoestrogens bisphenol a, 4-tert-octylphenol, and tech. 4-nonylphenol in two German wastewater treatment plants. Environ Sci Pollut Res 2008; 15: 405-16. [CrossRef]
- Sousa A, Schönenberger R, Jonkers N, Suter MJ, Tanabe S, Barroso CM. Chemical and biological characterization of estrogenicity in effluents from WTPs in Ria De Aveiro (Nw Portugal). Arch Environ Contam Toxicology 2010; 58 (1): 1-8. [CrossRef]

The Mitochondrial Origins of the Hellenistic Individuals of Ayasuluk Hill

Fatih Tepgeç¹ , Mehmet Gorgulu¹ 

¹Vocational School of Health Services, Altınbaş University, Istanbul, Türkiye

ORCID ID: F.T. 0000-0001-8413-6949; M.G. 0000-0002-9185-4225

Cite this article as: Tepgeç F, Gorgulu M. The mitochondrial origins of the hellenistic individuals of ayasuluk hill. Experimed 2022; 12(3): 139-48.

ABSTRACT

Objective: The present study aimed to extract ancient DNA from the remains of three individuals from the 4th century BC in order to determine the haplogroups through a mitochondrial DNA study, thus providing information about Anatolian migrations in ancient times.

Materials and Methods: For this purpose, the study examined the remains of three bodies found at the bottom of the city walls from the archeological excavations between 2007-2008 and dated to the 4th century BC. After taking anthropometric measurements, the study examined the mitochondrial *HVR1* and *HVR2* regions by using Sanger sequencing and then used online programs to evaluate the data from the sequencing.

Results: As a result of the study, death due to a possible injury from a sharp object was observed on the right femur of one of the three individuals. The maternal haplogroups of the individuals were determined to belong to the T2b group of European origin.

Conclusion: The present study obtained genetic information regarding three individuals found at the bottom of the ancient city walls on Ayasuluk Hill. These results will provide important information about the commander of the ruins found on the walls of the Ayasuluk Hill of the ancient city of Ephesus, which constantly changed hands during the Wars of the Diadochi.

Keywords: Mitochondria, genetics, ancient DNA

INTRODUCTION

The contributions of genetics to the field of archeology have increased over the past years and have influenced the re-examination of most of the information found in previous excavations or written texts (1-6).

During the Hellenistic period, Anatolia was a region where different societies reigned and fought each other. Those lands became a part of the empire with the conquests of Alexander the Great, but after his death in Babylon in 323 BC, their commanders divided them into kingdoms (7). The city of Ephesus occupies a very important place in Anatolia for hosting the Wars of the Diadochi during the Hellenistic period. The city of Ephesus was the first built independently under the control of Demetrius and with the assurance of Antigonus in 315 BC following Alexander the Great's death (7).

Due to Ayasuluk Hill constantly having changed hands, current archaeological data has yet to fully identify in which period or by which commander the walls of the city of Ephesus had been built. The pottery findings excavated in the area point to the late classical and early Hellenistic periods (4th-3rd centuries BC), but the exact date still remains uncertain.

As a result of the studies carried out using X-ray diffractometry (XRD) and scanning electron microscopy (SEM), the walls in the area on Ayasuluk Hill and the walls used in the reconstruction of Ephesus are thought to have been built in the 4th century BC. This leads to the idea about the skeletons that were found at the bottom of the city wall alongside the ceramic finds were soldiers who'd fought before Ephesus was moved. In order to prove this, the study examined the skeletons paleoanthropologically and genetically.

Corresponding Author: Fatih Tepgeç **E-mail:** fatih.tepgec@altinbas.edu.tr

Submitted: 02.10.2022 **Revision Requested:** 31.10.2022 **Last Revision Received:** 23.11.2022 **Accepted:** 24.11.2022 **Published Online:** 29.12.2022



Content of this journal is licensed under a Creative Commons Attribution-NonCommercial 4.0 International License.

The D-loop in the hypervariable region (HVR) is a 1.1 kb non-coding region in the human mitochondrial genome involved in the regulation of transcription and replication and has a highly variable sequence at the population level compared to the rest of the genome. It contains three short regions: *HVR1* (between nucleotides 16024-16400), *HVR2* (between nucleotides 44-340), and *HVR3* (between nucleotides 438-576). Among these, *HVR1* is the most frequently used one in population genetic studies (8-9). According to the literature, the mitochondrial genomes involved in this region were the first that used by the Cambridge group in 1981 and numbered in terms of the light strand defined as the Cambridge reference sequence (CRS) (10). However, this definition has since been updated due to an error in the used technique, with its final form being taken as the revised Cambridge reference sequence (rCRS) in 1999 and the reconstructed Sapiens reference sequence (RSRS) in 2012 as a result of the latest revisions (11, 12).

This study carried out mitochondrial DNA (mtDNA) analyses on samples of ancient DNA (aDNA) from the Seljuk Ayasuluk Castle on Ayasuluk Hill in southwest Anatolia. The study will contribute to the historical and archaeological findings regarding the makeup of the societies in the region and also identify the individuals who are presumed to have died in conflicts for the defense of Ephesus, one of the most active centers during the Wars of the Diadochi when regional turmoil occurred and the city frequently changed hands.

MATERIALS AND METHODS

The samples included in the study were based on the data obtained from archaeological studies and findings in the area and consisted of bones dated from the 4th-3rd century BC that were found alongside ceramic pieces at the bottom of the city wall during the excavation of 2007-2008. Evaluations of suitability of the sample for anthropometric measurement occurred prior to the analyses (13-15). The necessary permissions were obtained for the materials used in the study, which was approved for being conducted in the Altınbaş University Scientific Research Projects unit (Project code: PB2020-SHMYO-1).

Isolation of the aDNA

The aDNA was isolated from the samples in the Altınbaş University Ancient DNA Laboratory. Sterile laminar flow cabinets (sections where DNA isolation, PCR, and Post PCR are performed) where the pre-study procedures would be performed were first sterilized with sodium hypochlorite (NaClO; Cat no: 7681-52-9, Sigma, Germany) and UV lights (15 WATT, 265 nm wavelength, duration 45 minutes) (16). Sterile pipette tips, disposable sterile gloves, and masks were also used in the study.

In order to minimize DNA contamination before the procedure, the upper portion of 1-2 mm of the bone fragment was removed from the target area using sterile Dremel tips (Cat no: 4000-1/45; Dremel, USA) around the area to be treated, with these tips being replaced after each procedure. The new UV-sterilized disposable Dremel tips were used on

the powdered bone (0.04 to 0.5 g) that was to be taken for DNA sampling (17).

Isolation of the aDNA from the obtained bone powder (~50 mg) was carried out within a closed robotic system that had been sterilized before (and after) the study. This material was incubated in a 2 mL Eppendorf tube in 200 µL of incubation buffer and 10 µL proteinase K taken from the solutions in the isolation kit (TanBead Nucleic Acid Extraction Kit; Tissue Total DNA, Cat no: M6T2S46; TanBead; Taiwan) for 1 hour at room temperature before being processed.

The aDNA isolation was performed using the TanBead isolation robot and the tissue total DNA kits. Isolated samples were taken from the robot in 100 µL isolates and kept at 4°C until further use.

Following the isolation, the densities (ng/µL) and absorption measurements ($A_{260/280}$: 1.80 - 1.89) of the DNA samples were measured with a spectrophotometer and recorded (Cat No: ND-2000, ThermoFisher Scientific, USA; Table 1).

Table 1. Samples absorption measurements and concentrations.

Sample No	Conc. (ng/µL)	260/280	260/230
C320-1	135.1	1.43	0.63
C320-2	135.1	1.43	0.61
C320-3	14.8	1.37	0.76

Sanger Sequencing

AmpliAq Gold DNA Polymerase (Cat No: N8080246, ThermoFisher Scientific, USA) and UDG (Uracil-DNA Glycosylase, Cat No: 78310100UN, ThermoFisher Scientific, USA) were used during the PCR stage due to its effectiveness on degraded regions with low copy numbers. For each PCR reaction, the study used 1 Unit of UDG, 1 µL of 360 GC Enhancer (Cat No: N8080246, ThermoFisher Scientific, USA), 1X buffer solution (AmpliAq Gold® 360 Buffer, Cat No: N8080246, ThermoFisher Scientific, USA), 25 mM MgCl₂ (Cat No: N8080246, ThermoFisher Scientific, USA), 200 µM dNTP Mix (Cat No: N8080246, ThermoFisher Scientific, USA), 0.3 µM forward and reverse primers, 0.5 Unit Gold Taq polymerase enzyme, and 2 µL aDNA templates. The mixture was prepared by filling it with up to 25 µL of double distilled water (ddH₂O). All studies were performed on ice. Each PCR cycle studied the region to be amplified alongside the control PCR (negative control) that contained no DNA. If bands were seen in the control PCRs, the PCR process was repeated for the problematic samples from the aDNA extraction step.

The PCR were performed in the thermal cycler following the protocol designed for the *HVR1* and *HVR2* regions of mtDNA (Table 2). Initial denaturation was performed over 30 min at 37°C followed by 10 min at 95°C. Then for 30 cycles, denaturation occurred over 30 sec at 95°C, primer binding over 30 sec at

Table 2. Primer list for PCR.

Primer Name	Primer Sequence
15876F	5'-TCAATGGGCTGTCCTTGAG-3'
132R	5'-GACAGATACTGCGACATAGG-3'
15946F	5'-CAAGGACAAATCAGAGAAAA-3'
639R	5'-GGGTGATGTGAGCCCGTCTA-3'

60°C, elongation over 120 sec at 72°C (1 kb/c), and finally a 10 min extension time at 72°C. After the PCR, 5 µL of the products were taken and screened in the agarose gel electrophoresis containing 1.4% agarose (Cat No: 9012-36-6, Sigma, Germany) and 8 µg/mL ethidium bromide in the 1X TBE buffer, together with the 50 bp ladder marker (Cat No: D3812, Sigma, Germany) at 130 V for 20-25 min. The bands were visualized under UV light and recorded.

Enzymatic PCR purification (Exonuclease-I (Lot:00173016-ThermoFisher Scientific, USA) and rapid alkaline phosphatase (Cat No:04898133001, Roche, Switzerland) were performed on the products detected in the gel. After the purification step, the products were stored in the dark at 4°C until the sequence PCR reaction.

Sanger sequencing was performed on ABI3130 (Cat No: 3130XLR, ThermoFisher Scientific, USA). Electropherogram images were evaluated in the program Chromas, and the *HVR1* and *HVR2* regions of the mitochondria were identified according to RSRS based on the sequence results (18).

RESULTS

As a result of the paleopathological examination, the bones found in the area were determined to have belonged to 3 different adult males (Table 3) (15). The lesion seen on the

anterior region of the right femur bone in one of these three individuals extends linearly from top to bottom and shows slight bends; it is thought to be a possible piercing injury (Figure 1) (19, 20). Upon examining the cut, the person is thought to have died shortly after receiving this blow as no signs of recovery were found.

Table 3. Samples anthropometric measurements.

Sample No	Sex	Age	Lenght	Sample Tissue
C320-1	Male	>20	1.74	Left Tibia
C320-2	Male	>20	1.73	Left Femur
C320-3	Male	N/A	N/A	Left Femur

N/A: not available



Figure 1. C320-2 Right femur injury

As a result of investigation of the individuals included in the genetic evaluation, all the samples were identified to belong to the T2b2b haplogroup (Table 4). The same results were obtained in the independent PCR study performed for checking the results. Electropherogram images are given in

Table 4. Genetic results.

Sample No:	<i>HVR1</i>	<i>HVR2</i>	DNA Damage	Repeat	Haplogroup	Defining Markers for Haplotypes		Damaging Areas
						<i>HVR1</i>	<i>HVR2</i>	
C320-1	+	+	-	Sequencing	T (T2b2b)	T16126C C16294T C16296T (C16304T!)	73G	-
C320-2	+	+	+	Sequencing	T (T2b2b)	T16126C C16294T C16296T (C16304T!)		16126,16261,16294,16296, 16298, 16519
C320-3	+	+	+	Sequencing	T (T2b2b)	T16126C C16294T C16296T (C16304T!)	60C 73G	16189, 16289, 16400, 16519

!: back mutations

supplementary materials, with Table 4 providing the target regions in comparison for the haplogroup analysis.

DISCUSSION

Although developments in genetics and studies in the field of aDNA reveal new information about many historical events, consideration of these as pieces of auxiliary information rather than a definitive statement for questions to be asked is important. Recent decades have added the origin markers in mitochondria and Y chromosomes to the markers in the autosomal chromosomes. Without references to historical sources, such studies would have some difficulties for examining beyond the general screening tests, as the obtained data remains very weak without blending historical information with genetic information (3).

Although identifying DNA origin is based on mathematical proportions of the changes in the genomes of the living things under study, their sensitivity is directly proportional to an increase in the number of such studies. Although comprehensive methods exist for identifying origins in aDNA studies these days, one of the most practical ways for conducting a preliminary examination is to analyze easily examined mitochondrial *HVR* regions (21-23). The main reason for this and the accompanying problem is that the covered genomic region is relatively small (24).

Tracing the dominant alleles in gene pools in populations or the ancestry of important individuals is one of the important outcomes of the current study (6). Similarly, finding the place and time when a certain mutation first appeared (founding mutation) are also valuable in terms of genetics. Reflecting on the mutation rates in certain regions allows one to take into account the effects of not only geography but also time with regard to understanding the nature of variants in DNA (25, 26).

aDNA studies on excavations close to Ayasuluk Hill that cover similar historical periods have occurred with the Sagalassos and Kadikalesi excavations (27-29). Both regions involve the European macrohaplogroups and, hence, the T haplogroup. The historical periods that followed observed the T group to start appearing prominently after the density of the region's H, HV, and RO groups.

The maternal T haplogroup is one of the common haplogroups seen in Europe during the middle and early Neolithic period (30). The T2b group is one of the subgroups of the T group and is thought to have come to Europe from Anatolia during the last Ice Age and then to have spread during the Neolithic period (31). In order to confirm this, the T2b group in the Bronze Age also appears in the Eastern European Pontic-Castian steppes, such as the Srubnaya, Yamnaya, and Tripoli cultures (32, 33). Modi et al. (34) identified the T2b group in their findings from the early Bronze Age in Bulgaria.

Currently in maternal haplogroup studies, the T group is observed mostly in Europe and rarely in India (35, 36). This

strengthen the argument that this haplogroup is of Indo-European origin. Recent studies have also reported the T2 group to be one of the highest observed maternal haplogroups in the Macedonian population at 6.2% (37).

The soldiers provided by the city of Ephesus to the regions on Ayasuluk Hill during the struggle of Demetrius against Lysimakhos and the other Wars of the Diadochi in the region are said to have been sent from Kingdom of Macedon. The same source also states that Lysimakhos had left the slain soldiers where they were (7). The actual aim of this study was to obtain preliminary information about the possible origins of these soldiers. Evidence of at least the maternal origins of the samples was obtained by isolation of the aDNA and subsequently sequencing the HVR1 and HVR2 regions.

As a result of the study, the mitochondrial (maternal) haplogroups were found to be of European origin (T2b), and the skeletons found in the paleoanthropological examination are thought to have been soldiers probably from the army of Antigonos' son Demetrius or from Lysimachus, who came to Ayasuluk Hill to fight. The fact that the soldiers were not buried in a proper grave might show that they had lost the war, and this supports the view that Lysimachus was not a militaristic settlement.

In ancient DNA studies, while mitochondrial studies on their own give very general population data, they are very suitable for preliminary studies. However, the supplementation of Y chromosomal and autosomal markers when necessary, as well as using C14 carbon dating to date the materials, will lead to more detailed information being obtained about the samples in question. Examining the data from such individual or regional genetic identification studies using population genetics leads to larger data pools being obtained (16). In this way, all these data will not only be important in their own right but will also become important as the vast data they allow access to once the data regarding modern human genome sets accumulate. Although the information obtained as a result of such studies provides less information than broader sets, it does provide more rapid and cheaper preliminary results for excavation areas.

Acknowledgement: We deeply appreciate Assoc. Prof. Sinan Mimaroglu and Res. Asst. Firat Baranaydin for her guidance in data retrieval.

Ethics Committee Approval: There is no need for ethics committee approval, since the study was carried out on samples taken from ancient individuals belonging to the year 4th century BC.

Peer-review: Externally peer-reviewed.

Author Contributions: Conception/Design of Study – F.T., M.G.; Data Acquisition – F.T., M.G.; Data Analysis/Interpretation – F.T., M.G.; Drafting Manuscript – F.T., M.G.; Critical Revision of Manuscript – F.T., M.G.; Final Approval and Accountability – F.T., M.G.;

Conflicts of Interest: The authors declare no conflict of interest.

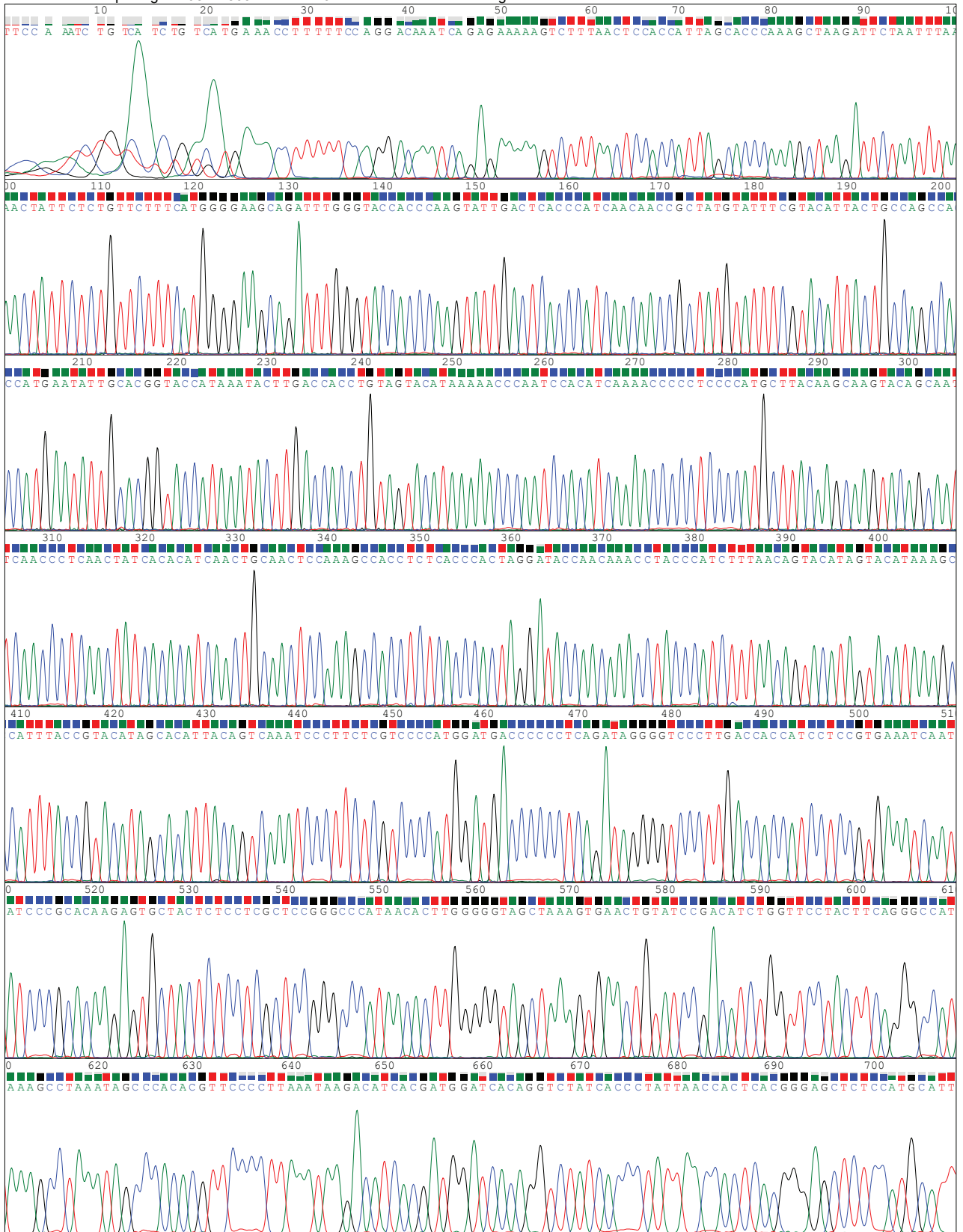
Financial Disclosure: The authors declare that this study has received no financial support.

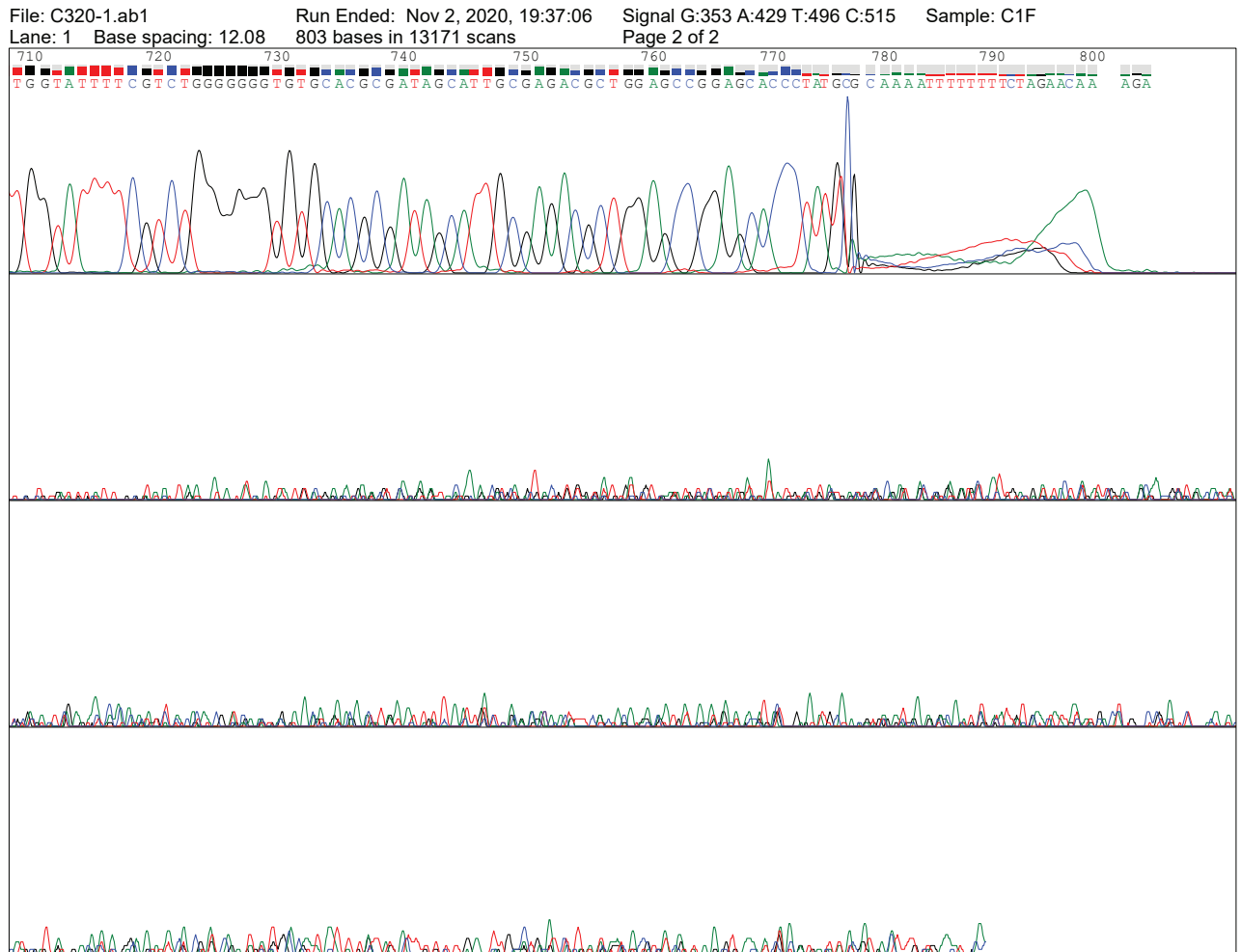
REFERENCES

1. Marciniak S, Perry GH. Harnessing ancient genomes to study the history of human adaptation. *Nat Rev Genet* 2017; 18(11): 659-74. [\[CrossRef\]](#)
2. Quintana-Murci L. Genetic, linguistic and archaeological perspectives on human diversity in Southeast Asia. *Am J Hum Genet* 2002; 71(5): 1253-5. [\[CrossRef\]](#)
3. De Chadarevian S. Genetic evidence and interpretation in history. *BioSocieties* 2010; 5(3): 301-5. [\[CrossRef\]](#)
4. Posth C, Nakatsuka N, Lazaridis I, Skoglund P, Mallick S, Lamnidis TC, et al. Reconstructing the deep population history of Central and South America. *Cell* 2018; 175(5): 1185-97. [\[CrossRef\]](#)
5. Moreno-Mayar JV, Vinner L, de Barros Damgaard P, De La Fuente C, Chan J, Spence JP, et al. Early human dispersals within the Americas. *Science* 2018; 362(6419): eaav2621. [\[CrossRef\]](#)
6. Feldman M, Master DM, Bianco RA, Burri M, Stockhammer PW, Mittnik A, et al. Ancient DNA sheds light on the genetic origins of early Iron Age Philistines. *Sci Adv* 2019; 5(7): eaax0061. [\[CrossRef\]](#)
7. Kaya MA. Anadolu'daki Galatlar ve Galatya tarihi: Ege Üniversitesi; 2000.
8. Brandstätter A, Niederstätter H, Parson W. Monitoring the inheritance of heteroplasmy by computer-assisted detection of mixed basecalls in the entire human mitochondrial DNA control region. *Int J Legal Med* 2004; 118(1): 47-54. [\[CrossRef\]](#)
9. Brandstätter A, Peterson CT, Irwin JA, Mpoke S, Koech DK, Parson W, et al. Mitochondrial DNA control region sequences from Nairobi (Kenya): inferring phylogenetic parameters for the establishment of a forensic database. *Int J Legal Med* 2004; 118(5): 294-306. [\[CrossRef\]](#)
10. Anderson S, Bankier AT, Barrell BG, de Bruijn MH, Coulson AR, Drouin J, et al. Sequence and organization of the human mitochondrial genome. *Nature* 1981; 290(5806): 457-65. [\[CrossRef\]](#)
11. Andrews RM, Kubacka I, Chinnery PF, Lightowlers RN, Turnbull DM, Howell N. Reanalysis and revision of the Cambridge reference sequence for human mitochondrial DNA. *Nat Genet* 1999; 23(2): 147. [\[CrossRef\]](#)
12. Behar DM, Van Oven M, Rosset S, Metspalu M, Loogväli E-L, Silva NM, et al. A "Copernican" reassessment of the human mitochondrial DNA tree from its root. *Am J Hum Genet* 2012; 90(4): 675-84. [\[CrossRef\]](#)
13. Mensforth RP, Latimer BM. Hamann-Todd collection aging studies: Osteoporosis fracture syndrome. *Am J Phys Anthropol* 1989; 80(4): 461-79. [\[CrossRef\]](#)
14. Meindl RS, Russell KF, Lovejoy CO. Reliability of age at death in the Hamann-Todd collection: validity of subselection procedures used in blind tests of the summary age technique. *Am J Phys Anthropol* 1990; 83(3): 349-57. [\[CrossRef\]](#)
15. İşcan MY. A Comparison of the Hamann-Todd and Terry collections. *Anthropologie (1962-)*. 1992; 30(1): 35-40.
16. Ou C, Moore J, Schochetman G. Use of UV irradiation to reduce false positivity in polymerase chain reaction. *Biotechniques* 1991; 10(4): 442-6.
17. Rohland N, Hofreiter M. Ancient DNA extraction from bones and teeth. *Nat Protoc* 2007; 2(7): 1756-62. [\[CrossRef\]](#)
18. Van Oven M, Kayser M. Updated comprehensive phylogenetic tree of global human mitochondrial DNA variation. *Hum Mutat* 2009; 30(2): E386-E94. [\[CrossRef\]](#)
19. Vazzana A, Scalise LM, Traversari M, Figus C, Apicella SA, Buti L, et al. A multianalytic investigation of weapon-related injuries in a Late Antiquity necropolis, Mutina, Italy. *J Archaeol Sci Rep* 2018; 17: 550-9. [\[CrossRef\]](#)
20. Mikulski RN, Schutkowski H, Smith MJ, Doumet-Serhal C, Mitchell PD. Weapon injuries in the crusader mass graves from a 13th century attack on the port city of Sidon (Lebanon). *PLoS One* 2021; 16(8): e0256517. [\[CrossRef\]](#)
21. Skoglund P, Sjödin P, Skoglund T, Lascoux M, Jakobsson M. Investigating population history using temporal genetic differentiation. *Mol Biol Evol* 2014; 31(9): 2516-27. [\[CrossRef\]](#)
22. Llamas B, Fehren-Schmitz L, Valverde G, Soubrier J, Mallick S, Rohland N, et al. Ancient mitochondrial DNA provides high-resolution time scale of the peopling of the Americas. *Sci Adv* 2016; 2(4): e1501385. [\[CrossRef\]](#)
23. Orlando L, Allaby R, Skoglund P, Der Sarkissian C, Stockhammer PW, Ávila-Arcos MC, et al. Ancient DNA analysis. *Nat Rev Methods Primers* 2021; 1(1): 1-26. [\[CrossRef\]](#)
24. Bolnick DA, Fullwiley D, Duster T, Cooper RS, Fujimura JH, Kahn J, et al. The science and business of genetic ancestry testing. *Science* 2007; 318(5849): 399-400. [\[CrossRef\]](#)
25. Kerner G, Laval G, Patin E, Boisson-Dupuis S, Abel L, Casanova J-L, et al. Human ancient DNA analyses reveal the high burden of tuberculosis in Europeans over the last 2,000 years. *Am J Hum Genet* 2021; 108(3): 517-24. [\[CrossRef\]](#)
26. Liu X, Orlando L. mapDATAge: a ShinyR package to chart ancient DNA data through space and time. *Bioinformatics* 2022; 38(16): 3992-4. [\[CrossRef\]](#)
27. Ottoni C, Ricaut F-X, Vanderheyden N, Brucato N, Waelkens M, Decorte R. Mitochondrial analysis of a Byzantine population reveals the differential impact of multiple historical events in South Anatolia. *Eur J Med Genet* 2011; 19(5): 571-6. [\[CrossRef\]](#)
28. Ottoni C, Rasteiro R, Willet R, Claeys J, Talloen P, Van de Vijver K, et al. Comparing maternal genetic variation across two millennia reveals the demographic history of an ancient human population in southwest Turkey. *R Soc Open Sci* 2016; 3(2): 150250. [\[CrossRef\]](#)
29. Tepgeç F, Görgülü M. Kadıkalesi Geç Bizans Dönemi Gömülerinin Mitokondriyel Kökenleri. *Acta Med Nicomedia* 2022 5(3): 98-103.
30. Brandt G, Haak W, Adler CJ, Roth C, Szécsényi-Nagy A, Karimnia S, et al. Ancient DNA reveals key stages in the formation of central European mitochondrial genetic diversity. *Science* 2013; 342(6155): 257-61. [\[CrossRef\]](#)
31. Pala M, Olivieri A, Achilli A, Accetturo M, Metspalu E, Reidla M, et al. Mitochondrial DNA signals of late glacial recolonization of Europe from near eastern refugia. *Am J Hum Genet* 2012; 90(5): 915-24. [\[CrossRef\]](#)
32. Juras A, Krzewińska M, Nikitin AG, Ehler E, Chyleński M, Łukasik S, et al. Diverse origin of mitochondrial lineages in iron age Black Sea Scythians. *Sci Rep* 2017; 7(1): 1-10. [\[CrossRef\]](#)
33. Fernández-Domínguez E, Reynolds L. The Mesolithic-Neolithic transition in Europe: a perspective from ancient human DNA. *Times of Neolithic transition along the Western Mediterranean*: Springer; 2017. p. 311-38. [\[CrossRef\]](#)
34. Modi A, Nesheva D, Sarno S, Vai S, Karachanak-Yankova S, Luiselli D, et al. Ancient human mitochondrial genomes from Bronze Age Bulgaria: new insights into the genetic history of Thracians. *Sci Rep* 2019; 9(1): 1-10. [\[CrossRef\]](#)
35. Rishishwar L, Jordan IK. Implications of human evolution and admixture for mitochondrial replacement therapy. *BMC genomics* 2017; 18(1): 1-11. [\[CrossRef\]](#)
36. Pipek OA, Medgyes-Horváth A, Dobos L, Stéger J, Szalai-Gindl J, Visontai D, et al. Worldwide human mitochondrial haplogroup distribution from urban sewage. *Sci Rep* 2019; 9(1): 1-9. [\[CrossRef\]](#)
37. Cvjetan S, Tolik H-V, Barać Lauc L, Čolak I, Đorđević D, Efremskova L, et al. Frequencies of mtDNA haplogroups in southeastern Europe-Croatians, Bosnians and Herzegovinians, Serbians, Macedonians and Macedonian Romani. *Coll Antropol* 2004; 28(1): 193-8.

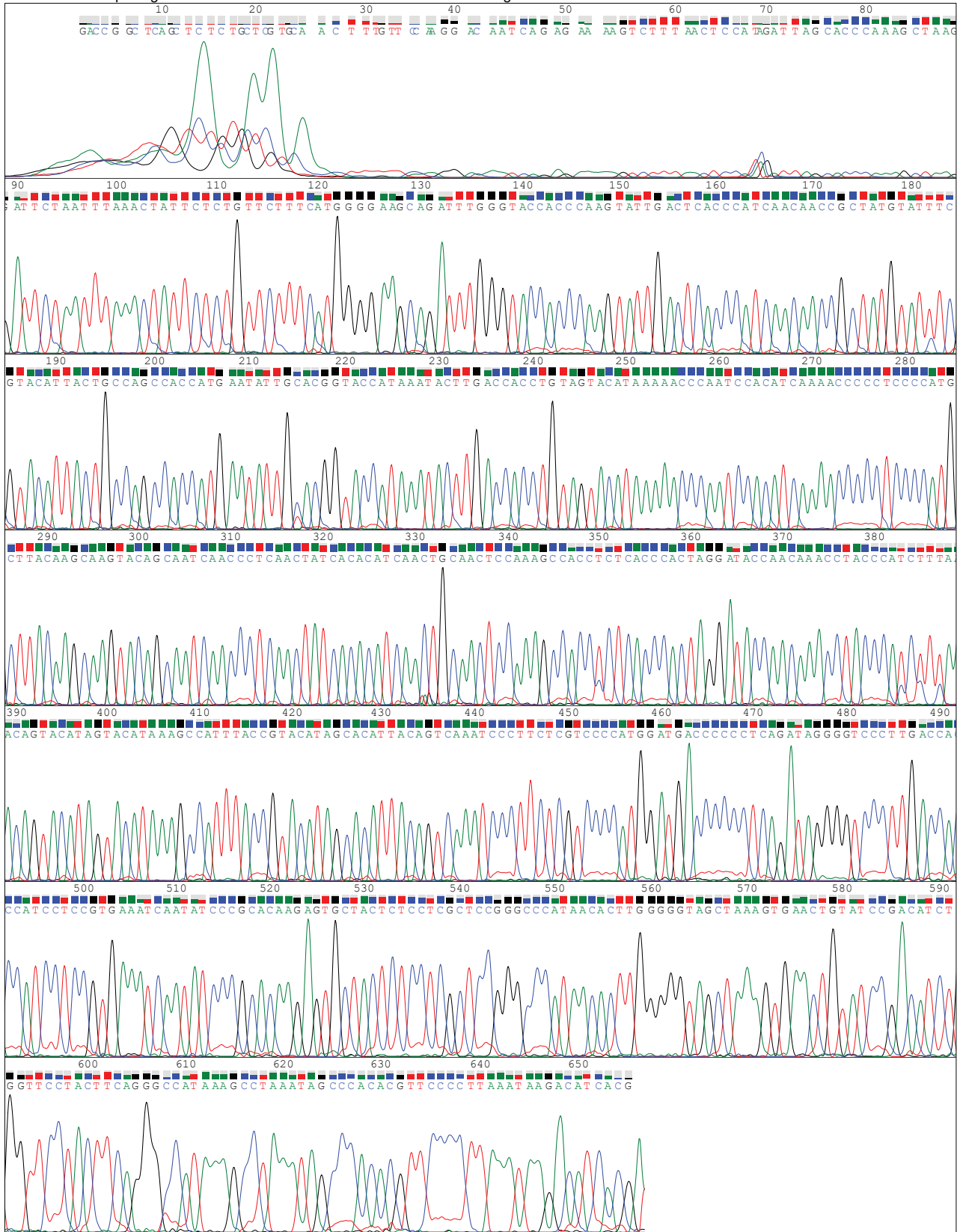
SUPPLEMENTARY FILE

File: C320-1.ab1 Run Ended: Nov 2, 2020, 19:37:06 Signal G:353 A:429 T:496 C:515 Sample: C1F
Lane: 1 Base spacing: 12.08 803 bases in 13171 scans Page 1 of 2

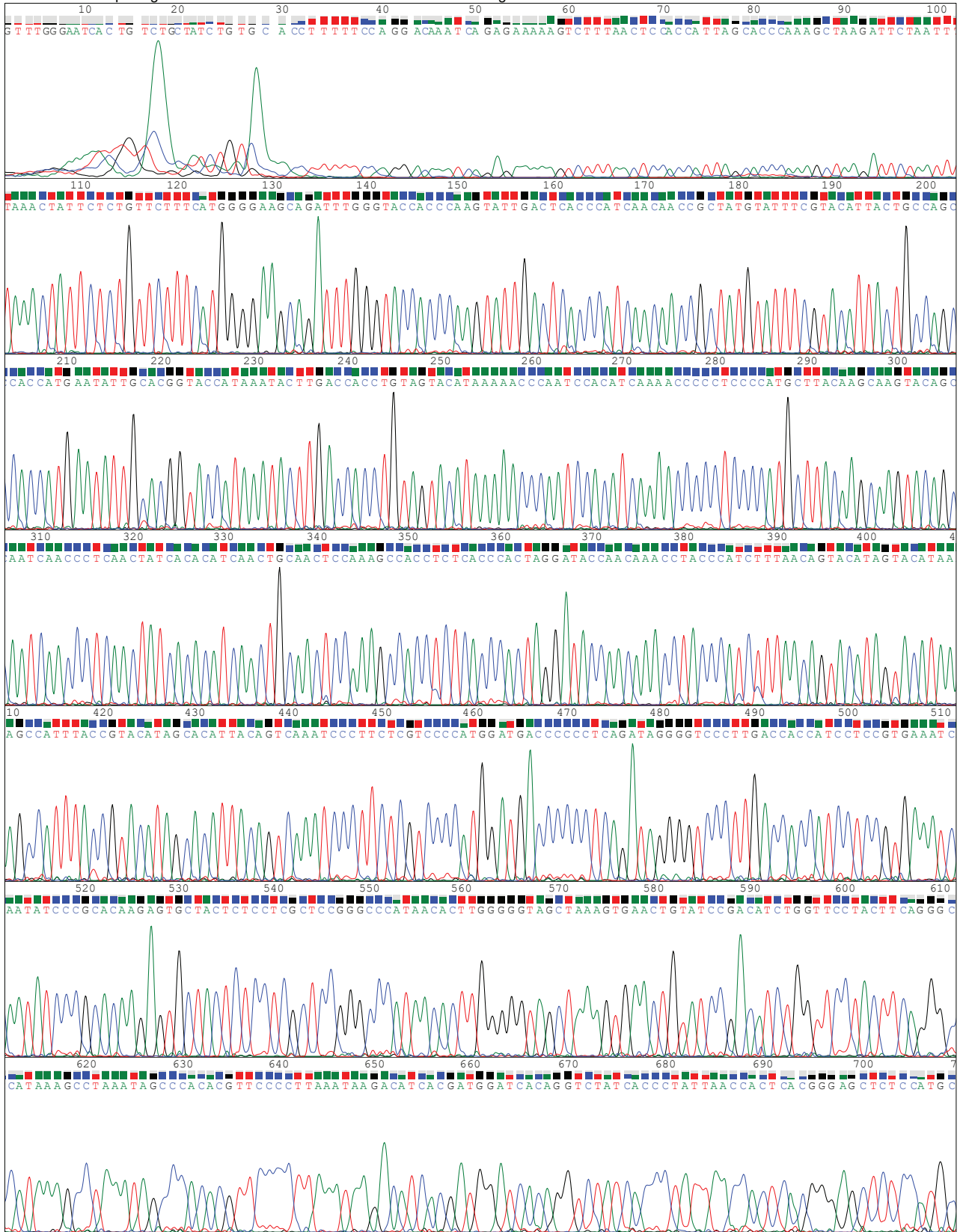


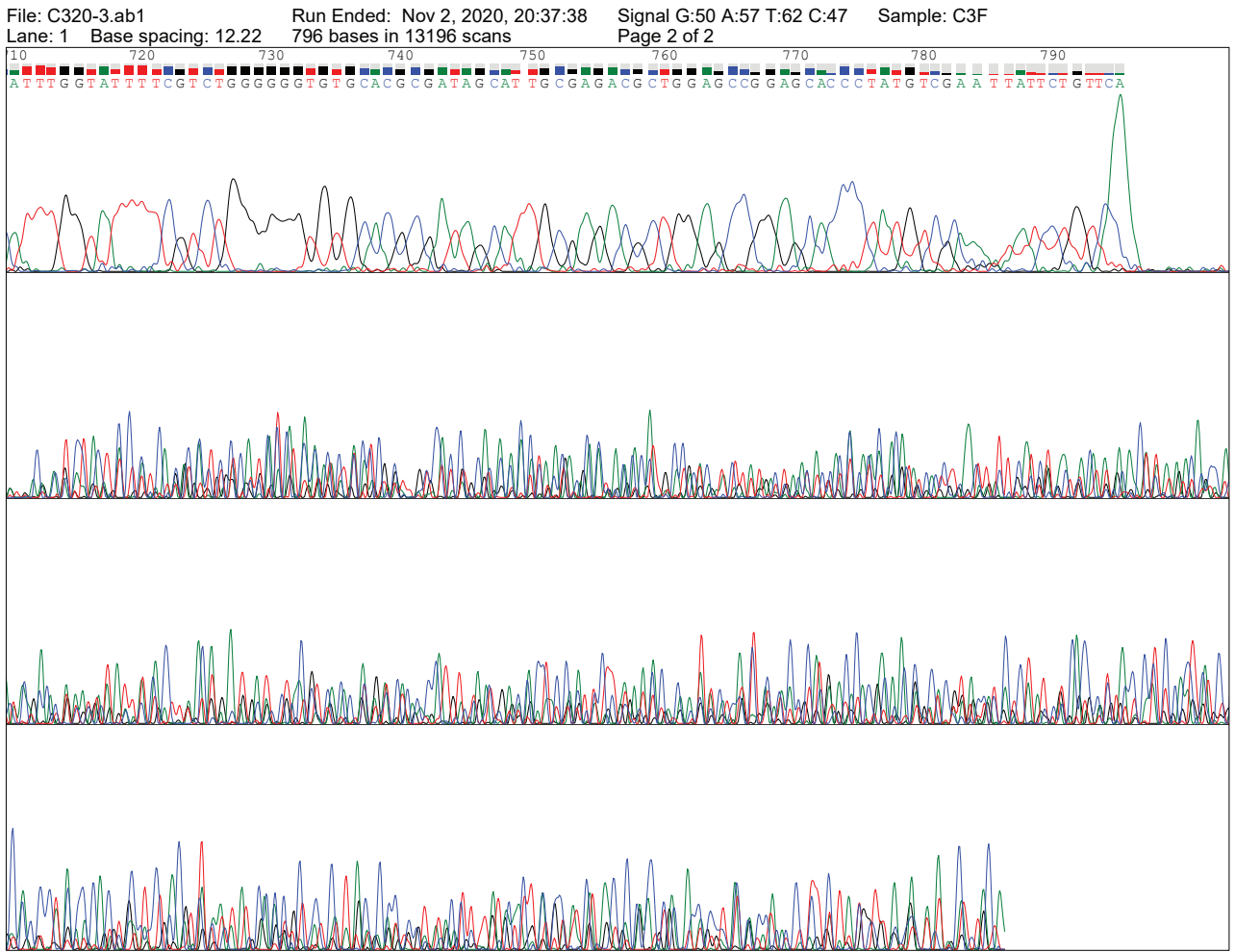


File: C320-2.ab1 Run Ended: Oct 30, 2020, 19:44:06 Signal G:89 A:169 T:125 C:103 Sample: C2F
Lane: 3 Base spacing: 15.31 655 bases in 8141 scans Page 1 of 1



File: C320-3.ab1 Run Ended: Nov 2, 2020, 20:37:38 Signal G:50 A:57 T:62 C:47 Sample: C3F
Lane: 1 Base spacing: 12.22 796 bases in 13196 scans Page 1 of 2





Fetal Hand Anomalies: 18 Cases Diagnosed Between 2020-2022 from a Single Tertiary Care Center

Ayça Dilruba Aslanger¹ , Tugba Sarac Sivrikoz² , Tugba Kalayci¹ , Seher Basaran¹ , Oya Uyguner¹ 

¹Department of Medical Genetics, Istanbul Faculty of Medicine, Istanbul University, Istanbul, Turkiye

²Division of Perinatology, Department of Obstetrics and Gynecology, Istanbul Faculty of Medicine, Istanbul University, Istanbul, Turkiye

ORCID ID: A.D.A. 0000-0003-1770-1762; T.S.S. 0000-0001-5482-9429; T.K. 0000-0002-9963-5916; S.B. 0000-0001-8668-4746; O.U. 0000-0002-2035-4338

Cite this article as: Aslanger AD, Sarac Sivrikoz T, Kalayci T, Basaran S, Uyguner O. Fetal hand anomalies: 18 cases diagnosed between 2020-2022 from a single tertiary care center. *Experimed* 2022; 12(3): 149-54.

ABSTRACT

Objective: The aim of this study was to present and investigate fetal cases with hand anomalies by discussing their antenatal and postmortem findings.

Materials and Methods: This retrospective review re-evaluates fetal cases identified antenatally with hand anomalies including polydactyly, syndactyly, reduction defects, and oligodactyly. The following data were collected from the patients' medical records: Demographic information, family histories, X-ray images, photographs, and cytogenetic/molecular findings. The study also performed a chromosome analysis, array-comparative genomic hybridization (CGH), and Sanger sequencing of *FGFR2* and *GLI3* genes.

Results: This study involved 18 cases with hand anomalies, all of which were diagnosed antenatally. Three cases were diagnosed with Greig cephalopolysyndactyly, Apert Syndrome, and triploidy, respectively.

Conclusions: Fetal ultrasonography is the most valuable tool for providing prenatal diagnosis. Prenatal detection of hand anomalies causes great anxiety for parents; therefore, making an accurate diagnosis list is important for the prenatal period. Prenatal diagnosis and management of hand anomalies must involve a multidisciplinary team composed of a perinatologist, a clinical geneticist, and a hand surgeon.

Keywords: Polydactyly, syndactyly, prenatal diagnosis

INTRODUCTION

The prevalence of upper limb congenital anomalies is 5.25-27.2 in 10,000 live births among the various populations. Hand anomalies are included in upper limb anomalies, with polydactyly being an extremely common type of hand anomaly, followed by transverse reduction defects, syndactyly, and oligodactyly (1, 2).

Upper limb development occurs between the 4th-8th week of gestation from the mesoderm and ectoderm. The temporal and spatial expressions of different gene families are involved in limb formation. Homeobox (HOX)

transcription factors regulate the position of the limbs along the craniocaudal axis. The upper limb bud develops on the ventrolateral wall of the embryo on the 26th day of gestation. The apical ectodermal ridge (AER) is a thickened ectoderm layer at the apex of the limb bud and produces the fibroblast growth factors (FGFs) that control the development of the underlying mesoderm. The zone of polarizing activity (ZPA) occurs in the posterior border of the limb bud and produces the Sonic hedgehog (SHH) protein, which regulates the anteroposterior development of the limbs. Dorsal ectoderm controls limb dorsalization through the secretion of WNT7a, which induces the transcription factor LMX1 in the underlying dorsal mesoderm (3-5).

Corresponding Author: Ayça Dilruba Aslanger **E-mail:** aaslanger@yahoo.com

Submitted: 17.10.2022 **Revision Requested:** 11.11.2022 **Last Revision Received:** 22.11.2022 **Accepted:** 24.11.2022 **Published Online:** 27.12.2022



Content of this journal is licensed under a Creative Commons Attribution-NonCommercial 4.0 International License.

The etiology of limb anomalies is very complex and can occur due to chromosomal abnormalities, single gene disorders, or disruptive conditions. However, the cause in many cases is still unknown. Polydactyly is a condition in which extra fingers form on the hands or toes. It usually occurs as a sixth digit, with the extra finger on the radial, ulnar or central side, respectively known as preaxial, postaxial, or mesoaxial polydactyly. Polydactyly affects the right hand more than the left hand and may appear isolated (non-syndromic) or combined with other anomalies (syndromic) as part of a syndrome (6). Isolated polydactyly is mostly passed from parent to child through the genes associated with non-syndromic polydactyly. Syndactyly, or congenital webbing, is characterized by containment of the skin, soft tissues, or osseous interconnections between adjacent digits at an estimated incidence rate of 1 in 2,000–3,000 live births and is more common in males than females (7). Syndactyly is assumed to arise as a failure of interdigital apoptosis, which falls under the control of bone morphogenetic proteins (BMPs) and is associated with FGFs in the AER. It can appear isolated or as part of a syndrome (8).

Because hand anomalies may be syndromic, the clinician should evaluate for other findings associated with polydactyly and consider other syndromic presentations. Case diagnoses of fetal hand anomalies are complicated. Detailed dysmorphological assessment of the fetus should be performed to detect additional minor anomalies or facial dysmorphism. In terms of preliminary and differential diagnoses, options such as karyotype, array-CGH, single gene sequencing, and whole exome sequencing (WES) should be offered to the family. This study aimed to investigate the types of 18 antenatally diagnosed fetal cases with hand anomalies and to discuss the genetic etiopathogenesis.

MATERIALS AND METHODS

The study involved the antenatally diagnosed fetal cases of intrauterine fetal demise (IUFD) or termination of pregnancy (ToP) with hand anomalies that have been referred to postmortem examination at Istanbul Faculty of Medicine, Department of Medical Genetics clinic at Istanbul University between 2020-2022; 18 fetal cases among 2,342 patients who had been evaluated by the multidisciplinary team for major congenital anomalies were included in the study as a result of additional anomalies accompanying the hand anomalies. The study was reviewed and approved by the institutional review board, and written informed consent (No: 17.10.2022-1316113) was obtained from all parents of the patients included in the study. The study retrospectively reviewed the clinical, radiological, and genetic results. Chromosome analysis was performed using standard cytogenetic Giemsa-Pancreatin-Leishman (GPL) banding technique in long term cultures on cells obtained from the chorionic villus biopsy in five cases (Cases 4, 5, 10, 13, 18), amniocentesis in four cases (Cases 6, 7, 11, 12), and fetal blood in eight cases (Cases 1, 2, 3, 8, 9, 14, 15, 17). To rule out other submicroscopic chromosomal abnormalities, a array-CGH test was performed for the available 11 cases (Case

3, 5, 6, 7, 8, 11, 15, 17). Genomic DNA was extracted from the long-term cultures of the cases, as well as peripheral blood from the parents for Cases 3 and 18 using commercial kits according to manufacturer's instruction (Mammalian Blood and Cells and Tissue DNA Isolation Kit/High Pure Kit, Roche Diagnostics GmbH, Mannheim Germany). Primers for the *FGFR2* (NM_000141.5) and *GLI3* (NM_000168.6) genes were designed to cover all the coding exons and deep exon intron boundaries. Sanger methods on an ABI 3500 Genetic Analyzer (Applied Biosystems, ThermoFisher Scientific, Foster City, CA, USA) and electropherograms in the Sanger sequencing were analyzed using SeqScape software (SeqScape Version 3.0; Applied Biosystems, Calsbad, CA, USA). The human genome GRCh37/hg19 was used as the reference version for alignments of the variants. The variants were investigated in the dbSNP ClinVar (<https://www.ncbi.nlm.nih.gov/clinvar/>) and HGMD (<http://www.hgmd.cf.ac.uk/ac/>) databases. These are classified according to the comments from the American College of Medical Genetics and Genomics (ACMG, 2015) standards (9).

RESULTS

This study involved a total of 18 fetal cases (5 females and 13 males) from unrelated families that had been diagnosed with hand anomalies. TOP was performed at a median gestational age of the 23rd week of gestation (GW; range = 15th-31st GW). The pregnancies had ended in an IUFD during the 34th GW in Case 7 and the 32nd GW in Case 16. Case 5 had bilateral syndactyly of the 3rd and 4th digits and was diagnosed as triploidy. The karyotype analyses of the remaining cases were normal except for Case 16, as her parents refused the invasive procedure. In cases where a single-gene disease was considered in the preliminary diagnosis, the diagnosis was made by performing the sequence analysis related to that disease. The clinical, cytogenetic and molecular results of the cases are summarized in Table 1, and hand anomalies are shown in Figure 1.

Polydactyly was found in five cases with syndromic features (Cases 1, 3, 9, 13, and 18), while one case (Case 2) was identified with a co-occurrence of neural tube defects (NTD) and polydactyly. Meckel-Gruber syndrome was evaluated in the preliminary diagnosis due to occipital encephalocele in two of three cases (Cases 13 and 18), with renal findings accompanying the polydactyly. Short-rib polydactyly syndrome (SRPS) was considered in one case with a narrow thorax (Case 9). Greig cephalopolysyndactyly syndrome was confirmed with the detection of the c.958_959insA (p.Ile320Asnfs*4) novel variant in the *GLI3* gene, which was the predicted pathogenic in Case 3 that had broad thumbs and halluces accompanying postaxial polysyndactyly in the upper extremity and preaxial polysyndactyly in the lower extremity. According to the ACMG criteria, this truncating variant received scores for PVS1 and PM2 and has been determined as the likely pathogenic. Case 6 had acrosyndactyly in the upper/lower extremity with severe craniosynostosis. Apert syndrome has been diagnosed through molecular testing, with a heterozygous c.755C>G (p.Ser252Trp) pathogenic variant being identified in the *FGFR2*

Table 1. Clinical and cytogenetic/molecular findings of fetal cases with hand anomalies.

Case	Hand anomalies	Other anomalies	Karyotype Results	Diagnosis & Molecular Results
Case 1	Bilateral postaxial polydactyly of hands and toes	Bilateral polycystic renal disease, absence of renal corticomedullary differentiation	46, XY	MCA R/O: Ciliopathies
Case 2	Postaxial rudimentary polydactyly on the left hand, bilateral camptodactyly on the 4 th and 5 th fingers	Meningomyelocele, hydrocephaly, kyphoscoliosis, hemivertebra	46, XY	MCA R/O: Neural tube defect plus polydactyly
Case 3	Bilateral postaxial polydactyly on the hands and syndactyly on 3 rd and 4 th fingers and preaxial polydactyly on the foots and syndactyly on 1 st and 3 rd toes, bilateral broad halluces and thumbs	Polyhydramnios, overgrowth Macrocephaly, facial dysmorphism Cavum velum interpositum cysts Interhemispheric cyst	46, XY	Greig cephalopolysyndactyly heterozygote c.958_959insA (p.Ile320Asnfs*4) in the <i>GLI3</i> gene
Case 4	Partial cutaneous syndactyly on 3 rd and 4 th Thumbs hypoplasia on the left Bilateral clinodactyly on the 5 th fingers	Anhidramnios, pericardial effusion, tricuspid regurgitation, PEV, forearm hypoplasia on the left	46, XX	MCA
Case 5	Bilateral syndactyly of 3 rd and 4 th of hands	Alobar HPE, cleft palate, VSD, PA, IUGR, anal atresia	69, XXX	Triploidy
Case 6	Bilateral acrosyndactyly, bilateral broad distal phalanx of thumbs	Craniosynostosis, cleft palate, segmental intestinal dilatation	46, XY	Apert syndrome c.755C>G (p.Ser252Trp) in the <i>FGFR2</i> gene
Case 7	Oligodactyly and ectrodactyly on right hand Camptodactyly of the 4 th fingers on the right hand, bilateral 5 th clinodactyly	Polyhydramnios, VSD, pulmonary stenosis, fallot tetralogy, facial dysmorphism	46, XX	MCA
Case 8	a single digit on the right hand, brachydactyly on the left hand	severe ulnar hypoplasia	46, XY	MCA R/O: Cornelia de Lange syndrome
Case 9	Bilateral postaxial polydactyly on hands and toes	Unilateral cleft lip and palate, labiogingival frenulum, short ribs with narrow trunk, rhizo-meso-acromelic shortness	46, XY	MCA R/O: Short-Rib Polydactyly syndrome
Case 10	Bilateral partial cutaneous syndactyly on 3 rd -5 th fingers	Bilateral renal agenesis, oligohydramnios, hyperechogenic bowel, facial dysmorphism	46, XY	MCA R/O: Fraser syndrome
Case 11	Oligodactyly (with preserved thumb) and syndactyly on 3 rd and 4 th enlarged fingers (macroductyly) on the left hand	Facial dysmorphism, lower limb hypoplasia on the right	46, XY	MCA R/O: Segmental overgrowth
Case 12	Oligodactyly (single finger on both hands)	Facial dysmorphism, bilateral severe mesomelia with elbow webbing, single bone (ulna?) on the forearm	46, XY	MCA R/O: Radial longitudinal deficiency
Case 13	Bilateral postaxial polydactyly on hands and toes	Occipital encephalocele, polycystic renal disease, omphalocele, bilateral PEV	46, XX	MCA R/O:Meckel-Gruber syndrome
Case 14	Bilateral thumb agenesis, camptodactyly Clinodactyly and brachydactyly on hands	Facial dysmorphism, bilateral elbow contractures, bilateral mesomelic shortness	46, XX	MCA R/O: Nager syndrome
Case 15	Terminal amputation and constriction rings of the 2 nd , 3 rd and 4 th digits on the left Constriction rings of the 1 st digit on the right and total cutaneous syndactyly between 2 nd and 5 th digits on the right	Facial dysmorphism, cleft lip and palate, borderline ventriculomegaly, cavum velum interpositum cysts, suspected aortic coarctation and corpus callosum dysgenesis	46, XY	MCA A/O: Amniotic Band Sequence + congenital cardiac and brain abnormalities+ cleft lip and palate

Table 1. Clinical and cytogenetic/molecular findings of fetal cases with hand anomalies. (continued)

Case	Hand anomalies	Other anomalies	Karyotype Results	Diagnosis & Molecular Results
Case 16	Constriction rings of the 2 nd and 3 rd digits on the right and 1 st and 3 rd digits on the left Terminal amputation and constriction rings of the 2 nd , 4 th and 5 th on the left	Constriction rings of the 2 nd and 4 th on the right, terminal transvers deficiency on the right hallux, tibial and fibular bowing on the right	N/D	MCA R/O: Amniotic Band Sequence + tibial bowing
Case 17	Terminal amputation and constriction rings of the 2 nd , 4 th digits on the left with distal swelling Terminal amputation and constriction rings of the 2 nd , 3 rd and 4 th digits on the left	Unilateral PEV, polyhydramnios	46, XY	MCA R/O: Amniotic Band Sequence
Case 18	Bilateral postaxial polydactyly on hands and toes	Occipital encephalocele, polycystic renal disease, omphalocele, bilateral PEV	46, XY	MCA R/O:Meckel-Gruber syndrome

MCA, Multiple Congenital Anomalies; R/O, Rule out diagnosis; PEV, Pes EquinoVarus; HPE, Holoprosencephaly; VSD, Ventricular Septal Defects; PA, Pulmonary Atresia; IUGR, IntraUterin Growth Retardation; N/D, Not Done



Figure 1. Clinical features of our cases.

A-B = Ectrodactyly in Case 7. **C-D** = Thumbs hypoplasia in Case 4. **E-F** = Partial cutaneous syndactyly in Case 10 with preliminary diagnosis of Fraser syndrome. **G-L** = Postaxial polydactyly in Case 1 (G-H), in Case 2 (I-J), in Case 3 with bilateral syndactyly of the 3rd and 4th digits with Greig cephalopolysyndactyly (K), and in Case 9 with a preliminary diagnosis of SRPS (L). **M-N** = Thumb hypoplasia in Case 14. **O-P** = Single finger on both hands in Case 12. **R-S** = Mitten-like acrosyndactyly in Case 6 with Apert syndrome. **T-U** = Segmental overgrowth in Case 11. **V-X** = Amniotic band sequence in Cases 16, 15, and 17. **Y** = Severe ulnar hypoplasia of the forearm with only a single digit in Case 8 with a preliminary diagnosis of CdLs.

gene. No variant was found in parents and with the clinical significance of this variant pathogenic being determined according to the ClinVar database. Three cases were considered in the differential diagnosis to involve Nager syndrome (Case 14), Cornelia de Lange syndrome (CdLS; Case 8), and Fraser syndrome (Case 10).

DISCUSSION

Congenital hand anomalies involve complex disorders such as polydactyly, syndactyly, reduction defects, or amniotic band sequence (ABS). Generally, cases detected around 20. GW should be carefully evaluated in terms of other structural abnormalities. These anomalies were first classified by Swanson according to the morphology of limb development and surgical procedures, with such classifications as 1) failure of formation (transverse deficiency (terminal arrest) or longitudinal (radial/ulnar longitudinal deficiency, central cleft of the hand)), 2) failure of differentiation (syndactyly, camptodactyly, clinodactyly), 3) duplications (preaxial/ thumb duplications, postaxial/5th finger duplications, mesoaxial polydactyly), 4) overgrowth (macroductyly), 5) undergrowth (thumb hypoplasia, brachydactyly), 6) amniotic band syndrome, and 7) generalized skeletal syndromes (4, 10). Since 2012, the International Federation of Societies for Surgery of the Hand (IFSSH) has recommended the Oberg-Manske-Tonkin (OMT) classification system as the new classification system for all congenital upper extremity anomalies (11). This embryology-based classification system includes malformations, deformities, dysplasias, and syndromes along the three axes of limb development. Malformations are divided in three subgroups: axis formation/differentiation of the entire upper limb, hand plate, or unspecified axis with respect to the proximal-distal, radial-ulnar (anteroposterior), and dorsal-ventral axes. Deformations mostly involve constriction rings. Dysplasias consist of segmental overgrowth or hypertrophy of the fingers (macroductyly) and/or unilaterally upper limb or tumoral growth. Approval has been given to the independent classification of syndromes. Recent publications have classified their cases according to the OMT system (3, 11, 14), which this study has done as well. Three syndromic cases were definitively diagnosed as having Greig cephalopolysyndactyly (Case 3), triploidy (Case 5), and Apert Syndrome (Case 6). Furthermore, seven cases were preliminary diagnosed, with ciliopathies in Case 1, Meckel-Gruber syndrome in Cases 13 and 18, SRPS in Case 9, Nager syndrome in Case 14, Fraser syndrome in Case 10, and CdLS in Case 8. Case 11 was presented with segmenter overgrowth complicated by macroductyly and oligodactyly, which can be classified in the group of dysplasia. Case 12 with isolated hand anomaly was considered a radial longitudinal deficiency and classified as a malformation. Meanwhile, Cases 2, 4, and 7 were evaluated as multiple congenital anomalies because of major anomalies accompanying the hand anomalies. Three cases (Cases 15, 16, and 17) were affected by ABS.

Just as in the literature, polydactyly here was also the most common type of hand anomaly in our case series. Occasionally, an extra finger including a fingernail was connected to the

hand with a small skin tag. When polydactyly is accompanied by a polycystic or dysplastic kidney anomaly, ciliopathies should be considered. Ciliopathies include primary ciliary dyskinesia, cystic kidney disease, nephronophthisis, retinitis pigmentosa, Bardet-Biedl syndrome, oral-facial-digital syndrome, SRPS, Joubert syndrome, and Meckel-Gruber syndrome, which involve genetic mutations regarding the encoding proteins involved in cilia function (15). Meckel-Gruber syndrome should be on the differential diagnosis list, especially in the presence of occipital encephalocele (16). The remaining cases were evaluated in the ciliopathy group, and WES was planned as a case with a preliminary diagnosis of SRPS. Common syndromic craniosynostosis syndromes including Crouzon, Pfeiffer, and Saethre-Chotzen are caused by mutations in the *FGFR2* gene and can have similar clinical manifestations. Mutations in the *FGFR2* comprise the majority of known mutations in syndromic forms of craniosynostosis. Our case with the syndactyly craniosynostosis diagnosed as Apert with mitten-like acrosyndactyly involved a wide abdominal circumference, segmental intestinal dilated colon, and rectum anomaly. Intestinal findings of the case where no postmortem autopsy had been conducted were found to be consistent with other intestinal findings such as intestinal malrotation, obstruction, and atresia, which in the literature are reported more frequently in the general population in patients with FGFR-related craniosynostosis syndrome (17).

ABS is a disruptive condition which surrounds the limbs or any part of the fetal body by the congenital constriction rings formed by fibrous bands of the amniotic sac. Constriction bands can cause permanent or transient disruption of the tissues under pressure. ABS is classified within the spectrum ranging from mild to severe as: 1) simple constriction rings, 2) rings with distal soft tissue deformity with or without lymphedema, 3) distal bone syndactyly, and 4) terminal amputation. In our case series, Cases 15, 16 and 17 were affected by ABS. Interestingly, Case 16 with ABS was complicated by tibial bowing, which is difficult to predict for *in-utero* ABS. However, the literature does contain some ABS reports with tibial bowing. A transient constriction by an amniotic band *in utero* may cause congenital bowing of the tibia (18). However, ABS should be distinguished from symbrachydactyly and transverse deficiency. Symbrachydactyly is an anomaly of the hand caused by Poland sequence or other similar anomalies of vascular disruption that affects all fingers unilaterally. Unlike ABS, the nail structure is present because ectodermal development is not affected in symbrachydactyly (19, 20). Fetal cases involving hand abnormalities should be referred to a perinatologist and clinical geneticist for further evaluation and counselling (21). These cases should be carefully evaluated for other structural abnormalities. If chromosomal abnormalities are suspected, invasive tests such as chorionic villus sampling and amniocentesis should be recommended, and if the karyotype analysis returns normal, an array-CGH should be performed.

The identification of hand anomalies should prompt a careful and detailed anomaly survey for any other structural

abnormality. After careful evaluation, the diagnosis should be made by advanced cytogenetic and molecular tests with a multidisciplinary team consisting of perinatologists, clinical geneticists, and a hand surgeon.

Providing families with the right genetic counseling is very important in terms of the treatment, prognosis, and recurrence risks of such diseases.

Ethics Committee Approval: This study procedure was approved by the relevant animal experimental local ethics committee of Istanbul University (E-29624016-050.99-52402).

Peer-review: Externally peer-reviewed.

Author Contributions: Conception/Design of Study – A.D.A., T.S.S., T.K.; Data Acquisition – A.D.A., T.S.S., T.K., S.B., O.U.; Data Analysis/ Interpretation – A.D.A., T.S.S., T.K., S.B., O.U.; Drafting Manuscript – A.D.A., T.S.S., T.K., S.B., O.U.; Critical Revision of Manuscript - A.D.A., T.S.S., T.K., S.B., O.U.; Final Approval and Accountability – A.D.A., T.S.S., T.K., S.B., O.U.

Conflicts of Interest: The authors declare no conflict of interest.

Financial Disclosure: The authors declare that this study has received no financial support.

REFERENCES

- Goldfarb CA, Shaw N, Steffen JA, Wall LB. The prevalence of congenital hand and upper extremity anomalies based upon the New York congenital malformations registry. *J Pediatr Orthop* 2017; 37(2): 144-8. [\[CrossRef\]](#)
- Ekblom AG, Laurell T, Arner M. Epidemiology of congenital upper limb anomalies in 562 children born in 1997 to 2007: a total population study from Stockholm, Sweden. *J Hand Surg Am* 2010; 35: 1742-54. [\[CrossRef\]](#)
- Oberg KC, Feenstra JM, Manske PR, Tonkin MA. Developmental biology and classification of congenital anomalies of the hand and upper extremity. *J Hand Surg Am* 2010; 35(12): 2066-76. [\[CrossRef\]](#)
- Manske PR, Oberg KC. Classification and developmental biology of congenital anomalies of the hand and upper extremity. *J Bone Joint Surg Am* 2009; 91(Suppl 4): 3-18. [\[CrossRef\]](#)
- Barham G, Clarke NM. Genetic regulation of embryological limb development with relation to congenital limb deformity in humans. *J Child Orthop* 2008; 2(1): 1-9. [\[CrossRef\]](#)
- Umair M, Ahmad F, Bilal M, Ahmad W, Alfadhel M. Clinical genetics of polydactyly: an updated review. *Front Genet* 2018; 9: 447. [\[CrossRef\]](#)
- Ahmed H, Akbari H, Emami A, Akbari MR. Genetic overview of syndactyly and polydactyly. *Plast Reconstr Surg Glob Open* 2017; 5(11): 1549. [\[CrossRef\]](#)
- Jose R, O'Brien M, Burke F. Congenital hand anomalies. In: Bentley G, editor. *European Surgical Orthopaedics and Traumatology*. Berlin, Heidelberg: Springer; 2014.p.1653-73. [\[CrossRef\]](#)
- Richards S, Aziz N, Bale S, Bick D, Das S, Gastier-Foster J, et al. ACMG Laboratory Quality Assurance Committee. Standards and guidelines for the interpretation of sequence variants: a joint consensus recommendation of the American College of Medical Genetics and Genomics and the Association for Molecular Pathology. *Genet Med* 2015; 17(5): 405-24. [\[CrossRef\]](#)
- De Smet L. IFSSH. International Federation for Societies for Surgery of the Hand JSSH. Japanese Society for Surgery of the Hand. Classification for congenital anomalies of the hand: the IFSSH classification and the JSSH modification. *Genet Couns* 2002; 13(3): 331-8.
- Ezaki M, Baek GH, Horii E, Hovius S. IFSSH scientific committee on congenital conditions. *J Hand Surg Eur* 2014; 39: 676-8. [\[CrossRef\]](#)
- Tonkin MA, Tolerton SK, Quick TJ, Harvey I, Lawson RD, Smith NC, et al. Classification of congenital anomalies of the hand and upper limb: development and assessment of a new system. *J Hand Surg Am* 2013; 38(9): 1845-53. [\[CrossRef\]](#)
- Uzun H, Özdemir FDM, Üstün GG, Sakarya AH, Bitik O, Aksu AE. Oberg-Manske-Tonkin classification of congenital upper extremity anomalies: The first report from Turkey. *Ann Plast Surg* 2020; 85(3): 245-50. [\[CrossRef\]](#)
- Wall LB, McCombe D, Goldfarb CA, Lam WL; ICHAD study group. The Oberg, Manske, and Tonkin classification of congenital upper limb anomalies: A consensus decision-making study for difficult or unclassifiable cases. *J Hand Surg Am* 2022; S0363-5023(22)423-3. [\[CrossRef\]](#)
- Waters AM, Beales PL. Ciliopathies: an expanding disease spectrum. *Pediatr Nephrol* 2011; 26(7): 1039-56. [\[CrossRef\]](#)
- Hildebrandt F, Benzing T, Katsanis N. Ciliopathies. *N Engl J Med* 2011; 364(16): 1533-43. [\[CrossRef\]](#)
- Hibberd CE, Bowdin S, Arudchelvan Y, Forrest CR, Brakora KA, Marcucio RS, Gong SG. FGFR-associated craniosynostosis syndromes and gastrointestinal defects. *Am J Med Genet A* 2016; 170(12): 3215-21. [\[CrossRef\]](#)
- Shah HH, Doddabasappa SN, Joseph B. Congenital posteromedial bowing of the tibia: a retrospective analysis of growth abnormalities in the leg. *J Pediatr Orthop B* 2009; 18(3): 120-8. [\[CrossRef\]](#)
- Moran SL, Jensen M, Bravo C. Amniotic band syndrome of the upper extremity: diagnosis and management. *J Am Acad Orthop Surg* 2007; 15: 397-407. [\[CrossRef\]](#)
- Gogola, G. Constriction Band Syndromes. In: Abzug J, Kozin S, Zlotolow D, editors. *The Pediatric Upper Extremity*. New York: Springer; 2015.p.413-29. [\[CrossRef\]](#)
- Ermito S, Dinatale A, Carrara S, Cavaliere A, Imbruglia L, Recupero S. Prenatal diagnosis of limb abnormalities: role of fetal ultrasonography. *J Prenat Med* 2009; 3(2): 18-22.

Activation-Induced Cytidine Deaminase Expression in Patients with Chronic Myeloid Leukemia

Emin Oguz¹ , Aynur Daglar Aday² , Akif Selim Yavuz³ 

¹Department of Internal Medicine, Division of Rheumatology, Van Education and Research Hospital, Van, Turkiye

²Department of Internal Medicine, Division of Medical Genetics, Istanbul Faculty of Medicine, Istanbul University, Istanbul, Turkiye

³Department of Internal Medicine, Division of Hematology, Istanbul Faculty of Medicine, Istanbul University, Istanbul, Turkiye

ORCID ID: E.O. 0000-0001-8165-7650; A.D.A. 0000-0001-8072-0646; A.S.Y. 0000-0001-9049-4654

Cite this article as: Oguz E, Daglar Aday A, Yavuz AS. Activation-induced cytidine deaminase expression in patients with chronic myeloid leukemia. *Experimed* 2022; 12(3): 155-9.

ABSTRACT

Objective: The findings on chronic myeloid leukemia (CML) patients suggest that clonal tumoral cells tend to have additional mutations besides the formation of the *BCR-ABL* fusion gene. Previous studies have demonstrated abnormal activation-induced cytidine deaminase (*AID*) expression in various types of cancer, showing *AID* transcript levels to be elevated in the CML blast phase. The study aimed to investigate the *AID* gene expression levels in CML and to investigate the etiopathogenic role of *AID*, which is not yet fully understood.

Materials and Methods: This study analyzed the *AID* transcript levels of 80 CML patients and 50 controls using real-time quantitative reverse transcription polymerase chain reaction (qRT-PCR).

Results: The study found the *AID* transcript levels to be significantly elevated ($p < 0.001$) in the CML patients compared to the control group, with no significance in *AID* transcript levels with regard to the patients' age, gender, clinical characteristics, or laboratory findings. No correlation was found between the *AID* and *BCR-ABL* transcript levels, while a positive correlation was present between *AID* transcript levels and presence of polymorphonuclear leukocytes (PMNL; $r = 0.320, p = 0.021$). No significant relationship occurred in *AID* transcription levels with the tyrosine-kinase-inhibitor (TKI) resistant mutation profile or cytogenetic response during TKI therapy.

Conclusion: This study found *AID* expression levels to be significantly elevated in CML patients and *AID* to be able to contribute to the etiopathogenesis of CML.

Keywords: Chronic myeloid leukemia, gene expression, cytidine deaminase

INTRODUCTION

Chronic myeloid leukemia (CML) is a myeloproliferative disease characterized by a reciprocal t(9;22) translocation leading to the formation of the Philadelphia chromosome. The newly formed fusion gene product *BCR-ABL* protein has aberrant tyrosine kinase activity, constituting the pathogenesis of CML (1).

Class-switching recombination (CSR) and somatic hypermutation (SHM) happen after naive B cells meet antigens in secondary lymphoid tissues. The activation-induced cytidine deaminase (*AID*), a member of the apolipoprotein B mRNA editing catalytic polypeptide-like family (APOBEC), takes part in these diversification processes (2). The *AICDA* gene encodes the 24 kDa *AID*

enzyme (3), and SHMs produce mutations in the DNA sequence (4). The *AID* enzyme converts cytosine residues in the immunoglobulin (Ig) variable region to uracil, and the body attempts to repair this error using base excision or mismatch repair mechanisms (5). *AID* can also alter gene expression through its effect on DNA demethylation, which can induce tumorigenesis due to genomic instability (6). Recent studies have reported ten–eleven translocation (TET) family members, particularly *TET2* and *AID*, to collaborate in DNA demethylation processes (7). *AID* is usually expressed in stimulated B cells, has been shown to be ectopically expressed, and induces CSR and SHM in a variety of non-lymphoid cells (8). Abnormal expression and secretion of Igs has also been reported in non-lymphoid cancer cells (6, 9). The expression of *AID* is strictly controlled

Corresponding Author: Aynur Daglar Aday **E-mail:** aynur.aday@istanbul.edu.tr

Submitted: 24.10.2022 **Revision Requested:** 14.11.2022 **Last Revision Received:** 16.11.2022 **Accepted:** 25.11.2022 **Published Online:** 30.12.2022



Content of this journal is licensed under a Creative Commons Attribution-NonCommercial 4.0 International License.

due to its mutagenic and recombinogenic ability, which can target the non-Ig genes as well as Ig genes that contribute to lymphogenesis (10).

Numerous reports are found stating deregulated AID activity to be able to induce various types of cancer, mainly as a result of its overexpression (11-14). This study aimed to identify the state of AID expression in CML patients and to reveal AID's etiopathogenic role, which is not yet fully understood.

MATERIALS AND METHODS

Study Population

This study was comprised of 80 CML cases being followed up in the Hematology Department of Istanbul Medical Faculty between November 1995-January 2014. Laboratory and clinical data, as well as computer records of the CML patients' information were reviewed. The patients' leukocyte, hemoglobin, and platelet counts at the time of diagnosis; leukocyte formula; bone marrow biopsy findings (bone marrow cellularity, fibrosis status); presence/absence of hepatomegaly; splenomegaly level; Sokal Score; disease stage; drug use history; and final status were recorded. Patient diagnoses were based on the criteria the World Health Organization had recommended in 2008 (15). The control group consisted of 50 healthy volunteers with no history of CML. 10 mL peripheral blood samples were drawn in sterile tubes containing EDTA, and complete blood counts were assayed during sampling. The study protocol was handled in accordance with the Declaration of Helsinki (16), with approval being obtained from the local ethics committee. Signed written informed consent was also obtained from all participants.

RNA Extraction and cDNA Synthesis

Total RNA extraction and cDNA synthesis were conducted using the respective High Pure RNA Isolation Kit and RevertAid First Strand cDNA Synthesis Kit (Roche Diagnostics, Mannheim, Germany).

Analysis of AID Gene Expression

Analysis of AID expression was carried out using real-time quantitative reverse transcription polymerase chain reaction (qRT-PCR) with the Real-Time Ready Universal Probelibrary Assay on the LightCycler 480 II Instrument (Roche Diagnostics, Mannheim, Germany) under the following PCR conditions: 95°C for 5 minutes, 95°C for 10 seconds, 58°C for 10 seconds, and 72°C for 15 seconds (40 cycles). The AID gene was amplified using forward 5'-TGGACACACCACTATGGAGAGC-3' and reverse 5'-GCGGACATTTTGAATTGGT-3' oligonucleotides. The HPRT1 gene was amplified using forward 5'-GACCAGTCAAACAGGGGACAT-3' and reverse 5'-GTGTC AATTATATCTCCACAATCAAG-3' oligonucleotides. Gene expressions were normalized using the internal control gene hypoxanthine phosphoribosyltransferase 1 (HPRT1) and calculated using the 2^{-ΔΔCT} method.

Statistical Analyses

Statistical analysis was performed using the statistical software program SPSS (ver. 21.0). The Mann-Whitney U and Student's t tests were used to analyze the distributions of the data. The chi-square test was used to analyze the categorical data. The

Spearman correlation test was conducted for the correlation analysis. Continuous variables were determined as mean ± standard deviation (SD), with a *p* < 0.05 being accepted as statistically significant.

RESULTS

The patient group consisted of 80 CML cases with a patient mean age of 53.7 ± 15.2 (range = 22-87; 33 females and 47 males). The mean age of the controls was 50.1 ± 16.4 (range = 24-85; 25 females, 25 males). The mean age and female-to-male ratio of the patient and control groups were similar (*p* = 0.515 and *p* = 0.329, respectively). Laboratory findings and clinical features of the patient group are given in Table 1.

Table 1. Laboratory findings and clinical features of the patient group.

Age (mean±SD)	53.7±15.2
Female: male ratio (n)	33: 47
Leukocyte at diagnosis (X10 ⁹ /L) (mean±SD)	15.8±10.9
Hemoglobin count at diagnosis (mean±SD) (g/dl)	11.0±1.8
Platelet count at diagnosis (X10 ⁹ /L) (mean±SD)	402.7±180.8
Polymorphonuclear leukocytes (PMNL) (%)	48.4 ±15.8
Red cells (%)	17.8±7.7
Eosinophil (%)	1.8±1.8
Basophil (%)	4.4±6.0
Blast (%)	1.6±2.2
Presence of splenomegaly at diagnosis n (%)	24 (30)
Spleen size at diagnosis (cm)	5.9±5.6
Disease phase at diagnosis n (%)	
Accelerated phase	5 (6.25)
Chronic phase	75 (93.75)
Bone marrow cellularity at diagnosis n (%)	
Hypercellular	78 (98.3)
Normocellular	2 (1.7)
Bone marrow reticulin fibrosis degree n (%)	
0	10 (12.5)
1	43 (53.75)
2	26 (32.5)
3	1 (1.25)
Sokal Score (mean ± SD)	1.0±0.4
Sokal classification n (%)	
Low	25 (31.25)
Intermediate	33 (41.25)
High	22 (27.5)
Presence of drug usage before TKI	21 (26.9)
Presence of TKI resistance mutation (n:15)	5 (35)
Presence of complete cytogenetic response	67 (83.3)
Disease duration, years (mean ± SD)	9.6±3.8
TKI: Tyrosine kinase inhibitor	

The mean *AID* expression level was 0.11 ± 0.1205 in the patient group and 0.0073 ± 0.0049 in the control group, with the mean *AID* expression level being significantly higher in the patients than in the controls ($p < 0.001$). The *AID* expression levels for the CML patient and control groups are given in Figure 1. *AID* expression levels do not seem to differ in terms of gender,

presence of splenomegaly, disease phase at diagnosis, degree of bone marrow reticulin fibrosis, Sokal score, presence of drug usage before tyrosine-kinase-inhibitor (TKI), or presence of complete cytogenetic response. Table 2 presents the relationships between patients' *AID* expression levels and their clinical features.

A strong correlation exists between patients' *AID* gene expression levels and polymorphonuclear leukocyte (PMNL) counts ($r = 0.320$; $p = 0.021$). The CML patients have a mean *BCR-ABL* fusion gene transcripts level of 0.07 ± 0.31 , with *AID* expression not being correlated to *BCR-ABL* expression ($r = -0.101$, $p = 0.374$).

DISCUSSION

Since the late 1990s, tremendous progress has been made in understanding the biology of CML. Studies indicate the *BCR-ABL* fusion gene to be essential for the initiation and progression of CML, while transformation from the chronic phase (CP) to the blast phase (BP) requires additional genetic and epigenetic abnormalities (18). Although the defining event is uniform, a progressive genetic instability is present, especially in patients in the accelerated phase (AP) or BP of CML, with the dependence of the disease on *BCR-ABL* activity decreasing as it progresses to the AP and BP (19, 20).

Genome sequencing has shed light on the finding regarding non-random mutation signatures in a variety of cancers. Studies

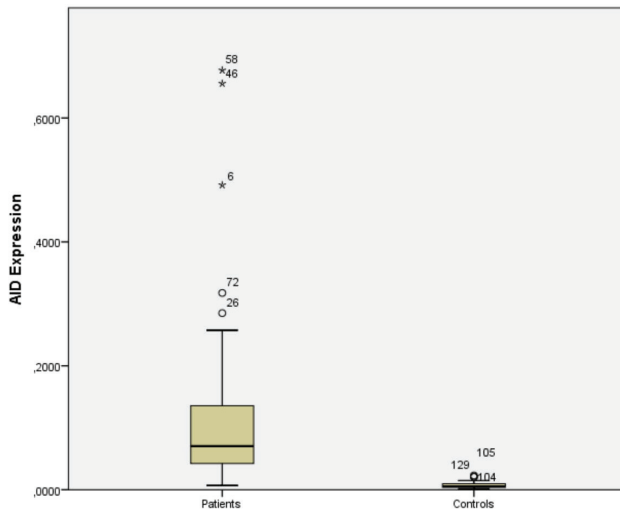


Figure 1. Figure 1. *AID* expression levels in CML patients' and control groups.

Table 2. Relationship between *AID* expression levels and clinical features of CML patients.

	AID mRNA expression	p-value
Gender		
Female	0.085±0.061	0.506
Male	0.128±0.146	
Presence of splenomegaly at diagnosis	0.116±0.143	
Disease phase at Diagnosis		
Accelerated phase	0.240±0.266	0.324
Chronic phase	0.103±0.102	
Bone marrow reticulin fibrosis degree (%)		
0	0.100±0.069	0.377
1	0.093±0.100	
2	0.134±0.149	
Sokal classification		
Low	0.087±0.069	0.951
Intermediate	0.126±0.152	
High	0.132±0.169	
Presence of drug usage before TKI	0.094±0.069	0.888
Presence of TKI resistance mutation (n:15)	0.132±0.202	0.462
Presence of complete cytogenetic response	0.113±0.119	0.175

TKI: Tyrosine Kinase Inhibitor

have shown the AID enzyme to recognize these specific motifs in DNA and to create mutations (13). Apart from enhancing the immune response, AID also acts to drive tumorigenesis by causing genome-wide mutations and double-strand breaks (21-23). Subsequently, continued AID expression increases the genetic plasticity of tumors (24, 25).

Studies on various types of cancers have provided evidence of aberrant AID expression to be able to induce mutations in non-Ig genes, including cancer-related genes, and to possibly participate in the development of solid tumors (e.g., colon, bladder, renal tumors) and hematological malignancies (e.g., B-cell lymphoma, multiple myeloma, CLL, ALL) (11, 12, 26, 27).

Previous studies on myelodysplastic syndrome and myeloproliferative neoplasms have found a strong association between AID overexpression and these malignancies (14, 17). Furthermore, Kunimoto et al. (7) demonstrated the important role AID has in myeloid and erythroid lineage differentiation by epigenetically regulating genes through active DNA methylation. Liu et al. (28) reported AID expression in CML cells to trigger general genetic instability by mutating tumor-suppressor and DNA-repair genes. In addition, they showed overexpression of AID to also promote lymphoid blast crisis (BC) in BCR-ABL+ CML and the AID and BCR-ABL genes to be overexpressed in lymphoid BC compared to CP in CML. Klemm et al. (24) demonstrated a causal role for AID activity in the formation of BCR-ABL mutations leading to TKI resistance and rapid progression to BC. Feldhahn et al. (11) and Gruber et al. (29) reported the kinase activity of BCR-ABL to upregulate AID expression and increase genetic instability, thus contributing to the progression of CML to BC and the leukemogenesis of BCR-ABL+ B-ALL. Assuming AID to be an oncogene that initiates tumorigenesis, a therapy targeting AID has been suggested for possibly suppressing processes such as cell proliferation and migration (17).

The current study found AID expression to be much higher in the CML patient group compared to the control group. However, AID overexpression was not detected in patients who were imatinib resistant or in the AP. Considering CML's phases, ABL1 mutations are most frequently encountered in the AP and BP, with the current study finding most of the patients to be in the CP and no patients in the BC ($n_{CP} = 75$, $n_{AP} = 5$). Although patients' AID expression levels were higher than the patients in CP, the difference was insignificant, the reason for this finding could possibly be the small number of patients in the AP. However, the highest AID gene expression levels detected in this study occurred in a patient in the AP. This finding is consistent with studies reporting increased AID gene expression in patients with advanced CML.

The study found a strong correlation between AID mRNA levels and the PMNL counts, which involve terminally differentiated myeloid cells that normally travel to the site of infection and destroy foreign bodies (30). Thus, AID appears to have a proliferative effect on PMNL cells.

CONCLUSION

The results of this study suggest the aberrant expression of the AID gene to be able to play a role in the etiopathogenesis of CML due to its mutation-inducing ability causing genetic instability. Further studies with larger groups are needed to elucidate the role of AID in CML.

Ethics Committee Approval: The study was approved by the Istanbul Faculty of Medicine Ethics Committee (Approval number: 2013/1759 date: 13.12.2013).

Informed Consent: Written informed consent was taken from all patients and healthy controls.

Peer-review: Externally peer-reviewed.

Author Contributions: Concept - A.S.Y.; Literature Search - E.O., A.D.A.; Data Collection and/or Processing - A.S.Y., E.O., A.D.A.; Analysis and/or Interpretation - A.D.A.; Writing: A.D.A.; Supervision - A.S.Y.; Final Approval and Accountability - E.O., A.D.A., A.S.Y.

Conflicts of Interest: The authors declare no conflict of interest.

Financial Disclosure: This research was granted by the Scientific Research Projects Unit of Istanbul University, Grant Number: 40224.

REFERENCES

1. Chereda B, Melo JV. Natural course and biology of CML. *Ann Hematol* 2015; 94(Suppl 2): S107-21. [\[CrossRef\]](#)
2. Muramatsu M, Kinoshita K, Fagarasan S, Yamada S, Shinkai Y, Honjo T. Class switch recombination and hypermutation require activation-induced cytidine deaminase (AID), a potential RNA editing enzyme. *Cell* 2000; 102(5): 553-63. [\[CrossRef\]](#)
3. Conticello SG. The AID/APOBEC family of nucleic acid mutators. *Genome Biol* 2008; 9(6): 229. [\[CrossRef\]](#)
4. Sablitzky F, Wildner G, Rajewsky K. Somatic mutation and clonal expansion of B cells in an antigen-driven immune response. *EMBO J* 1985; 4(2): 345-50. [\[CrossRef\]](#)
5. Rios LAS, Cloete B, Mowla S. Activation-induced cytidine deaminase: in sickness and in health. *J Cancer Res Clin Oncol* 2020; 146(11): 2721-30. [\[CrossRef\]](#)
6. Hu D, Zheng H, Liu H, Li M, Ren W, Liao W, et al. Immunoglobulin expression and its biological significance in cancer cells. *Cell Mol Immunol* 2008; 5(5): 319-24. [\[CrossRef\]](#)
7. Kunimoto H, McKenney AS, Meydan C, Shank K, Nazir A, Rapaport F, et al. AID is a key regulator of myeloid/erythroid differentiation and DNA methylation in hematopoietic stem/progenitor cells. *Blood* 2017; 129(13): 1779-90. [\[CrossRef\]](#)
8. Yu K, Huang FT, Lieber MR. DNA substrate length and surrounding sequence affect the activation-induced deaminase activity at cytidine. *J Biol Chem* 2004; 279(8): 6496-500. [\[CrossRef\]](#)
9. Chen Z, Qiu X, Gu J. Immunoglobulin expression in non-lymphoid lineage and neoplastic cells. *Am J Pathol* 2009; 174(4): 1139-48. [\[CrossRef\]](#)
10. Dominguez PM, Shaknovich R. Epigenetic function of activation-induced cytidine deaminase and its link to lymphomagenesis. *Front Immunol* 2014; 5: 642. [\[CrossRef\]](#)
11. Feldhahn N, Henke N, Melchior K, Duy C, Soh BN, Klein F, et al. Activation-induced cytidine deaminase acts as a mutator in BCR-ABL1-transformed acute lymphoblastic leukemia cells. *J Exp Med* 2007; 204(5): 1157-66. [\[CrossRef\]](#)

12. Maura F, Rustad EH, Yellapantula V, Łuksza M, Hoyos D, Maclachlan KH, et al. Role of AID in the temporal pattern of acquisition of driver mutations in multiple myeloma. *Leukemia* 2020; 34(5): 1476-80. [\[CrossRef\]](#)
13. Rebhandl S, Huemer M, Greil R, Geisberger R. AID/APOBEC deaminases and cancer. *Oncoscience* 2015; 2(4): 320-33. [\[CrossRef\]](#)
14. Torun ES, Dağlar Aday A, Nalçacı M. Activation-induced cytidine deaminase expression in patients with myelodysplastic syndrome and its relationship with prognosis and treatment. *Turk J Med Sci* 2021; 51(5): 2451-60. [\[CrossRef\]](#)
15. Tefferi A, Vardiman JW. Classification and diagnosis of myeloproliferative neoplasms: the 2008 World Health Organization criteria and point-of-care diagnostic algorithms. *Leukemia* 2008; 22(1): 14-22. [\[CrossRef\]](#)
16. World Medical Association. World Medical Association Declaration of Helsinki: Ethical principles for medical research involving human subjects. *JAMA* 2013; 310(20): 2191-4. [\[CrossRef\]](#)
17. Dermenci H, Daglar Aday A, Akadam Teker AB, Hancer V, Gelmez MY, Nalcaci M, et al. Aberrant activation-induced cytidine deaminase gene expression links BCR/ABL1-negative classical myeloproliferative neoplasms. *Med Bull Haseki* 2022; 60: 228-33. [\[CrossRef\]](#)
18. Ren R. Mechanisms of BCR-ABL in the pathogenesis of chronic myelogenous leukaemia. *Nat Rev Cancer* 2005; 5(3): 172-83. [\[CrossRef\]](#)
19. Ochi Y, Yoshida K, Huang YJ, Kuo MC, Nannya Y, Sasaki K, et al. Clonal evolution and clinical implications of genetic abnormalities in blastic transformation of chronic myeloid leukaemia. *Nat Commun* 2021; 12(1): 2833. [\[CrossRef\]](#)
20. Maiti A, Franquiz MJ, Ravandi F, Cortes JE, Jabbour EJ, Sasaki K, et al. Venetoclax and BCR-ABL tyrosine kinase inhibitor combinations: outcome in patients with philadelphia chromosome-positive advanced myeloid leukemias. *Acta Haematol* 2020; 143(6): 567-73. [\[CrossRef\]](#)
21. Okazaki IM, Hiai H, Kakazu N, Yamada S, Muramatsu M, Kinoshita K, et al. Constitutive expression of AID leads to tumorigenesis. *J Exp Med* 2003; 197(9): 1173-81. [\[CrossRef\]](#)
22. Pasqualucci L, Bhagat G, Jankovic M, Compagno M, Smith P, Muramatsu M, et al. AID is required for germinal center-derived lymphomagenesis. *Nat Genet* 2008; 40(1): 108-12. [\[CrossRef\]](#)
23. Robbiani DF, Bunting S, Feldhahn N, Bothmer A, Camps J, Deroubaix S, et al. AID produces DNA double-strand breaks in non-Ig genes and mature B cell lymphomas with reciprocal chromosome translocations. *Mol Cell* 2009; 36(4): 631-41. [\[CrossRef\]](#)
24. Klemm L, Duy C, Iacobucci I, Kuchen S, von Levetzow G, Feldhahn N, et al. The B cell mutator AID promotes B lymphoid blast crisis and drug resistance in chronic myeloid leukemia. *Cancer Cell* 2009; 16(3): 232-45. [\[CrossRef\]](#)
25. Muñoz DP, Lee EL, Takayama S, Coppé JP, Heo SJ, Boffelli D, et al. Activation-induced cytidine deaminase (AID) is necessary for the epithelial-mesenchymal transition in mammary epithelial cells. *Proc Natl Acad Sci USA* 2013; 110(32): E2977-86. [\[CrossRef\]](#)
26. Godsmark G, DE Souza Rios LA, Mowla S. Activation-induced cytidine deaminase promotes proliferation and enhances chemoresistance and migration in B-cell lymphoma. *Anticancer Res* 2021; 41(1): 237-47. [\[CrossRef\]](#)
27. Hancer VS, Kose M, Diz-Kucukkaya R, Yavuz AS, Aktan M. Activation-induced cytidine deaminase mRNA levels in chronic lymphocytic leukemia. *Leuk Lymphoma* 2011; 52(1): 79-84. [\[CrossRef\]](#)
28. Liu Z, Wu X, Duan Y, Wang Y, Shan B, Kong J, et al. AID expression is correlated with Bcr-Abl expression in CML-LBC and can be down-regulated by As₂O₃ and/or imatinib. *Leuk Res* 2011; 35(10): 1355-9. [\[CrossRef\]](#)
29. Gruber TA, Chang MS, Sposto R, Müschen M. Activation-induced cytidine deaminase accelerates clonal evolution in BCR-ABL1-driven B-cell lineage acute lymphoblastic leukemia. *Cancer Res* 2010; 70(19): 7411-20. [\[CrossRef\]](#)
30. Zingde S. The neutrophil in chronic myeloid leukaemia: Molecular analysis of chemotaxis, endocytosis and adhesion. *Cancer J* 1998; 11: 167-75.

Evaluating the Long-Term Outcomes of Medical and Surgical Treatments in Fibrostenotic Crohn's Disease Patients Treated with Anti-TNF/Biologic Therapy

Cagatay Ak¹ , Suleyman Sayar² , Resul Kahraman² , Kamil Ozdil² 

¹Department of Gastroenterology, Nigde Training and Research Hospital, Nigde, Turkiye

²Department of Gastroenterology, Umraniye Training and Research Hospital, Health Sciences University, Istanbul, Turkiye

ORCID ID: C.A. 0000-0002-2474-873X; S.S. 0000-0001-7089-6082; R.K. 0000-0001-5534-0860; K.Ö. 0000-0003-2556-3064

Cite this article as: Ak C, Sayar S, Kahraman R, Ozdil K. Evaluating the long-term outcomes of medical and surgical treatments in fibrostenotic Crohn's disease patients treated with anti-TNF/biologic therapy. *Experimed* 2022; 12(3): 160-7.

ABSTRACT

Objective: This study analyzed the follow-up findings on hospitalization requirements and clinical activities for fibrostenotic Crohn's disease (CD) patients who received biological/anti-TNF treatment without undergoing surgery as well as CD patients who were treated medically and surgically.

Materials and Methods: This study compared the Harvey-Bradshaw scores, control colonoscopy results, and hospitalization times regarding the long-term follow-ups for fibrostenotic CD patients who've undergone surgery and for those who only received medical treatment. In addition, the study analyzed the factors associated with disease activation.

Results: The study was consisted of 117 patients receiving anti-TNF therapy. Patients who underwent surgery for stenotic CD had a lower one year Harvey-Bradshaw score and shorter hospitalization regarding their long-term follow-up compared to those who did not undergo surgery. Patients who underwent surgery had a lower albumin level ($p < 0.001$) and developed perianal CD ($p = 0.046$) less than those who had not undergone surgery. C-reactive protein elevation ($p = 0.024$) and smoking ($p < 0.001$) have been associated with disease activity, and the absence of granuloma ($p = 0.003$) and neural plexitis ($p = 0.006$) on the surgical specimen was found to be associated with disease activation.

Conclusion: Surgical treatment is seen to improve the quality of life and result in fewer hospitalizations for fibrostenotic CD patients. Also, hypoalbuminemia may be a marker indicating a surgical decision.

Keywords: Crohn's disease, anti-TNF therapy, surgical therapy, disease activation

INTRODUCTION

Crohn's disease (CD) is a highly heterogeneous inflammatory bowel disease with different disease phenotypes, including perianal disease, fistulas, and strictures (1). CD is a chronic recurrent disease characterized by a decrease in the quality of life as a result of symptoms and a global health problem posing a significant financial burden for both patients and healthcare systems (2). One of CD's common complications is intestinal strictures, which occur in one-

third of patients within 10 years. CD strictures are classified as inflammatory, fibrotic, or mixed, but all symptomatic inflammatory strictures have some components of fibrosis (3). Many challenges still remain regarding treatment selection and management for patients with fibrostenotic CD. Medical therapy for inflammatory strictures is considered as the first-line therapy, with anti-TNF agents being one of the most important therapeutic agents used for this purpose. However, medical treatment is ineffective against strictures with a fibrotic component, with some

Corresponding Author: Cagatay Ak **E-mail:** cagatayak88@gmail.com

Submitted: 05.10.2022 **Revision Requested:** 31.10.2022 **Last Revision Received:** 30.11.2022 **Accepted:** 02.12.2022 **Published Online:** 29.12.2022



Content of this journal is licensed under a Creative Commons Attribution-NonCommercial 4.0 International License.

further studies suggesting anti-TNF agents to possibly increase the development of stenosis. A high proportion of patients on anti-TNF therapy will require surgery. In addition, although radiological imaging methods (magnetic resonance enterography (MRE), computed tomography enterography, ultrasonography and inflammatory indicators (C-reactive protein (CRP) and fecal calprotectin) can be useful in detecting the presence of the inflammatory component, these examination methods have limitations and low specificity. Therefore, predicting the success of a patient's response to medical therapy can be difficult. Meanwhile, the literature data on which medical and surgical treatment options might be more beneficial in terms of the effects of the natural course of the disease and its clinical outcomes are also unclear (4, 5). This study aimed to analyze and compare the follow-up findings in terms of hospitalization requirements, clinical activities, and laboratory findings for fibrostenotic CD patients who've received biological treatment as a medical treatment without undergoing surgery compared to patients who received medicine in addition to surgical therapy. In addition, the study analyzed the factors associated with disease activation in patients who were followed up with the biological/anti-TNF therapy in their long-term follow-up.

MATERIALS AND METHODS

The study involved 542 CD patients who visited the University of Health Sciences Gastroenterology Clinic of the Umraniye Training and Research Hospital between January 2010-June 2021. This study analyzed the patients who'd been diagnosed with CD based on clinical, laboratory, radiological, endoscopic, and histopathological findings and were followed up both through electronic files and the inflammatory bowel disease (IBD) outpatient clinic file. The study retrospectively recorded the data (clinical, laboratory, radiological, endoscopic data, operation epicrisis, hospitalization data) gathered during the diagnosis and follow-up of 64 patients with fibrostenotic CD who were monitored regularly at least twice a year and of 117 patients undergoing anti-TNF therapy. Figure 1 shows the inclusion and exclusion criteria of patients.

The study has also recorded the patients' demographic characteristics, age at disease onset, disease involvement (according to the Montreal classification), duration of biological treatment and medication (e.g., adalimumab, infliximab, vedolizumab), drug switching, and use of immunomodulatory drugs (azathioprine). MRE was used to measure stenosis in cm. The termination and onset of anti-TNF therapy were recorded for patients who'd developed ileocecal valve resection due to stenosis. The study also made use of the records pertained to the postoperative follow-up period; the Harvey Bradshaw scores before the operation and for the third, sixth, ninth, and twelfth months after the operation; and the Rutgeerts score at the 12th-month control colonoscopy for patients who'd undergone surgery. Records were also used regarding the initial, third, sixth, ninth, and twelfth month Harvey Bradshaw scores as well as the simple endoscopic score for Crohn's disease (SES-CD) during the 12th-month control colonoscopy for the

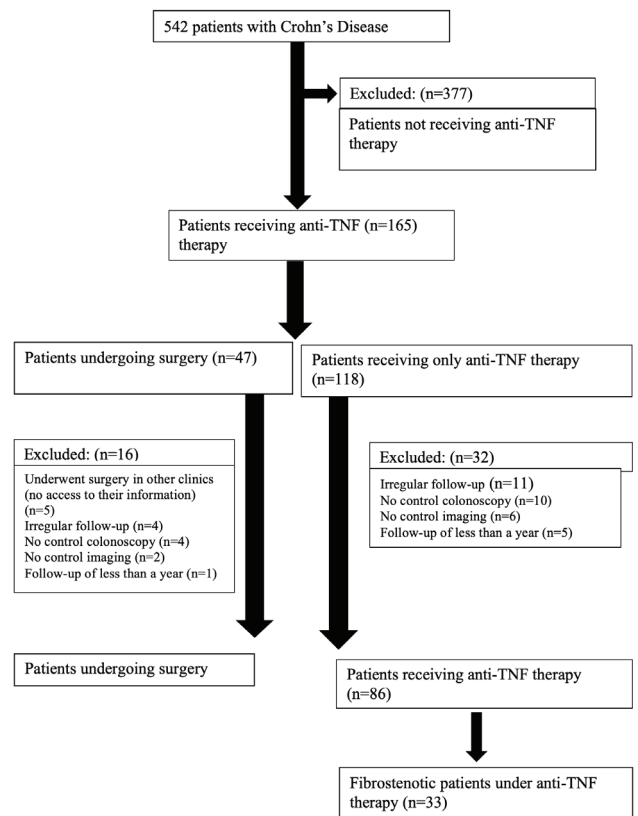


Figure 1. Inclusion and exclusion criteria of patients.

patients who were followed up with medical therapy. Albumin, sedimentation, CRP levels, tobacco use status, perianal CD, fistulas, abscess development, and the number and length of hospitalizations during long-term follow-up (after the onset of anti-TNF therapy) were recorded for all patients upon starting anti-TNF therapy. A Rutgeerts score of < 2 and an SES-CD score of < 6 in the control colonoscopy indicates endoscopic remission. Non-operated patients who were hospitalized for stenosis at least once and whose stenosis was documented through control imaging and/or endoscopically were defined as stenotic non-operated patients. Non-operated and non-stenotic patients receiving anti-TNF therapy were defined as non-operated non-stenotic patients. Perianal CD, abscesses, fistula development, and/or stenosis detection endoscopically during the long-term follow-up after the treatment or operation were considered as indicators of disease activation. The Harvey Bradshaw scores and length of hospitalization stays in the long-term follow-up were compared in terms of the patients who'd been operated on for fibrostenotic stenosis and the patients who were only followed up through medical treatment. In addition, the study has analyzed the associations with disease activation in the long-term follow-up for all patients receiving biologic and anti-TNF therapy.

Statistical Analyses

This study accepted statistical significance level as $p < 0.05$ and used the program SPSS (ver. 25) to perform the analysis and the

Kolmogorov-Smirnov test for normality testing. The study used means and standard deviations for the normally distributed data, while medians and interquartile range methods (IQR) were used for the non-normally distributed data. The study analyzed the normally distributed data using the independent t-test and the non-normally distributed data using the Mann-Whitney U test. The chi-square test has been used for evaluating the categorical data.

RESULTS

The patients ($n = 542$) had a mean age of 41.4 ± 11.4 years, and more than half the patients were men (56.4%). Table 1 shows the patients' general characteristics, treatments, complication rates, tobacco use status, and laboratory findings during the follow-up. Of the patients, 31 underwent ileocecal resection (26.5%), two of whom underwent surgery again due to having developed stenosis during the long-term follow-up (6.5%). Of all the patients, 33 were non-operated stenotic patients (28.2%). Table 2 shows these patients' general characteristics, treatments, clinical and endoscopic scores, and complication rates during the long-term follow-up. Patients were monitored for an average of 69.1 ± 37.4 months in total. Table 3 shows the analysis of the activity-related factors during the long-term follow-up.

DISCUSSION

Fibrotic CD is a prevalent and compelling clinical phenomenon. A considerable number of patients may require surgical intervention due to medical treatment being unlikely to reverse intestinal damage and fibrosis. Surgical treatment due to the absence of anti-fibrotic therapy depends on the location and length of the disease, concomitant complications, and patient preference (6). Although anti-TNF therapy has been proven effective in inducing and maintaining successful treatment of moderate-to-severe active CD patients, long-term bowel resection is inevitable in most patients (7). CD patients have a cumulative surgical risk of 16.3% in the first, 33.3% in the fifth, and 46.6% in the tenth year (8). Riss et al. (9) also reported an 8.6% recurrence rate for required surgery after an average follow-up of more than eight years. The current study has found 31 patients (26.5%) to have undergone surgery and two (6.5%) to have undergone a second surgery due to relapse. These rates were slightly lower when compared with the other study, possibly due to the fact that all patients who underwent surgery had also undergone anti-TNF therapy.

Research has also revealed postoperative treatment with an anti-TNF agent to decrease the risk of both clinical and endoscopic recurrence (10-12). Schwartz et al. (13) found the risk of perianal CD to be 55% at a median of 4.8 years post-diagnosis. Fistulizing CD is likely to develop in 35% of patients, 46% of which are non-perianal (14). The rate of perianal CD decreases with the increased use of thiopurine and anti-TNF therapy (15). The present study found the perianal CD and non-perianal fistulizing CD rates to respectively be 24.8% and 18.8% during the long-term follow-up under anti-TNF therapy

with and without thiopurine treatment. These lower rates of perianal CD and fistulizing CD compared to previous studies may possibly be related to the fact that all patients had received the anti-TNF therapy, either with or without the thiopurine treatment. The European Crohn's and Colitis Organization

Table 1. General characteristics, treatments, complication rates, tobacco use status, and laboratory findings during follow-up.

Parameters	
Age (year)	41.4±11.4
Female	51 (43.6%)
Male	66 (56.4%)
Disease type L1/ L2/ L3	37 (31.6%) / 9 (7.7%) / 71 (60.7%)
Operated stenotic patients	31 (26.5%)
Non-operated stenotic patients	33 (28.2%)
Non-operated non-stenotic patients	53 (45.3%)
Follow-up time (month)	69.1±37.4
Treatment	
Infliximab	60 (51.3%)
Adalimumab	52 (44.4%)
Vedolizumab	5 (4.3%)
Azathioprine	79 (67.5%)
Drug switching	12 (10.3%)
Activation	36 (30.8%)
Fistula	22 (18.8%)
Enterocutaneous	14 (63.6%)
Enteroenteric	5 (22.7%)
Enterovesican	2 (9.1%)
Enterovaginal	1 (4.5%)
Perianal Disease	29 (24.8%)
Abscess	14 (12.0%)
Smoking	22 (18.8%)
Albumin (g/dL)	3.66±0.44
ESR (mm /hour)	26.74±11.55
CRP (mg/dL)	3.10±2.54

L1: Ileal, L2: Colonic, L3: Ileocolonic, ESR: Erythrocyte Sedimentation Rate, CRP: C-reactive protein. Otherwise not mentioned, the values indicate (mean±SD) of the groups or number of individuals (percentages) in mentioned groups.

Table 2. Operated and non-operated stenotic patients' general characteristics, treatments, clinical and endoscopic scores, and complication rates during the long-term follow-up.

Parameters	Operated Patients (n=31)	Non-Operated Stenotic Patients (n=33)	p
Age (year)	42.3 ± 12.4	39.8 ± 10.7	0.390*
Female	11 (35.5%)	12 (36.4%)	0.942†
Male	20 (64.5%)	21 (63.6%)	
Disease type			
L1	13 (41.9%)	12 (36.4%)	
L2	0 (0.0%)	1 (1.6%)	0.900†
L3	18 (58.1%)	20 (59.4%)	
Diagnosis Time (month)	86 (Median) 69 (IQR)	52 (Median) 26 (IQR)	0.017‡
Medicated follow-up period (month)	50.1 ± 24.3	50.8 ± 27.4	0.902*
Preoperative medication (month)	20.2 ± 9.2		
Number of patients hospitalized	5 (16.1%)	17 (51.5%)	0.011†
Hospital (day)	8.40 ± 6.77	7.65 ± 6.74	0.829*
Medication			
Infliximab	15 (48.4%)	16 (48.5%)	-
Adalimumab	16 (51.6%)	16 (48.5%)	-
Vedolizumab	0 (%0)	1 (%3)	-
Azathioprine	17 (54.8%)	23 (69.7%)	0.343†
Drug switching	6 (19.4%)	3 (9.1%)	0.317†
Activity	8 (25.8%)	14 (42.4%)	0.201†
Fistula	7 (22.6%)	8 (24.2%)	0.796†
Perianal Disease	4 (12.9%)	12 (36.4%)	0.046†
Abscess	5 (16.1%)	7 (21.2%)	0.546†
Smoking	6 (19.4%)	9 (27.3%)	0.439†
Endoscopic Remission	26 (83.9%)	21 (63.6%)	0.466†
	Median(IQR)	Median(IQR)	
Harvey Bradshaw (month 0)	9 (3)	10 (2)	0.176‡
Harvey Bradshaw (month 3)	7 (3)	9 (2)	0.013‡
Harvey Bradshaw (month 6)	4 (3)	7 (3)	0.000‡
Harvey Bradshaw (month 9)	4 (1)	6 (2)	0.000‡
Harvey Bradshaw (month 12)	3 (2)	5 (3)	0.000‡
Stenosis length (cm)	11 (4)	8 (4)	0.011‡
Albumin (gr/dL)	3.3 (0.6)	3.8 (0.3)	0.000‡
ESR (mm /hour)	31.2 ± 9.7	30.6 ± 12.5	0.826*
CRP (mg/dL)	4.1 (4)	3.1 (2.9)	0.350‡

*: Independent t test, †: Chi-Square test, ‡: Man-Whitney U test, L1: Ileal, L2: Colonic, L3: Ileocolonic, ESR: Erythrocyte Sedimentation Rate, CRP: C-reactive protein. Otherwise not mentioned, the values indicate (mean ± SD) of the groups or number of individuals (percentages) in mentioned groups.

Table 3. Analysis of activity-related factors during the long-term follow-up.

Parameters	Activated (n = 36) (30.8%)	Non-Activated (n = 81) (69.2%)	p
Age (year)	39.5 ± 9.7	42.23 ± 12.1	0.237*
Gender			
Female	11 (30.6)	40 (49.4)	0.058†
Male	25 (69.4)	41 (50.6)	
Disease type			
L1	13 (36.1%)	24 (29.6%)	0.437†
L2	4 (11.1%)	5 (6.2%)	
L3	19 (52.8%)	52 (64.2%)	
	Median (IQR)	Median (IQR)	
Disease age (month)	56 - 63	53 - 59	0.571‡
Operated stenotic patients	8 (22.2%)	23 (28.4%)	0.231†
Non-operated stenotic patients	14 (38.9%)	19 (23.5%)	
Non-operated non-stenotic patients	14 (38.9%)	39 (48.1%)	
Medication			
Infliximab	18 (29.0%)	44 (71.0%)	0.666†
Adalimumab	18 (32.7%)	37 (67.3%)	
Azathiopirine	23 (63.9%)	56 (69.1%)	0.576†
Albumin (g/dL)	3.7 - 0.7 (IQR)	3.8 - 0.3 (IQR)	0.202‡
ESR (mm/hour)	28.0 ± 12.4	26.2 ± 11.2	0.425*
CRP (mg/dL)	3.7 - 3.5 (IQR)	2.2 - 2.2 (IQR)	0.024‡
Smoking	16 (44.4%)	6 (7.4%)	0.000†
Stenosis length (cm)	12.6 ± 4.1	9.0 ± 3.3	0.000*
Operated patients	n = 8 (25.8%)	n = 23 (74.2%)	
No granuloma	3 (15.8%)	16 (84.2%)	0.003†
No neural plexitis	6 (23.1%)	20 (76.9%)	0.006†
Medication termination day	19.7 ± 9.1	28.0 ± 19.8	0.335*
Medication onset day	80 ± 76.3	51.2 ± 25.8	0.327*

*: Independent t test, †: Chi-Square test, ‡: Mann-Whitney U test, L1: Ileitis CD, L2: Colonic CD, L3: Ileocolonic CD, ESR: Erythrocyte sedimentation rate, CRP: C-reactive protein. Otherwise not mentioned, the values indicate (mean ± SD) of the groups or number of individuals (percentages) in mentioned groups.

(ECCO) suggested that researchers perform studies comparing infliximab and surgery rates and stated, "Surgery is a sensible alternative for patients with disease refractory to conventional medical treatment and should also be discussed" (16). The present study observed the operated and non-operated

patients who'd received stenotic anti-TNF therapy to have similar baseline clinical and demographic characteristics and Harvey Bradshaw scores. The operated patients had statistically lower Harvey Bradshaw scores compared to the non-operated patients during the one-year follow-up at three-month

intervals. In addition, only 16% of the operated patients had hospitalizations due to stenosis compared to 51.5% of the non-operated stenotic patients during the long-term follow-up ($p = 0.011$). In the 12th month, 83.9% of the operated patients were in endoscopic remission compared to 63.6% of the non-operated patients with strictures, but the difference is not statistically significant ($p = 0.466$). Ponsioen et al. (17) compared laparoscopic ileocaecal resection and infliximab for terminal ileitis in CD and found the early surgical and anti-TNF groups to have similar endoscopic remission rates at one year but the former to have a better general quality of life and lower medical costs than the latter. The current study has found no remarkable difference in sedimentation or CRP values between operated patients and non-operated patients with strictures. However, the operated and non-operated patients with strictures had respective albumin levels of 3.3 gr/dL (IRQ = 0.6) and 3.8 gr/dL (IRQ = 0.3; $p < 0.001$). Zhou et al. (18) found patients with albumin levels under 3.5 g/dL to have a higher rate of penetrating disease and emergency surgery compared to those with albumin levels over 3.5 g/dL. In CD, hypoalbuminemia is correlated with disease activation without no association to malnutrition, and low preoperative albumin is an independent risk factor for postoperative complications (19, 20). However, no data is found regarding the effect of hypoalbuminemia on surgery decisions. Significantly low albumin levels being detected in the operated group suggests that albumin levels may be a marker for decision to perform surgery; however, further studies are still needed on this subject.

No significant difference was found regarding fistula and abscess development in the long-term follow-up with regard to operated and non-operated patients ($p = 0.796$, $p = 0.546$, respectively). Operated patients and non-operated stenotic patients had similar disease involvement according to the Montreal classification, with perianal CD being more common in stenotic patients in the long-term follow-up compared to the non-operated patients ($p = 0.046$). This may be related to the transport of inflammatory cytokine load from the inflamed intestinal segment to the anal region by means of stool transport.

Domenech et al. (21) focused on the clinical outcomes of newly diagnosed CD patients before and after infliximab availability and found infliximab availability to have not reduced the need for surgery. The current study's results revealed fibrostenotic CD patients undergoing anti-TNF therapy to likely need surgery in the natural course of the disease, to have a better quality of life in the postoperative period, and to have experienced less disease-related hospitalization. Research studies have also reported better quality of life and less hospitalization during long-term follow-ups (17, 22).

The present study observed long-term disease activation in 36% of all patients undergoing anti-TNF therapy. Patients with the presence and absence of disease activation are also observed to have similar demographic and clinical characteristics and to have made similar treatment choices. Tobacco use was statistically higher in patients with disease activation ($p <$

0.001). Gracie and Ford's (23) systematic meta-analysis of 33 studies on the adverse effects of tobacco use on CD ($n = 11,000$) reported smokers to have 55%–85% higher rates of flare-up regarding disease activity compared to non-smokers. The present study found patients with disease activation to have higher CRP levels compared to those without disease activation ($p = 0.024$). Nevertheless, no remarkable difference was found regarding erythrocyte sedimentation rates between patients with and without disease activation ($p = 0.425$). Fagan et al. (24) found a correlation for disease activation with both CRP and erythrocyte sedimentation rate (ESR). However, they reported a more robust correlation between disease activation and CRP. Boschetti et al. (25) conducted a study on 86 CD patients who'd undergone ileocolonic resection and found a weak but significant difference in CRP concentrations between patients in endoscopic remission and those in recurrence. Earlier studies have also reported the effect of tobacco use and higher CRP levels on disease activation (24, 25). With regard to fibrostenotic CD, a surgical operation is performed on the refractory medical disease, with the most common procedure being bowel resection. Pathological evaluation of a resected bowel segment may also provide information about disease activation during long-term follow-up (26). Anselme et al. (27) found a significant association between granulomas and recurrence among patients who'd undergone surgery for CD ($n = 130$). Sokol et al. (28) also reported submucosal plexitis to be predictive of clinical recurrence ($n = 171$). The current study's results show the absence of granuloma in the surgical specimen ($p = 0.003$) and plexitis at the surgical margin ($p = 0.006$) to be correlated with no disease activation in the long-term follow-up. The time for termination and restart of anti-TNF therapy was also evaluated in terms of activation in operated patients during the long-term follow-up. Anti-TNF therapy was discontinued earlier for patients who experienced activation compared to those with no activation (19.7 ± 9.1 day vs. 28.0 ± 19.8 day). Anti-TNF therapy was initiated earlier in patients with activation compared to those with no activation (80 ± 76.3 day vs. 51.2 ± 25.8 day). The relationship between the discontinuation of preoperative anti-TNF therapy and postoperative onset time and postoperative disease activation remains unclear. Earlier termination and later initiation of anti-TNF therapy may be correlated with disease activation in long-term follow-up due to the loss of long-term anti-inflammatory pressure.

This study is one that compared the endoscopic and clinical long-term outcomes regarding the surgical and medical treatment of fibrostenotic CD and analyzed the factors related to activation during the long-term follow-up period. The study has two limitations: 1) it was conducted in only one center, and 2) it is a retrospective study.

CONCLUSION

Surgical treatment has been correlated with improved quality of life and fewer hospitalizations for fibrostenotic CD patients. Hypoalbuminemia may be a marker for a decision to perform surgery. Operated patients had no neural plexitis

and granuloma in their pathology specimen, which may be a marker for the lack of activation in long-term follow-up. Tobacco use and high CRP levels may predict disease activation during the long-term follow-up, with further comprehensive studies being needed in this regard.

Ethics Committee Approval: This study procedure was approved by the Istanbul Health Sciences University Umraniye Training and Research Hospital Clinical Research Ethics Committee (B.10.1.TKH.4.3 4.H.GP.0.01/230).

Peer-review: Externally peer-reviewed.

Author Contributions: Conception/Design of Study - C.A.; Data Acquisition - R.K.; Data Analysis/Interpretation - C.A., R.K.; Supervision - S.S.; Drafting Manuscript - C.A.; Critical Revision of Manuscript - C.A., R.K., K.O.; Final Approval and Accountability - C.A., R.K., S.S., K.O.

Conflicts of Interest: The authors declare no conflict of interest.

Financial Disclosure: The authors declare that this study has received no financial support.

REFERENCES

- Satsangi J, Silverberg MS, Vermeire S, Colombel JF. The Montreal classification of inflammatory bowel disease: controversies, consensus, and implications. *Gut* 2006; 55(6):749-53. [CrossRef]
- De Cruz P, Kamm MA, Prideaux L, Allen PB, Desmond PV. Postoperative recurrent luminal Crohn's disease: a systematic review. *Inflamm Bowel Dis* 2012; 18(4): 758-77. [CrossRef]
- Rieder F, Zimmermann EM, Remzi FH, Sandborn WJ. Crohn's disease complicated by strictures: a systematic review. *Gut* 2013; 62(7): 1072-84. [CrossRef]
- Yoo JH, Holubar S, Rieder F. Fibrostenotic strictures in Crohn's disease. *Intest Res* 2020; 18(4): 379-401. [CrossRef]
- Lu C, Baraty B, Lee Robertson H, Filyk A, Shen H, Fung T, et al. Stenosis Therapy and Research (STAR) Consortium. Systematic review: medical therapy for fibrostenosing Crohn's disease. *Aliment Pharmacol Ther*. 2020; 51(12): 1233-46. [CrossRef]
- Rieder F, Bettenworth D, Ma C, Parker CE, Williamson LA, Nelson SA, et al. An expert consensus to standardise definitions, diagnosis and treatment targets for anti-fibrotic stricture therapies in Crohn's disease. *Aliment Pharmacol Ther* 2018; 48(3): 347-57. [CrossRef]
- Murthy SK, Begum J, Benchimol EI, Bernstein CN, Kaplan GG, McCurdy JD, et al. Introduction of anti-TNF therapy has not yielded expected declines in hospitalisation and intestinal resection rates in inflammatory bowel diseases: a population-based interrupted time series study. *Gut* 2020; 69(2): 274-82. [CrossRef]
- Frolkis AD, Dykeman J, Negrón ME, Debruyne J, Jette N, Fiest KM, et al. Risk of surgery for inflammatory bowel diseases has decreased over time: a systematic review and meta-analysis of population-based studies. *Gastroenterology* 2013; 145(5): 996-1006. [CrossRef]
- Riss S, Schuster I, Papay P, Herbst F, Mittlböck M, Chitsabesan P, et al. Surgical recurrence after primary ileocolic resection for Crohn's disease. *Tech Coloproctol* 2014; 18(4): 365-71. [CrossRef]
- Regueiro M, Velayos F, Greer JB, Bougatsos C, Chou R, Sultan S, et al. American Gastroenterological Association Institute technical review on the management of Crohn's disease after surgical resection. *Gastroenterology* 2017; 152(1): 277-295. [CrossRef]
- Regueiro M, Feagan BG, Zou B, Johanns J, Blank MA, Chevrier M, et al. PREVENT Study Group. Infliximab reduces endoscopic, but not clinical, recurrence of Crohn's disease after ileocolonic resection. *Gastroenterology* 2016; 150(7): 1568-78. [CrossRef]
- Regueiro M, Schraut W, Baidoo L, Kip KE, Sepulveda AR, Pesci M, et al. Infliximab prevents Crohn's disease recurrence after ileal resection. *Gastroenterology* 2009; 136(2): 441-50. [CrossRef]
- Schwartz DA, Loftus EV, Tremaine WJ, Panaccione R, Sandborn WJ. The natural history of fistulizing Crohn's disease: a population based study. *Dig Liver Dis* 2000; 32(1): A18. [CrossRef]
- Schwartz DA, Loftus EV Jr, Tremaine WJ, Panaccione R, Harmsen WS, Zinsmeister AR, et al. The natural history of fistulizing Crohn's disease in Olmsted County, Minnesota. *Gastroenterology*. 2002; 122(4): 875-80. [CrossRef]
- Chhaya V, Saxena S, Cecil E, Subramanian V, Curcin V, Majeed A, et al. Have perianal surgery rates decreased with the rise in thiopurine use in Crohn's disease? *Gut* 2014; 63: A176. [CrossRef]
- Gomollón F, Dignass A, Annese V, Tilg H, Van Assche G, Lindsay JO, et al. ECCO. 3rd European Evidence-based Consensus on the diagnosis and management of Crohn's Disease 2016: Part 1: Diagnosis and medical management. *J Crohns Colitis*. 2017; 11(1): 3-25. [CrossRef]
- Ponsioen CY, de Groof EJ, Eshuis EJ, Gardenbroek TJ, Bossuyt PM, Hart A, et al. Laparoscopic ileocaecal resection versus infliximab for terminal ileitis in Crohn's disease: a randomised controlled, open-label, multicentre trial (published correction appears in *Lancet Gastroenterol Hepatol* 2017; 2(11): 785-92).
- Zhou J, Li Y, Gong J, Zhu W. No Association between staging operation and the 5-Year risk of reoperation in patients with Crohn's Disease. *Sci Rep* 2019; 9(1): 275. [CrossRef]
- Cabral VL, de Carvalho L, Miszputen SJ. Importância da albumina sérica na avaliação nutricional e de atividade inflamatória em pacientes com doença de Crohn (Importance of serum albumin values in nutritional assessment and inflammatory activity in patients with Crohn's disease). *Arq Gastroenterol* 2001; 38(2): 104-8. [CrossRef]
- Ge X, Liu H, Tang S, Wu Y, Pan Y, Liu W, et al. Preoperative hypoalbuminemia is an independent risk factor for postoperative complications in Crohn's disease patients with normal BMI: A cohort study. *Int J Surg*. 2020; 79: 294-9. [CrossRef]
- Domènech E, Zabana Y, Garcia-Planella E, López San Román A, Nos P, Ginard D, et al. Clinical outcome of newly diagnosed Crohn's disease: a comparative, retrospective study before and after infliximab availability. *Aliment Pharmacol Ther* 2010; 31(2): 233-9. [CrossRef]
- de Groof EJ, Stevens TW, Eshuis EJ, Gardenbroek TJ, Bosmans JE, van Dongen JM, et al. Cost-effectiveness of laparoscopic ileocaecal resection versus infliximab treatment of terminal ileitis in Crohn's disease: the LIRIC Trial. *Gut* 2019; 68(10): 1774-1780. [CrossRef]
- To N, Gracie DJ, Ford AC. Systematic review with meta-analysis: the adverse effects of tobacco smoking on the natural history of Crohn's disease. *Aliment Pharmacol Ther* 2016; 43(5): 549-61. [CrossRef]
- Fagan EA, Dyck RF, Maton PN, Hodgson HJ, Chadwick VS, Petrie A, et al. Serum levels of C-reactive protein in Crohn's disease and ulcerative colitis. *Eur J Clin Invest* 1982; 12(4): 351-9. [CrossRef]
- Boschetti G, Laidet M, Moussata D, Stefanescu C, Roblin X, Phelip G, et al. Levels of fecal calprotectin are associated with the severity of postoperative endoscopic recurrence in asymptomatic patients with Crohn's Disease. *Am J Gastroenterol* 2015; 110(6): 865-72. [CrossRef]
- Yamamoto T, Watanabe T. Surgery for luminal Crohn's disease. *World J Gastroenterol* 2014; 20(1):78-90. [CrossRef]

27. Anseline PF, Włodarczyk J, Murugasu R. Presence of granulomas is associated with recurrence after surgery for Crohn's disease: experience of a surgical unit. *Br J Surg* 1997; 84(1): 78-82. [\[CrossRef\]](#)
28. Sokol H, Polin V, Lavergne-Slove A, Panis Y, Treton X, Dray X, et al. Plexitis as a predictive factor of early postoperative clinical recurrence in Crohn's disease. *Gut* 2009; 58(9): 1218-25. [\[CrossRef\]](#)

Comparing the VDR Gene *BsmI* and *CDX2* Polymorphisms in Healthy Turks and Healthy Somalians Living in Turkiye

Ender Coskunpinar¹ , Betul Nilgun Engin² 

¹Department of Medical Biology, Faculty of Medicine, University of Health Sciences, Istanbul, Turkiye

²School of Medicine, University of Health Sciences, Istanbul, Turkiye

ORCID ID: E.C: 0000-0002-1003-5544; B.N.E. 0000-0002-9242-9909

Cite this article as: Coskunpinar E, Engin BE. Comparing the VDR gene *BsmI* and *CDX2* polymorphisms in healthy Turks and healthy Somalians living in Turkiye. *Experimed* 2022; 12(3): 168-73.

ABSTRACT

Objectives: This study aimed to evaluate genotypic and allelic differences by comparing the Vitamin D (Vit-D) receptor (VDR) gene *BsmI* (rs1544410) and *CDX2* (rs11568820) polymorphisms in healthy Turks and healthy Somalians living in Turkiye.

Materials and Methods: The study involved 100 healthy Turkish individuals and 60 healthy Somali individuals residing in Turkiye for at least 5 years. The genotyping study was performed using the polymerase chain reaction-restriction fragment length polymorphism (PCR-RFLP) and allele-specific PCR methods. Statistical analysis was performed to identify the possible differences between groups using the Chi-square and Student's t tests for pair-wise comparisons.

Results: According to the data obtained in the study with regard to the *BsmI* (rs1544410 A/G) and *CDX2* (rs11568820 A/G) genotypes, no statistically significant difference was determined to be present regarding the frequency of carrying the mutant GG genotype in the two groups ($p = 0.95$ and $p = 0.221$, respectively).

Conclusion: The study has found no significant genotypic or allelic difference to be present in terms of the *BsmI* (rs1544410) and *CDX2* (rs11568820) gene variants between healthy Turkish individuals and Somali individuals who have spent most of their lives exposed to less sunlight while living in Turkiye for the past five years.

Keywords: VDR, *BsmI* (rs1544410), *CDX2* (11568820), polymorphism

INTRODUCTION

Vitamin D (Vit-D) is a steroid hormone that is synthesized from cholesterol and binds to its intracellular polypeptide Vit-D receptor (VDR) to start its active mechanisms. The VDR regulates the expression of genes in Vit-D sensitive tissues and initiates the pathways necessary for the formation of biological effects. The VDR gene has eight introns and nine exons and is located in chromosome region 12q13.1. The most well-known function of Vit-D is to regulate bone metabolism through a calcium-phosphorus balance; as such, its deficiency is significant in the development of cardiovascular diseases and hypertension. Vit-D also has immune-regulatory functions, regulating both innate and

adaptive immunity (1). Vit-D is also known as an important regulator of innate immune responses to microbial challenges (2) and was accepted at the beginning of the 20th century as having a critical role in preventing rickets (3). Most of the Vit-D the human body consumes is produced by the skin as a result of exposure to sunlight. Vit-D is then processed by the liver and kidney to make it beneficial for bones (4). Sunlight is a very important factor for Vit-D production (5), and Vit-D has two forms: Vitamin D₂ (Ergocalciferol) and vitamin D₃ (Cholecalciferol) (6). When human skin is exposed to solar UVB radiation (wavelengths: 290-315 nm), 7-dehydrocholesterol is converted in the skin first to preVit-D₃, then from preVit-D₃ to Vit-D₃. Meanwhile, Vit-D₂ has yeast and fungal origins and can be converted

Corresponding Author: Ender Coskunpinar **E-mail:** ecoskunpinar@gmail.com

Submitted: 01.11.2022 **Revision Requested:** 23.11.2022 **Last Revision Received:** 23.11.2022 **Accepted:** 02.12.2022 **Published Online:** 00.00.2022



Content of this journal is licensed under a Creative Commons Attribution-NonCommercial 4.0 International License.

into Vit-D₃ when consumed with food. During the formation of Vit-D, the 25-hydroxyvit-D (25(OH)D) form is synthesized in the liver, and then the 1 α , 25-dihydroxyvit-D form is synthesized in the kidney (7). The amount of Vit-D production in the skin can vary depending on skin color, latitude, season and, surprisingly according to the time of day (8, 9). Supplementation of 400-1,000 IU per day for infants in the first year of life, 600-1,000 IU per day for children and adolescents between 1-18 years, and 1,500-2,000 IU per day for adults over 18 years is considered appropriate for preventing Vit-D deficiency (10).

Vit-D plays a central role in bone- and calcium-related processes, regulating bone metabolism by stimulating calcium and phosphate absorption in the intestine. Studies have shown a relationship to exist between many acute and chronic diseases such as cardiovascular diseases, liver and kidney diseases, preeclampsia, periodontitis, some autoimmune disorders, cancer, diabetes, and neurological disorders due to a Vit-D deficiency (4, 11). Vit-D also has several effects on bone metabolism, regulating arterial blood pressure, preventing cardiovascular complications, modulating immunological responses, regulating insulin production and preventing diabetes, and protecting against certain cancers (12).

The VDR is expressed in various parts of the brain throughout embryonic development, and the active form of Vit-D enables the activation of various target genes through the VDR (13). Therefore, some neuropsychiatric diseases have been associated with polymorphisms in the VDR (14). The stability of Vit-D-mediated signaling pathways is important for brain development (15), with functional polymorphisms affecting gene expression having been reported in this gene (16). Mutations in the *BsmI* rs1544410 variant have also been shown to be associated with neurodegenerative diseases (14, 16). As a result of studies, the association of polymorphisms with various diseases draws attention to the effectiveness of these genomic changes; however, the data are still quite limited (17-19). The *CDX2* (rs11568820) variant is associated with transcriptional activity, which can affect calcium absorption (20).

Considering that only 20% of all Vit-D needed by the body is obtained from food, geographical differences are thought to be important in terms of VDR gene polymorphisms. Evaluating the differences in skin color in this context may additionally

be appropriate. The number of studies conducted on healthy Somalians in the literature is extremely limited. Moreover, no study is found to have investigated the VDR gene *BsmI* and *CDX2* polymorphisms among Turkish and Somali individuals.

This study aimed to evaluate genotypic and allelic differences by comparing the VDR gene *BsmI* (rs1544410) and *CDX2* (rs11568820) polymorphisms between healthy Turks and healthy Somalians living in Türkiye. This study is the first study to examine these two gene regions (*BsmI* and *CDX2*) together.

MATERIALS AND METHODS

Study Design

The study involved 160 volunteers (90 female and 70 male) between the ages of 18-35 (Table 1). Ethics committee approval was obtained on December 1, 2021 with Decision no. 2015-KAEK-56-21-03 from the Biruni University Clinical Research Ethics Committee. After obtaining informed consent from the volunteers to participate in the study, 2 mL peripheral blood samples were taken. Next, the study conducted genotyping using DNA isolation, polymerase chain reaction (PCR), and then following restriction length polymorphism (RFLP) methods. The gene regions amplified by the PCR and restriction cut results have been visualized using agarose gel electrophoresis.

Volunteer Selection and Sample Obtainment

One hundred healthy Turks and 60 healthy Somalians living in Türkiye for at least 5 years between the ages of 18-35 have been included in the study, with 2 mL samples of peripheral blood being taken from the volunteers who signed the informed consent form. The samples were kept in a refrigerator at +4 °C until further processing.

DNA Isolation and PCR

DNA samples were extracted according to the kit protocol (High Pure PCR Template Preparation Kit /Product No: 11796828001) and stored in a -20°C refrigerator for use in subsequent processes. The DNA concentrations obtained as a result of the isolation method were measured using a Denovix DS-11 FX spectrophotometer, with a specific primer design being made for the *BsmI* (rs1544410) and *CDX2* (rs11568820) gene regions (Table 2).

Table 1. Comparison of age and gender in Turkish and Somali volunteers.

Gender	Turkish group					Somali group					p value
	(N=100)		%			(N=60)		%			
Female	66		66			24		40			*0.001
Male	34		34			36		60			
Age	N	Mean	Min.	Max.	SD	N	Mean	Min.	Max.	SD	p value
	100	26	18	35	4.008	60	23	19	26	1.610	0.241

N=Total number, SD=Standard deviation, Min=Minimum, Max=Maximum

Table 2. Primers designed for the VDR Gene *BsmI* (rs1544410) and *CDX2* rs11568820 regions.

Gene	Forward	Reverse
<i>CDX2</i> (rs11568820)	G-(5' AGGATAGAGAAAATAATAGAAAACATT 3') A-(5' TCCTGAGTAAACTAGGTCACAA 3')	5' AACCCATAATAAGAAATAAGTTTTCAC 3' 5' ACGTTAAGTTCAGAAAGATTAATTC 3'
<i>BsmI</i> (rs1544410)	5' CAACCAAGACTACAAGTACCGCGTCAGTGA 3'	5' AACCCAGCGGGAAGAGGTCAAGGG 3'

The PCR mix content for the *BsmI* (rs1544410) gene region was prepared as follows: 18.2 µL dH₂O; 2.5 µL buffer; 2 µL dNTP (2.5 mm); 0.5 µL forward primer; 0.5 µL reverse primer; 0.3 µL Taq polymerase. The PCR mix content was prepared for the *CDX2* (rs11568820) gene region as follows: 15.7 µL dH₂O; 2.5 µL buffer; 1.5 µL MgCl₂; 2 µL dNTP (2.5 mm); 0.5 µL forward primer1; 0.5 µL forward primer2; 0.5 µL reverse primer1; 0.5 µL reverse primer2; 0.3 µL Taq polymerase.

Appropriate binding conditions for the primers designed for the *BsmI* (rs1544410) region are as follows: pre-denaturation at 94°C for 1 minute, denaturation for 30 seconds at 94°C, primer attachment for 45 seconds at 58.9°C, chain elongation for 30 seconds at 72°C, and elongation at 72°C for 5 minutes. Appropriate binding conditions for primers designed for the *CDX2* (rs11568820) region are as follows: pre-denaturation at 94°C for 5 minutes, denaturation at 94°C for 30 seconds, primer binding at 54.8°C for 45 seconds, chain elongation at 72°C for 30 seconds, and elongation at 72°C for 5 minutes. The template was amplified using the Thermal Cycler (Blue-Ray/ tcst-9620) device over 35 cycles for *BsmI* (rs1544410) and 43 cycles for *CDX2* (rs11568820). Genotyping was done using the PCR and PCR-RFLP methods for the rs1544410 region. PCR and enzyme digestion products were amplified by the PCR method and carried out through restriction enzyme digestion for the *BsmI* (rs1544410) region followed by the agarose gel electrophoresis. These products were visualized in a transilluminator using a CCD camera under UV light. To evaluate the *CDX2* (rs11568820) region of the VDR gene, the study used the allele-specific PCR. The amplified rs11568820 region of the PCR products were separated by size in a 3% agarose gel electrophoresis. Gel staining was performed with ethidium bromide and also visualized in a transilluminator using a CCD camera under ultraviolet light.

Genotyping

Site-specific restriction enzymes were determined in order to detect variant changes in specific regions of the genes from different DNA regions that had been amplified using PCR. The reaction was prepared with the components whose specific amounts were adjusted for each enzyme for a total volume of 15 µL. Specific restriction enzymes were used for restriction cutting. The obtained product was run through the agarose gel electrophoresis to determine whether or not it has a mutation. The cut made by the restriction enzyme in certain regions was visualized in a transilluminator using a CCD camera under ultraviolet light following the agarose gel electrophoresis.

Analyzing the *BsmI* (rs1544410) Variant

The rs1544410 variant in the *BsmI* gene consists of 813 base pairs (bp). Using primers specifically designed for this region, the 813 bp regions were amplified using PCR and visualized over a 2% agarose gel. The amplified PCR products were then digested with the *MvaI*269I restriction enzyme. The mutant GG allele was displayed as a single 813-bp fragment, with the wild-type AA allele being displayed as two fragments of 478 bp and 335 bp, and the heterozygous AG allele being displayed as 3 fragments of 813 bp, 478 bp, and 335 bp (Figure 1).

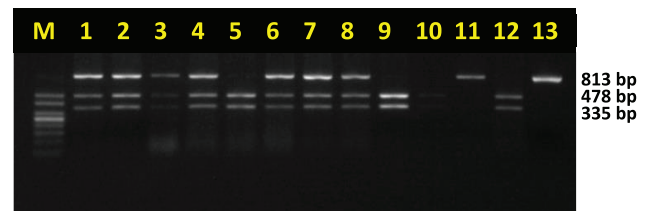


Figure 1. VDR gene *BsmI* digestion polymorphism products: Lane 1,2,3,4,6,7,8: AG heterozygous products, lane 5,9,12: AA wild type products, lane 11: GG homozygous product, lane 13 uncut control PCR product. M: Marker

Analyzing the *CDX2* (rs11568820) Variant

To analyze the *CDX2* (rs11568820) region, the study used the allele-specific PCR, which is a popular method for the DNA typing of SNPs. The single-tube PCR genotyping does not require enzyme cutting or manipulation of the PCR products (Figure 2).



Figure 2. Allele specific PCR analysis of the VDR gene *CDX2* polymorphism. Lane 12: positive control, lane 13: negative control, lane 1,2,4: GG homozygous products, lane 3,5,6,7,8,9,10,11: AG heterozygous products. M: 100 bp ladder.

Statistical Analyses

The program SPSS (ver. 25.0) was used to analyze the data, and the data were evaluated using the chi-square and Student’s t tests, with the statistical significance being accepted at $p < 0.05$.

RESULTS

The genotype and allele distributions for both groups are shown in Table 3. According to the data obtained in the study regarding the *BsmI* (rs1544410 A/G) and *CDX2* (11568820 A/G) genotypes, no statistically significant difference was determined in terms of the frequency individuals carrying the mutant GG genotype ($p = 0.95$ and $p = 0.221$, respectively), or alleles ($p = 0.97$ and $p = 0.18$, respectively) in the Somali group compared to the Turkish group.

Table 3. Genotype and allele distributions of *BsmI* (rs1544410) and *CDX2* (11568820) gene variants.

VDR <i>BsmI</i>	Somali Group		Turkish Group		X ²	P value
	N=60	%	N=100	%		
Genotyping						
AA	18	30	29	29.37	0.089	0.95
AG	31	51.67	54	53.13		
GG	11	18.33	17	17.5		
Allele						
A	67	55.83	112	56	0.0008	0.97
G	53	44.17	88	44		
VDR <i>CDX2</i>						
Genotyping						
AA	22	36.67	50	50	3.01	0.221
AG	25	41.67	30	30		
GG	13	21.66	20	20		
Allele						
A	69	57.5	130	65	1.79	0.18
G	51	42.5	70	35		

DISCUSSION

Vit-D deficiency arises when a person does not get enough Vit-D through the skin (from sun exposure) or food, as well as when their liver and/or kidneys have pathologies processing Vit-D. Each individual has different Vit-D requirements, and Vit-D expression and levels of the VDR gene may vary in different geographies. VDR gene polymorphisms have been investigated

all over the world due to their association with susceptibility to various diseases, as Vit-D plays a very important role in preventing multifactorial pathologies including osteoporosis and bone metabolism disorders in particular. The biological action of Vit-D occurs through its receptor encoded by the VDR gene. Therefore, VDR gene polymorphisms can affect bone mineral density, susceptibility to osteoporosis, and response to Vit-D supplementation.

Vit-D deficiency can cause bone problems in both children (e.g., rickets, osteomalacia) and adults (osteoporosis). Many studies have reported links between Vit-D deficiency and various health problems including depression, fractures, diabetes, heart diseases, kidney diseases, cancer, and infection. However, most of these connections do not emit the same results in each society, and the publications in the literature are quite inconsistent with each other (4). In Marozik et al. (21) published an article in 2021 and reported the results that the rs1544410 T/T polymorphism increases the risk of osteoporosis and decreases bone mineral density, while the rs11568820 polymorphism has a significant dose effect with 25(OH)D. González Rojo et al.’s 2022 study (22) on 246 cardiovascular disease patients from Southern Spain and 246 controls of Caucasian origin reported *BsmI* (rs1544410) and *CDX2* (rs11568820) polymorphisms to increase susceptibility to cardiovascular disorders when Vit-D intake varies. Liu et al. published in the article in 2015 (23) reported rs11568820 and rs1544410 polymorphisms in the VDR to be associated with gout in the Chinese Han male population. Nevertheless, despite that study obtaining no genotypic significance, a predisposition was observed in allelic frequencies. In an article by Maciejewski et al. (24) investigated the relationship between thyroid-related orbitopathy, an autoimmune disease that typically occurs in the course of Graves’ disease, and VDR gene polymorphisms and, while different publications in the literature have stated these polymorphisms to provide a predisposition, Maciejewski et al. (24) reported the gene polymorphisms of the relevant region to not be associated with the disease, adding a new example to the contradictory results. Tantawy et al. (25) published in 2016 article on Egyptian pediatric acute lymphocytic leukemia (ALL) patients found no association for the rs1544410 and rs11568820 genotypes with ALL, despite the significant genetic heterogeneity present in the VDR gene. Studies conducted in recent years have also shown Vit-D deficiency to be at very low levels in Somali individuals who have migrated to Northern European countries when compared to local individuals (26-28). Nelson et al. (29) studied on African men and reported no association between rs1544410 polymorphism and aggressive prostate cancer, while also reporting 25(OH)D levels and the rs11568820 polymorphism to be associated with the disease. One study conducted with healthy volunteers living in the Emirati population stated the Emirati population genotype and allele distribution of VDR gene polymorphisms to not differ from Caucasians living in the USA and France but to have a significant difference with Asian populations (30). As seen in the examples above, Vit-D receptor gene polymorphisms have shown inconsistent results in both comparisons of healthy volunteers and when comparing individuals with various diseases to

healthy volunteers. The current study found no significant genotypic or allelic difference in terms of the *BsmI* (rs1544410) and *CDX2* (rs11568820) gene variants between healthy Turkish individuals and Somali individuals who have spent most of their lives exposed to less sunlight and been living in Türkiye for the last five years.

Acknowledgment: We thanks to TUBITAK for support to our project.

Ethics Committee Approval: Ethical approval was taken from the Biruni University Clinical Research Ethics Committee (Decision Number: 2015-KAEK-56-21-03). All procedures were followed in accordance with the Helsinki Declaration of 1975, as revised in 2000.

Peer-review: Externally peer-reviewed.

Author Contributions: Conception/Design of Study - E.C., B.N.E.; Data Acquisition - E.C., B.N.E.; Data Analysis/Interpretation - E.C., B.N.E.; Drafting Manuscript - E.C., B.N.E.; Critical Revision of Manuscript - E.C., B.N.E.; Final Approval and Accountability - E.C., B.N.E.

Conflicts of Interest: The authors declare no conflict of interest.

Financial Disclosure: This study was supported by the TUBITAK under Grant 2021/I (project number: 1919B012101611).

REFERENCES

- Bizzaro G, Antico A, Fortunato A, Bizzaro N. Vitamin D and autoimmune diseases: Is vitamin D receptor (VDR) polymorphism the culprit? *Isr Med Assoc J* 2017; 19(7): 438-43.
- Ismailova A, White JH. Vitamin D, infections and immunity. *Rev Endocr Metab Disord* 2022; 23(2): 265-277. [CrossRef]
- Jones G. The discovery and synthesis of the nutritional factor vitamin D. *Int J Paleopathol* 2018; 23: 96-99. [CrossRef]
- Jin J. Screening for Vitamin D Deficiency in Adults. *JAMA* 2021; 325(14): 1480. [CrossRef]
- Tangpricha V. Vitamin D in food and supplements. *Am J Clin Nutr* 2012; 95(6): 1299-300. [CrossRef]
- Hymøller L, Jensen SK. 25-Hydroxyvitamin D circulates in different fractions of calf plasma if the parent compound is vitamin D₂ or vitamin D₃, respectively. *J Dairy Res* 2016; 83(1): 67-71. [CrossRef]
- DeLuca HF. Vitamin D: Historical overview. *Vitam Horm* 2016; 100: 1-20. [CrossRef]
- Al-Ghafari AB, Balamash KS, Al Doghaither HA. Relationship between serum vitamin D and calcium levels and vitamin D receptor gene polymorphisms in colorectal cancer. *Biomed Res Int* 2019; 26;2019: 8571541. [CrossRef]
- Greenhagen RM, Frykberg RG, Wukich DK. Serum vitamin D and diabetic foot complications. *Diabet Foot Ankle* 2019; 19;10(1): 1579631. [CrossRef]
- Wacker M, Holick MF. Vitamin D - effects on skeletal and extraskeletal health and the need for supplementation. *Nutrients* 2013; 10;5(1): 111-48. [CrossRef]
- Sana S, Kayani MA. Role of vitamin D deficiency and mRNA expression of VDR and RXR in haematological cancers. *Mol Biol Rep* 2021; 48(5): 4431-4439. [CrossRef]
- Eyles DW, Burne TH, McGrath JJ. Vitamin D, effects on brain development, adult brain function and the links between low levels of vitamin d and neuropsychiatric disease. *Front Neuroendocrinol* 2013; 34(1): 47-64. [CrossRef]
- Balabanova S, Richter HP, Antoniadis G, Homoki J, Kremmer N, Hanle J, Teller WM. 25-Hydroxyvitamin D, 24, 25-Dihydroxyvitamin D and 1,25-Dihydroxyvitamin D in human cerebrospinal fluid. *Klin Wochenschr* 1984; 15; 62(22): 1086-90. [CrossRef]
- Lee YH, Kim JH, Song GG. Vitamin D receptor polymorphisms and susceptibility to Parkinson's Disease and Alzheimer's Disease: A meta-analysis. *Neurol Sci* 2014; 35(12): 1947-53. [CrossRef]
- Schmidt RJ, Hansen RL, Hartiala J, Allayee H, Sconberg JL, Schmidt LC, et al. Selected vitamin D metabolic gene variants and risk for autism spectrum disorder in the CHARGE study. *Early Hum Dev* 2015; 91(8): 483-9. [CrossRef]
- Cui X, Gooch H, Petty A, McGrath JJ, Eyles D. Vitamin D and the brain: Genomic and non-genomic actions. *Mol Cell Endocrinol* 2017; 453:131-143. [CrossRef]
- Coşkun S, Şimşek Ş, Camkurt MA, Çim A, Çelik SB. Association of polymorphisms in the vitamin D receptor gene and serum 25-hydroxyvitamin D levels in children with autism spectrum disorder. *Gene* 2016; 588(2): 109-14. [CrossRef]
- Balta B, Gumus H, Bayramov R, Korkmaz Bayramov K, Erdogan M, Oztop DB, et al. Increased vitamin D receptor gene expression and rs11568820 and rs4516035 promoter polymorphisms in autistic disorder. *Mol Biol Rep* 2018; 45(4): 541-6. [CrossRef]
- Zhang Z, Li S, Yu L, Liu J. Polymorphisms in vitamin D receptor genes in association with childhood autism spectrum disorder. *Dis Markers* 2018; 2018: 7862892. [CrossRef]
- Yamamoto H, Miyamoto K, Li B, Taketani Y, Kitano M, Inoue Y, et al. The caudal-related homeodomain protein CDX2 regulates vitamin D receptor gene expression in the small intestine. *J Bone Miner Res* 1999; 14(2): 240-7. [CrossRef]
- Marozik P, Rudenka A, Kobets K, Rudenka E. Vitamin D status, bone mineral density, and VDR gene polymorphism in a cohort of belarusian postmenopausal women. *Nutrients* 2021; 13(3): 837. [CrossRef]
- González Rojo P, Pérez Ramírez C, Gálvez Navas JM, Pineda Lancheros LE, Rojo Tolosa S, Ramírez Tortosa MDC, et al. Vitamin D-related single nucleotide polymorphisms as risk biomarker of cardiovascular disease. *Int J Mol Sci* 2022; 23(15): 8686. [CrossRef]
- Liu SG, Li YY, Sun RX, Wang JL, Li XD, Han L, et al. Polymorphisms in the vitamin D receptor and risk of gout in Chinese Han male population. *Rheumatol Int* 2015; 35(6): 963-71. [CrossRef]
- Maciejewski A, Kowalczyk MJ, Gasińska T, Szeliga A, Predecki M, Dorszewska J, et al. The Role of vitamin D receptor gene polymorphisms in thyroid-associated orbitopathy. *Ocul Immunol Inflamm* 2020; 28(3): 354-61. [CrossRef]
- Tantawy M, Amer M, Raafat T, Hamdy N. Vitamin D receptor gene polymorphism in Egyptian pediatric acute lymphoblastic leukemia correlation with BMD. *Meta Gene* 2016; 9: 42-6. [CrossRef]
- Demeke T, Osmancevic A, Gillstedt M, Krogstad AL, Angesjö E, Sinclair H, et al. Comorbidity and health-related quality of life in Somali women living in Sweden. *Scand J Prim Health Care* 2019; 37(2): 174-81. [CrossRef]
- Kalliokoski P, Widarsson M, Rodhe N, Löfvander M. Positive impact on vitamin D related lifestyle of medical advice in pregnant Somali-born women and new mothers: A mixed method study in Swedish primary care. *BMC Public Health* 2021; 21(1): 297. [CrossRef]
- Adebayo FA, Itkonen ST, Lilja E, Jääskeläinen T, Lundqvist A, Laatikainen T, et al. Prevalence and determinants of vitamin D deficiency and insufficiency among three immigrant groups in Finland: Evidence from a population-based study using standardised 25-Hydroxyvitamin D data. *Public Health Nutr* 2020; 23(7): 1254-65. [CrossRef]

29. Nelson SM, Batai K, Ahaghotu C, Agurs-Collins T, Kittles RA. Association between serum 25-hydroxy-vitamin D and aggressive prostate cancer in African American Men. *Nutrients* 2016; 9(1): 12. [\[CrossRef\]](#)
30. Osman E, Al Anouti F, El Ghazali G, Haq A, Mirgani R, Al Safar H. Frequency of rs731236 (TaqI), rs2228570 (FokI) of Vitamin-D Receptor (VDR) gene in Emirati healthy population. *Meta Gene* 2015; 15;6: 49-52. [\[CrossRef\]](#)

Self-Discontinuation of Antiseizure Medication During Pregnancy Increases Postpartum Seizure Frequency

Miray Atacan Yasguclukal¹ , Zeynep Acar¹ , Birgul Bastan¹ , Aytul Mutlu¹ , Ozlem Cokar¹ 

¹Neurology Clinic of Haseki Training and Research Hospital, Health Sciences University, Istanbul, Turkiye

ORCID ID: M.A.Y. 0000-0002-9529-1343; Z.A. 0000-0003-2369-3711; B.B. 0000-0002-8285-4901; A.M. 0000-0002-1710-0783; O.C. 0000-0003-0231-1091

Cite this article as: Atacan Yasguclukal M, Acar Z, Bastan B, Mutlu A, Cokar O. Self-discontinuation of antiseizure medication during pregnancy increases postpartum seizure frequency. *Experimed* 2022; 12(3): 174-80.

ABSTRACT

Objectives: The study aimed to investigate the rate of unplanned pregnancies, changes in seizure frequencies during the 6 months before the pregnancy, during the pregnancy, and the 6 months after the pregnancy, and antiseizure medication (ASM) compliances in women with epilepsy (WWEs).

Materials and Methods: The study retrospectively evaluated WWEs who were followed up in the epilepsy outpatient clinic of a training and research hospital between 1997-2021 and had used ASMs for at least 6 months prior to their pregnancy.

Results: The study assessed a total of 158 pregnancies for 77 WWEs, with 112 pregnancies resulting in live births, 71.4% of which were unplanned pregnancies. Unplanned pregnancies are more common in less educated women ($p = 0.02$). Of the women, 35 self-discontinued their ASMs during pregnancy, and these women were younger than the WWEs who continued taking their ASMs ($p = 0.003$). In addition, folic acid supplement use was lower in women who self-discontinued their ASMs ($p = 0.031$). The rate of increase in seizure frequency during postpartum period compared to pregnancy was higher in women who self-discontinued ASMs ($p = 0.032$).

Conclusion: Self-discontinuation of ASM during pregnancy is related to an increase in postpartum seizure frequency. WWEs should be given advice on how to minimize the risk of seizure during the postpartum period.

Keywords: Epilepsy, pregnancy, seizures, postpartum period

INTRODUCTION

Epilepsy is a common neurological disease affecting 0.3% to 0.6% of pregnant women (1, 2). Managing pregnancy for women with epilepsy (WWEs) is challenging in terms of both the mother's and child's health. Antiseizure medications (ASMs) increase the risk of congenital defects, intrauterine growth retardation, miscarriage, stillbirth, and preterm birth in WWEs, and recent reports have also mentioned the negative impact of ASMs on children's mental functions (3–6). This is concerning for the physician as well as for mothers with epilepsy and their family.

Despite the well-known adverse effects of ASMs, pregnant WWEs may be required to continue their medications to protect both themselves and the fetus from seizures that may occur during pregnancy. Even though dose reduction may be possible if the seizures are under control, WWEs should be advised to have been free of seizures for at least 1 year before the pregnancy (7, 8). Furthermore, due to sleep deprivation and postpartum depression, the postpartum period is hazardous for seizure recurrence (9). Preconception counseling is important for WWEs to minimize adverse events and have a complication-free pregnancy (3). However, studies have also indicated

Corresponding Author: Miray Atacan Yaşgüçlülük **E-mail:** mirayatacan@hotmail.com

Submitted: 10.10.2022 **Revision Requested:** 02.11.2022 **Last Revision Received:** 08.11.2022 **Accepted:** 02.12.2022 **Published Online:** 30.12.2022



Content of this journal is licensed under a Creative Commons Attribution-NonCommercial 4.0 International License.

unplanned pregnancy rates to range from 16.2%-60.6% (10-12). With unplanned pregnancies in general, WWEs abruptly discontinue their ASMs or reduce their dosage once they find out they are pregnant due to the anxiety of the teratogenic effects of ASMs. Noncompliance with ASMs during pregnancy is reported to be around 20% in the literature (13). For these reasons, managing the pregnancy of WWEs can be challenging.

This study aimed to investigate the rate of unplanned pregnancies, changes in seizure frequencies during the 6 months before the pregnancy, during the pregnancy, and the 6 months after the pregnancy, ASM compliances, and pregnancy outcomes for WWEs.

MATERIALS AND METHODS

This study retrospectively evaluated female patients who'd been seeking treatment in an epilepsy outpatient clinic of a training and research hospital between January 1997-November 2021. The study involves women who'd been diagnosed with epilepsy prior to a pregnancy and who had used ASMs for at least 6 months prior to their pregnancy.

The study retrieved its data from patient files that include their demographic characteristics, education level, type of epileptic seizures, seizure frequency (before, during, and after pregnancy), whether the pregnancy was planned or not, and the use of folic acid supplements. The types of epileptic seizures have been defined according to the International League Against Epilepsy (ILAE) 2017 classification using electroencephalography (EEG) findings along with seizure history, and ASM adherence was monitored through patients' statements. The unplanned pregnancy group consists of WWEs who experienced unexpected pregnancies and who consulted an epileptologist post-conception. With regard to planned pregnancies, 5 mg of folate supplementation was started three months before the planned conception. With regard to the unplanned pregnancies, however, folic acid supplementation was introduced in the first follow-up visit following the start of the pregnancy. Follow-up visits were done in 3-month intervals.

Seizure frequency was evaluated over three periods: the 6 months before the pregnancy (T1), during the pregnancy (T2), and the 6 months after the pregnancy (T3). Changes in seizure frequency between each of these three periods was assessed and classified under three categories: Unchanged, increased, or decreased. Pregnancies that resulted in a miscarriage, stillbirth, medical abortion, or curettage have been excluded from the comparison regarding seizure frequency. More than a 50% increase in seizure frequency during and after a pregnancy compared to before is considered as increased seizure frequency, while a more than 50% decrease is considered as decreased seizure frequency.

Pregnancy outcomes have been grouped in terms of live births, spontaneous miscarriages, medical abortions, curettage, stillbirths, and ectopic pregnancies. Stillbirths are defined as pregnancies that result in fetal death after the 23rd week of

pregnancy.

Antiseizure medications used during pregnancy and their doses have been noted for all pregnancies. Seizure frequencies have been compared between WWEs who self-discontinued ASMs and those who maintained their treatment.

These retrospectively collected data have been anonymized. Therefore, no need exists for written consent. This study was approved by a Haseki Training and Research Hospital Institutional Review Board committee (approval number: 2021-273).

Statistical Analyses

Statistical analyses have been performed using the program SPSS 21.0 for Windows. Descriptive statistics are presented as numbers and percentages for categorical variables and as means, standard deviations, minimums, and maxima for numeric variables. The chi-square test is used to compare two independent groups, while the numeric variables in two independent groups are compared using Student's t test when normality is not met. For more than two independent groups, numeric variables are compared using the one-way ANOVA test when normally distributed and using the Kruskal-Wallis test when normality is not. McNemar's test has been preferred for comparing percentages of independent groups, and subgroup analyses have been interpreted using the Bonferroni correction. All *p* values are two-sided with a statistical significance of 0.05.

RESULTS

The demographic and clinical characteristics of the patients included in the study are summarized in Table 1. The outcomes of the pregnancies are shown in Figure 1. Among the 30 miscarriages, 18 pregnancies involved mothers undergoing monotherapy, five involve mothers undergoing polytherapy, and seven involved mothers who'd self-discontinued their ASM. Among the four medical abortions, one pregnancy was terminated because the fetus had anencephaly and the mother was taking 750 mg/day of valproic acid (VPA), one fetus had unknown developmental problems and the mother was taking 600 mg/day of carbamazepine (CBZ), one fetus had hydronephrosis and the mother was taking 400 mg/day of CBZ, and one pregnancy was terminated because the mother had severe seizures while taking 600 mg/day of CBZ and 50 mg/day of lamotrigine (LTG).

The characteristics of the 112 pregnancies that resulted in a live birth are presented in Table 2. Of these live births, 35 women had self-discontinued their ASMs, 14 of whom restarted upon seizure recurrence. The remaining 21 pregnancies (plus another two who'd stopped their ASMs under the close care of their physician for a total of 23 pregnancies) went to term without medications. Reduced ASM dosage occurred in 23 pregnancies in an attempt to lessen the teratogenesis risk, while the ASM dosage was increased in four pregnancies in order to improve seizure control.

Table 1. Demographical and clinical characteristics of women with epilepsy.

	N=77	
Age at epilepsy onset (year) (mean±sd)	14.13±0.62	
Age at presentation (year) (mean±sd)	23.69±0.77	
Age at first pregnancy (year) (mean±sd)	23.08±0.47	
Follow-up duration (year) (mean±sd)	8.50±0.63	
Number of pregnancies (mean±sd)	2.58±0.21	
	N	%
Consanguineous marriage	14	18.2
Number of years of education		
≤8 years	61	79.2
≥8 years	16	20.8
Type of epileptic seizures*		
Focal	26	33.8
Generalized	51	66.2
Number of pregnancies		
1	22	28.6
2	24	31.2
3	16	20.8
≥4	6	19.5

* There were 26 patients with focal (6 structural/lesional, 19 with unknown causes) and 51 patients (5 juvenile absence epilepsy (JAE), 27 juvenile myoclonic epilepsy (JME), 19 others) with generalized seizures

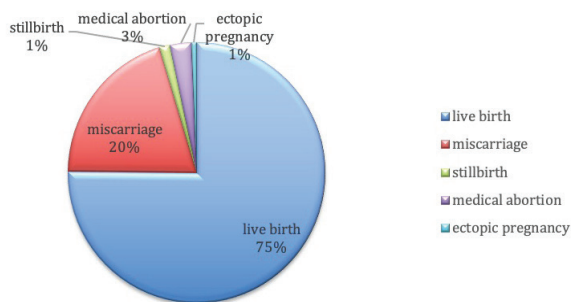


Figure 1. Outcomes of pregnancies.

The rate of planned pregnancies was observed to be 28.6%. No association was found between planned/unplanned pregnancies with change in seizure frequency or ASM use before pregnancy (e.g., monotherapy/polytherapy; $p > 0.05$). The mean age at conception and mean duration of disease were significantly higher with regard to planned pregnancies ($p = 0.013$ and $p = 0.049$, respectively). Planned pregnancies were more common for women who'd received eight or more years of education and women experiencing their first pregnancies ($p = 0.034$ and $p = 0.011$, respectively; Table 3).

Table 2. Characteristics of pregnancies with live births.

	N=112	%
Route of delivery		
Vaginal route	69	61.6
Cesarean section	43	38.4
Planned pregnancy	32	28.6
Folic acid use	78	69.6
Treatment discontinuation	35	31.3
ASM use during pregnancy		
No ASMs	23	20.5
Monotherapy	68	60.7
Polytherapy	21	18.8

ASM: Antiseizure medication

The changes in seizure frequency between T1 and T2 differ significantly from the changes in seizure frequency between T2 and T3 ($p = 0.000$). Between T2 and T3, the rates for unchanged

Table 3. Pregnancy planning and associated factors.

		Pregnancy planning		P-value
		Planned N=32 N(%)	Unplanned N=80 N(%)	
ASM use before pregnancy	Monotherapy	26 (81.3)	60 (75.0)	.645
	Polytherapy	6 (18.8)	20 (25.0)	
Number of years of education	≤8 years	11 (34.4)	47 (58.8)	.034
	≥8 years	21 (65.6)	33 (41.3)	
First pregnancy	Yes	22 (68.8)	32 (40.0)	.011
	No	10 (31.3)	48 (60.0)	
Mean age at conception (year) (mean±sd)*		28.19±4.96	25.54±4.91	.013
Mean duration of disease (year) (mean±sd)*		13.56±5.94	11.06±7.07	.049
Change in seizure frequency during pregnancy compared to preconceptional period	Unchanged	16 (50.0)	43 (53.8)	.904
	Decreased	8 (25.0)	20 (25.0)	
	Increased	8 (25.0)	17 (21.3)	
Change in seizure frequency during postpartum period compared to pregnancy	Unchanged	14 (43.8)	33 (41.3)	.951
	Decreased	7(21.9)	17 (21.3)	
	Increased	(34.4)	30 (37.5)	
	No	28(80.0)	52(65.0)	

ASM: Antiseizure medication
 *Mann Whitney U test

and decreased seizure frequencies declined while the rates for increased seizures grew compared to the respective frequency changes from T1 to T2 (Figure 2). Furthermore, an increase in seizure frequency was observed between T2 and T3 in 65.2% of pregnancies where the women were being monitored without ASM ($p = 0.008$). No association was found between the change in seizure frequency between T2 and T3 with regard to the type of epileptic seizure, duration of disease, or age at conception ($p > 0.05$; Table 4).

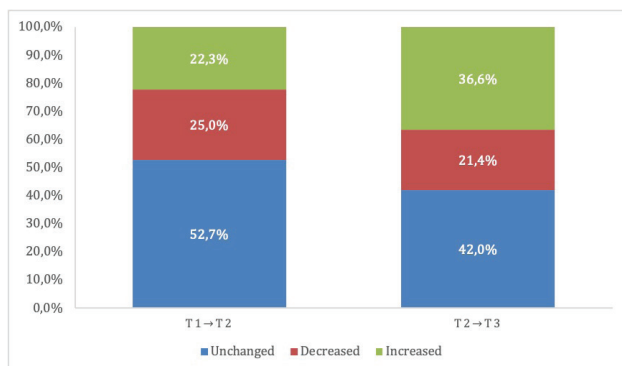


Figure 2. Change in seizure frequencies.
 T1→T2: Comparison between T1 and T2
 T2→T3: Comparison between T2 and T3

The results for noncompliance with antiepileptic treatment during pregnancy are presented in Table 5. The mean age of women who'd discontinued ASMs during pregnancy was significantly lower ($p = 0.002$). The use of folic acid supplementation was also significantly associated with drug discontinuation, with 75.6% of patients who used folic acid supplements continuing their ASMs, while 47.1% of patients who did not take folic acid discontinued their ASMs ($p = 0.031$). Noncompliance with ASM therapy was higher in patients who'd received eight years or less of education or who were in their first pregnancies, although the difference was not statistically significant ($p = 0.333$ and $p = 0.284$, respectively). No significant association was found between ASM self-discontinuation and change in seizure frequency between T1 and T2 ($p = 0.702$). However, the rate of increase in seizure frequency between T2 to T3 was higher in women who'd discontinued their ASM while pregnant ($p = 0.032$).

DISCUSSION

This study has evaluated the pregnancies of 77 WWEs undergoing treatment in an epilepsy outpatient clinic whose rate of unplanned pregnancies was observed to be 71.4%. The ratio of planned pregnancies has been shown to vary according to countries' development levels, with unplanned pregnancies being reported at 16.2% in the Natsal-3 study in Britain (10), 46.2% in Japan (11), and 60.6% in China

Table 4. Change in seizure frequency during postpartum period compared to pregnancy and associated factors.

		Change in seizure frequency during postpartum period compared to pregnancy			P-value
		Unchanged N=47 N(%)	Decreased N=24 N(%)	Increased N=41 N(%)	
ASM use during pregnancy	No ASMs	6 (12.8)	2 (8.3)	15 (36.6)	.008
	Monotherapy	34 (72.3)	14 (58.3)	20 (48.8)	
	Polytherapy	7 (14.9)	8 (33.3)	6 (14.6)	
Type of epileptic seizures	Focal	16 (34.0)	12 (50.0)	9 (22.0)	.067
	Generalized	31 (66.0)	12 (50.0)	32 (78.0)	
Mean age at conception (year) (mean±sd)*		26.94±5.37	26.00±4.91	25.73±4.78	.513
Mean duration of disease (year) (mean±sd)*		11.89±6.72	10.58±6.34	12.34±7.31	.603

ASM: Antiseizure medication
*One way ANOVA test

Table 5. Noncompliance with antiepileptic treatment and associated factors.

		Drug discontinuation		P-value
		Yes N=35 N(%)	No N=77 N(%)	
Pregnancy planning	Planned	7(20.0)	25(32.5)	.259
	Unplanned	28(80.0)	52(67.5)	
ASM use before pregnancy	Monotherapy	27 (77.1)	59 (76.6)	.952
	Polytherapy	8 (22.9)	18 (23.4)	
Folic acid use	Yes	19 (54.3)	59 (76.6)	.031
	No	16 (45.7)	18 (23.4)	
Number of years of education	≤8 years	21 (60.0)	37 (48.1)	.333
	≥8 years	14 (40.0)	40 (51.9)	
First pregnancy	Yes	20 (57.1)	34 (44.2)	.284
	No	15 (42.9)	43 (55.8)	
Mean age at conception (year) (mean±sd)*		24.23±4.82	27.23±4.89	.002
Mean duration of disease (year) (mean±sd)*		10.20±6.98	12.49±6.69	.108
Change in seizure frequency during pregnancy compared to preconceptional period	Unchanged	20 (57.1)	39 (50.6)	.702
	Decreased	7 (20.0)	21 (27.3)	
	Increased	8 (22.9)	17 (22.1)	
Change in seizure frequency during postpartum period compared to pregnancy	Unchanged	11 (31.4)	36 (46.8)	.032
	Decreased	5 (14.3)	19 (24.7)	
	Increased	19 (54.3)	(28.6)	

ASM: Antiseizure medication
*Mann Whitney U test

(12). Data from the Pregnancy Risk Assessment Monitoring System (PRAMS) reported 55% of pregnancies for WWEs to be unplanned (15), while data from the Epilepsy Birth Control Registry (EBCR) reported this rate to be 65% (16). The rate of planned pregnancies among WWEs in Turkiye has been found to range from 28.6%-41.6% (17, 18). According to data from field research conducted on the general population in Turkiye, 26% of pregnancies are unplanned. Similar to the current study, unexpected pregnancies are lower in women who have at least eight years of education and for first pregnancies (19). WWEs noteworthy have a high rate of unplanned pregnancies despite having a chronic disease.

The rate of ASM self-discontinuation was found to be 31.3%. Noncompliance with ASM during pregnancy among the WWEs has been reported to vary between 15%-62.3% in the literature (1, 13). According to Turkish studies, this rate ranges between 10.7%-25% (18, 20). Pregnant WWEs are twice as likely to stop ASM as nonpregnant WWEs (21). The current study discovered WWEs who'd self-discontinued their ASMs had a lower mean age. This finding is consistent with the findings from Sweileh et al. (22). Women who don't use folic acid supplements were also found to have higher rates of ASM self-discontinuation in the current study. Similarly, one study (23) investigating adherence to medication among pregnant women with chronic diseases found women who do not use folic acid supplementation to have a higher risk of non-compliance with their treatment. Fear of the teratogenic consequences of ASMs was the main reason in this study for WWEs' poor adherence. A lack of folate supplements further increased the risk of congenital abnormalities. Therefore, negative beliefs about ASMs and self-discontinuation could be lessened through proper counseling during the preconception period and by ensuring the use of folic acid supplementation.

The postpartum period saw a greater increase in seizure frequency. Moreover, the current study demonstrated the increase in seizure frequency to be higher in pregnancies of women who were monitored while not taking medication during pregnancy. Vajda et al. (24) noted obtaining seizure control both before and during pregnancy to increase the chance of remaining seizure-free during the postpartum period. Although a comparison of seizure frequencies during the preconception and postpartum periods has not been thoroughly explored, postpartum sleep deprivation, exhaustion, and increased stress may increase the risk of seizure in WWEs (9, 25). Therefore, it was recommended to keep the dose of ASM higher than in the preconceptional period (9). Different life modifications should also be made during this period. Sleep deprivation is inevitable, especially for breastfeeding mothers. WWEs should be advised to take precautions such as sharing burden of nighttime feeding with other people and attempting to make up for the lack of sleep during the infant's daytime naps (26, 27).

As this study involves a records-based search, it is subject to the accompanying limitations involving restricted details

about the patient population and the potential of missing or misinterpreting data. The information in the study is based on the reliability of the patient's self-recall without the use of seizure diaries. The small sample size and lack of a control group are other limitations of the study. Additionally, the characteristics of pregnancies with and without live births could not be compared.

The current research reveals a significantly greater rate of unplanned pregnancies to have occurred among WWEs, as well as a high rate of ASM self-discontinuation. In a survey study, it was found that for 87% of the WWEs that considered having children, the potential effect of epilepsy and ASMs on the unborn child was their most crucial concern. Furthermore, this study also emphasizes preconception counseling to have been inadequate, so much so that 33% of the WWEs hadn't even received any information about their pregnancy and epilepsy medication (28). For this reason, negative beliefs about ASMs should be lessened through proper counseling during the preconception period. Finally, postpartum seizure frequency was seen to have increased more significantly for WWEs who'd self-discontinued their ASMs. WWEs should be provided counseling on how to minimize the risk of having a seizure during the postpartum period. This includes emphasizing the significance of drug adherence as well as proper sleep with the help of another person.

Ethics Committee Approval: This study was approved by the Haseki Training and Research Hospital Institutional Review Board committee (approval number: 2021-273).

Peer-review: Externally peer-reviewed.

Author Contributions: Conception/Design of Study - M.A.Y., Z.A., B.B.; Data Acquisition - M.A.Y., Z.A.; Data Analysis/Interpretation - B.B., A.M., O.C.; Drafting Manuscript - M.A.Y.; Critical Revision of Manuscript - Z.A., B.B., A.M., O.C.; Final Approval and Accountability - M.A.Y., Z.A., B.B., A.M., O.C.

Conflicts of Interest: The authors declare no conflict of interest.

Financial Disclosure: The authors declare that this study has received no financial support.

REFERENCES

1. Fairgrieve SD, Jackson M, Jonas P, Walshaw D, White K, Montgomery TL, et al. Population based, prospective study of the care of women with epilepsy in pregnancy. *Br Med J* 2000; 321(7262): 674-5. [\[CrossRef\]](#)
2. Olafsson E, Hallgrímsson JT, Hauser WA, Ludvigsson P, Gudmundsson G. Pregnancies of women with epilepsy: a population-based study in Iceland. *Epilepsia* 1998; 39(8): 887-92. [\[CrossRef\]](#)
3. Bollig KJ, Jackson DL. Seizures in pregnancy. *Obstet Gynecol Clin North Am* 2018; 45(2): 349-67. [\[CrossRef\]](#)
4. Veroniki AA, Cogo E, Rios P, Straus SE, Finkelstein Y, Kealey R, et al. Comparative safety of anti-epileptic drugs during pregnancy: A systematic review and network meta-analysis of congenital malformations and prenatal outcomes. *BMC Med* 2017; 15(1): 1-20. [\[CrossRef\]](#)

5. Kjaer D, Christensen J, Bech BH, Pedersen LH, Vestergaard M, Olsen J. Preschool behavioral problems in children prenatally exposed to antiepileptic drugs - a follow-up study. *Epilepsy Behav* 2013; 29(2): 407-11. [\[CrossRef\]](#)
6. Viale L, Allotey J, Cheong-see F, Arroyo-Manzano D, Mccorry D, Bagary M, et al. Epilepsy in pregnancy and reproductive outcomes : A systematic review and meta-analysis. *Lancet* 2015; 6736(15): 1-8. [\[CrossRef\]](#)
7. Vajda FJE, Hitchcock A, Graham J, O'Brien T, Lander C, Eadie M. Seizure control in antiepileptic drug-treated pregnancy. *Epilepsia* 2008; 49(1): 172-6. [\[CrossRef\]](#)
8. Vajda FJE, O'Brien TJ, Graham JE, Hitchcock AA, Lander CM, Eadie MJ. Predicting epileptic seizure control during pregnancy. *Epilepsy Behav* 2018; 78: 91-5. [\[CrossRef\]](#)
9. Nucera B, Brigo F, Trinka E, Kalss G. Treatment and care of women with epilepsy before, during, and after pregnancy: a practical guide. *Ther Adv Neurol Disord* 2022; 15: 17562864221101688. [\[CrossRef\]](#)
10. Wellings K, Jones KG, Mercer CH, Tanton C, Clifton S, Datta J, et al. The prevalence of unplanned pregnancy and associated factors in Britain: Findings from the third National Survey of Sexual Attitudes and Lifestyles (Natsal-3). *Lancet* 2013; 382(9907): 1807-16. [\[CrossRef\]](#)
11. Goto A, Yasumura S, Reich MR, Fukao A. Factors associated with unintended pregnancy in Yamagata, Japan. *Soc Sci Med* 2002; 54(7): 1065-79. [\[CrossRef\]](#)
12. Zhang Y yao, Song C geng, Wang X, Jiang Y li, Zhao J jing, Yuan F, et al. Clinical characteristics and fetal outcomes in women with epilepsy with planned and unplanned pregnancy: A retrospective study. *Seizure* 2020; 79: 97-102. [\[CrossRef\]](#)
13. Shahla M, Hijran B, Sharif M. The course of epilepsy and seizure control in pregnant women. *Acta Neurol Belg* 2018; 118(3): 459-64. [\[CrossRef\]](#)
14. EUROCAT. EUROCAT Guide 1 . 4 and Reference Documents ((Last update version 28/12/2018). 2013; (2013). Available from: www.eurocat-network.eu/
15. Johnson EL, Burke AE, Wang A, Pennell PB. Unintended pregnancy, prenatal care, newborn outcomes, and breastfeeding in women with epilepsy. *Neurology* 2018; 91(11): e1031 LP-e1039. [\[CrossRef\]](#)
16. Herzog AG, Mandle HB, Cahill KE, Fowler KM, Hauser WA. Predictors of unintended pregnancy in women with epilepsy. *Neurology* 2017; 88(8): 728-33. [\[CrossRef\]](#)
17. Bayrak M, Bozdog H, Karadag C, Gunay T, Goynumer G. Retrospective analysis of obstetric and perinatal outcomes in pregnant women with epilepsy. *Istanbul Kanuni Sultan Süleyman Tıp Derg* 2014; 6(3): 127-32. [\[CrossRef\]](#)
18. Ozdemir O, Sari ME, Kurt A, Sakar VS, Atalay CR. Pregnancy outcome of 149 pregnancies in women with epilepsy: Experience from a tertiary care hospital. *Interv Med Appl Sci* 2015; 7(3): 108-13. [\[CrossRef\]](#)
19. Hacettepe Üniversitesi Nüfus Etütleri Enstitüsü. 2018 Türkiye Nüfus ve Sağlık Araştırması. Hacettepe Üniversitesi Nüfus Etütleri Enstitüsü, TC Cumhurbaşkanlığı Strat ve Bütçe Başkanlığı ve TÜBİTAK, Ankara, Türkiye. 2019; Available from: https://hips.hacettepe.edu.tr/tr/2018_turkiye_nufus_ve_saglik_arastirmasi-55
20. Madazlı R, Öncül M, Albayrak M, Uludağ S, Eşkazan E, Ocak V. Gebelik ve epilepsi: 44 olgunun değerlendirilmesi. *Cerrahpaşa Med J* 2004; 35: 126-30.
21. Man SL, Petersen I, Thompson M, Nazareth I. Antiepileptic drugs during pregnancy in primary care: A UK Population based study. *PLoS One* 2012; 7(12). [\[CrossRef\]](#)
22. Sweileh WM, Ihabesheh MS, Jarar IS, Taha ASA, Sawalha AF, Zyoud SH, et al. Self-reported medication adherence and treatment satisfaction in patients with epilepsy. *Epilepsy Behav* 2011; 21(3): 301-5. [\[CrossRef\]](#)
23. Lupattelli A, Spigset O, Nordeng H. Adherence to medication for chronic disorders during pregnancy: Results from a multinational study. *Int J Clin Pharm* 2014; 36(1): 145-53. [\[CrossRef\]](#)
24. Vajda FJE, O'Brien TJ, Graham JE, Hitchcock AA, Perucca P, Lander CM, et al. Epileptic seizure control during and after pregnancy in Australian women. *Acta Neurol Scand* 2022; 145(6): 730-6. [\[CrossRef\]](#)
25. Crawford P. Best practice guidelines for the management of women with epilepsy. 2005; 46(3): 117-24. [\[CrossRef\]](#)
26. Pennell PB. Pregnancy in the woman with epilepsy: Maternal and fetal outcomes. *Semin Neurol* 2002; 22(3): 299-307. [\[CrossRef\]](#)
27. Walker SP, Permezel M, Berkovic SF. The management of epilepsy in pregnancy. *BJOG An Int J Obstet Gynaecol* 2009; 116(6): 758-67. [\[CrossRef\]](#)
28. Crawford P, Hudson S. Understanding the information needs of women with epilepsy at different lifestages: Results of the "Ideal World" survey. *Seizure* 2003; 12(7): 502-7. [\[CrossRef\]](#)

Germline Screening of Cancer-Related Genes in Turkish Ovarian Cancer Patients

Esra Arslan Ates^{1,2} , Ceren Alavanda³ , Bilgen Bilge Geckinli³ , Ahmet Ilter Guney³ , Tuba Gunel² 

¹Department of Medical Genetics, Faculty of Medicine, Istanbul University-Cerrahpaşa, Istanbul, Turkiye

²Department of Molecular Biology and Genetics, Faculty of Sciences, Istanbul University, Istanbul, Turkiye

³Department of Medical Genetics, Faculty of Medicine, Marmara University, Istanbul, Turkiye

ORCID ID: E.A.A. 0000-0001-5552-8134; C.A. 0000-0002-7327-3849; B.B.G. 0000-0003-0317-5677; A.I.G. 0000-0002-1661-1282; T.G. 0000-0003-3514-5210

Cite this article as: Arslan Ates E, Alavanda C, Geçkinli BB, Guney AI, Gunel T. Germline screening of cancer-related genes in Turkish ovarian cancer patients. *Experimed* 2022; 12(3): 181-7.

ABSTRACT

Objective: Ovarian cancer (OC) is one of the most fatal types of cancer and affects 1%-1.5% of women worldwide. The most common genes causing OC are the *BRCA1* and *BRCA2* genes. However, improvements in next-generation sequencing (NGS) technologies have allowed for screening of the various genes related to hereditary cancer syndromes. The aim of this study was to evaluate cancer-related gene variations among cases of ovarian cancer.

Materials and Methods: The study evaluated 63 cases that were referred to the Marmara University Pendik Training and Research Hospital Genetic Diseases Diagnostic Center between 2016-2021 with a diagnosis of OC for germline variations in 25 cancer-related genes using NGS. Large intragenic rearrangements of the *BRCA1* and *BRCA2* genes were screened using multiplex ligation-dependent probe amplification (MLPA).

Results: The study detected 12 distinct pathogenic variations in the *BRCA1*, *BRCA2*, *BRIP1*, and *RAD50* genes in 13 OC cases. Four of the 13 cases involved copy number variations that included at least one exon of the *BRCA1* gene.

Conclusion: This study detected pathogenic *BRCA1* variations to be the leading cause of hereditary OC. The study showed just screening for *BRCA1* to reveal the underlying hereditary defect in 76.9% of the cases, which seems higher compared to literature. More studies involving larger cohorts are necessary to figure out the exact frequency of *BRCA1* variations in Turkish OC cases.

Keywords: Ovarian cancer, hereditary cancer syndromes, germline variation

INTRODUCTION

Ovarian cancer (OC) is one of the leading causes of cancer-related deaths worldwide among women. Every year, 240,000 women are diagnosed with OC, making it the seventh most common cancer globally. OC is frequently diagnosed in the later stages of the disease and is known as the most fatal gynecologic cancer with a five-year survival rate of less than 45% (1, 2).

Germline predisposition is one of the most significant risk factors for developing OC (3). A germline pathogenic

variation is detected in cancer-related genes in approximately 23% of OC cases (4). *BRCA1* and *BRCA2* are the most common genes associated with hereditary ovarian cancer (5), with the worldwide population of women having a 1.8% lifetime risk for ovarian cancer. However, this risk increases up to 15%-45% for germline *BRCA1* pathogenic variant carriers, and 10%-20% for *BRCA2* pathogenic variant carriers (6). Among all hereditary OC patients, 15%-35% of pathogenic variations may be present in other tumor suppressor genes or oncogenes including mismatch repair (MMR) genes, *TP53*, *ATM*, *CHEK2*, *PALB2*, *RAD50*, and *BRIP1* (5, 7). Identifying the underlying molecular defects in ovarian

Corresponding Author: Esra Arslan Ates **E-mail:** esraarslan.md@gmail.com

Submitted: 12.10.2022 **Revision Requested:** 09.11.2022 **Last Revision Received:** 02.12.2022 **Accepted:** 03.12.2022 **Published Online:** 30.12.2022



Content of this journal is licensed under a Creative Commons Attribution-NonCommercial 4.0 International License.

cancer is an important approach for the medical management of patients and guidance regarding treatment options, and this study aimed to reveal the relationship between genetic variations and clinical outcomes.

MATERIALS AND METHODS

Patients Data

The study involved 63 patients who were referred to the medical genetics department with a diagnosis of OC between 2016-2021 and has obtained approval from the institutional review board with the protocol number 09.2020.751. Informed consent was obtained from all patients during the face-to-face interviews. The patients were evaluated in terms of age of diagnosis, clinical outcomes, and family history. CA-125 levels were obtained from their patient follow-up documents at the time of diagnosis.

Genetic Tests

DNA isolation from peripheral blood samples was performed using the QIAamp DNA Mini Kit (Qiagen, MD, USA). The *BRCA1* and *BRCA2* genes were amplified using the Multiplicom BRCA Master Dx (Agilent, CA, USA). Copy number variations (CNVs) in the *BRCA1* and *BRCA2* genes were screened using the SALSA multiplex ligation-dependent probe amplification (MLPA) Probemix P002 BRCA1 and P045 BRCA/CHEK2 kits (MRC Holland, Amsterdam, the Netherlands). The 25 genes associated with cancer predisposition (i.e., *ATM*, *BARD1*, *BRCA1*, *BRCA2*, *BRIP1*, *CDH1*, *CHEK2*, *FAM175A*, *MRE11A*, *NBN*, *PALB2*, *PIK3CA*, *RAD50*, *RAD51C*, *RAD51D*, *TP53*, *XRCC2*, *MLH1*, *MSH2*, *MSH6*, *PMS2*, *MUTYH*, *APC*, *PTEN*, and *STK11*) were amplified using the Multiplicom BRCA Hereditary Cancer MASTR Plus kit (Agilent, CA, USA). Sequencing was performed on the Illumina NextSeq platform (Illumina Inc., San Diego, CA, USA). The obtained data have been analyzed in the analysis program Sophia DDM (Sophia Genetic Inc. Boston, MA 02116, USA). For the confirmation and segregation analyses of the detected variants, the target region was replicated with the designed primers and then sequenced with the ABI Prism 3500 Genetic Analyzer (Thermo Fisher Scientific, MA, USA) device using the Sanger sequencing method. Human reference genome Hg 19 was used for variant annotation and evaluated according to the American College of Medical Genetics and Genomics (ACMG) criteria (8).

Statistical Analysis

Data were evaluated via Microsoft Excel for Mac (version 15.33) application. Mean ages and percentage values were obtained using this software.

RESULTS

Between 2016-2021, 63 ovarian cancer cases were referred to the medical genetics department for genetic testing. These patients' ages ranged between 24-83, with the age at diagnosis ranging from 22-83 and a median age of diagnosis of 50 years. Two (3%) cases involved bilateral ovarian cancer, while three (4.7%) cases also had a history of breast cancer. Among the 63 cases, 48 (76%) reported at least one cancer case among family

members, with 31 being first-degree, 13 being second-degree, and four being third-degree relatives. At least one family member had also been diagnosed with ovarian cancer in 17 (26.9%) of the cases, while 13 (20%) cases also had at least one family member who suffered from breast cancer.

Other cancer types such as gastrointestinal tract, lung, and endometrium cancers were reported for family members in 18 (28%) of the cases; these cases also showed no family history of ovarian or breast cancer. In 15 (23.8%) cases, no family history was found for any kind of cancer.

Firstly, the *BRCA1/2* genes were evaluated for single nucleotide variations (SNVs) and CNVs, with a pathogenic variation related to hereditary breast/ovarian cancer being detected in 11 (17%) patients, 10 of the 11 variants were found in the *BRCA1* gene and one of the 11 variant was found in the *BRCA2* gene. In three cases, two missense mutations, one nonsense mutation, and two frameshift mutations in the *BRCA1* gene were detected. In four cases, the MLPA revealed three distinct intragenic deletions and one duplication. No variations were detected in the related exons or adjacent sequences within at least 20 base pairs in the introns. A frameshift *BRCA2* variation be detected in only one case.

Non-BRCA cases were screened for 25 breast cancer-causing genes. Among 52 cases, only two (2.8%) cases, pathogenic variations were detected in the *BRIP1* and *RAD50* genes. The *BRIP1* c.139C>G (p.Pro47Ala) variation was detected in a 55-year-old OC patient who had multiple family members diagnosed with breast and/or ovarian cancer. The *RAD50* c.2083C>T (p.Gln695*) variation causing a truncated protein was detected in a 28-year-old OC patient with no records in the ClinVar or Human Gene Mutation Database (HGMD). According to ACMG criteria, this variation is predicted to be deleterious. She had an aunt who died at the age of 60 from skin cancer, but no further data was available regarding her cancer histopathology or clinical outcome. The CNVs analyses of these 25 genes using the Sophia DDM CNV detection algorithm detected no copy number variations; however, the study was not able to screen CNVs using MLPA. This case was also reported in a previous study (9) evaluating hereditary cancer cases independent of cancer type. Table 1 specifies all pathogenic variations and characteristics of the patients carrying pathogenic variations, Figure 1 presents the visualizations from the Integrative Genomics Viewer (IGV), and Figure 2 shows the data from the MLPA.

A positive family history was present in 11 of 13 (84%) cases involving a pathogenic variation, with four reported ovarian cancer diagnoses in a first-degree relative, three reported breast cancer cases in first- and second-degree relatives, and three cases reporting other types of cancers including gastrointestinal, lung, and endometrial cancers in more than two relatives.

In six cases, the study detected six variations in the *BRCA1*, *BRCA2*, *PALB2*, *CHEK2*, and *CDH1* genes that were classified as "variant of uncertain significance" (VUS) according to the ACMG criteria (Table 2; Figure 3).

Table 1. Clinical features and molecular findings of ovarian cancer cases having pathogenic/likely pathogenic variants.

Age at Diagnosis	Clinical Presentation	Family History	Gene (Transcript)	Variation	Coding Consequence	HGMD
45	Unilateral Ovarian Ca	-	<i>BRCA1</i> (NM_007294)	c.181T>G (p.Cys61Gly)	Missense	CM940172-DM (Breast cancer)
34	Unilateral Ovarian Ca	+ Pancreas Ca (Second degree relative)	<i>BRCA1</i> (NM_007294)	c.2019delA (p.Glu673Aspfs*28)	Frameshift	CD021407-DM (Ovarian cancer)
57	Unilateral Ovarian Ca	-	<i>BRCA1</i> (NM_007294)	c.2800C>T (p.Gln934*)	Nonsense	CM004607-DM (Ovarian cancer)
50	Unilateral Ovarian Ca	+ Breast and Ovarian ca (First and second degree relative)	<i>BRCA1</i> (NM_007294)	c.5074G>C (p.Asp1692His)	Missense	CM129092-DM? (Breast cancer)
47	Bilateral Ovarian Ca+ Breast Ca	+ Breast and Ovarian ca (First degree relative)	<i>BRCA1</i> (NM_007294)	c.5266dupC (p.Gln1756Profs*74)	Frameshift	CI941841-DM (Breast cancer)
56	Unilateral Ovarian Ca	+ Ovarian Ca (First degree relative)	<i>BRCA1</i> (NM_007294)	c.5266dupC (p.Gln1756Profs*74)	Frameshift	CI941841 (Breast cancer)
54	Unilateral Ovarian Ca	+ Breast Ca (First degree relative) Thyroid ca (Second Degree Relative)	<i>BRCA1</i> (NM_007294)	Exon 3-8 dup	CNV	CN025048-DM (Breast and/or ovarian cancer)
42	Unilateral Ovarian Ca+ Breast Ca	+ Breast Ca (First degree relative)	<i>BRCA1</i> (NM_007294)	EX 18-19 DEL	CNV	CG146559-DM (Breast cancer)
45	Unilateral Ovarian Ca	+ Breast Ca (First degree relative)	<i>BRCA1</i> (NM_007294)	EX21-23 DEL	CNV	CG052603-DM (Breast and/or ovarian cancer)
40	Unilateral Ovarian Ca+ Breast Ca	+ Endometrium Ca (First degree relative)	<i>BRCA1</i> (NM_007294)	Exon 24 del	CNV	CG146555-DM (Ovarian cancer)
50	Unilateral Ovarian Ca+ Breast Ca	+ Endometrium Ca (second degree relative)	<i>BRCA2</i> (NM_000059)	c.6405_6409del (p. Asn2135Lysfs*3)	Frameshift	CD972084-DM (Breast cancer)
55	Unilateral Ovarian Ca	+ Breast and Ovarian Ca (First Degree relative) Pancreas Ca (Second Degree Relative)	<i>BRIP1</i> (NM_032043)	c.139C>G (p.Pro47Ala)	Missense	CM014756-DM (Breast cancer)
28	Unilateral Ovarian Ca	+ Malign Melanoma (second degree relative)	<i>RAD50</i> (NM_005732)	c.2083C>T (p.Gln695*)	Nonsense	Novel

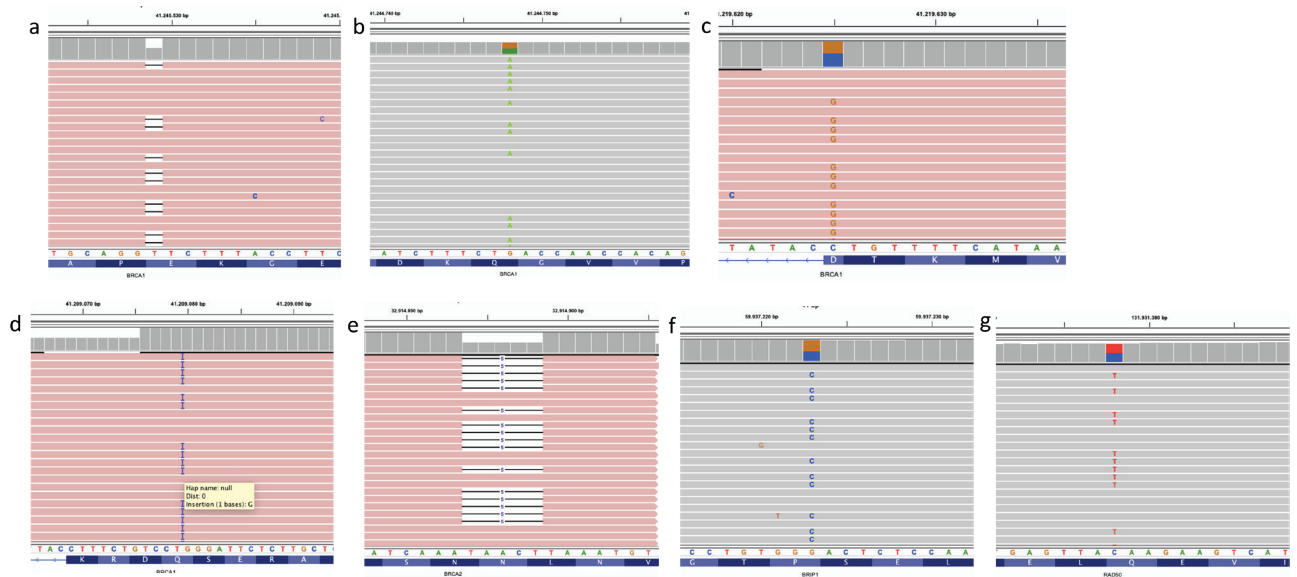


Figure 1. Integrative genomics viewer (IGV) visualizations of detected pathogenic variants.

- a) BRCA1 heterozygous c.2019delA (p.Glu673Aspfs*28),
- b) BRCA1 heterozygous c.2800C>T (p.Gln934*),
- c) BRCA1 heterozygous c.5074G>C (p. Asp1692His),
- d) BRCA1 heterozygous c.5266dupC (p.Gln1756Profs*74),
- e) BRCA2 heterozygous c.6405_6409del (p. Asn2135Lysfs*3),
- f) BRIP1 heterozygous c.139C>G (p.Pro47Ala),
- g) RAD50 heterozygous c.2083C>T (p.Gln695*)

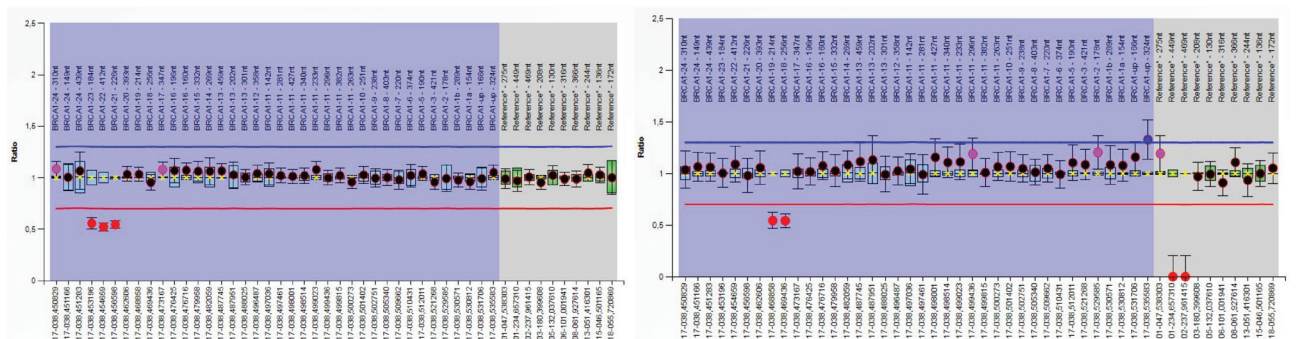


Figure 2. Multiplex Ligation-Dependent Probe Amplification (MLPA) data of copy number variants.

- a) BRCA1 heterozygous exon 21-23 deletion,
- b) BRCA1 heterozygous exon 18-19 deletion.

DISCUSSION

This study has investigated 63 ovarian cancer patients for germline variations among 25 cancer-related genes. A family history of ovarian cancer and certain other neoplasms including breast, colorectal, and endometrium cancers are also well-known risk factors for OC (10). The current study reported 49% of cases ($n = 31$) to have at least one first-degree relative with

a history of cancer. This finding is consistent with a previous study which had reported as 40% in a large cohort (11). The current study also evaluated family history up to third-degree relations, which observed this ratio increase up to 76% ($n = 48$). Although family history was not an inclusion criterion for this study, this high rate is thought to be due to the tendency of clinicians to refer patients to genetics department when a family history of cancer is already present.

Table 2. The VUSs detected in the study.

Age at diagnosis	Gene/ Transcript	Variation	Frequency in our Inhouse database	MAF (GnomAD)	Mutation Taster	DANN	GERP	ClinVar/ HGMD	dbSNP
36	<i>PALB2</i> NM_024675	c.3306C>G (p.Ser1102Arg)	0.00005	0.000007953	Polymorphism	0.7592	6.1399	VUS/DM? (Breast cancer)	rs515726112
55	<i>PALB2</i> NM_024675	c.3508C>A p.His1170Asn	0,00005	-	Polymorphism	0.9857	5.9	VUS/-	rs200283306
60	<i>CDH1</i> NM_004360	c.2602C>T p.(Arg868Cys)	0.00006	-	Disease Causing	0.9984	6.17	VUS/-	rs864622630
50	<i>CHEK2</i> NM_001005735	c.157T>A (p.Ser53Thr)	0.00005	0.00004773	Disease Causing	0.9981	5.42	VUS/-	rs371657037
53	<i>BRCA1</i> NM_007294	c.401_403dupCCA (p.Ala134_ Lys135insThr)	0.00003	-	Polymorphism	-	5.32	VUS/-	rs1555596338
30	<i>BRCA2</i> NM_000059	c.8416T>C (p.Ser2806Pro)	0.00003	-	Disease Causing	0.9989	5.19	VUS/DM (Prostate cancer)	rs1280487930

VUS: Variant of uncertain significance, MAF: Minor allele frequency, DANN: Deep neural network variant predictor, GERP: Genomic evolutionary rate profiling, DM: Disease mutation.

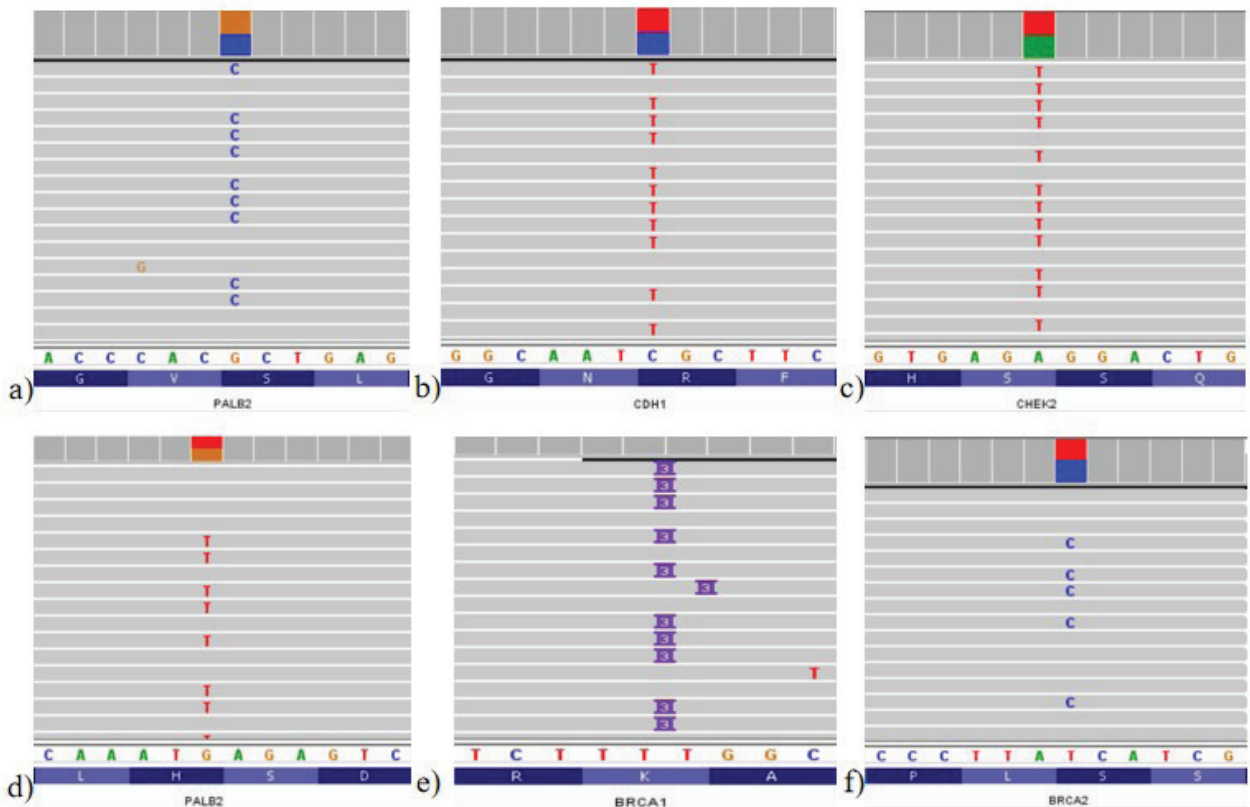


Figure 3. Integrative genomics viewer (IGV) visualizations of detected VUS.

- a) PALB2 heterozygous c.3306C>G (p.Ser1102Arg),
- b) CDH1 heterozygous c.2602C>T (p.Arg868Cys),
- c) CHEK2 heterozygous c.157T>A (p.Ser53Thr),
- d) PALB2 heterozygous c.3508C>A (p.His1170Asn),
- e) BRCA1 heterozygous c.401_403dupCCA (p.Ala134_Lys135insThr),
- f) BRCA2 heterozygous c.8416T>C (p.Ser2806Pro).

Among the 48 family-history positive patients, 30 (62.5%) reported breast and/or ovarian cancer in other family members, which suggests that hereditary breast and ovarian cancer syndrome (HBOCS) is related to the *BRCA1* and *BRCA2* genes. Germline pathogenic variations in *BRCA1* and *BRCA2* have also been detected in about 65%-85% of hereditary OC as its most common cause (5). Based on these data, the study screened the *BRCA1* and *BRCA2* genes for pathogenic variations as a first step. Pathogenic *BRCA1* and *BRCA2* variations are known to be related with HBOCS and were detected in a total of 11 cases, with pathogenic *BRCA1* variations being detected in 10 (90.9%) cases diagnosed as HBOCS. Only one case saw a pathogenic *BRCA2* variation (c.6405_6409del; p. Asn2135Lysfs*3) was detected in only one case. The 1:10 ratio for *BRCA2:BRCA1* variations is an unexpected result, as variations have been reported as being one and a half to two times higher in *BRCA1* than in *BRCA2* with regard to ovarian cancer (5). The ratio in this study could not be explained through the ancestry of the population as a previous study (12) of 102 Turkish ovarian cancer patients contrarily detected this ratio to be 7:10. Although their study group had a predominance of non-familial cases, which is slightly different from the current study and its predominance of familial cases, the current study's data are not supportive enough to compare the penetrance of *BRCA* genes for ovarian cancer, as performing a segregation analysis was not possible here. However, another study (13) from Turkey involved 44 ovarian cancer patients, similar to the current study, and detected pathogenic *BRCA1* variations in 18 of the cases, while detecting only one patient with a *BRCA2* variation. The pathogenic variation detection rate of sequencing of whole exons and the deletion duplication analysis for *BRCA1* and *BRCA2* genes are known to respectively be around 90% and 10% in *BRCA*-related HBOCS. Maistro et al. (14) reported *BRCA1* rearrangements in two out of 100 OC cases, while Zhang et al.'s study (15) on 1,342 OC patients reported a gross deletion rate of 3.9% for all detected pathogenic variations in 0.5% of the cohort. This study detected CNVs in four out of 11 (36%) cases, all of which affected at least one exon of the *BRCA1* gene and corresponding to 6.3% of all the OC cases. This study speculates that the approximately 10x higher rate of gross deletion duplications may be due to the small number of patients included in the study. However, the largest cohort study screening large *BRCA1* rearrangements among a Turkish population including 667 OC patients detected 27 large genomic rearrangements, which corresponded to 4% of the cohort and 78% of the *BRCA1* pathogenic variation carriers (16). Because of the insufficient information regarding a methodology for SNV screening, the SNV detection rates from these two studies cannot be compared. However, these two studies do indicate a higher CNV detection rate in Turkish OC patients. Yazıcı et al.'s study (17) also reported a *BRCA1* rearrangement rate of 4% in ovarian cancer cases, which supports the previous statement.

Among the 52 non-*BRCA* cases, this study detected pathogenic variations in the *BRIP1* and *RAD50* genes of two cases. *BRIP1* encodes the *BRCA1*-associated C-terminal helicase 1 and

is one of the most commonly affected genes in non-*BRCA* OC patients, with approximately one-third of OC patients carrying a pathogenic variation in their *BRIP1* gene (18). The *BRIP1* c.139C>G (p.Pro47Ala) variation was reported previously and shown to result in complete loss of helicase activity (19). The case in the current study carrying the *BRIP1* c.139C>G (p.Pro47Ala) variant had been diagnosed at the age of 55 and had first- and second-degree relatives with breast and ovarian cancer. The study detected a novel variation in the *RAD50* gene (c.2083C>T; p.Gln695*) in one case, and this is predicted as being a likely pathogenic variation related to the ACMG criteria. The patient in this case was one of the youngest in the study's cohort, with a diagnosis age of 28. Her aunt (father's sister) was the only other known cancer case in her family, with the aunt having been diagnosed with skin cancer and dying at the age of 60. The *RAD50* gene is a relatively rare one to be affected in OC patients, with Minion et al. reporting a 3% incidence rate of non-*BRCA* in OC cases (17). The *RAD50* gene encodes an essential protein that plays an important role in repairing DNA double-strand breaks, with biallelic variations being related to a Nijmegen breakage syndrome-like disorder (OMIM: #613078) that presents itself with dysmorphic features, growth retardation, and developmental delay (20).

BRCA2 and *BRIP1* biallelic variations have been related to Fanconi anemia (21), with patients possessing monoallelic variations in the *BRCA2* and *BRIP1* genes having been evaluated with the related autosomal recessive disorders and no such history being reported in the families. However, segregation analysis and genetic counseling were planned for at risk family members.

CONCLUSION

This study has evaluated 63 OC cases for underlying molecular deficiencies and detected the *BRCA1* gene as the most commonly affected gene in OC cases, with the *BRCA2*, *BRIP1*, and *RAD50* genes being the other ones in which germline cancer-related variations were detected. The high rate of CNVs in *BRCA1* indicates the sequencing of cancer predisposition genes to be insufficient for OC cases and the CNV analysis of genes (especially *BRCA1*) should be done as the second step in molecular analysis following the *BRCA1* sequencing. However, the widespread use of multigene panel tests and improvement of the CNV analysis algorithms in sequence analysis tools would help accelerate diagnostic processes. Additionally, countries with high consanguineous marriage rates such as Turkey will benefit by informing the families of patients to be aware that preconception and/or prenatal diagnostic opportunities through genetic counseling are very important with regard to these autosomal recessive conditions and that a family-oriented approach is a required.

Ethics Committee Approval: This study was approved by the Clinical Research Ethics Committee of Marmara University Medical Faculty (24.07.2020-09.2020.751).

Peer-review: Externally peer-reviewed.

Author Contributions: Conception/Design of Study – E.A.A., C.A., B.B.G., A.İ.G., T.G.; Data Acquisition – E.A.A., C.A., B.B.G., A.İ.G., T.G.; Performing experiments – E.A.A., C.A., B.B.G., A.İ.G., T.G.; Data Analysis/ Interpretation – E.A.A., C.A., B.B.G., A.İ.G., T.G.; Statistical Analyses – E.A.A., C.A., B.B.G., A.İ.G., T.G.; Drafting Manuscript – E.A.A., C.A., B.B.G., A.İ.G., T.G.; Critical Revision of Manuscript – E.A.A., C.A., B.B.G., A.İ.G., T.G.; Final Approval and Accountability – E.A.A., C.A., B.B.G., A.İ.G., T.G.;








Conflicts of Interest: The authors declare no conflict of interest.

Financial Disclosure: The authors declare that this study has received no financial support.

REFERENCES

1. Stewart C, Ralyea C, Lockwood S. Ovarian cancer: An integrated review. *Semin Oncol Nurs* 2019; 35(2): 151-6. [\[CrossRef\]](#)
2. Webb PM, Jordan SJ. Epidemiology of epithelial ovarian cancer. *Best Pract Res Clin Obstet Gynaecol* 2017; 41: 3-14. [\[CrossRef\]](#)
3. Eccles DM, Balmana J, Clune J, Ehlik B, Gohlke A, Hirst C, et al. Selecting patients with ovarian cancer for germline brca mutation testing: Findings from guidelines and a systematic literature review. *Adv Ther* 2016; 33(2): 129-50. [\[CrossRef\]](#)
4. Shanbhogue KP, Prasad AS, Ucisik-Keser FE, Katabathina VS, Morani AC. Hereditary ovarian tumour syndromes: Current update on genetics and imaging. *Clin Radiol* 2021; 76(4): 313e315-313 e326. [\[CrossRef\]](#)
5. Toss A, Tomasello C, Razzaboni E, Contu G, Grandi G, Cagnacci A, et al. Hereditary ovarian cancer: Not only BRCA 1 and 2 genes. *Biomed Res Int* 2015; 2015: 341723. [\[CrossRef\]](#)
6. Ledermann JA, Raja FA, Fotopoulou C, Gonzalez-Martin A, Colombo N, Sessa C. Newly diagnosed and relapsed epithelial ovarian carcinoma: ESMO Clinical Practice Guidelines for diagnosis, treatment and follow-up. *Ann Oncol* 2013; 24 Suppl 6:vi24-32. [\[CrossRef\]](#)
7. Fierheller CT, Alenezi WM, Tonin PN. The Genetic analyses of French Canadians of Quebec facilitate the characterization of new cancer predisposing genes implicated in hereditary breast and/or ovarian cancer syndrome families. *Cancers (Basel)* 2021; 13(14). [\[CrossRef\]](#)
8. Richards S, Aziz N, Bale S, Bick D, Das S, Gastier-Foster J, et al. Standards and guidelines for the interpretation of sequence variants: a joint consensus recommendation of the American College of Medical Genetics and Genomics and the Association for Molecular Pathology. *Genet Med* 2015; 17(5): 405-24. [\[CrossRef\]](#)
9. Arslan Ates E, Turkyilmaz A, Alavanda C, Yildirim O, Guney AI. Multigene panel testing in Turkish hereditary cancer syndrome patients. *Medeni Med J* 2022; 37(2): 150-8. [\[CrossRef\]](#)
10. La Vecchia C. Ovarian cancer: Epidemiology and risk factors. *Eur J Cancer Prev* 2017; 26(1): 55-62. [\[CrossRef\]](#)
11. Zheng G, Yu H, Kanerva A, Forsti A, Sundquist K, Hemminki K. Familial ovarian cancer clusters with other cancers. *Sci Rep* 2018; 8(1): 11561. [\[CrossRef\]](#)
12. Yazici H, Glendon G, Burnie SJ, Saip P, Buyru F, Bengisu E, et al. BRCA1 and BRCA2 mutations in Turkish familial and non-familial ovarian cancer patients: A high incidence of mutations in non-familial cases. *Hum Mutat* 2002; 20(1): 28-34. [\[CrossRef\]](#)
13. Demir S, Tozkir H, Gurkan H, Atli El, Yalcintepe S, Atli E, et al. Genetic screening results of individuals with high risk BRCA-related breast/ovarian cancer in Trakya region of Turkey. *J BUON* 2020; 25(3): 1337-47.
14. Maistro S, Teixeira N, Encinas G, Katayama ML, Niewiadonski VD, Cabral LG, et al. Germline mutations in BRCA1 and BRCA2 in epithelial ovarian cancer patients in Brazil. *BMC Cancer* 2016; 16(1): 934. [\[CrossRef\]](#)
15. Zhang S, Royer R, Li S, McLaughlin JR, Rosen B, Risch HA, et al. Frequencies of BRCA1 and BRCA2 mutations among 1,342 unselected patients with invasive ovarian cancer. *Gynecol Oncol* 2011; 121(2): 353-7. [\[CrossRef\]](#)
16. Aktas D, Gultekin M, Kabacam S, Alikasifoglu M, Turan AT, Tulunay G, et al. Identification of point mutations and large rearrangements in the BRCA1 gene in 667 Turkish unselected ovarian cancer patients. *Gynecol Oncol* 2010; 119(1): 131-5. [\[CrossRef\]](#)
17. Yazici H, Kilic S, Akdeniz D, Sukruoglu O, Tuncer SB, Avsar M, et al. Frequency of rearrangements versus small indels mutations in BRCA1 and BRCA2 genes in Turkish patients with high risk breast and ovarian cancer. *Eur J Breast Health* 2018; 14(2): 93-9. [\[CrossRef\]](#)
18. Minion LE, Dolinsky JS, Chase DM, Dunlop CL, Chao EC, Monk BJ. Hereditary predisposition to ovarian cancer, looking beyond BRCA1/BRCA2. *Gynecol Oncol* 2015; 137(1): 86-92. [\[CrossRef\]](#)
19. Cantor S, Drapkin R, Zhang F, Lin Y, Han J, Pamidi S, et al. The BRCA1-associated protein BACH1 is a DNA helicase targeted by clinically relevant inactivating mutations. *Proc Natl Acad Sci USA* 2004; 101(8): 2357-62. [\[CrossRef\]](#)
20. Waltes R, Kalb R, Gatei M, Kijas AW, Stumm M, Soback A, et al. Human RAD50 deficiency in a Nijmegen breakage syndrome-like disorder. *Am J Hum Genet* 2009; 84(5): 605-16. [\[CrossRef\]](#)
21. Del Valle J, Rofes P, Moreno-Cabrera JM, Lopez-Doriga A, Belhadj S, Vargas-Parra G, et al. Exploring the role of mutations in fanconi anemia genes in hereditary cancer patients. *Cancers (Basel)* 2020; 12(4). [\[CrossRef\]](#)

Differential Cytotoxic Activity of a New Cationic Pd(II) Coordination Compound with N₄-Tetradentate Hybrid Ligand in Cancer Cell Lines

Merve Erkisa Genel^{1,2,3} , Selin Selvi³ , Ismail Yilmaz⁴ , Remzi Okan Akar^{3,6} , İlhan Yaylim¹ , Abdurrahman Sengul^{5,*} , Engin Ulukaya^{3,6,*} 

*asterik indicates two corresponding authors

¹Department of Molecular Medicine, Aziz Sancar Institute of Experimental Medicine, Istanbul University, Istanbul, Turkiye

²Institute of Graduate Students in Health Sciences, Istanbul University, Istanbul, Turkiye

³Molecular Cancer Research Center (ISUMKAM), Istinye University, Istanbul, Turkiye

⁴Department of Chemistry, Faculty of Science, Karabuk University, Karabuk, Turkiye

⁵Department of Chemistry, Faculty of Arts and Sciences, Zonguldak Bulent Ecevit University, Zonguldak, Turkiye

⁶Department of Clinical Biochemistry, Faculty of Medicine, Istinye University, Istanbul, Turkiye

ORCID ID: M.E.G. 0000-0002-3127-742X; S.S. 0000-0003-2762-4780; İ.Y. 0000-0002-0139-0122; R.O.A. 0000-0001-8687-2034; İ.Y. 0000-0003-2615-0202; A.S. 0000-0001-6851-4612; E.U. 0000-0003-4875-5472

Cite this article as: Erkisa Genel M, Selvi S, Yilmaz I, Akar RO, Yaylim I, Sengul A, Ulukaya E. Differential cytotoxic activity of a new cationic Pd(II) coordination compound with n4-tetradentate hybrid ligand in cancer cell lines. *Experimed* 2022; 12(3): 188-201.

ABSTRACT

Objective: Successful cancer treatment still requires the discovery of novel compounds that hold promise for chemotherapeutics. The objective of this study was to examine the effectiveness of a newly synthesized cationic palladium(II) coordination compound that functions via several pathways to provide an efficient therapeutic option for various cancer cells.

Materials and Methods: A new cationic palladium(II) coordination compound, [Pd(L)]Cl₂·H₂O, denoted as Complex 1, where the ligand L is the compound 6,6'-bis(NH-benzimidazol-2-yl)-2,2'-bipyridine, was synthesized and characterized by the attenuated total reflectance (ATR) - fourier-transform infrared spectroscopy (FT-IR), proton nuclear magnetic resonance (¹H NMR), electrospray ionization mass spectrometry (ESI-MS), and carbon-hydrogen-nitrogen (CHN) analyses. The density functional theory (DFT) calculations show the coordination sphere around the metal center in Complex 1 to be made up of tertiary N atoms of the pyridine (py) and benzimidazole (bim) rings completing the square-planar geometry with significant distortion. The anti-growth/cytotoxic activity of the complex was determined using the sulforhodamine B (SRB) and adenosine triphosphate (ATP) viability assays for 24 and 48 h *in vitro*. The study evaluates the determinations for annexin V-propidium iodide (PI) positivity, mitochondrial membrane potential loss, Bcl-2 protein inactivation, and deoxyribonucleic acid (DNA) damage to investigate the cell death mode and its partial mechanism.

Results: Complex 1 caused cytotoxicity in a dose-dependent manner in all the cell lines used, with IC₅₀ values ranging from 2.6-8.8 μM for 48 h. Among the cancer models, colon and breast cancer cell lines underwent cell death by well-described apoptosis through the intrinsic pathway involving the mitochondria. However, the other cell lines did not show such a cell death modality. This implies that differential cell death modes operate based on the cancer type.

Conclusion: For the treatment of breast and colon cancers, the complex 1 appears to be a unique, promising complex. Therefore, complex 1 deserves further attention for proof of concept in animal models.

Keywords: Palladium complexes, N₄-donor ligand, benzimidazole, bipyridine, apoptosis, anticancer effect

Corresponding Author1: Engin Ulukaya **E-mail:** eulukaya@istinye.edu.tr

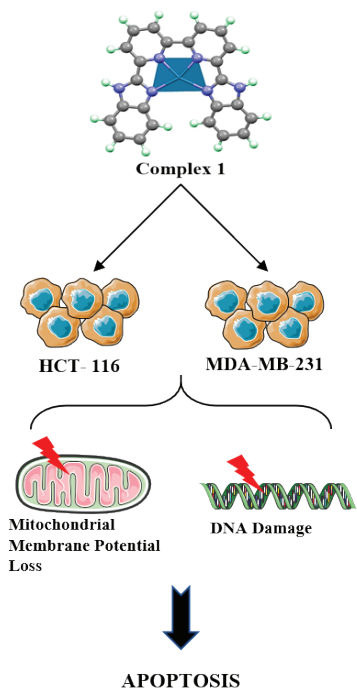
Corresponding Author2: Abdurrahman Sengul **Email:** sengul@beun.edu.tr

Submitted: 14.10.2022 **Revision Requested:** 26.10.2022 **Last Revision Received:** 03.12.2022 **Accepted:** 05.12.2022 **Published Online:** 27.12.2022



Content of this journal is licensed under a Creative Commons Attribution-NonCommercial 4.0 International License.

GRAPHICAL ABSTRACT



Highlights

- A new cationic Pd(II) complex is synthesized with N_4 -donor ligand
- DFT calculations show that complex 1 has a distorted square planar geometry
- Complex 1 dependent cell death mode differs depending on the type of cancer.
- Complex 1 induces intrinsic apoptosis and DNA damage in colon and breast cancer cells.

INTRODUCTION

Successful cancer treatment still needs new complexes to be developed that hold promise for chemotherapeutics due to a few reasons such as acquired resistance to anticancer drugs during the treatment period with few exceptions. Another problem is the heterogeneity of tumor tissue, the presence of a variety of clones in the same tissue that respond differently to the applied treatments. Another important problem is the serious side effects of the drugs, sometimes even resulting in discontinued treatment. Therefore, developing novel compounds would provide a chance at gaining a new set of anticancer drugs. These may even have a new class of mechanisms of action that will be profoundly appreciated. Metal-based complexes (e.g., cisplatin) are particularly efficient in terms of their DNA-damaging effects that eventually cause cell death. Since the discovery of cisplatin (i.e., cis-diamminedichloroplatinum II, or $cis-[Pt(NH_3)_2Cl_2]$), countless research advances have been performed for preventing and

treating cancer. Chemotherapeutic drugs that are currently on the market have poor efficacy and harmful side effects (1). Therefore, a focus in this particular discipline involves the creation and development of new anticancer medications with greater cytotoxic efficacy against cancer cells and minimal side effects. Due to their capacity to interact with a variety of different enzymes and receptors, benzimidazoles are well known as biologically significant chromophores in medicinal chemistry (2). Transition metal complexes of such biologically significant ligands exhibit better pharmacological activity than the corresponding free ligand.

Studies of transition metal coordination complexes with N_4 -donor tetradentate ligands are appealing due to their interesting coordination modes, catalytic activities, and electronic and photo-physical properties (3, 4). In particular, square-planar d^8 metal complexes with these types of ligands have gained enormous interest in the field of anticancer drug agents due to these planar metal complexes providing a large aromatic surface as a prerequisite for DNA intercalators (5). Cisplatin is one of clinics' most effective and widely used chemotherapeutic agents. However, cisplatin causes serious side effects like nephrotoxicity, ototoxicity, nausea, and vomiting. Due to its limited efficacy and severe side effects, researchers are focused on developing new platinum drugs that have fewer side effects and the ability to overcome drug resistance (6). Although intense research on the biological activities of metallointercalators has been performed, the intrinsic relationship between their molecular structure and cytotoxicity has yet to be elucidated. Researchers aim to modify the structure of the intercalator ligand to develop new drugs possessing different biological activities. In this respect, studies have shown that changing the metal ion and modifying the organic ligand in the coordination complexes results in the changes in the DNA affinity, binding mode, and strength of the transition metal complexes (7). Even though palladium and platinum are members of the same chemical group, their modes of action may be distinct from those of cisplatin and from one another. In comparison to their Pt(II) counterparts, Pd(II) complexes have a stronger capacity to coordinate with DNA bases and, as a result, more effectively suppress the proliferation of cancer cells such as KB, A549, and MCF7 (8). When coupled with N-donor ligands, Pd(II) and Pt(II) assume the same square-planar geometry and exhibit similar properties as a d^8 -metal ion. The Pt(II) is kinetically more stable than the Pd(II) counterpart as revealed by the ligand-exchange kinetics during the aquation reaction Pd(II) estimated to be 10^6 times faster than Pt(II) (9). As a tridentate chelating ligand, 2,6-bis(NH-benzimidazol-2-yl)pyridine coordinates with the metal center stronger than the tridentate 2,2':6',2''-terpyridine ligand due to the benzimidazole rings being more basic than the pyridine rings (10). Therefore, the present complex of the N_4 -donor hybrid ligand which acts as a π -donor and π -acceptor can be compared to analogous metal complexes with QP, such as $(Pt(QP))^{2+}$ which has been shown to bind to double-helix DNA more strongly than the terpyridine (terpy)- and bipyridine (bpy)-Pt(II) complexes (11). The DNA binding of the substrate depends

on the surface extension of the aromatic moiety. The Pt(II) complex (i.e., Pt(QP)²⁺) was demonstrated to have comparable cytotoxicity to cisplatin against human carcinoma cell lines (e.g., breast, colorectal, lung), and cisplatin-resistant cell lines (5). As previously established, metal complexes' biological activity can be regulated by changing the metal ion and modifying the ligand structure through the introduction of NH functionalities along with the extension of the aromatic ring system, as exemplified by the study from Chi-Ming Che et al. (12). In this regard, the current study would like to report the synthesis of a new Pd(II) coordination complex with a tetradentate 2,2'-bipyridine ligand bearing biologically significant benzimidazole chromophores that extends the aromatic surface and provides NH functional groups for hydrogen bonding interactions with DNA (13, 14). Also, the ligand (L) having an N₄-tetradentate binding pocket, which forms a stable chelate (Pd(L))Cl₂·H₂O under physiological conditions, is expected to show higher cytotoxic activity as has been observed for the polypyridine-iron(II) complexes (15). Such structural and chemical properties of the new cationic palladium(II) complex are significantly important for a potential drug targeting DNA due to the present *in vitro* studies of the platinum(II) counterpart having been found to exhibit higher cytotoxic activity in comparison to cisplatin toward certain cancer lines (14). In present study has found the Complex 1 to show promise toward prostate cancer treatment with an IC₅₀ value of 2.6 μM, which deserves further attention from proof-of-concept studies.

MATERIALS AND METHODS

Materials

Analytical pure reagents were obtained from Merck. IR spectra were analyzed in the 4,000-600 cm⁻¹ region using PerkinElmer Spectrum 100 fourier-transform infrared (FT-IR) spectrophotometer. Nuclear magnetic resonance analysis (NMR) results were obtained using the Bruker DPX-400 NMR spectrometer. Analysis of the elements was carried out on the element analyzer. Liquid chromatography-mass spectrometry/mass spectrometry (LC-MS/MS), electrospray ionization mass spectrometry (ESI-MS) were obtained with an AB 4000 QTRAP LC-MS. Pd(COD)₂Cl₂ where COD = 1,5-cyclooctadiene was prepared according to the methods in the literature (15). Ground-state geometry optimization was studied as described elsewhere (16, 17). The software Gaussian 09 was used for calculations and the software Gaussview 5.0 was used for visualizations (18). The B3LYP/6-31G(d,p) level was chosen because the B3LYP functionality has been proven to give good results for organic molecules (19) and the LANL2DZ basis set for the metal coordination compound. A similar previous study discovered the B3LYP/6-31G(d,p) level results to correlate with the experimental data (20).

Synthesizing the Ligand 6,6'-bis(NH-benzimidazol-2-yl)-2,2'-bipyridine (L)

The synthesis and purification details of the ligand have been previously reported (14, 21), and the characterization data are identical with the literature data (14). ESI-MS: *m/z* 411.1

[M+Na]⁺ (Figure S1). ¹H NMR (DMSO-*d*₆): δ = 13.09 (s, 2H, NH), 9.09 (d, 2H, *J* = 7.83 Hz, bpy-H3,3'), 8.54 (d, 2H, *J* = 7.76 Hz, bpy-H5,5'), 8.26 (t, 2H, *J*_{4,5} = 7,80 Hz, *J*_{4,3} = 7,82 Hz, bpy-H4,4'), 7.76 (d, 2H, *J* = 8 Hz, bim), 7.66 (d, 2H, *J* = 8 Hz, bim), 7.30 (m, 4H, bim) (Figure S2). ¹³C NMR (DMSO-*d*₆): δ = 155 (bpy-C2,2'), 152 (bim-C2,2'), 148 (bpy-C6,6'), 144 (bim), 139 (bpy-C4,4'), 124 (bpy-C3,3'), 123 (bim), 120 (bpy-C5,5') ve 113 (bim) (Figure S3). Attenuated total reflectance (ATR)-FT-IR (4000-600 cm⁻¹): 3286 (br, w, ν_{as}(N-H)), 3074 (w, ν_{as} Ar-H), 1657(m), 1624(m), 1589(m), 1573(m) (bim and py rings), 1434 (br, s, δ (N-H)), 1371 (s, δ CH)), 1231(s, ν(C-N)), 1079 (s), 991(m), 935 (m), 877 (m), 808 (m), 741 (s, δ (C-H)) (Figure S4).

Synthesizing the 6,6'-bis(NH-benzimidazol-2-yl)-2,2'-bipyridylpalladium(II)chloride Monohydrate [Pd(L)]Cl₂·H₂O

The mixture of [Pd(L)]Cl₂·H₂O (0.019 g, 0.065 mmol) in MeOH was mixed with a solution of 6,6'-bis(NH-benzimidazol-2-yl)-2,2'-bipyridine (0.003 g, 0.065 mmol) in MeOH (25.0 mL) (25.0 mL). The reaction solution was mixed for 3 h at reflux. The yellow solid that precipitated at room temperature was then filtered and air dried (22 mg, 60% humidity) after washing with about 200 mL of methanol and diethyl ether, respectively. Analysis calculated for C₂₄H₁₆N₆Cl₂·Pd·H₂O: C 49.48; H 3.11; N 14.44. Found: C 49.52; H 2.98; N 14.55. FT-IR (KBr, ν/cm⁻¹): 3427 (w, ν_{as}(N-H)), 3067 (w, ν (Ar-H)), 1592 (m) and 1570 (s) (py and bim rings), 1457 (s), 1411(s), 1271 (s), 812 (s), 735 (s), 708 (m) (Figure 1). LC-ESI-MS *m/z* 246 [Pd(L)]²⁺, 389 [L+Na]⁺, 495.4 [Pd(L)-H]⁺, 554.9 [Pd(L)+Cl+Na]⁺ (Figure S5). ¹H NMR (DMSO-*d*₆): δ = 14.15 (brd, s, NH), 9.11 (d, *J* = 8 Hz, 2H), 8.45 (d, *J* = 8 Hz, 2H), 8.29 (t, *J* = 8 Hz, 2H), 7.74 (m, 4H), 7.34 (m, 4H) (Figure S6).

Cell Culture

The A549, MDA-MB-231, PC-3, HCT-116, and BEAS-2B cell lines were cultured in the RPMI 1640 (Gibco, Grand Island, NY, USA) medium supplemented with 100U/mL penicillin+100μg/mL streptomycin (P/S; Gibco, Grand Island, NY, USA), 2 mM L-glutamine (Gibco, Grand Island, NY, USA), and a 10% fetal bovine serum (FBS; Lonza, Verviers, Belgium). MDA-MB-231 cells were cultured in the RPMI-1640 medium supplemented with P/S, 2 mM L-glutamine, and 5% FBS. All cells were incubated at 37°C in a humidified atmosphere containing 5% CO₂.

Determination of the Antiproliferative Effect Using the SRB and ATP Viability Assays

For the sulforhodamine B assay (SRB; Invitrogen S1307, Massachusetts, USA) and the adenosine triphosphate assay (ATP ; SIGMA 32160414, Missouri, USA) assays, all cells were cultured at a density of 5×10³ cells per well on a 96-well plate in triplicates. After 24 h, Complex 1 was added at different concentrations (Range = 1.25-40 μM) over 48 h. After the treatment period, the SRB and ATP assays were studied, as described elsewhere (14).

Evaluation of the Cell Death Using Flow Cytometry

To specify Complex 1's effects on apoptosis, the study measured γ-H2A.X (phosphorylation of the Ser-139 residue of the histone variant (H2A.X)) activation (MCH200101 Millipore, Darmstadt,

Germany), the MitoPotential assay (MCH100110, Millipore, Darmstadt, Germany), Bcl-2 inactivation (MCH200105, Millipore, Darmstadt, Germany), and phosphatidylserine translocation (MCH100105, Millipore, Darmstadt, Germany) using flow cytometry. All cell lines were seeded at 3×10^5 cells/well into 6-well plates and treated with Complex 1 at the previously calculated IC_{90} values and incubated for 24 and 48 h. At the end of the treatment period, all of the assays were implemented as described to the cells (22).

Statistical Analyses

GraphPad Prism 6.0 statistical software (San Diego, CA) for Windows was used to perform one-way ANOVA on all of the data before the Tukey post-hoc test. Statistical significance was defined as $p < 0.05$.

RESULTS AND DISCUSSION

Geometry Optimization

The geometry-optimized structure of Complex 1 has been obtained through density functional theory (DFT) calculations with the exception of the crystallization water and the counter ion chlorides (Figure 1). Table S1 gives the selected bond distances, angles, and dihedral angles for the optimized metal Complex 1. The palladium(II) ion in Complex 1 is seen to have adopted a distorted square-planar geometry with a N_4 -donor tetradentate ligand akin to that of the structurally related coordination compound 2,2':6',2"':6"':2"''-quaterpyridine (QP) with platinum(II), $[Pt(QP)]^{2+}$ (23). The Pd atom in Complex 1 deviates by 4.7° from the square planar geometry (Figure 3a). Bipyridine and benzimidazole moieties are not coplanar (Figure 3b). The mean planes of the two bim rings intersect at 9.7° (the difference between C17-N2-Pd-N4 and C18-N5-Pd-N4), and the dihedral angle between the py and bim rings is nearly 176.8° (N4-C1-C24-N6), with bond lengths and bond angles being affected by these deviations. Pd-N bond lengths on the bim side (Pd-N2 and Pd-N5) are longer than Pd-N bond lengths on the py side (Pd-N3 and Pd-N4 in Table 1). The trans angles N2-Pd-N4 and N3-Pd-N5 are 159.12° , indicating a distorted square geometry. As far as the study has noted, this seems to be the first palladium(II) complex with the N_4 -donor 6,6'-bis(NH-benzimidazol-2-yl)-2,2'-bipyridine ligand.

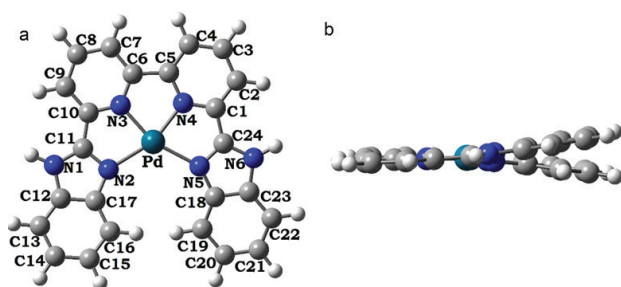
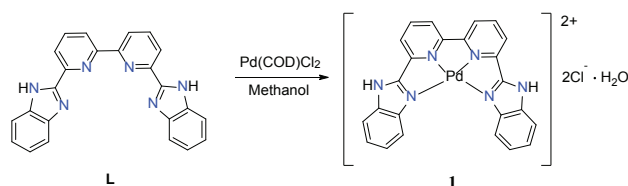


Figure 1. Optimized gas-phase structure of Complex 1 at B3LYP/6-31G(d,p) level with LANL2DZ on metal (a: top view, b: side view)

Synthesis and Characterization

The N_4 -donor tetradentate hybrid ligand (**L**) was synthesized as reported previously (21), with the specifics of the synthesis and characterization of the ligand having been recently detailed (24). The characterization data for **L** are identical to those of the reported data (24). The ESI-MS spectrum (Figure S1) shows the molecular ion peak at m/z 411.1 to be attributed to $[L+Na]^+$.

The Pd(II) coordination Complex 1 was readily obtained by the treatment of $[Pd(COD)Cl_2]$ with **L** in refluxing methanol at good yield, as illustrated in Scheme 1. The compound dissolves in



Scheme 1. The synthetic route of the palladium(II) complex

the coordinating solvents of DMF and DMSO, but is insoluble in common solvents. All attempts to obtain single crystals of Complex 1 were met with failure. The elemental analysis of Complex 1 offered a 1:1 (metal:ligand) stoichiometry, as expected. For Complex 1, a water molecule was added as a result of the analytical findings supporting this (*vide infra*). In the mass spectrum of Complex 1 (Figure S5), the mono-charged ion at m/z 495.4 corresponds to $[Pd(L)-H]^+$ ($C_{24}H_{17}N_6Pd$). The low-intensity parental peak at m/z 246 corresponds to the doubly charged ion $[Pt(L)]^{2+}$, thus confirming the proposed cationic structure as depicted in Scheme 1. The peak at m/z 554.9 corresponds to $[Pd(L)+Cl+Na]^+$ ($C_{24}H_{16}N_6ClPdNa$) and agrees well with the molecular structure. The peak corresponding to the ligand is observed at m/z 381.6.

NMR Study

The 1H NMR (Figure S2) and ^{13}C NMR (Figure S3) spectra of **L** are included for a better comparison with the corresponding palladium(II) Complex 1. The proposed structure is perfectly compatible with the 1H NMR spectra of **L**. The N-H proton signals appear at 13.09 ppm as a singlet. The protons on the py rings resonate at 9.09 ppm (2H, doublet), 8.54 ppm (2H, doublet), and 8.26 ppm (2H, triplet), respectively. The protons on the benzene rings are observed at 7.76 ppm (2H, doublet), 7.66 ppm (2H, doublet), and 7.30 ppm (4H, multiplet), respectively. The molecule holds the C_2 symmetry in solution, indicating the bim rings to be magnetically equivalent. This is further confirmed by the ^{13}C NMR spectrum, which shows five different C atoms on the py ring and four different C atoms on the bim ring, as illustrated in Figure S6. The metal complex's 1H NMR spectra has been provisionally assigned due to not being well-resolved. The 1H NMR spectrum (Figure S6) shows the N-H signal at 14.15 ppm as a broad singlet, which is the most deshielded in comparison to that of the free ligand (13.09 ppm). The rise in the N-H acidic character upon coordination of

the benzimidazole ring to the palladium(II) center through the imine N atoms is attributed to the substantial downfield shift in the bim N-H signal. The signals of the 2,2'-bipyridine protons appear in the expected pattern and region as observed for the free ligand. The three signals observed at 9.11 ppm as a doublet for H3,3', 8.45 ppm as a doublet for H5,5' and 8.29 as a triplet for H4,4' indicate the molecule to have adopted a C₂ symmetry in solution. The bpy protons show insignificant shifts compared to those of the free ligand. The benzene protons seem unaffected by the coordination. The benzene protons resonate in the same region (7.7-7.3 ppm) observed for the free ligand.

FT-IR Spectra

Figure S4 depicts the IR spectra of the substance L. The presence of intermolecular hydrogen bonds between the benzimidazole rings in the molecule is shown by the extensive absorption in the range of 3,600-2,400 cm⁻¹ (25). According to the predictions made for a polar molecule with strong H-bond donor and acceptor groups that easily interact with the polar solvent, this broad absorption encompasses the OH stretching of the hydration water. The O-H bending overtone of water can be responsible for the extra dip at around 3,200 cm⁻¹ (26). No absorption occurs corresponding to the free O-H stretches of water above 3,600 cm⁻¹. The frequency at 1,589 cm⁻¹ may be assigned to the N-H in-plane bending mode (25). The aromatic ring's C-H stretching vibration is blamed for the weak absorption at 3,074 cm⁻¹. The frequencies at 1,573 and 1,522 cm⁻¹ can be assigned to the stretching of the bim and py rings (27). The absorptions between 900 and 600 cm⁻¹ are mostly due to the C-H out-of-plane and N-H out-of-plane bends as well as the in-plane ring bending modes.

R spectroscopy can be used to gain a better understanding of how the ligand and metal coordinate. Comparing the IR spectra of the complexes to those of the free ligands reveals noteworthy differences. The FT-IR (Figure 3) further supports the existence of the hydrated complex by showing broad bands in the range of 3,500-2,400 cm⁻¹ that are caused by intermolecular hydrogen bonds between the benzimidazole N-H. The N-H stretching peak at 3,427 cm⁻¹, which is sharper than that of the unbound ligand, may be an indication of the N-H groups not being engaged in the coordination. The characteristic aromatic CH stretching is observed at 3,067 cm⁻¹, and those related to the benzimidazole and pyridine ring stretching modes are observed in the region of 1,591-1,411

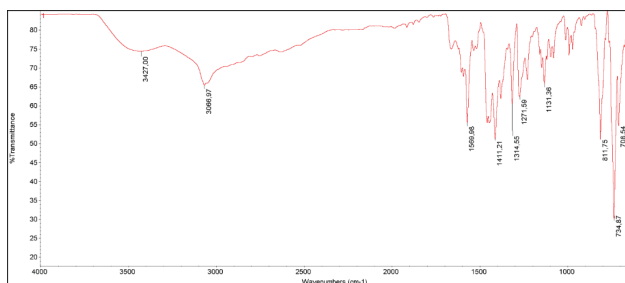


Figure 3. FT-IR spectra of Complex 1.

cm⁻¹. Except for minor changes in their locations and intensities brought on by coordination, the other bands in the complex's spectra are essentially identical to those in the spectrum of the ligand. The peaks at 1,570 and 734 cm⁻¹ in Complex 1 are stronger and sharper than the corresponding peaks at 1,573 and 741 cm⁻¹ in the free ligand. This may imply Complex 1 to have a more rigid structure compared to the flexible ligand showing N-H tautomerism.

Effect of the Complex on Cell Viability

First, the study examined the cytotoxic effects of Complex 1 on the four most prevalent human cancer cell lines (i.e., A549, lung; MDA-MB-231, breast; HCT-116, colorectal; PC-3, prostate cancer), as well as one healthy human bronchial epithelial cell

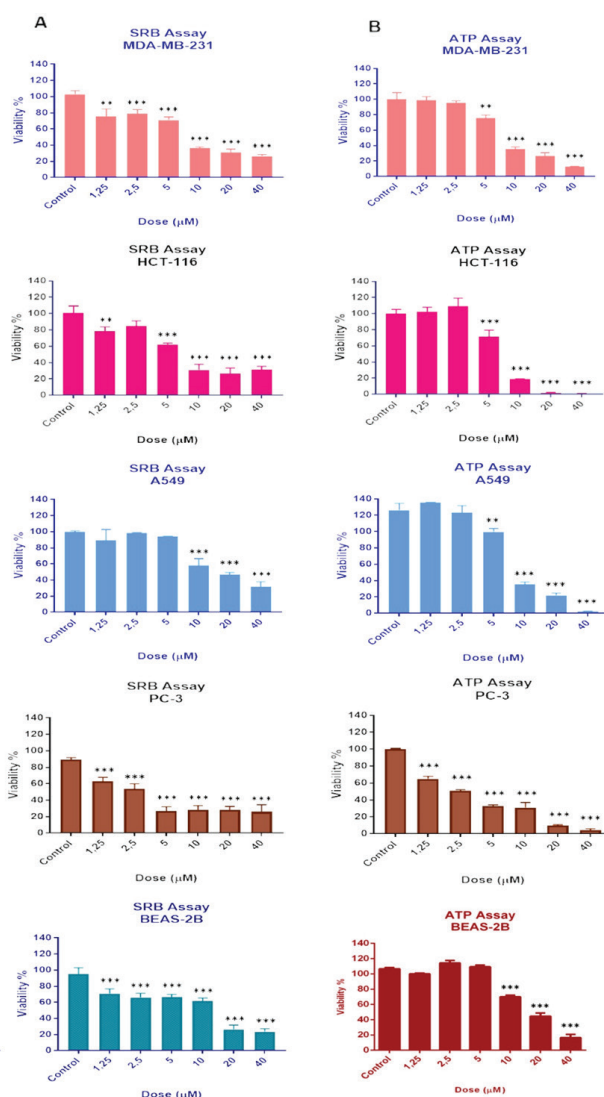


Figure 4. Measuring the effect of Complex 1 using the SRB (A) and ATP (B) assays. A549, PC-3, MDA-MB-231, HCT-116, and BEAS-2B cells were treated for 48 h at a concentration of 1.25-40 μM. *** p < 0.001. Data are presented as mean ± SD (n = 3).

line (BEAS-2B), for 48 h at various concentrations (1.25–40 μM ; Figure 4). As a result of the SRB assays, Complex 1 significantly decreased the viability of all cell lines. Although Complex 1 showed a cytotoxic effect on all cell lines, it was effective at a much lower dose on the PC-3 cells. The IC_{50} (the concentration that kills 50% of cells) and IC_{90} (the concentration that kills 90% of cells) values were calculated with the results confirmed by the ATP assays (Table 1).

Table 1. IC_{50} , IC_{90} and, selectivity index values for Complex 1 calculated based on the results of the ATP assay with cells treated for 48 h. The SI was calculated for Complex 1 using the formula $\text{SI} = (\text{IC}_{50} \text{ for normal cell line BEAS-2B}) / (\text{IC}_{50} \text{ for the respective cancer cell line})$.

Complex 1	IC_{50} Dose (μM) \pm	IC_{90} Dose (μM) \pm	Selectivity Index (SI)
PC-3	2.6 \pm 1.3	19.8 \pm 0.4	1.15
MDA-MB-231	8.2 \pm 0.6	> 40	0.37
A549	8.8 \pm 1.2	32.2 \pm 0.8	0.34
HCT-116	7.02 \pm 0.9	15.1 \pm 1.4	0.42
BEAS-2B	3.0 \pm 1.6	> 40	-

The comparison of the IC_{50} results obtained from the different cancer cell lines with those of the cationic complexes has revealed the IC_{50} values presented here to be effective at much lower doses (28). That the dose that kills 90 % the cells is especially high in the healthy human bronchial epithelial cell line is noteworthy. While it is effective on cancer cells at lower doses, this low dose range is seen to be ineffective on healthy cells. These *in vitro* studies also need to be validated *in vivo*. Therefore, Complex 1 deserves further attention for its proof of concept in animal models. At the same time, the study compared the selectivity index (SI) values of Complex 1 tested on these cells. A favorable $\text{SI} > 1.0$ indicates a drug with efficacy against tumor cells greater than the toxicity against normal cells. Accordingly, the SI was observed to be particularly high in prostate cancer cells.

To investigate whether the cytotoxicity was caused by the complex or the ligand, the SRB assay was performed on the ligand only-treated cells. No cytotoxic effect of the ligand was observed in the SRB assay, as shown in another study (24). In order to certify the occurrence of cell death, a dose usage equivalent to IC_{90} is inevitable. Therefore, the IC_{90} dose was used for flow cytometry analysis to determine cell death and related parameters.

Apoptosis-inducing Effect of the Complex

The annexin V-FITC staining assay was carried out using the flow cytometer to further analyze whether or not the cell death mode was apoptosis. At 24h and 48h respectively, 14.65% and 14.95% of cells for A549, 35.45% and 46.58% of cells for

MDA-MB-231, 11.35% and 18.50% of cells for PC-3, 35.7% and 50.55% of cells for HCT-116, and 15.45 % and 12.22% of cells for BEAS-2B underwent apoptosis (the total amount of both early and late-stage apoptosis; Figure 5). The complex has been shown to significantly induce apoptosis of the MDA-MB-231 and HCT-116 cell lines. However, the complex was found to induce cell death through primary necrosis for the A549, PC-3, and BEAS-2B cells. These findings clearly show Complex 1's ability to induce cell death through different pathways based on the cell line type.

Mitochondria are one of the regulators that have an important role in apoptosis. Membrane depolarization of mitochondria is an important marker for intrinsic apoptosis. After 24 h and 48 h of treatment with Complex 1 in all cell lines, a respective 41.3% and 97.15% of cells for A549, 41.35% and 95% for MDA-MB-231, 37.5% and 94.85% for PC-3, 34.85% and 95.95% for HCT-116, and 38.37% and 88.16% for BEAS-2B were found to be in state of mitochondria membrane-depolarization (Figure 6). Studies have reported mitochondrial membrane depolarization to increase in all cell lines based on time regardless of apoptosis or necrosis (29).

The decrease in Bcl-2 activity is related to the regulation of mitochondrial-mediated apoptosis and as a result, the change in activation of Bcl-2 was investigated regarding flow cytometry. To detect Bcl-2 inactivation after 24 h and 48 h of treatment with Complex 1 in all cell lines, the Bcl-2 inactivation assay was performed using the flow cytometer. Bcl-2 inactivation was found to be respectively 3.10% and 2.10% for A549, 40.6% and 54.70% for MDA-MB-231, 1.30% and 0.70% for PC-3, 8% and 72.80% for HCT-116, and 0.2% and 0% for BEAS-2B at the 24 h and 48 h marks (Figure S7). Since necrotic cell death occurred in the A549, PC-3, and BEAS-2B cells, no inactivation of Bcl-2 happened despite the mitochondrial membrane depolarization. In the MDA-MB-231 cell line, Bcl-2 inactivation further enhanced apoptosis in a time-dependent manner in addition to the mitochondrial membrane depolarization. Also, all these findings indicate that Complex 1 might have caused intrinsic apoptosis in MDA-MB-231. Similar to this, an increase in Bcl-2 inactivation occurred in the HCT-116 cell line as well, especially in the 48 hour application. This implies that Complex 1 may have a distinct killing effect that is based on cancer type.

$\gamma\text{-H2A.X}$ activation is one of the significant markers that contribute to DNA damage. After double-strand breaks form in DNA, H2A.X is phosphorylated through the ATM and ATR pathways. The palladium-based complexes are well known for covalently bonding to DNA strands and causing DNA damage (30). To detect DNA damage after 24 h and 48 h of treatment with Complex 1 in all cell lines, the H2A.X activation assay was performed using the flow cytometer. H2A.X activation was found to respectively be 3.1% and 3.3% for A549, 19.7% and 34.5% for MDA-MB-231, 2.76% and 1.34% for PC-3, 44.8% and 39.7% for HCT-116, and 4% and 6.6% for BEAS-2B for the 24 h and 48 h cycles (Figure S8). While Complex 1-induced DNA damage was not detected in the A549, PC-3, or BEAS-2B cell

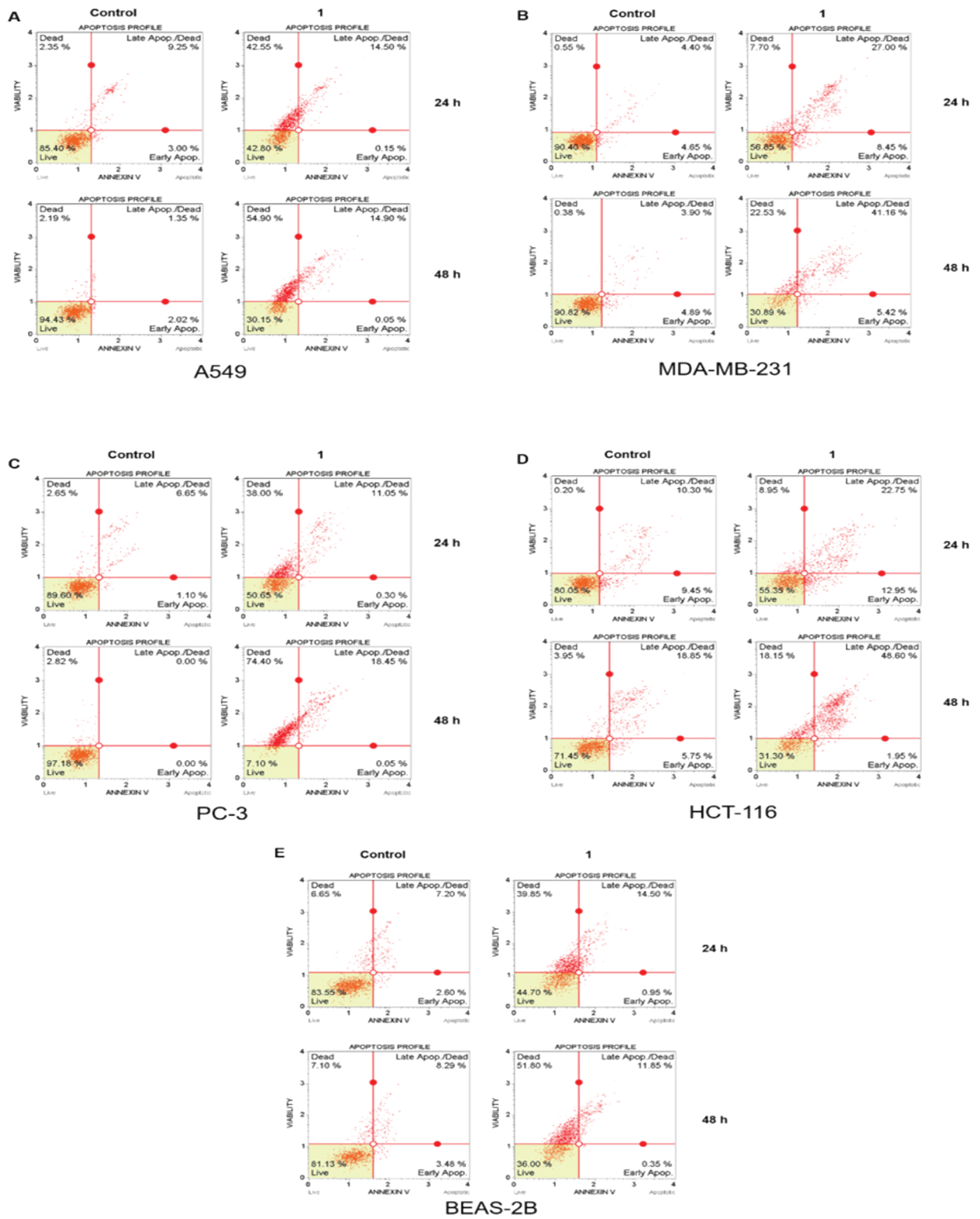


Figure 5. Assessment of phosphatidylserine translocation using flow cytometry. A549 (A), MDA-MB-231 (B), PC-3 (C), HCT-116 (D), and BEAS-2B (E) cells were treated with doses of Complex 1 at a concentration of IC₉₀ for 24 h and 48 h.

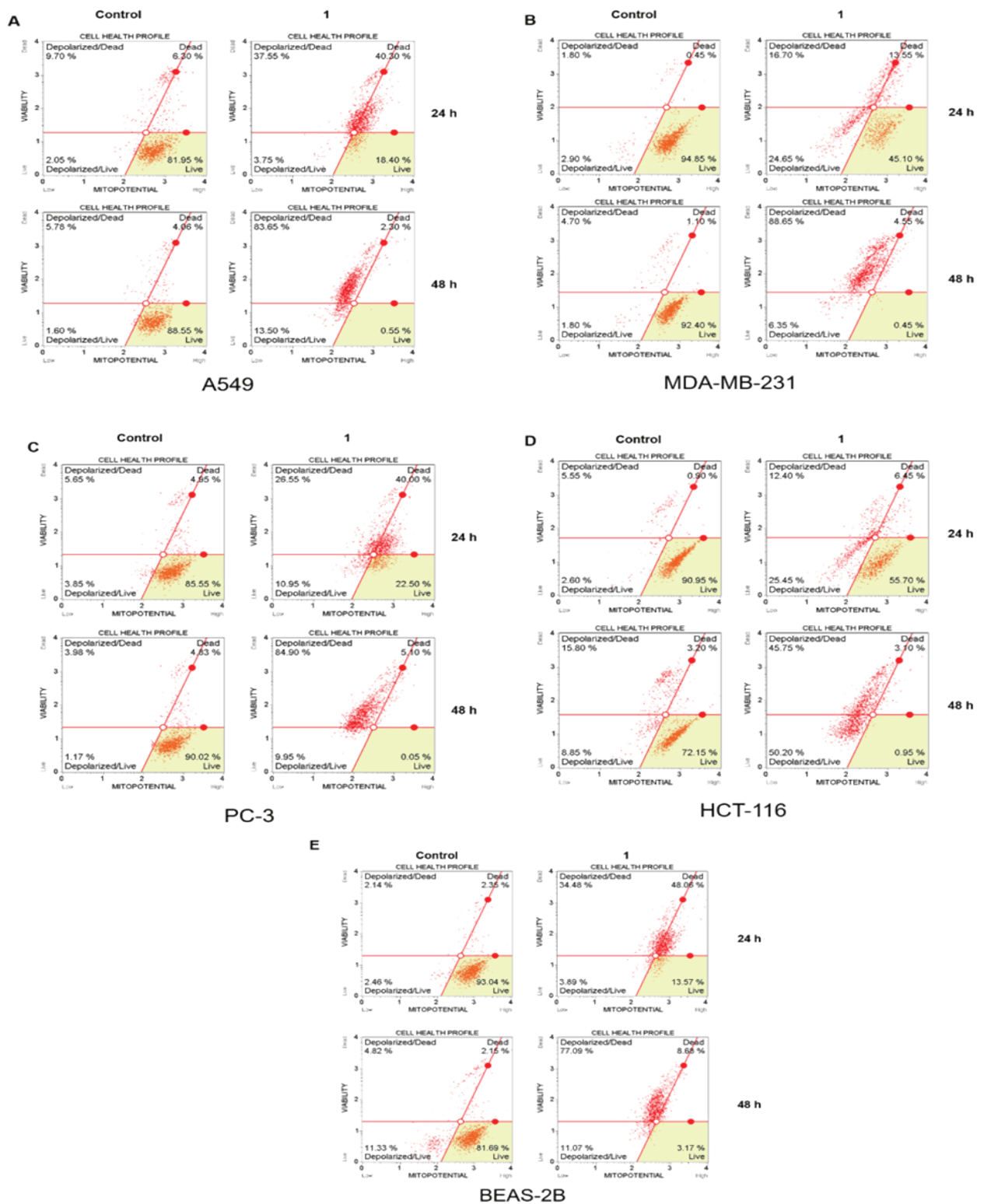


Figure 6. Mitochondria-dependent apoptosis in A549 (A), MDA-MB-231 (B), PC-3 (C), HCT-116 (D), and BEAS-2B (E) cells treated with Complex 1 doses at a concentration of IC_{90} for 24 and 48 h.

lines, MDA-MB-231 and HCT-116 cell lines did show a time-dependent increase in DNA damage. This finding is particularly important, as these assays seem to confirm each other in terms of their role in the apoptotic process.

CONCLUSION

This study has synthesized and thoroughly characterized the cationic palladium(II) complex with N_4 -donor tetradentate ligand using spectroscopic methods. The study also performed DFT calculations to obtain the optimized geometry. The palladium(II) adopted a significantly distorted square planar geometry with regard to Complex 1 due to the steric repulsion of the bulky benzimidazole chromophores in the 6,6'-positions of the 2,2'-bipyridine. Both the ligand and the palladium(II) complex are hydrated in a crystal form. The NMR and the FT-IR spectra of the complex show the ligand coordinates to the Pd center via imine N atoms to afford a doubly charged cationic complex.

When considering all these findings, Complex 1 seems to induce cell death by apoptosis through DNA damage and involvement of mitochondria in the HCT-116 and MDA-MB-231 cells while not having much of an effect in the other cell lines that were used. As such, Complex 1 may be considered particularly effective against colon and triple-negative breast cancers. Therefore, Complex 1 as a novel palladium-based complex deserves to be studied further with regard to proof-of-concept studies on animal models.

Ethics Committee Approval: Ethics committee approval was not obtained because there was no use of human and animal data in this study.

Peer-review: Externally peer-reviewed.

Author Contributions: Conception/Design of Study - E.U., A.S., M.E.G., S.S.; Data Acquisition - E.U., A.S., M.E.G., S.S.; Data Analysis/ Interpretation - E.U., A.S., M.E.G., S.S., I.Y.; Drafting Manuscript - M.E.G., R.O.A., E.U., A.S.; Critical Revision of Manuscript - I.Y., M.E.G., R.O.A., E.U., A.S.; Final Approval and Accountability - E.U., A.S., I.Y.

Conflicts of Interest: The authors declare no conflict of interest.

Financial Disclosure: This work was partly supported by the Turkish Scientific and Technical Research Council (TÜBİTAK) (grant number TBAG-2450(104T060)).

Acknowledgments: We gratefully acknowledge Nursel Açar Selçuki for carrying out computational DFT studies and we thank for the computer time on FenCluster (Ege University Faculty of Science).

REFERENCES

- Phillips MC, Mousa SA. Clinical application of nano-targeting for enhancing chemotherapeutic efficacy and safety in cancer management. *Nanomedicine* 2022; 17(6): 405-21. [CrossRef]
- Racané L, Zlatar I, Perin N, Cindrić M, Radovanović V, Banjanac M, et al. Biological Activity of Newly Synthesized Benzimidazole and Benzothiazole 2, 5-Disubstituted Furane Derivatives. *Molecules* 2021; 26(16): 4935. [CrossRef]
- Roopashree B, Gayathri V, Gopi A, Devaraju KS. Syntheses, characterizations, and antimicrobial activities of binuclear ruthenium (III) complexes containing 2-substituted benzimidazole derivatives. *J Coord Chem* 2012; 65(22): 4023-40. [CrossRef]
- Renouard T, Fallahpour RA, Nazeeruddin MK, Humphry-Baker R, Gorelsky SI, Lever ABP, et al. Novel ruthenium sensitizers containing functionalized hybrid tetradentate ligands: synthesis, characterization, and INDO/S analysis. *Inorg Chem* 2002; 41(2): 367-78. [CrossRef]
- Yau HC, Chan HL, Yang M. Determination of mode of interactions between novel drugs and calf thymus DNA by using quartz crystal resonator. *Sens Actuators B Chem* 2002; 81(2-3): 283-88. [CrossRef]
- Heringova P, Kasparkova J, Brabec V. DNA adducts of antitumor cisplatin preclude telomeric sequences from forming G quadruplexes. *J Biol Inorg Chem* 2009; 14(6): 959-68. [CrossRef]
- Büyükeksi SI, Orman EB, Şengül A, Altındağ A, Özkaya AR. Electrochemical and photovoltaic studies on water soluble triads: Metallosupramolecular self-assembly of ditopic bis (imidazole) perylene diimide with platinum (II)-, and palladium (II)-2, 2': 6', 2''-terpyridyl complex ions. *Dyes Pig* 2017; 144: 190-202. [CrossRef]
- Largy E, Hamon F, Rosu F, Gabelica V, De PE, Guédin A, et al. Tridentate N-Donor Palladium (II) Complexes as Efficient Coordinating Quadruplex DNA Binders. *Chemistry* 2011; 17(47): 13274-283. [CrossRef]
- Burda JV, Zeizinger M, Leszczynski J. Activation barriers and rate constants for hydration of platinum and palladium square-planar complexes: An ab initio study. *J Chem Phys* 2004; 120(3): 1253-62. [CrossRef]
- Muller G, Bunzli, JCG, Schenk KJ, Piquet C, Hopfgartner G. Influence of bulky N-substituents on the formation of lanthanide triple helical complexes with a ligand derived from bis (benzimidazole) pyridine: structural and thermodynamic evidence. *Inorg Chem* 2001; 40(12): 2642-51. [CrossRef]
- Cusumano M, Di Pietro ML, Giannetto A. Stacking surface effect in the DNA intercalation of some polypyridine platinum (II) complexes. *Inorg Chem* 1999; 38(8): 1754-58. [CrossRef]
- Wong, ELM, Fang GS, Che CM, Zhu N. Highly cytotoxic iron (III) complexes with pentadentate pyridyl ligands as a new class of anti-tumor agents. *Chem Commun* 2005; (36): 4578-80. [CrossRef]
- Davidson JP, Faber PJ, Fischer JrRG, Mansy S, Peresie HJ, Rosenberg B, et al. "Platinum-pyrimidine blues" and related complexes: a new class of potent antitumor agents. *Cancer Chemother Rep* 1975; 59(2 Pt 1): 287-300.
- Yılmaz I, Akar OR, Erkisa M, Selvi S, Şengül A, Ulukaya E. Highly promising antitumor agent of a novel Platinum (II) complex bearing a tetradentate chelating ligand. *ACS Med Chem Lett* 2020; 11(5): 940-8. [CrossRef]
- Drew D, Doyle JR, Shaver AG. Cyclic diolefin complexes of platinum and palladium. *Inorg Syn* 1972; 13: 47-55. [CrossRef]
- Russo TV, Martin RL, Hay PJ. Density functional calculations on first-row transition metals. *J Chem Phys* 1994; 101(9): 7729-37. [CrossRef]
- Hay PJ. *Methods of Electronic Structure Theory*: Plenum Press, 1977.
- Dennington RD, Keith TA, Millam JM. *GaussView 5.0*, Gaussian, Inc., Wallingford, 20, 2008.
- Zhang IY, Wu J, Xu X. Extending the reliability and applicability of B3LYP. *Chem Commun* 2010; 46(18): 3057-70. [CrossRef]
- Czarnecki MA, Wojtków D. Effect of varying water content on the structure of butyl alcohol/water mixtures: FT-NIR two-dimensional correlation and chemometric studies. *J Mol Struct* 2008; 883: 203-8. [CrossRef]

21. Yılmaz I, Acar NS, Coles SJ, Şengül A. Spectroscopic, EPR, X-ray structural, and DFT studies of the complex compound of N4-donor ligand with copper (II). *J Mol Struct* 2020; 1214: 128204. [\[CrossRef\]](#)
22. Buyukeksi SI, Erkisa Genel M, Şengül A, Ulukaya E, Oral AY. Structural studies and cytotoxic activity of a new dinuclear coordination compound of palladium (II)-2,2':6,2'-terpyridine with rigid dianionic 1,2,4-triazole-3-sulfonate linker. *Appl Organomet Chem* 2018; 32(8): e4406. [\[CrossRef\]](#)
23. Lee C, Yang W, Parr RG. Development of the Colle-Salvetti correlation-energy formula into a functional of the electron density. *Phys Rev B* 1988; 37: 785-9. [\[CrossRef\]](#)
24. Kohn W, Sham LJ. Self-consistent equations including exchange and correlation effects. *Phys Rev* 1965; 140: A1133-8. [\[CrossRef\]](#)
25. Yurdakul Ş, Kurt M. Vibrational spectroscopic studies of metal (II) halide benzimidazole. *J Mol Struct* 2003; 650(1-3): 181-190. [\[CrossRef\]](#)
26. Bhattacharjee A, Wategaonkar S. Water bridges anchored by a C-H... O hydrogen bond: the role of weak interactions in molecular solvation. *Phys Chem Chem Phys* 2016; 18(40): 27745-49. [\[CrossRef\]](#)
27. Miao SB, Ji BM, Deng DS, Xu C, Ma N. Crystal structures and luminescence of two zinc (II) complexes with benzimidazole ligands. *J Struct Chem* 2010; 51(2): 386-91. [\[CrossRef\]](#)
28. Yıldız U, Şengül A, Kandemir I, Cömert F, Akkoç S, Coban B. The comparative study of the DNA binding and biological activities of the quaternized dicnq as a dicationic form and its platinum (II) heteroleptic cationic complex. *Bioorg Chem* 2019; 87: 70-7. [\[CrossRef\]](#)
29. Kim JS, He L, Lemasters JJ. Mitochondrial permeability transition: a common pathway to necrosis and apoptosis. *Biochem Biophys Res Commun* 2003; 304(3): 463-70. [\[CrossRef\]](#)
30. Kumar A, Naaz A, Prakasham AP, Gangwar MK, Butcher RJ, Panda D, Ghosh P. Potent anticancer activity with high selectivity of a chiral palladium N-Heterocyclic Carbene Complex. *ACS omega* 2017; 2(8): 4632-46. [\[CrossRef\]](#)

SUPPORTING INFORMATION

Differential Cytotoxic Activity of A New Cationic Pd(II) Coordination Compound with N₄-Tetradentate Hybrid Ligand in Cancer Cell Lines

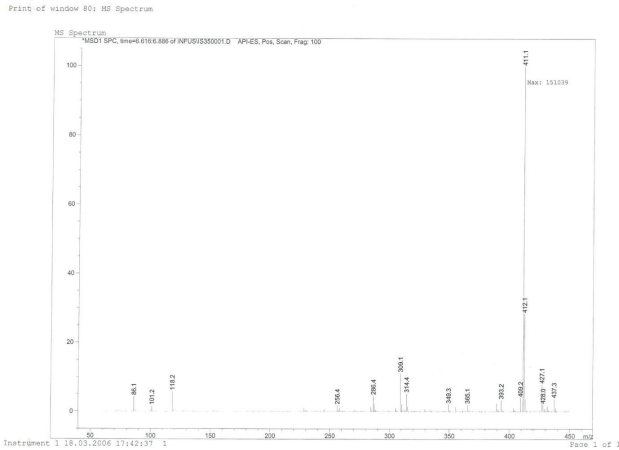


Figure S1. ESI-MS spectrum of L

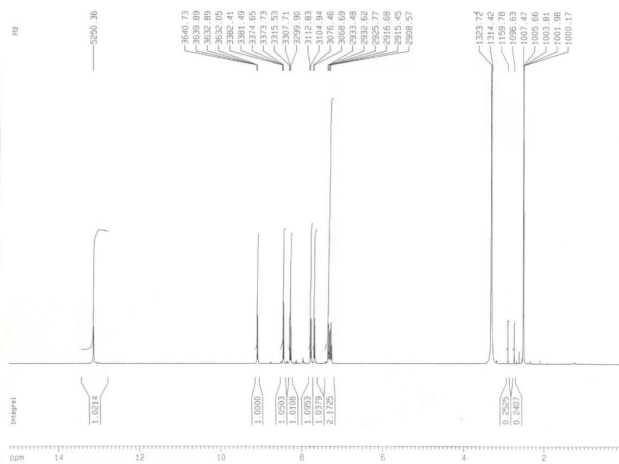


Figure S2. ¹H NMR spectrum of L

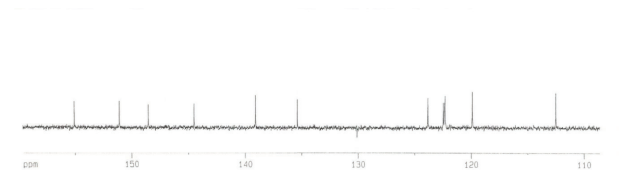


Figure S3. ¹³C NMR spectrum of L

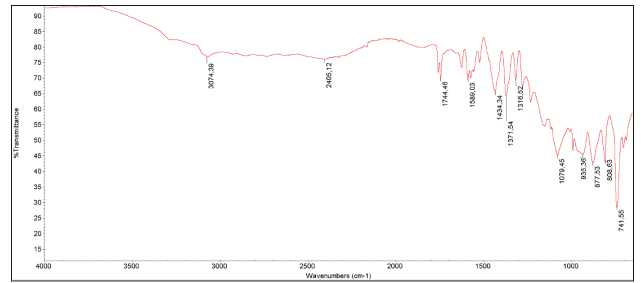


Figure S4. FT-IR (ATR) spectrum of L

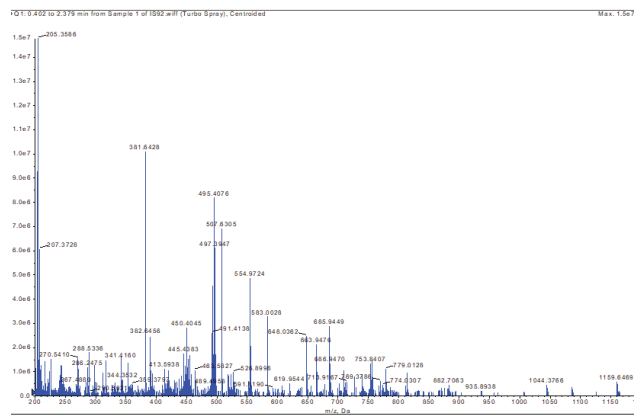


Figure S5. LC-ESI-MS spectrum of 1

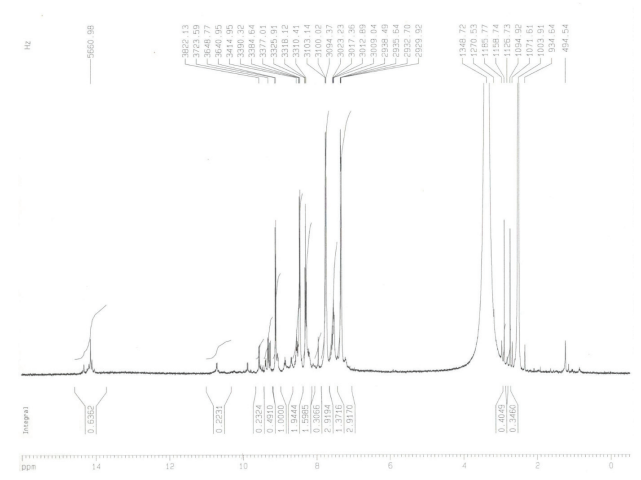


Figure S6. ¹H NMR spectrum of 1

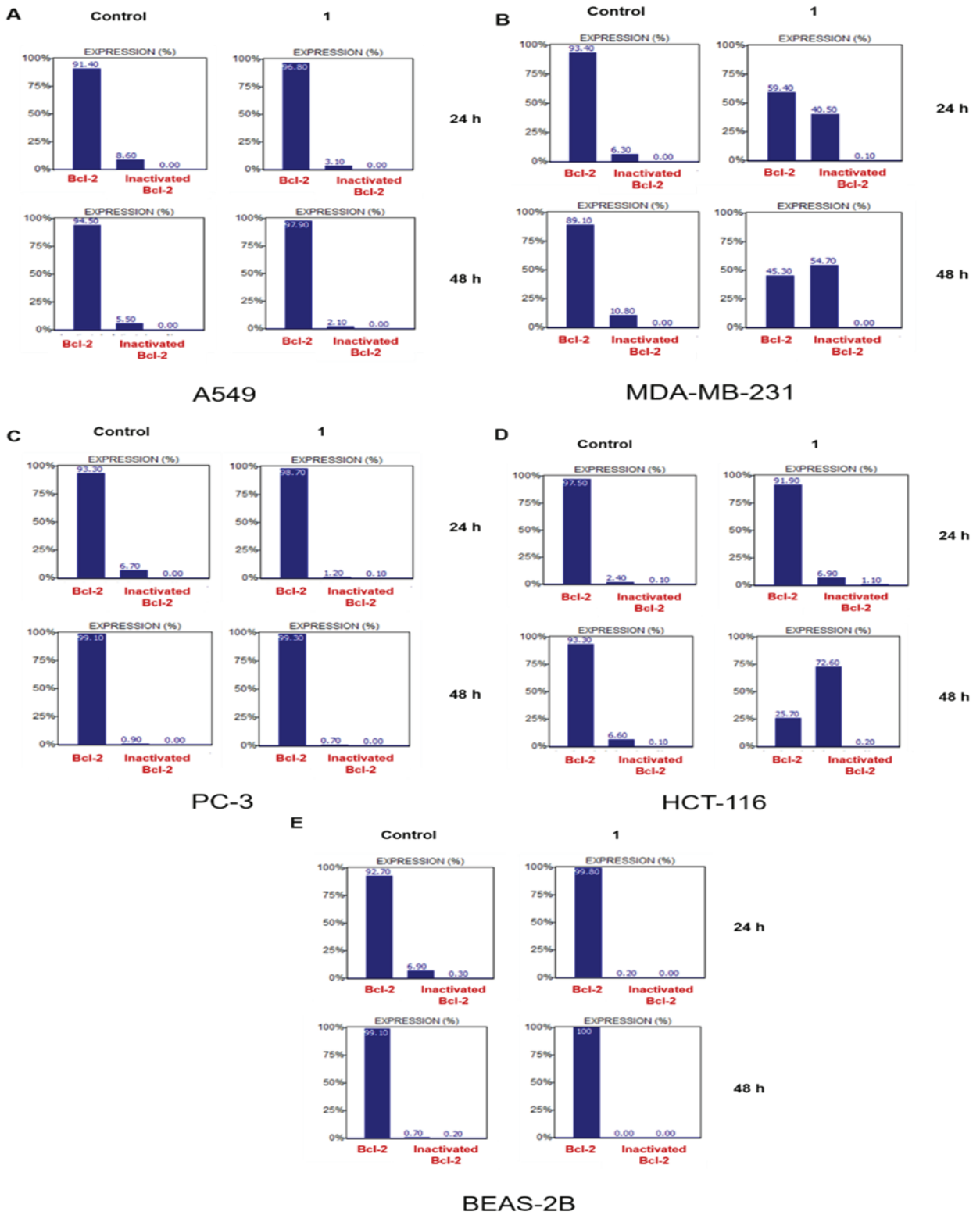


Figure S7. Bcl-2 phosphorylation (Ser70) in (A) A549, (B) MDA-MB-231, (C) PC-3, (D) HCT-116 and (E) BEAS-2B cell lines after treatment with complex 1 (IC₉₀ doses) for 24 and 48 h.

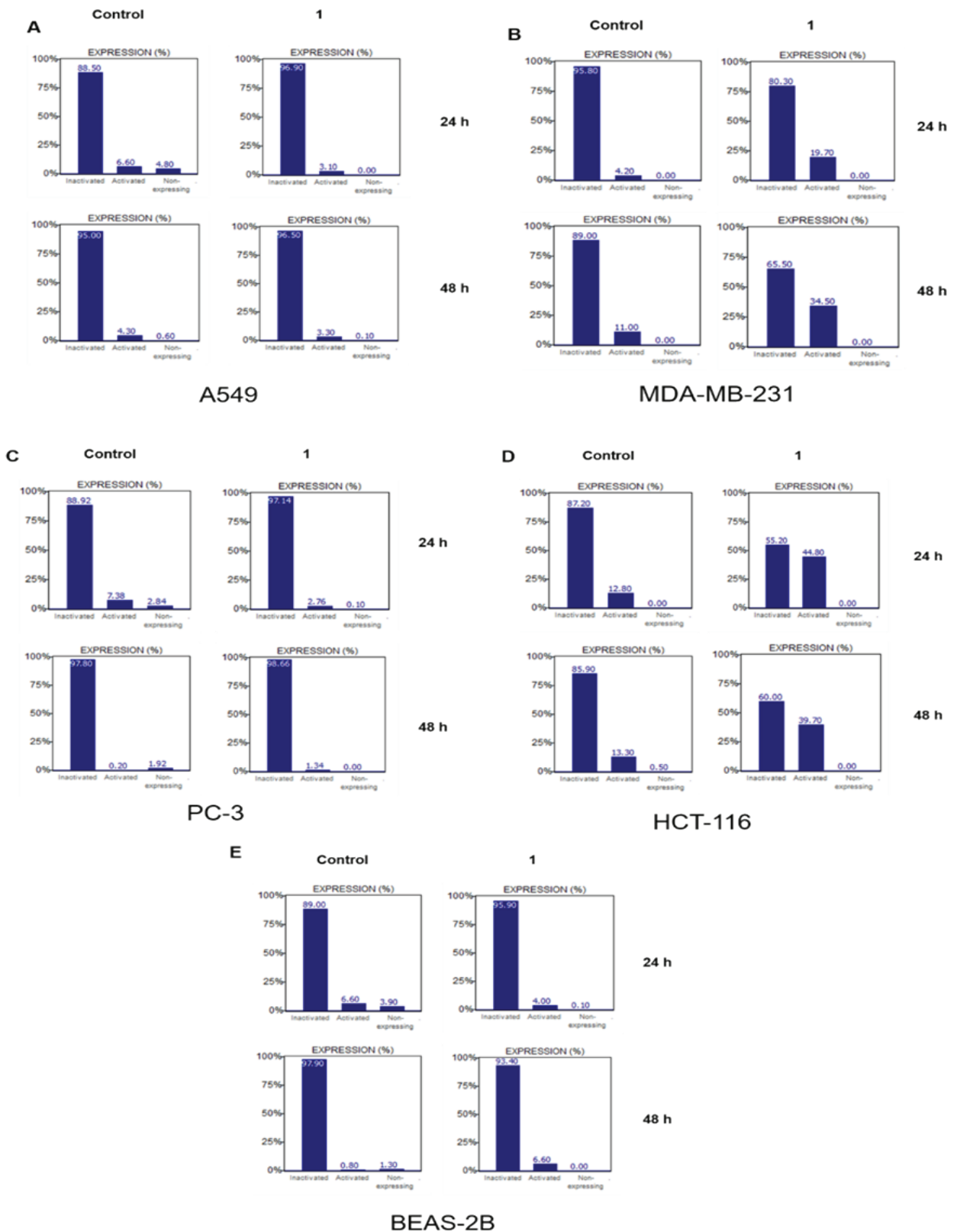


Figure S8. DNA damage in (A) A549, (B) MDA-MB-231, (C) PC-3, (D) HCT-116, and (E) BEAS-2B cell lines after treatment with complex 1 (IC₅₀ doses) for 24 and 48 h.

Table S1. Calculated (in the gas phase) selected bond lengths (Å), angles (°), and dihedral angles for compound 1.

	Bond lengths (Å)		Angles(°)		Dihedral Angles(°)
Pd-N2	2.130	N2-Pd-N4	159.12	N2-Pd-N4-C1	168.25
Pd-N3	1.985	N3-Pd-N5	159.12	C17-N2-Pd-N5	7.99
Pd-N4	1.985	N2-Pd-N3	79.36	C16-C17-N2-Pd	4.00
Pd-N5	2.130	N3-Pd-N4	80.05	N2-C11-C10-N3	0.60
N2-C11	1.347	N4-Pd-N5	79.36	Pd-N2-C11-C10	-4.72
N2-C17	1.385	N2-Pd-N5	121.38	C17-N2-Pd-N4	-164.86
C17-C12	1.419	C11-N2-C17	106.68	C18-N5-Pd-N4	-174.59
C12-N1	1.384	C11-C10-N3	111.25	N4-C1-C24-N6	176.80
C12-C13	1.398	N3-C9-C10	119.14	N3-C10-C11-N1	176.80
C17-C16	1.403	C10-N3-C6	123.98		
C11-C10	1.458	N3-C6-C5	113.22		
C10-N3	1.347	C6-C5-N4	113.22		
N3-C6	1.356	C5-N4-C1	123.98		
C6-C5	1.484	N4-C1-C24	111.25		
C5-N4	1.356	C1-C24-N5	120.44		
N4-C1	1.347	N5-C24-N6	111.14		
C1-C24	1.458	C24-N5-C18	106.68		
C1-N5	1.347				
N5-C18	1.385				
C18-C23	1.419				
C23-N6	1.384				
C23-C22	1.398				
C18-C19	1.403				

Cytotoxic and Cytostatic Effects of Targeting mTOR and Hedgehog Pathways in Acute Myeloid Leukemia

Enes Cicek^{1*} , Fulya Mina Kucuktas^{1*} , Munevver Yenigul² , Emel Basak Gencer Akcok¹ 

¹Department of Molecular Biology and Genetics, Faculty of Life and Natural Sciences, Abdullah Gül University, Kayseri, Türkiye

²Bioengineering Department, Graduate School of Engineering and Science, Abdullah Gül University, Kayseri, Türkiye

*E.Ç. and F.M.K. equally contributed to this work.

ORCID ID: E.C. 0000-0002-7452-2253; F.M.K. 0000-0001-7682-4012; M.Y.- 0000-0003-0468-721X; E.B.G.A. 0000-0002-6559-9144

Cite this article as: Cicek E, Kucuktas FM, Yenigul M, Gencer Akcok EB. Cytotoxic and cytostatic effects of targeting mTOR and Hedgehog pathways in acute myeloid leukemia. *Experimed* 2022; 12(3): 202-8.

ABSTRACT

Objectives: Acute myeloid leukemia (AML) is a highly aggressive heterogeneous hematopoietic malignancy characterized by a rapid and abnormal proliferation of immature myeloid leukemia cells in the bone marrow and peripheral blood. Aberrant alterations in signal transduction pathways are strongly associated with the progression of AML. This study aimed to investigate cell viability and the cell cycle in AML cells by targeting the Hedgehog and mTOR signaling pathways with rapamycin and GANT61.

Materials and Method: The antiproliferative effect of rapamycin and GANT61 was assessed by the MTT cell viability assay in two AML cell lines: CMK and MOLM-13. The effect of the inhibitors on cell-cycle distribution was determined using propidium iodide staining and measured with flow cytometry.

Results: Rapamycin, an mTOR inhibitor, and GANT61, a Gli-1 inhibitor, decreased the cell proliferation of CMK and MOLM-13 cells. The IC₂₀ values, which is the drug concentration that inhibits cell growth by 20%, were combined and administered to the cells. The results show the drugs to have a combinatorial inhibitory effect on CMK cells but not on MOLM-13 cells. In addition, the combination of drugs arrested the cells during the G₀/G₁ phase.

Conclusion: This study suggests a novel combination therapy approach for AML via mTOR and Hedgehog signaling pathway inhibition using rapamycin and GANT61, respectively. It also suggest further studies be performed to reveal the mechanism of action.

Keywords: Hedgehog, mTOR, leukemia, combination therapy, cell cycle

INTRODUCTION

Acute myeloid leukemia (AML) is a highly aggressive heterogeneous hematopoietic malignancy characterized by a rapid proliferation of immature myeloid leukemia cells in the bone marrow and peripheral blood (1-3). According to Saultz and Garzon (3), AML arises from the genetic abnormalities of leukemia cells that accumulate with age. AML has an effect on marrow in the majority of patients, with 20% of the affected bone marrow cells being immature or undifferentiated leukemia blasts (2).

Altered proliferation and survival mechanisms are common deregulations in AML cells. These mechanisms

are under the control of signal transduction pathways, and some of the signal transduction pathways affected in AML cells are receptor tyrosine kinases such as FLT3 and KIT and non-receptor tyrosine kinases such as RAS family members, RAF/MEK/ERK, and PI3K/AKT, as well as the Hedgehog (HH) and mTOR signaling pathways. These pathways are mostly affected by means of gain-of-function mutations in upstream elements that alter the activation mechanism. Constitutive activation of these pathways leads to the survival and proliferation of hematopoietic progenitor cells (4). Although AML is the second most commonly seen leukemia in children, the survival rate of AML patients has not improved due to the heterogeneity of the disease. The

Corresponding Author: Emel Basak Gencer Akcok **E-mail:** emelbasak.gencerakcok@agu.edu.tr

Submitted: 24.10.2022 **Revision Requested:** 28.11.2022 **Last Revision Received:** 02.12.2022 **Accepted:** 05.12.2022 **Published Online:** 29.12.2022



Content of this journal is licensed under a Creative Commons Attribution-NonCommercial 4.0 International License.

need exists to target specific signaling pathways to accomplish an efficient treatment approach toward AML.

The HH signaling pathway is conserved and functions in developmental processes such as regeneration, differentiation, and proliferation (5). Even though the HH signaling pathway is conserved, its function varies in different species. For adult humans, the HH signaling pathway has responsibilities in tissue repair, stem cell renewal, and oncogenesis (6). The role of the HH signaling pathway regarding stem cell renewal in both somatic stem cells and pluripotent cells can be correlated with cancer stem cell activity when alterations occur in the signaling pathway and its activity (7). HH signaling is aberrantly expressed in AML cells, suggesting a link between poor prognosis and drug resistance (8). The HH signaling pathway includes glioma-associated oncogene (Gli) proteins (Gli1, Gli2, and Gli3), which are transcription factors. GANT61 is a selective inhibitor of Gli-1 gene transactivation. *In vitro* studies have been conducted for many types of cancer, including neuroblastoma, rhabdomyosarcoma, colon, lung, pancreatic, leukemia, cervix, gastric, skin, and head-neck (9-11).

The mammalian target of rapamycin, also known as mTOR, is the pathway responsible for the regulation of growth and cellular metabolism in eukaryotic cells by regulating cell proliferation, autophagy, and apoptosis through multiple signaling pathways. mTOR is a serine/threonine protein kinase that forms two distinct catalytic subunits of the mTOR complexes, mTORC1 and mTORC2 (12, 13). PI3K/AKT and mTOR signaling have been documented to support the proliferation and survival of AML cells (14). mTOR activation is mostly observed in AML blasts, but the precise function and the downstream targets of mTOR in the AML are poorly understood. Meanwhile, rapamycin, which is an mTOR inhibitor, has been proven as a promising class of agents for treatment of malignant blood cancer, either alone or in combination with other treatments (15).

The inhibition of a single pathway, especially the mTOR or HH pathway, has been targeted by numerous researchers and reviewed previously. However, targeting a single pathway related to AML is an insufficient approach due to the presence of simultaneous alterations of multiple signaling transduction mechanisms. Therefore, the development of a combination therapy targeting the mTOR and HH pathways is needed in order to provide an efficient treatment option for AML patients. This study aimed to target the mTOR and HH pathways in AML patients to understand the crosstalk between these two pathways in order to find a possible therapeutic approach. This study hypothesizes that inhibiting the mTOR and HH signaling pathways using rapamycin and GANT61 is a combination that could be a therapeutic approach for AML. Inhibiting these pathways has been investigated by numerous studies due to their high potency as therapeutic targets. However, no reports are found concerning the effect of the drugs used in the current study on both of these pathways in AML cells.

MATERIALS AND METHODS

Chemicals

Rapamycin and GANT61 were purchased from Biovision and Sigma, respectively. Five mM stock drug solutions were prepared in dimethylsulfoxide (DMSO) in accordance with the recommendations and stored at -20°C. The RPMI 1640 and penicillin/streptomycin were obtained from Euro Clone. The heat-inactivated fetal bovine serum (FBS) was obtained from Biological Industries. RNase and propidium iodide (PI) were purchased from Sigma and used in the cell cycle assay.

Cell Culture and Maintenance

The AML cell lines CMK and MOLM-13 were obtained from the German National Resource Center for Biological Material (DSMZ). CMK was sourced from the AML M7 cell line of Down syndrome patients (DS-AMKL), and MOLM-13 was originated from a FLT3 mutation. The cells were cultured in the RPMI growth medium supplemented with 20% FBS and 1% penicillin/streptomycin at 37°C and 5% CO₂.

Cell Viability Assay

The cell viability assay was performed to determine cell proliferation using 3-(4,5-dimethylthiazol-2-yl)-2,5-diphenyl-2H-tetrazolium bromide (MTT) as previously described (16). In brief, 96 well plates were seeded with 1×10⁴ cells/wells treated with increasing concentrations of inhibitors. After 48 hours, the MTT solution was added and incubated for 2 h. Following the incubation time, the plates were centrifuged for 10 min. The formazan crystals that formed were dissolved using DMSO. The plates were left for 15 min on a rotator. Afterward, the absorbance was measured at 570 nm using the microplate reader (Varioskan™ LUX multimode, Thermo Scientific).

Cell Cycle Assay

1×10⁶ cells were plated into the cells and treated with rapamycin and GANT61 for 48 h. After collecting and centrifuging the cells at 260g for 10 min at 4°C, the supernatant was collected and the cells were washed twice in cold PBS. Following the removal of the supernatant, the pellet was dissolved with a mixture of 1 mL cold PBS and 4 mL ethanol (70%) and incubated at -20°C overnight for fixation. After incubation, the supernatant was removed by centrifugation, and the cell pellet was washed in PBS. The PBS/Triton X-100 was added next, followed by the addition of 100 µL of RNase-A, which were then incubated at 37°C for 30 minutes. Lastly, 100 µL of PI was added, incubated for 15 minutes, and analyzed using flow cytometry.

Statistical Analyses

Analysis of the viability data was done with the GraphPad PRISM (version 8.0; GraphPad Software Inc.). The Dunnett test and one-way analysis of variance (ANOVA) were performed for the statistical analysis, which showed $p = 0.0001$ for all results, with $p = 0.0005$ for the MOLM-13 combination cell viability results. Assays were repeated three times independently from one another.

Table 1. Combination index (CI) was calculated and isobolograms determined using the program CompuSyn.

CMK			MOLM-13		
GANT61	RAPAMYCIN	GANT61+RAPA	GANT61	RAPAMYCIN	GANT61+RAPA
Dose	Dose	CI Value	Dose	Dose	CI Value
5.2	0.1	0.56278	1.74	0.1	0.23773

The effects of the drug combination used in this study were evaluated using the CI based on Chou-Talalay's multidrug effect equation, with a CI of < 1, =1, or > 1 being respectively indicative of synergistic, additive, or antagonistic effects [17].

RESULTS

1. GANT61 and Rapamycin Decrease Cell Proliferation in AML Cell Lines

The study has assessed the cytotoxic effects of the HH inhibitor GANT61 and mTOR inhibitor rapamycin on the CMK and MOLM-13 AML cells. Increasing concentrations of the drugs were administered to the cells over 48 h, with the cell proliferations of both the CMK and MOLM-13 cell lines decreasing as the dosage increased. When GANT61 was administered between 5-100 μM, the IC20 values were determined as 5.2 μM for the CMK and 1.74 μM for the MOLM-13 cells. This result indicates GANT61 to be effective at inhibiting cancer cell survival by blocking Gli-1 activity (Figure 1a). Rapamycin also decreased cell viability when applied at 0.1-10 nM levels. However, the decrease was capped at 54.98% for a drug concentration of 0.5 nM or higher in both the CMK and MOLM-13 cell lines. After the rapamycin treatment, the IC20 value was calculated as 0.1 nM for both CMK and MOLM-13 cells (Figure 1b).

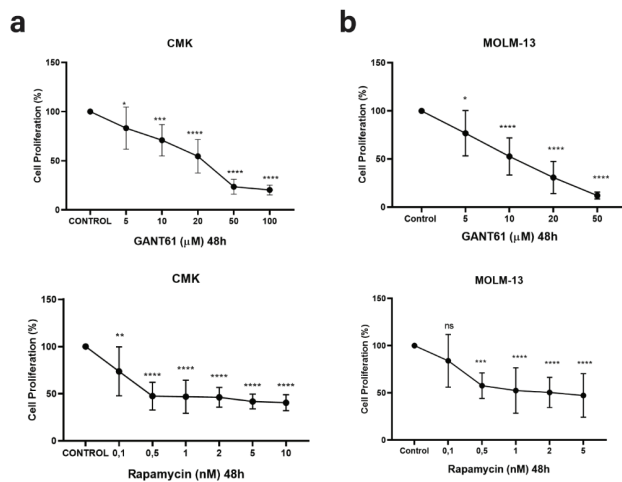


Figure 1. The effect of GANT61 and rapamycin on cell viability compared to the control for the (a) CMK and (b) MOLM-13 cells. These results represent data from samples in triplicates across three independent experiments ($n = 3$). * = $p < 0.05$; *** = $p < 0.001$; **** = $p < 0.0001$. *SD* = the mean value of the replicates; ns= Nonsignificant.

2. The Combined Cytotoxic Effects of GANT61 and Rapamycin on AML Cells

Next, the study evaluated the effect of drug combinations on AML cells. The cells were treated for 48 h with the IC20 concentration of rapamycin, which had been calculated as 0.1 nM for both cell lines, and the IC20 concentration of GANT61, which was detected as 5.2 μM and 1.74 μM for the respective CMK and MOLM-13 cells. Decreases in cell proliferation using the combination therapy were observed in the MOLM-13 cells by 46% and 38% for the respective untreated control and GANT61-only treatment. However, the cell viability following the combination treatment was surprisingly not significantly different when compared to the rapamycin-only treatment. The combination treatment for CMK cells decreased cell viability by 42%, 51%, and 10% when respectively compared to the untreated control, GANT61 treatment, and rapamycin-only treatment. Therefore, the results indicate the combination therapy to have reduced the cell proliferation levels more apparently in the CMK cells compared to the single treatments (Figure 2). However, when comparing the results regarding cell viability in terms of synergism, the combination of 5.2 μM and 1.74 μM GANT61 with 0.1 nM of rapamycin showed a synergistic effect (95% CI: 0.562-0.237) in the respective CMK and MOLM-13 cells (Table 1).

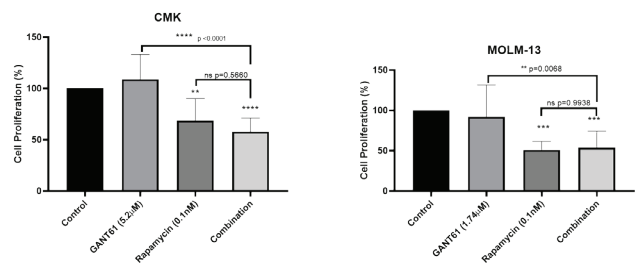


Figure 2. The cytotoxic effects of the different combinations of GANT61 and rapamycin on the CMK and MOLM-13 cells. These results represent the data from the triplicate samples across three independent experiments ($n = 3$). ** = $p < 0.01$; *** = $p < 0.001$; **** = $p < 0.0001$. *SD* = the mean value of replicates; ns= Nonsignificant.

Table 2. The cell cycle distribution and the percentage of the average cell population of CMK and MOLM-13 cells in G0, S, and G2/M phase.

	CMK cells			MOLM-13 cells		
	G0/G1	S	G2/M	G0/G1	S	G2/M
Untreated control	62.1	27.4	10.4	67.8	22.4	9.8
DMSO	63.2	26.5	10.3	66.4	23.85	9.5
GANT61 IC20	66.8	23.7	9.5	64.15	23.2	12.65
Rapamycin IC20	70.1	20	10	68.45	20.6	10.95
Combination	79.2	15	5.8	70	19.7	10.2

3. The Cytostatic Effect of the Combination Treatment on AML Cells

To enlighten the mechanism behind the decrease in cell proliferation, the cell cycle distribution was assessed in response to the drug combination treatment using the flow cytometric analysis. The results show the combination of GANT61 and rapamycin to have resulted in a 12% decrease in the S phase in the CMK cells when compared to the control. The combination treatment demonstrated a 17% increase in the G0/G1 phase, which shows the cells to have been arrested in this phase in response to the drug treatment (Figure 3a). In the MOLM-13 cells, similar effects were not observed as a result of the drug treatment. However, when compared to the CMK cells, a slight decrease was seen in the S phase, as well as a slight increase in the G0/G1 phase (Figure 3b). These results demonstrate the cytotoxic effect of the drug combination to perhaps have arisen from the cell cycle arrest (Table 2).

DISCUSSION

The therapeutic approach involves four types of standard treatments that are reported to have been used in chemotherapy, radiation therapy, and stem cell transplantation regarding AML. In addition to the standard treatments, new approaches are also being studied in clinics. Targeted therapy is one of the new therapies and uses drugs to attack cancer cells that cause less harm to normal cells. One subtype of targeted therapy is monoclonal antibody therapy, which uses antibodies for treatment to attach to and kill the cancer cells (18).

AML is a heterogeneous disease that makes targeting it with classical chemotherapeutic drugs difficult. Specific targeting of signaling pathways would be a more efficient way for treatment of this disease, and this study in particular has focused on simultaneously targeting the HH and mTOR signaling pathways with specific inhibitors due to the important role they represent in the progression of AML.

For instance, a correlation exists between the elevated expression of the HH-signaling protein Gli-1 and chemoresistance against therapeutic drugs and radiotherapy for AML (19, 20), with the proper HH signaling pathway activity being altered in AML cells. The induction of the signaling pathway in AML cells does not require HH to bind to PTCH1. Therefore, Gli-1 and SMO expression is persistent in AML cells. This persistence will increase the concentration of Gli-1 in AML cells (21). Subsequently, this increase in the Gli-1 alongside other elements of the signaling pathway result in AML becoming resistant to treatment. Queiroz et al. (21) demonstrated the HH pathway to be an important component of multidrug resistance in myeloid leukemia, as well as the need for it to be targeted. Inhibiting the HH signaling pathway has also been linked to the induction of apoptosis. Therefore, inhibiting this signaling pathway in AML cells is a viable and required strategy for treatment, in addition to administering HH inhibitors combined with chemotherapeutic agents targeting leukemic stem cells, as this pathway is involved in the maintenance and expansion of leukemic stem cells (22).

The second pathway targeted in the current study was mTOR signaling. mTORC1 functions as a cell growth and metabolism regulator and contains five components: mTOR, Raptor as the regulatory associated protein of mTOR, mLST8, PRAS40, and Deptor. mTORC2 has six components, some of which are common to mTOR, including mTOR again as well as Rictor, mSIN1, Proctor-1, mLST8, and Deptor again. In contrast to mTOR, the exact function of mTORC2 has not yet been revealed, but the known function of the complex is to control cell proliferation and cell survival (13, 23). By promoting anabolic processes and limiting catabolic processes, mTORC1 possesses a regulatory function in cell growth and proliferation (23). The base of knowledge about the function of mTORC1 involves bacterial macrolide rapamycin usage (24). Rapamycin is a macrocyclic antibiotic that was first discovered as an antifungal medication. However, its immunosuppressive effect is also considered useful as clinical medication (25). Rapamycin is an inhibitor that, by interacting with the FKBP12 protein and the FKBP12-

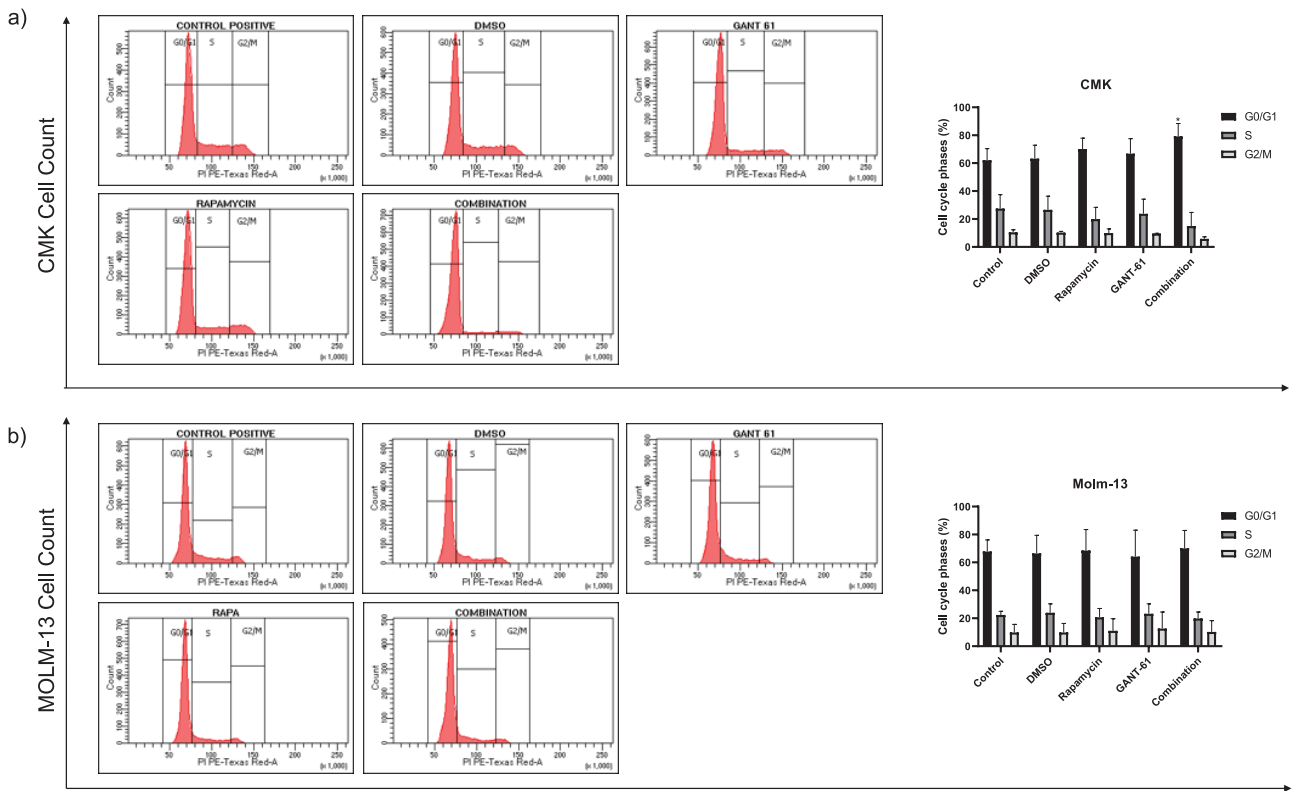


Figure 3. The effect of GANT61 and rapamycin alone or in combination on cell cycle progression of AML cells. CMK (n=3) and MOLM-13 (n=2). The representative histograms were shown. At least two independent experiments were performed, combined, and analyzed (* = $p < 0.05$).

rapamycin binding domain of mTOR, inhibits the mTORC1 functions. The inhibition happens in the transition of mTOR and G1 to the S phase by forming an immunosuppressive complex. However, rapamycin is not able to physically contact or inhibit mTORC2. With respect to rapamycin sensitivity, mTORC1 and mTORC2 can respectively be defined as rapamycin-sensitive and rapamycin-insensitive. However, the paradigm might not be accurate when considering the cases of mTORC2 activity blockage by means of rapamycin or the mTORC1 resistance to rapamycin (23, 24). AML cells have an upregulated mTOR pathway that reprograms metabolic activities. For example, Akt is constitutively active and promotes glycolysis due to the upregulated mTOR pathway (2). In AML, the mTOR pathway becomes dysregulated once mutations occur in association with oncogene activation, oncogene amplification, or tumor suppressor gene inactivation. For instance, the deletion of PTEN activates the mTOR pathway by inducing p53 expression and leukemogenesis (1).

Alterations of key mTOR signaling genes have shown regulation of AML leukemia stem cells. An example of this is the Rheb1 expression, which is overexpressed in patients with AML and also associated with lower survival rates in comparison to patients with a lower expression of Rheb1. Rheb1 deletion also has revealed an induced effect of apoptosis and enhanced cell

cycle arrest, leading to a prolonged lifetime in leukemia stem cells (1). Another study showed in their leukemia cell panel and pilot clinical study how rapamycin had demonstrated antileukemic effects (26). In addition, this aforementioned pathway implies constitutive activity in around 60% of the patients with AML, with constitutive activation causing a decrease in overall survival time (2). Therefore, inhibition of the mTOR pathway is crucial as a therapeutic approach for AML inhibition due to its vital functions such as proliferation and differentiation.

Together with these, the induced mTOR signaling pathway is seen to influence the HH signaling pathway via the phosphorylation of Gli-1 at Ser84. This phosphorylation ends up inhibiting SUFU binding, thereby inducing the HH pathway (27). This crosstalk between these two pathways has led this study to suggest that targeting them simultaneously would have a synergistic effect on AML cells due to the blockage of the signal that is triggered by both pathways. For this purpose, the study administered GANT61 as an inhibitor for the Gli-1 and Gli-2 proteins in the HH signaling pathway and rapamycin as an inhibitor of mTOR (9). GANT61 binds to Gli proteins inside the nucleus without targeting the direct binding of Gli to DNA. However, GANT61 also inhibits the transcriptional factor ability of the Gli proteins and significantly decreases the expression of HH target proteins, inclusive of the HH signaling pathway

inhibitors (28). The suppression of Gli-1 has been observed to enhance the chemosensitivity of CD34⁺-enriched AML progenitor cells, suggesting that Gli could be a potential target for AML treatments (9).

Numerous studies have investigated the inhibition of HH and mTOR signaling pathways due to their high potency as therapeutic targets for AML. Gli-1 and mTOR inhibition has been shown to induce apoptosis and demonstrated a synergistic effect in both solid tumors and hematological malignancies. In particular, GANT61 is seen to promote apoptosis in oral squamous cell carcinoma (OSCC) (28). Similarly, Miyazaki et al. (29) demonstrated the effect of the combination of GANT61 and rapamycin in pancreatic cancer stem cells, which showed an efficient reduction of 85% in cell proliferation. Moreover, this combination offered a decreased expression of the Gli-luciferase, along with the increased synergistic cytotoxic effect in different AML cells (30). A recent finding has also shown Gli-1, which is associated with poor prognosis in AML, to be found to activate the PI3K and cyclin-dependent kinases (CDKs) and thus promote the survival and cell-cycle progression. Synergistic inhibition of Gli-1 using GANT61 and CDK4/6 sensitized the cells to Ara-c therapy (31). Moreover, targeting of FLT3 wild-type AML cells with the combined FLT3, Gli-1, and PI3K inhibition resulted in a strong inhibitory effect on the FLT3 mutant AML cells (32). However, no reports are found concerning the effects of the combined GANT61 and rapamycin on both of those pathways in CMK or MOLM-13 cells. When compared with the literature, the results from the current study have proven a similar effect with a decrease in cell proliferation. The potential exists for a combination therapy approach to AML in the CMK and MOLM-13 cell lines by inhibiting the mTOR and HH signaling pathways using rapamycin and GANT61 in combination. The purpose of the present study has been to gain a better understanding of the effect of these two pathways in AML cells.

In agreement with the findings in the literature, the cell viability assays in the current study indicated the effect of the HH inhibitor GANT61 to decrease cell viability in a dose-dependent manner. However, the mTOR inhibitor rapamycin decreased cell viability by 50%, even though a high 1 μ M dose of rapamycin had been tested on cells. The literature has shown that when a panel of AML cells is subjected to increasing concentrations of rapamycin and their clonogenicity is tested, some cell lines remain insensitive, which resulted in no change in colony numbers (26). Similar to this study's results, this effect could be due to the cytostatic effect of rapamycin. Combining rapamycin with other pathway inhibitors such as the PI3K/AKT pathway could sensitize the cells to rapamycin. Previous studies have also demonstrated reduced cell proliferation with regard to time and dosage (33, 34). For the combination treatment of the CMK cell line using the IC₂₀ values for both Rapamycin and GANT61, a slight reduction occurred in cell proliferation when compared to the individual treatments. Therefore, the combined usage of these two drugs might prove to be more effective than when used individually. The differences in cell

lines might also arise from the different genetic backgrounds of the cells. The cell cycle analysis revealed 17% of the CMK and 2.7% of the MOLM-13 cells to have been arrested during the G₀/G₁ phase in response to the combination treatment. The cell cycle arrest could be a reflection of the decreased cell proliferation in response to the drug treatment.

In summary, the present study proposes that targeting the mTOR and HH pathways simultaneously inhibits the cell proliferation of the CMK and MOLM-13 cell lines in AML. Moreover, the combinational treatment led to a G₀/G₁ cell cycle arrest, especially in the CMK cell line. Further in-depth studies should be conducted to understand the mechanistic effects of these drugs by evaluating the apoptotic effects for instance, with an elucidation of the underlying impact of these pathways on AML also being recommended.

Acknowledgment: This study would like to thank the flow cytometry facility in the Genome and Stem Cell Center of Erciyes University, with thanks to Esma Saraymen, the flow cytometry specialist, for her technical assistance during the flow cytometry experiments.

Ethics Committee Approval: In the current study, only *in vitro* cell line study was performed, therefore there is no need for ethical approval.

Peer-review: Externally peer-reviewed.

Author Contributions: Conception/Design of Study - E.B.G.A.; Data Acquisition - E.B.G.A., F.M.K., E.C., M.Y.; Data Analysis/Interpretation - E.B.G.A., F.M.K., E.C., M.Y.; Drafting Manuscript - E.B.G.A., F.M.K., E.C., M.Y.; Critical Revision of Manuscript - E.B.G.A., F.M.K., E.C., M.Y.; Final Approval and Accountability - E.B.G.A., F.M.K., E.C., M.Y.

Conflicts of Interest: The authors declare no conflict of interest.

Financial Disclosure: The authors declare that this study has received no financial support.

REFERENCES

1. Darici S, Alkhalidi H, Horne G, Jørgensen HG, Marmioli S, Huang X. Targeting PI3K/Akt/mTOR in AML: Rationale and clinical evidence. *J Clin Med* 2020; 9(9): 2934. [CrossRef]
2. Nepstad I, Hatfield KJ, Grønningsæter IS, Reikvam H. The PI3K-Akt-mTOR signaling pathway in human acute myeloid leukemia (AML) cells. *Int J Mol Sci* 2020; 21(8): 2907. [CrossRef]
3. Saultz JN, Garzon R. Acute myeloid leukemia: A concise review. *J Clin Med* 2016; 5(3): 33. [CrossRef]
4. Scholl C, Gilliland DG, Fröhling S. Deregulation of signaling pathways in acute myeloid leukemia. *Semin Oncol* 2008; 35(4): 336-45. [CrossRef]
5. Terao T, Minami Y. Targeting Hedgehog (Hh) Pathway for the acute myeloid leukemia treatment. *Cells* 2019; 8(4): 312. [CrossRef]
6. Niyaz M, Khan MS, Mudassar S. Hedgehog signaling: An achilles' heel in cancer. *Transl Oncol* 2019; 12(10): 1334-44. [CrossRef]
7. Sari IN, Phi LTH, Jun,N, Wijaya YT, Lee S, Kwon HY. Hedgehog signaling in cancer: A prospective therapeutic target for eradicating cancer stem cells. *Cells* 2018; 7(11): 208. [CrossRef]
8. Shallis RM, Bewersdorf JP, Boddu PC, Zeidan AM. Hedgehog pathway inhibition as a therapeutic target in acute myeloid leukemia. *Expert Rev Anticancer Ther* 2019; 19: 717-29. [CrossRef]

9. Long B, Wang LX, Zheng FM, Lai SP, Xu DR, Hu Y, et al. Targeting GLI1 suppresses cell growth and enhances chemosensitivity in CD34⁺ enriched acute myeloid leukemia progenitor cells. *Cell Physiol Biochem* 2016; 38(4): 1288-302. [\[CrossRef\]](#)
10. Ruch JM, Kim EJ. Hedgehog signaling pathway and cancer therapeutics: Progress to date. *Drugs*. 2013; 73, 613-23. [\[CrossRef\]](#)
11. Harada K, Ohashi R, Naito K, Kanki K. Hedgehog signal inhibitor GANT61 inhibits the malignant behavior of undifferentiated hepatocellular carcinoma cells by targeting non-canonical GLI signaling. *Int J Mol Sci* 2020; 21(9): 3126. [\[CrossRef\]](#)
12. Saxton RA, Sabatini DM. mTOR signaling in growth, metabolism, and disease. *Cell* 2017; 168(6): 960-76. [\[CrossRef\]](#)
13. Zou Z, Tao T, Li H, Zhu X. mTOR signaling pathway and mTOR inhibitors in cancer: Progress and challenges. *Cell Biosci* 2020; 10(1): 31. [\[CrossRef\]](#)
14. Park S, Chapuis N, Tamburini J, Bardet V, Cornillet-Lefebvre P, Willems L, et al. Role of the PI3K/AKT and mTOR signaling pathways in acute myeloid leukemia. *Haematologica* 2010; 95(5): 819-28. [\[CrossRef\]](#)
15. Feng Y, Chen X, Cassidy K, Zou Z, Yang S, Wang Z and Zhang X. The Role of mTOR inhibitors in hematologic disease: From bench to bedside. *Front Oncol* 2021; 10: 611690. [\[CrossRef\]](#)
16. Yenigül M, Akçok İ, Gencer Akçok EB. Ethacrynic acid and cinnamic acid combination exhibits selective anticancer effects on K562 chronic myeloid leukemia cells. *Mol Biol Rep* 2022; 49(8): 7521-30. [\[CrossRef\]](#)
17. Chou TC. Drug combination studies and their synergy quantification using the Chou-Talalay method. *Cancer Res* 2010; 70: 440-6. [\[CrossRef\]](#)
18. PDQ Adult Treatment Editorial Board. Adult Acute Myeloid Leukemia Treatment (PDQ®): Patient Version. In PDQ Cancer Information Summaries. National Cancer Institute (US); 2002. Available from: <http://www.ncbi.nlm.nih.gov/books/NBK65939/>
19. Aberger F, Hutterer E, Sternberg C, del Burgo PJ, Hartmann TN. Acute myeloid leukemia -strategies and challenges for targeting oncogenic Hedgehog/GLI signaling. *Cell Commun Signal* 2017; 15(1): 8. [\[CrossRef\]](#)
20. Li X, Chen F, Zhu Q, Ding B, Zhong Q, Huang K, et al. Gli-1/PI3K/AKT/NF-κB pathway mediates resistance to radiation and is a target for reversion of responses in refractory acute myeloid leukemia cells. *Oncotarget* 2016; 7: 33004-15. [\[CrossRef\]](#)
21. Queiroz KC, Ruela-de-Sousa RR, Fuhler GM, Abernson HL, Ferreira CV, Peppelenbosch MP, et al. Hedgehog signaling maintains chemoresistance in myeloid leukemic cells. *Oncogene* 2010; 29(48): 6314-22. [\[CrossRef\]](#)
22. Jamieson C, Martinelli G, Papayannidis C, Cortes JE. Hedgehog pathway inhibitors: A new therapeutic class for the treatment of acute myeloid leukemia. *Blood Cancer Discov* 2020; 1(2): 134-45. [\[CrossRef\]](#)
23. Laplante M, Sabatini DM. mTOR signaling at a glance. *J Cell Sci* 2009; 122(20): 3589-94. [\[CrossRef\]](#)
24. Arriola Apelo SI, Lamming DW. Rapamycin: An inhibitor of aging emerges from the soil of Easter Island. *J Gerontol A Biol Sci Med Sci* 2016; 71(7): 841-9. [\[CrossRef\]](#)
25. Ballou LM, Lin RZ. Rapamycin and mTOR kinase inhibitors. *J Chem Biol* 2008; 1(1-4): 27-36. [\[CrossRef\]](#)
26. Récher C, Beyne-Rauzy O, Demur C, Chicanne G, Dos Santos C, Mansat-De Mas V, et al. Antileukemic activity of rapamycin in acute myeloid leukemia. *Blood* 2005; 105 (6): 2527-34. [\[CrossRef\]](#)
27. Wang Y, Ding Q, Yen CJ, Xia W, Izzo JG, Lang JY, et al. The Crosstalk of mTOR/S6K1 and Hedgehog pathways. *Cancer Cell* 2012; 21(3): 374-87. [\[CrossRef\]](#)
28. Bacelar Sacramento de Araújo T, de Oliveira Siquara da Rocha L, Torres Andion Vidal M, Cerqueira Coelho PL, Galvão dos Reis M, Solano de Freitas Souza B, et al. GANT61 Reduces Hedgehog Molecule (GLI1) Expression and Promotes Apoptosis in Metastatic Oral Squamous Cell Carcinoma Cells. *Int J Mol Sci* 2020; 21(17): 6076. [\[CrossRef\]](#)
29. Miyazaki Y, Matsubara S, Ding Q, Tsukasa K, Yoshimitsu M, Kosai K, et al. Efficient elimination of pancreatic cancer stem cells by hedgehog/GLI inhibitor GANT61 in combination with mTOR inhibition. *Mol Cancer* 2016; 15(1): 49. [\[CrossRef\]](#)
30. Pan D, Li Y, Li Z, Wang Y, Wang P, Liang Y. Gli inhibitor GANT61 causes apoptosis in myeloid leukemia cells and acts in synergy with rapamycin. *Leuk Res* 2012; 36(6): 742-8. [\[CrossRef\]](#)
31. Zhou C, Du J, Zhao L, Liu W, Zhao T, Liang H, Fang P, et al. GLI1 reduces drug sensitivity by regulating cell cycle through PI3K/AKT/GSK3/CDK pathway in acute myeloid leukemia. *Cell Death Dis* 12(3): 231. [\[CrossRef\]](#)
32. Latuske E, Stamm H, Klokow M, Vohwinkel G, Muschhammer J, Bokemeyer C, Jücker M, Kebenko M, Fiedler W, Wellbrock J. Combined inhibition of GLI and FLT3 signaling leads to effective anti-leukemic effects in human acute myeloid leukemia. *Oncotarget* 2017; 8: 29187-201. [\[CrossRef\]](#)
33. SiY, ChuH, ZhuW, XiaoT, ShenX, FuY, et al. Concentration-dependent effects of rapamycin on proliferation, migration and apoptosis of endothelial cells in human venous malformation. *Exp Ther Med* 2018; 16: 4595-601. [\[CrossRef\]](#)
34. Cheng KY, Hao M. Mammalian target of rapamycin (mTOR) regulates transforming growth factor-β1 (TGF-β1)-induced epithelial-mesenchymal transition via decreased pyruvate kinase M2 (PKM2) expression in cervical cancer cells. *Med Sci Monit* 2017; 23: 2017-28. [\[CrossRef\]](#)

Shotgun Lipidomics Elucidates the Lipidome Alterations of the Mcl-1 Inhibitor S63845 in AML Cell Lines with a Focus on Sphingolipids

Melis Kartal Yandim¹ , Mesut Bilgin² 

¹Department of Medical Biology, Faculty of Medicine, Izmir University of Economics, Izmir, Turkiye

²Lipidomics Core Facility, Center for Autophagy, Recycling and Disease (CARD), Danish Cancer Society Research Center (DCRC), Copenhagen, Denmark

ORCID ID: M.K.Y. 0000-0003-0573-4276; M.B. 0000-0002-5034-8465

Cite this article as: Kartal Yandim M, Bilgin M. Shotgun lipidomics elucidates the lipidome alterations of the Mcl-1 inhibitor S63845 in AML cell lines with a focus on sphingolipids. *Experimed* 2022; 12(3): 209-14.

ABSTRACT

Objective: Acute myeloid leukemia (AML) is a vigorous type of leukemia requiring effective treatment. Myeloid cell leukemia-1 (Mcl-1) is an anti-apoptotic molecule that is upregulated in AML and is studied as a target for treatment. The specific Mcl-1 inhibitor, S63845, has antiproliferative effects on AML cells. Bioactive sphingolipids have crucial roles in cells and regulate Mcl-1 stability. This study aimed to elucidate the changes in lipid profiles of AML cell lines in response to Mcl-1 inhibitor S63845 treatment, with a special focus on sphingolipids.

Materials and Methods: The cytotoxic effects of S63845 were identified in the AML cell lines MV4-11, HL60, and KG1 using the MTT cell proliferation assay. Lipidome analysis was conducted by quantitative shotgun lipidomics covering 378 individual lipid species in 26 classes within the major lipid categories.

Results: The IC₅₀ values of S63845 have been calculated as 7 nM for MV4-11, 53 nM for HL60, and 479 nM for KG1. The lipidome results reveal the S63845 treatment to increase ceramide (Cer) levels in the MV4-11 and KG1 cell lines at the expense of downstream sphingolipids while increasing the hexosylceramide (HexCer) levels in the HL60 cell line at the expense of the Cer and sphingomyelin (SM).

Conclusion: This study showed S63845 to be able to suppress cell proliferation by altering lipid compositions in AML cell lines. More importantly, the study suggested S63845 to differentially affect the lipid profiles of AML cell lines.

Keywords: Mcl-1, small molecule inhibitors, S63845, acute myeloid leukemia, shotgun lipidomics, bioactive sphingolipids

INTRODUCTION

Acute myeloid leukemia (AML) is caused by phenotypic and genetic abnormalities during hematopoietic stem cell differentiation. These abnormalities lead to proliferation and aggregation of immature blood cells (1). Among the acute leukemias, AML represents the most common type and is seen in approximately 80% of adult leukemia patients (1). While the overall survival rate is higher in younger age groups, AML prognosis is poor in older adults, resulting in death in 44% of adults over the age of 75 (2). In the clinic, standard intensive chemotherapy approaches combining cytarabine and anthracyclines are used to combat AML. Other approaches

such as targeted therapies have additionally been proposed as being effective in AML therapy with improvements in high-throughput techniques (2). However, the need exists for novel treatment approaches due to the limited current treatment alternatives, poor prognosis, limited tolerance to the treatment in older patients, and the resistance developed against anti-cancer drugs (3). In this context, small molecule inhibitors for Mcl-1 have been proposed as potentially effective agents in AML treatment (4).

Mcl-1 is a member of the Bcl-2 family, which is responsible for the regulation of apoptotic processes (5). In normal cells, Mcl-1 acts as the inhibitor of apoptosis by sequestering BH3-

Corresponding Author: Melis Kartal Yandim **E-mail:** melis.yandim@ieu.edu.tr

Submitted: 30.10.2022 **Revision Requested:** 28.11.2022 **Last Revision Received:** 03.12.2022 **Accepted:** 05.12.2022 **Published Online:** 30.12.2022



Content of this journal is licensed under a Creative Commons Attribution-NonCommercial 4.0 International License.

only molecules such as Bim, Bid, and Puma or by neutralizing Bax and Bak (5). Mcl-1 inhibits cytochrome c release by disrupting mitochondrial outer membrane permeabilization (6). Overexpression of Mcl-1 results in the disruption of the equilibrium between the anti-apoptotic and pro-apoptotic proteins, subsequently causing an excess proliferation of cancer cells (6). Due to its oncogenic properties and high expression levels in several types of cancers including hematological malignancies and solid cancers, Mcl-1 has been proposed as a powerful target in cancer treatment (6). S63845 was first discovered by Kotschy et al. (4) and has been characterized and reported as an effective small molecule inhibitor of Mcl-1 in many types of cancer. In AraC-resistant acute myeloid leukemia cell lines, S63845 in combination with venetoclax increases anti-leukemic effect, and this combination is strongly synergistic compared to combinations with hypomethylating agents (7). Moreover, S63845 combined with imatinib, nilotinib, dasatinib, or asciminib show synergistically apoptotic effects on chronic myeloid leukemia cells (8). In light of the information on the strong effects of S63845, it has been suggested as a promising therapeutic target for both solid tumors and hematological malignancies (6). However, the exact mechanism of action of S63845 remains unclear.

Lipid compositions are known to be altered in tumor cells, which may affect their cellular response to different agents (9). Fatty acids promote proliferation in tumor cells due to their contribution to the membrane lipid bilayer and additionally have a crucial function in cell signaling as well as in developing resistance against anti-cancer agents (9). Bioactive sphingolipids have important roles in cell proliferation, apoptosis, autophagy, inflammation, and migration (10). The central molecule of this family, ceramide, is related to pro-apoptotic outcomes, whereas the other members, sphingosine-1-P (S1P) and glucosylceramide, are related to anti-apoptotic outcomes and contribute to the development of multidrug resistance in cancer cells (10). Some studies have reported a relationship between sphingolipids and Mcl-1, even suggesting ceramide and S1P to regulate the degradation of Mcl-1 (11, 12). The agents targeting sphingolipid metabolism suppress Mcl-1 expression and subsequently affect Mcl-1 stability (13).

In light of this information, this study aimed to elucidate the effects of the Mcl-1 inhibitor, S63845, on the lipid profiles of three different AML cell lines, MV4-11, HL60, and KG1, with a special focus on sphingolipids. In total 378 individual lipid species have been profiled using mass spectrometry (MS)-based shotgun lipidomics. The results reveal the S63845 treatment influences lipid metabolism depending on the type of AML cell line.

MATERIALS and METHODS

Cell Lines, Chemicals, and Culture Conditions

HL60 and KG1 cell lines were obtained from the German Collection of Microorganisms and Cell Cultures (Germany). The MV4-11 cell line was a kind gift from Dr. A. Adan (Abdullah Gul University, Kayseri, Turkey). S63845 was obtained from Cayman Chemical (Michigan, USA), and the stock solution (1 mM) was

prepared by dissolving it in dimethyl sulfoxide (DMSO, VWR, Pennsylvania, USA). The cell culture medium and additives were obtained from Gibco (CA, USA). The chemical reagents, solutions, and internal lipid standards for the lipidomics analysis were obtained from Sigma-Aldrich (St. Louis, MO, USA), Rathburn Chemicals (Walkerburn, Scotland), Avanti Polar Lipids (Alabaster, AL, USA), and Larodan AB (Solna, Sweden). All cell lines were cultured in RPMI-1640 growth medium containing 10% fetal calf serum (FCS), 2 mM L-glutamine, and 1% penicillin-streptomycin at 37°C in a 5% CO₂ humidified incubator.

MTT Assay

The effects of S63845 on cell proliferation were determined using the MTT cell proliferation assay (Sigma-Aldrich, MO, USA). The protocol was applied for the MTT assay as described previously (14). In each experiment, the final concentration of DMSO exceeded no more than 0.2% in culture. In short, 1×10⁴ cells per well from the HL60, KG1, and MV4-11 cell lines were seeded into 96-well plates in 100 µL growth medium. Increased concentrations of S63845 were applied in 100 µL of RPMI-1640 onto the cells, and the cells were incubated at 37°C in 5% CO₂ for 72 h. Next, the cells were incubated for 4 h with 20 µL of MTT (5 mg/mL). After the incubation period, the plates were centrifuged for 10 min at 1800 rpm, and the MTT crystals were dissolved with 100 µL of DMSO. After shaking the plates for 5 min using an orbital shaker, the plates were analyzed under 570 nm wavelengths with a spectrophotometer (Thermo Fisher Scientific Multiskan Spectrum, Finland). IC₅₀ values of the S63845 for each cell line were calculated according to the cell proliferation plots.

Treating the Cells with S63845 for the Lipidomics Analysis

The cells were seeded into 6-well plates at 4×10⁵ cells per well in 1 mL of growth medium, and treated with IC₅₀ values of S63845 for 24 h at 37°C. Because the aim of this treatment is to stimulate the changes in lipid profiles rather than killing the cells, IC₅₀ values for the 72-h span were applied for 24 h. After the incubation period, the centrifuge was run at 400 g for 5 min at 4°C, then two washing steps were performed with 500 µL of ice-cold 155 mM ammonium bicarbonate. Next, the 155 mM ammonium bicarbonate were added as pellets to the 4×10⁵ cells in 200 µL (2000 cells/µL). The cells were stored at -80°C until the lipid extraction.

Lipid Extraction

The lipid extraction process was executed at 4°C or upon ice (15). Tubes with 200 µL of biological samples containing the 4×10⁵ cells were added to a 1,000 µL chloroform/methanol (2:1, v/v) and 12.5 µL internal standard solution. The composition of the internal standard solution is presented in Table 1. The lipids were extracted with 20 min of shake at 2000 rpm and then centrifuged for 5 min at 1000 g. The organic phase at the bottom was collected and put into a new tube. After being evaporated for 60 min with a vacuum evaporator, the samples were resuspended in the 200 µL chloroform/methanol (1:2, v/v).

Shotgun Lipidomics Analysis

For positive ionization, 10 µL of crude lipid extracts were mixed with 12.9 µL of 13.3 mM ammonium acetate in 2-propanol. For

Table 1. Internal standard solution composition.

Lipid	Amount (pmol)
Cholesteryl ester (CE) 15:0-D7	45.80
Ceramide (Cer) 18:1;2/12:0;0	31.25
Cholesterol (Chol)-D4	356.87
Diacylglycerol (DAG) 12:0/12:0	45.63
Dihexosylceramide (diHexCer) 18:1;2/17:0;0	23.21
Hexosylceramide (HexCer) 18:1;2/12:0;0	28.88
Lysophosphatidic acid (LPA) 17:0	31.15
Lysophosphatidylcholine (LPC) 12:0	25
Lysophosphatidylethanolamine (LPE) 17:1	30.75
Lysophosphatidylglycerol (LPG) 17:1	30.16
Lysophosphatidylinositol (LPI) 13:0	22.91
Lysophosphatidylserine (LPS) 17:1	14.26
Phosphatidic acid (PA) 12:0/12:0	28.35
Phosphatidylcholine (PC) 12:0/12:0	35.94
Phosphatidylethanolamine (PE) 12:0/12:0	39.95
Phosphatidylglycerol (PG) 12:0/12:0	29.31
Phosphatidylinositol (PI) 8:0/8:0	28.38
Phosphatidylserine (PS) 12:0/12:0	25.38
Sphingomyelin (SM) 18:1;2/12:0;0	21.28
Trihexosylceramide (triHexCer) 18:1;2/17:0;0	51.19

negative ionization, 10 μ L of crude lipid extract were mixed with 10 μ L of 0.2% (v/v) methylamine in methanol was used. The mass spectrometric analysis was performed on an Orbitrap Fusion Tribrid mass spectrometer (Thermo Fisher Scientific, USA) coupled to TriVersa NanoMate (Advion Biosciences, USA), a direct nanoelectrospray infusion robot. For the fourier transform (FT)-MS and FT MS/MS analyses, similar features were used as previously reported (16, 17).

Lipid Annotation

Annotation of the lipids was based on sum composition, where glycerolipids and glycerophospholipids are denoted as: <lipid class>< number of carbon atoms in acyl chains ><number of double bonds in acyl chains> (e.g., PC 34:1). While sphingolipid species are denoted as <lipid class><number of carbon atoms in the sphingoid base and acyl chain>< number of double bonds in the sphingoid base and acyl chain ><number of OH groups in the sphingoid base and acyl chain > (e.g., SM 34:1;2) (18-21).

Data Processing

LipidXplorer was used to report the data acquired from the FT MS and FT MS/MS analyses (22, 23). Absolute molar quantities were calculated using LipidQ, an R-based suite of scripts (17).

Statistical Analyses

All experiments were performed over three biological replicates. Statistical significance was determined using the Student's t test and one-way ANOVA, with $p < 0.05$ being considered statistically significant.

RESULTS

S63845 Inhibited Cell Proliferation in Three Different AML Cell Lines

The anti-proliferative effects of S63845 in AML cell lines were determined using the MTT cell proliferation assay. The cells were treated with increasing concentrations of S63845 (1-2,000 nM, depending on the cell type) for 72 h, and the MTT cell proliferation assay was executed. S63845 suppressed cell proliferation in each cell line as compared to the untreated control groups. IC₅₀ values were calculated as 7, 53, and 479 nM in MV4-11, HL60, and KG1 cell lines, respectively (Figure 1).

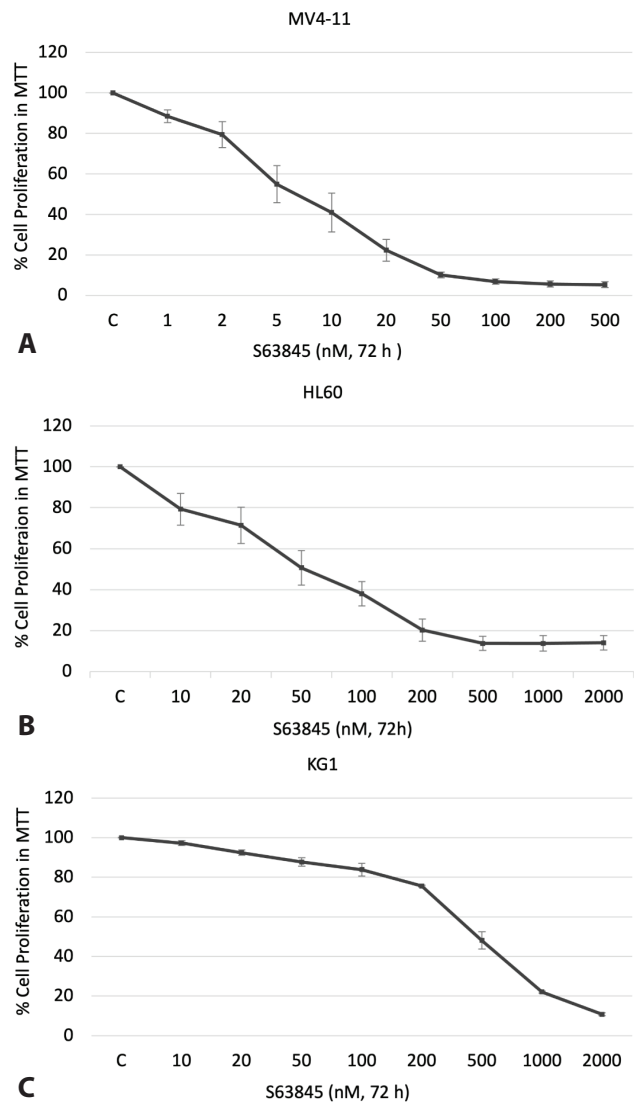


Figure 1. Antiproliferative effects of S63845 on the MV4-11 (A), HL60 (B), and KG1 (C) cell lines. IC₅₀ values of S63845 for each cell line were calculated from the cell proliferation plots. Three biological replicates were used for MTT cell proliferation assays, and the results are the means of the independent experiments. The standard deviations are represented with the error bars, with $p < 0.05$ being considered statistically significant.

S63845 Differentially Affected Lipid Profiles in Three Different AML Cell Lines

Quantitative shotgun lipidomics analysis was performed on each cell line treated with IC₅₀ values of S63845 for 24 h. The lipidomics profiling demonstrated quantification of 26 classes within major lipid categories and enabled profiling of 378 individual lipid species (Figure 2A). The class profile demonstrated a typical mammalian lipidome profile with PC and Chol as the major lipid components of the lipidome with 45.162±3.843 mol% and 17.341±1.311 mol% of all the cells, respectively (Figure 2A). The lipid with lowest detected levels belongs to lysoglycerophospholipid with 0.007±0.013 mol % for LPSO- (Figure 2A). Interestingly, comparing the three cell lines to their treated counterparts demonstrated the HL60 and

KG1 class profiles have similar changes in respect to S63845 treatment (Figure 2B). However, the MV4-11 cell lines treated with S63845 demonstrated few similarities with the treated HL60 and KG1 cell lines (Figure 2B).

Due to the presence of a relationship between Mcl-1 and sphingolipid metabolism, we focused on the sphingolipid species to reveal any possible trend with similar changes in all cell lines treated with S63845. We quantified 55 sphingolipid species belonging to five sphingolipid classes: Cer, HexCer, dihexosylceramide (diHexCer), trihexosylceramide (triHexCer), and SM. The cells treated with S63845 did not demonstrate similarities for the species profile within the HexCer and triHexCer classes (Figure 2C). Interestingly, the SM 34:1;2

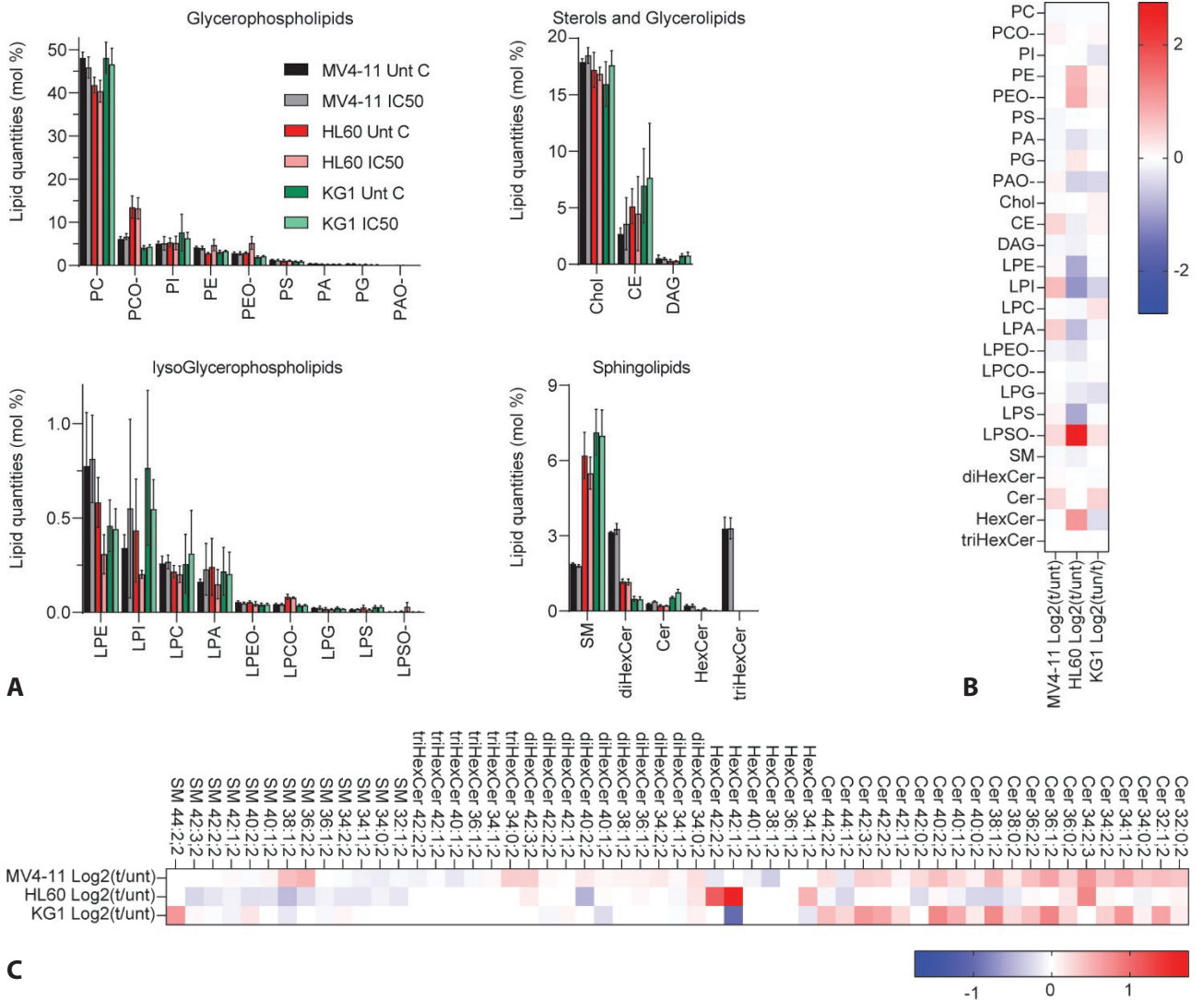


Figure 2. S63845 induced lipidome alterations of the MV4-11, HL60 and KG1 cell lines. A) The bar graph presents the mol % values of the 26 lipid classes. B) The heatmap presents the log₂-transformed lipid class abundance ratios of the treated and untreated cell lines. C) The heatmap presents the log₂-transformed sphingolipid species abundance ratios of the treated and untreated cell lines.

decreased and diHexCer 34:0;2 increased in all treated cell lines (Figure 2C). However, 10 of the 20 Cer species demonstrated increased levels for all treated counterparts of the MV4-11, HL60, and KG1 cell lines (Figure 2C). While the treated counterparts of the MV4-11 and KG1 cell lines demonstrated similar trends for 18 out of 20 Cer species with increased levels, the treated HL60 cell lines mostly showed an opposite trend compared to the treated MV4-11 and KG1 cell lines (Figure 2C). The HL60 cell line demonstrated increased levels of HexCer, which is one of the downstream sphingolipids of Cer (Figure 2C).

DISCUSSION

Despite of the novel investigations in the treatment of AML patients, approximately 1/3 of the patients can be cured. Therefore, the need still exists for more effective therapeutic approaches in the clinic (24). Targeting Mcl-1 in AML treatment has been proposed to have potential in *in vitro* and *in vivo* studies conducted by many groups (25). S63845 has been reported to have cytotoxic and apoptotic effects in AML cell lines with IC₅₀ values less than 1 μM (4).

Lipid composition may change with regard to several types of cancer cells, and these changes affect the cellular responses against chemotherapeutic agents (26). Sphingolipids are important elements of membrane lipids and have crucial roles in cell signaling, regulating several cellular events including cell proliferation, cell death, senescence, invasion, and angiogenesis (10). Many studies have reported the regulatory effects of Cer and S1P on Mcl-1 stability (11). However, no study has reported yet on the mechanism of action of the Mcl-1 inhibitor S63845 regarding the effects on lipid profiles in AML cell lines. Therefore, this study has aimed to elucidate the potential effects of S63845 on lipid profiles in the MV4-11, HL60, and KG1 cell lines using quantitative shotgun lipidomics. Upon treating the cells with increasing concentrations of S63845 for 72 h, the IC₅₀ values were calculated as 7, 53, and 479 nM in MV4-11, HL60, and KG1 cell lines, respectively. The study's aim has been to induce lipid alteration rather than suppressing cell proliferation for the lipidomics analysis. Therefore, we treated the cells for only 24 h while using the corresponding concentrations for the 72 h-IC₅₀-values of S63845. The results of profiling 378 individual lipid species in 26 classes showed that most of the Cer species levels increased in response to the S63845 treatment, whereas SM levels decreased (Figure 2A). These results suggest S63845 to be able to induce SM hydrolysis, leading to increases in Cer levels. Hydrolysis of SM is carried out by SMases and results in cell death and suppression of cell proliferation in cancer cells (27). However, S63845 mostly affects the lipidomes over a variety of different actions, depending on the type of cell. For instance, some types of SMs (i.e., SM 36:2;2 and SM 38:1;2) increase in MV4-11 cell lines, whereas they decrease in the other cell lines. SM accumulation has been suggested to possibly be related to the negative impact regarding autophagosomal membrane maturation in early stages (27). This accumulation of SM may suppress autophagy in these cells. Additionally, the S63845 treatment increased HexCer levels in the HL60 cell

lines, contrary to the other cells. In many types of cancer cells, increased HexCer levels have been related to the development of multidrug resistance and cell survival. Cer is converted into HexCer through UDP-glucose Cer glucosyltransferase and glucosylCer synthase (10, 28). The effects of these changes may be elucidated by examining the cell death mechanisms and gene expression levels in further studies. Moreover, due to AML being a very heterogenous disease, each type of cell line and patient sample may respond to the anti-cancer agents differently despite having the same disease type, and their lipid profiles may also change in distinct manners (9). The study's results depicting the distinct effects of S63845 depending on cell type also contribute to this rationale.

CONCLUSION

In conclusion, this study revealed the S63845 treatment to be able to inhibit cell proliferation by increasing Cer levels in AML cell lines. This increase in Cer levels may result from the hydrolysis of SM and may then lead to apoptosis. However, each cell line may respond to the S63845 treatment through different mechanisms. The results of the shotgun lipidomics analysis showed that, despite belonging to the same disease type, the same agent may affect lipidomes differently depending on the cell line. This result suggests the potential of using lipidomic profiles in terms of diagnostic and prognostic fingerprints. This study sheds light on the action of the S63845 mechanism. The exact mechanism of the S63845's action resulting in the changes in lipidomes should be elucidated in further studies regarding each cell line.

Acknowledgments: We would like to thank the technicians at the Danish Cancer Society Research Center for their support during the experiments, in particular Dianna Skousborg Larsen for her assistance during the lipidomics analyses.

Ethics Committee Approval: The study involves commercially available cell lines, therefore there is no need for ethical approval.

Peer-review: Externally peer-reviewed.

Author Contributions: Conception/Design of Study - M.K.Y., M.B.; Data Acquisition - M.K.Y., M.B.; Performing experiments - M.K.Y., M.B.; Data Analysis/Interpretation - M.K.Y., M.B.; Statistical Analyses - M.K.Y., M.B.; Drafting Manuscript - M.K.Y., M.B.; Critical Revision of Manuscript - M.K.Y., M.B.; Final Approval and Accountability - M.K.Y., M.B.

Conflicts of Interest: The authors declare no conflict of interest.

Financial Disclosure: The authors declare that this study has received no financial support.

REFERENCES

1. Padmakumar D, Chandrababha VR, Gopinath P, Vimala Devi ART, Anitha GRJ, Sreelatha MM, et al. A concise review on the molecular genetics of acute myeloid leukemia. Vol. 111, Leukemia Research. Elsevier Ltd; 2021. [CrossRef]

2. Newell LF, Cook RJ. Advances in acute myeloid leukemia. Vol. 375, BMJ (Clinical research ed.). NLM (Medline); 2021. p. n2026. [\[CrossRef\]](#)
3. Pearson JM, Tan SF, Sharma A, Annageldiyev C, Fox TE, Abad JL, et al. Ceramide analogue SACLAC modulates sphingolipid levels and MCL-1 splicing to induce apoptosis in acute myeloid leukemia. *Mol Cancer Res* 2020; 18(3): 352-63. [\[CrossRef\]](#)
4. Kotschy A, Szlavik Z, Murray J, Davidson J, Maragno AL, le Toumelin-Braizat G, et al. The MCL1 inhibitor S63845 is tolerable and effective in diverse cancer models. *Nature* 2016; 538(7626): 477-82. [\[CrossRef\]](#)
5. Bolomsky A, Vogler M, Köse MC, Heckman CA, Ehx G, Ludwig H, et al. MCL-1 inhibitors, fast-lane development of a new class of anti-cancer agents. *J Hematol Oncol* 2020;13: 173. [\[CrossRef\]](#)
6. Wang H, Guo M, Wei H, Chen Y. Targeting MCL-1 in cancer: current status and perspectives. *J Hematol Oncol* 2021; 14(1): 67. [\[CrossRef\]](#)
7. Moujalled DM, Pomilio G, Ghiurau C, Ivey A, Salmon J, Rijal S, et al. Combining BH3-mimetics to target both BCL-2 and MCL1 has potent activity in pre-clinical models of acute myeloid leukemia. *Leukemia* 2019; 33(4): 905-17. [\[CrossRef\]](#)
8. Malyukova A, Ujvari D, Yektaei-Karin E, Zovko A, Madapura HS, Keszei M, et al. Combination of tyrosine kinase inhibitors and the MCL1 inhibitor S63845 exerts synergistic antitumorigenic effects on CML cells. *Cell Death Dis* 2021; 12(10). [\[CrossRef\]](#)
9. Stefanko A, Thiede C, Ehninger G, Simons K, Grzybek M. Lipidomic approach for stratification of acute myeloid leukemia patients. *PLoS One* 2017; 12(2). [\[CrossRef\]](#)
10. Ogretmen B, Hannun YA. Biologically active sphingolipids in cancer pathogenesis and treatment. *Nat Rev Cancer* 2004; 4(8): 604-16. [\[CrossRef\]](#)
11. Powell JA, Lewis AC, Zhu W, Toubia J, Pitman MR, Wallington-Beddoe CT, et al. Targeting sphingosine kinase 1 induces MCL1-dependent cell death in acute myeloid leukemia. *Blood* 2017; 6: 771-82. [\[CrossRef\]](#)
12. Tan SF, Liu X, Fox TE, Barth BM, Sharma A, Turner SD, et al. Acid ceramidase is upregulated in AML and represents a novel therapeutic target. *Oncotarget* 2016; 7(50): 83208-22. [\[CrossRef\]](#)
13. Lewis AC, Wallington-Beddoe CT, Powell JA, Pitson SM. Targeting sphingolipid metabolism as an approach for combination therapies in haematological malignancies. *Cell Death Discov* 2018; 4(1): 72. [\[CrossRef\]](#)
14. Kozanoglu I, Yandim MK, Cincin ZB, Ozdogu H, Cakmakoglu B, Baran Y. New indication for therapeutic potential of an old well-known drug (propranolol) for multiple myeloma. *J Cancer Res Clin Oncol* 2013; 139(2): 327-35. [\[CrossRef\]](#)
15. Bligh EG, Dyer WJ. A rapid method of total lipid extraction and purification. *Can J Biochem Physiol* 1959; 37(8): 911-7. [\[CrossRef\]](#)
16. Almeida R, Pauling JK, Sokol E, Hannibal-Bach HK, Ejsing CS. Comprehensive Lipidome Analysis by Shotgun Lipidomics on a Hybrid Quadrupole-Orbitrap-Linear Ion Trap Mass Spectrometer. *J Am Soc Mass Spectrom* 2015; 26(1): 133-48. [\[CrossRef\]](#)
17. Nielsen IØ, Groth-Pedersen L, Dicroce-Giacobini J, Jonassen ASH, Mortensen M, Bilgin M, et al. Cationic amphiphilic drugs induce elevation in lysoglycerophospholipid levels and cell death in leukemia cells. *Metabolomics* 2020; 16(9): 91. [\[CrossRef\]](#)
18. Ejsing CS, Sampaio JL, Surendranath V, Duchoslav E, Ekroos K, Klemm RW, et al. Global analysis of the yeast lipidome by quantitative shotgun mass spectrometry. *Proc Natl Acad Sci USA* 2009; 106(7): 2136-41. [\[CrossRef\]](#)
19. Klose C, Surma MA, Gerl MJ, Meyenhofer F, Shevchenko A, Simons K. Flexibility of a eukaryotic lipidome—insights from yeast lipidomics. *PLoS One* 2012; 7(4): e35063. [\[CrossRef\]](#)
20. Sampaio JL, Gerl MJ, Klose C, Ejsing CS, Beug H, Simons K, et al. Membrane lipidome of an epithelial cell line. *Proc Natl Acad Sci USA* 2011; 108(5): 1903-7. [\[CrossRef\]](#)
21. Ejsing CS, Moehring T, Bahr U, Duchoslav E, Karas M, Simons K, et al. Collision-induced dissociation pathways of yeast sphingolipids and their molecular profiling in total lipid extracts: a study by quadrupole TOF and linear ion trap-orbitrap mass spectrometry. *J Mass Spectrom* 2006; 41(3): 372-89. [\[CrossRef\]](#)
22. Herzog R, Schuhmann K, Schwudke D, Sampaio JL, Bornstein SR, Schroeder M, et al. LipidXplorer: A Software for Consensual Cross-Platform Lipidomics. *PLoS One* 2012; 7(1): e29851. [\[CrossRef\]](#)
23. Herzog R, Schwudke D, Shevchenko A. LipidXplorer: Software for Quantitative Shotgun Lipidomics Compatible with Multiple Mass Spectrometry Platforms. *Curr Protoc Bioinformatics* 2013; 43(1). [\[CrossRef\]](#)
24. Ewald L, Dittmann J, Vogler M, Fulda S. Side-by-side comparison of BH3-mimetics identifies MCL-1 as a key therapeutic target in AML. *Cell Death Dis* 2019; 10(12). [\[CrossRef\]](#)
25. Wei AH, Roberts AW, Spencer A, Rosenberg AS, Siegel D, Walter RB, et al. Targeting MCL-1 in hematologic malignancies: Rationale and progress. *Blood Rev* 2020; 44: 100672. [\[CrossRef\]](#)
26. Escribá P v., Busquets X, Inokuchi J ichi, Balogh G, Török Z, Horváth I, et al. Membrane lipid therapy: Modulation of the cell membrane composition and structure as a molecular base for drug discovery and new disease treatment. *Prog Lipid Res* 2015; 59: 38-53. [\[CrossRef\]](#)
27. Ogretmen B. Sphingolipid metabolism in cancer signalling and therapy. *Nat Rev Cancer* 2018; 18(1): 33-50. [\[CrossRef\]](#)
28. Pal P, Atilla-Gokcumen GE, Frasor J. Emerging Roles of Ceramides in Breast Cancer Biology and Therapy. *Int J Mol Sci* 2022; 23(19): 11178. [\[CrossRef\]](#)

Cerrahpaşa Medical Faculty Hospital HIV-1/-2 Serological Test Data: 2019-2022 Retrospective Evaluation

Harika Oyku Dinc¹ , Elif Keskin² , Banu Tufan Kocak³ , Bekir Kocazeybek² 

¹Department of Pharmaceutical Microbiology, Faculty of Pharmacy, Bezmialem Vakif University, Istanbul, Turkiye

²Department of Medical Microbiology, Cerrahpaşa Medical Faculty, Istanbul University-Cerrahpaşa, Istanbul, Turkiye

³T.C. Ministry of Health, Erenkoy Mental Health and Neurology Training and Research Hospital, Istanbul, Turkiye

ORCID ID: H.Ö.D. 0000-0003-3628-7392; E.K. 0000-0001-8264-0703; B.T.K. 0000-0002-6435-0785; B.K. 0000-0003-1072-3846

Cite this article as: Dinc HO, Keskin E, Tufan Kocak B, Kocazeybek B. Cerrahpaşa Medical Faculty Hospital HIV-1/-2 serological test data: 2019-2022 retrospective evaluation. *Experimed* 2022; 12(3): 215-8.

ABSTRACT

Objective: The aim of this study was to retrospectively discuss the human immunodeficiency virus (HIV) scanning and verification test results and demographics of patients who were admitted to the Istanbul University Cerrahpaşa Medical Faculty's Medical Microbiology Laboratory Center Serology/ELISA division with suspected HIV infection or pre-operative serologic screening. In addition, the study aimed to compare HIV seroprevalence with data from the center's previous period.

Materials and Methods: HIV-1/-2 antibody +P24 antigen (HIV-1/-2 Ab/Ag) was studied routinely using the chemiluminescent microparticle immunoassay (CMIA) method with the same method also being used as the second repeat test. The sera verifications of patients who showed repeated reactivity after the HIV Ab/Ag test were studied using the line immunoassay (LIA) method.

Results: The study retrospectively studied 156,542 cases between 2019-2022, of which 237 (0.17%) showed repeated anti-HIV-1/-2 reactivity. From the repeated reactivity serum samples, LIA testing was performed to confirm the remaining 181 serum samples after excluding the previously confirmed samples, with 175 (96.6%) coming back positive. All these samples showed *sgp120* and *gp41* band positivity, thus confirming HIV1 positivity.

Conclusion: These retrospective data from one center regarding HIV seroprevalence for the 2019-2022 period are in line with other national studies. However, due to the COVID-19 pandemic, HIV prevalence during this period may have been higher than detected. HIV prevalence in Istanbul, being a cosmopolitan city that receives immigrants, should be monitored in the future.

Keywords: HIV-1/-2, serological diagnostics, CMIA, LIA

INTRODUCTION

In accordance with the World Health Organization (WHO) report published in July 2022, more than 34.8 million people live with the human immunodeficiency virus (HIV), with approximately 1.5 million people having been infected with HIV in 2021 globally (1). Through the intensive work of national and international health organizations and non-governmental organizations (NGOs), new HIV infections and HIV-related deaths respectively decreased by 39% and 51% between 2000-2019 (2). However, with only

approximately 81% of HIV-infected individuals knowing their own HIV status, the 90-90-90 treatment target of the Joint United Nations Program on HIV/AIDS (UNAIDS) has yet to be met (3). Therefore, HIV continues to be a serious public health problem. Antiretroviral therapy (ART) should be started immediately once a person is diagnosed with HIV, and these people should be monitored periodically using clinical and laboratory findings as well as blood tests that are performed to evaluate the viral load of HIV in blood. Diagnosing infected persons as soon as possible has great importance in this context.

Corresponding Author: Bekir Kocazeybek **E-mail:** bzeybek@iuc.edu.tr

Submitted: 19.10.2022 **Revision Requested:** 29.11.2022 **Last Revision Received:** 05.12.2022 **Accepted:** 06.12.2022 **Published Online:** 30.12.2022



Content of this journal is licensed under a Creative Commons Attribution-NonCommercial 4.0 International License.

The present study aimed to retrospectively evaluate the test results and demographic data of patients who applied to the medical department's serology laboratory with suspected HIV infection or presurgical serological screening for the anti-HIV -1/-2 between January 2019-October 2022. In addition, the study evaluated the seroprevalence of HIV infections by comparing the data obtained in this period with the data from the previous period (January 2015-December 2018).

MATERIALS AND METHODS

The study retrospectively evaluated the results from samples that had been sent to the laboratory for anti-HIV serology testing in line with presurgical screening or clinical suspicion between January 1, 2019-October 1, 2022. The patients' demographic information was obtained retrospectively from the ISHOP doctor and laboratory information system of the Istanbul University Cerrahpaşa Medical Faculty Hospital. The serological diagnosis of HIV infection at the center is based on the Republic of Türkiye Ministry of Health's HIV/AIDS Diagnostic Treatment Guide (6). Accordingly, once a serum sample arrives at the center with a request for the anti-HIV-1/-2 test, it is screened for the presence of HIV-1/-2 antibodies and p24 antigens using chemiluminescent microparticle immunoassay (CMIA) tests. Upon detecting reactivity with the first test, the test was then repeated two more times using the same kit,

(LIA) test (INNO-LIA® HIV I/II Score, Immunogenetics, Germany). In accordance with the recommendations from the Centers for Disease Control and Prevention (CDC) and WHO, the presence of at least two envelope proteins (sgp120/gp41 or sgp105, gp 36) or at least one envelope protein band (sgp120/gp41 or sgp105, gp36) together with the p24 antigen band was considered to confirm the WB/LIA test results for diagnosis (1, 5, 13). The detection of bands other than those specified was considered indeterminate, and the absence of the specified bands was considered negative.

Statistical Analyses

The study analyzed the obtained data using the program SPSS (IBM Corp., 2012: IBM SPSS Statistics for Windows, Version 21.0; Armonk, NY). The study used the chi-square test as well as descriptive statistical analyses (i.e., frequencies, percentages) for the statistical evaluation of the results.

RESULTS

The retrospective evaluation requested the data from 160,194 HIV-1/-2 Ag+Ab tests, with the sera results from 4,697 patients unable to be accessed from the department for various reasons. During the evaluation period, 0.15% (n = 237) of the 155,497 sera were repeatedly reactive to the HIV-1/-2 p24 Ag+Ab. Among these 237 patients, 90.7% (n = 215) were male

Table 1. Frequency of HIV infection by years.

Years	Total Number of Tests	Recurrent HIV-1/-2 Ag+Ab Reactivity n (%)	HIV-1/-2 Confirmation Positive n (%)
January - December 2019	44.900	70 (0.15)	48 (0.1)
January - December 2020	30.974	44 (0.14)	38 (0.12)
January - December 2021	42.168	72 (0.17)	53 (0.13)
January - October 2022	38.500	51 (0.13)	36 (0.09)
Total	156.542	237 (0.15)	175 (0.11)

provided that one of the blood samples was the same as the first tested sample. A confirmatory test is performed when two of the three total tests were found to be reactive, and patients with a positive confirmatory test are informed.

As stated above, the presence of the HIV-1/-2 antibody and p24 antigen had been evaluated using the CMIA method (ARCHITECT HIV Ag/Ab Combo, Abbott Diagnostics, Abbott Park, IL, USA) on the serum samples. According to the manufacturer's instructions, the serum samples that yielded a reactive result were subjected to repeated testing using the same method. The results were obtained in terms of signal/cut-off (S/CO) units. After testing the repeated reactivity, blood was drawn a second time from the respective patient and the same CMIA test was performed again. For confirming the results of repeatedly reactive samples, the line immunoassay

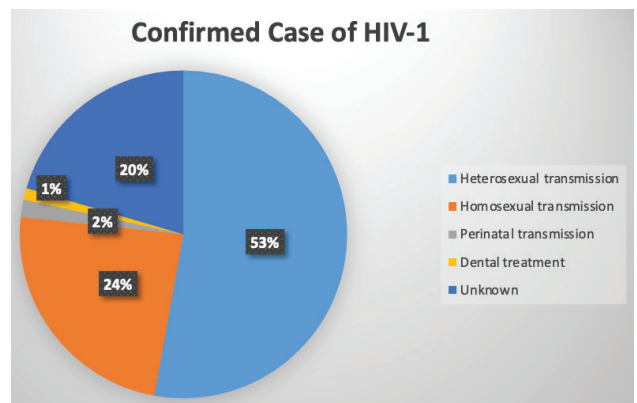


Figure 1. Possible transmission routes of HIV-1 confirmed cases.

and 9.3% ($n = 22$) were female, with a mean age of 38.7 years (Table 1, Figure 1). Six (2.5%) of the repeatedly reactive results to the anti-HIV belonged to patients under the age of 18. The confirmation test could not be performed with regard to 56 patients with repeated reactivity results for various reasons such as the patient interrupting the diagnosis/treatment process or the previous confirmation test being interrupted. As a result, the LIA test was performed on only 181 (76.3%) of the repeatedly reactive patients. The results came back positive for 175 (96.7%) and negative for six (3.3%) of these patients. LIA-positivity for HIV-1 was detected in all cases. When examining the transmission routes in the 175 cases with positive LIA results, 93 (53.1%) had had heterosexual intercourse, 42 (25.7%) had had homosexual intercourse, 3 (1.7%) had had a perinatal transmission, and 1 (0.5%) had had dental treatment. In 36 of the cases (20.5%), information about the possible transmission route could not be obtained (Figure 1). When examining the distribution of seropositive bands, the sgp120, gp41, p31, p24, and p17 bands were additionally found to be positive in 103 (58.8%) of the individuals (Table 2).

Table 2. Distribution of specific bands detected as reactive in HIV-1/-2 infected cases detected positive by LIA.

Bands	Number	Percentage (%) rate
HIV-1		
Sgp 120, gp41, p31, p24, p17	103	58.8
Sgp 120, gp41, p31, p24	41	23.5
Sgp 120, gp41, p24, p17	12	6.8
Sgp 120, gp41, p31, p17	5	2.9
Sgp 120, gp41, p24	4	2.3
Sgp 120, gp41, p31	7	4
Sgp 120, gp41	3	1.7

The age distribution of the 175 people who tested positive in the HIV confirmation tests was between 1-71 years old with an average age of 37.3 years. When considering the age distribution of patients with repeated reactivity regarding LIA

Table 3. Distribution of HIV-1/-2 positive cases according to age and gender.

Age Groups	GENDER	
	Female	Male
0-18	-	3
18-35	4	84*
36-50	11	43
>50	3	27
Total	18	157

* $p < 0.05$

positivity, HIV infection was most common in the 18-35 age group ($p < 0.05$) (Table 3). Three cases occurred where the individuals were under the age of 18, and their transmission involved the parenteral route (Table 3). Of the positively infected cases, 89.7% (157) were male and 10.2% (18) were female. When statistically analyzing the positivity rate in terms of gender, the high positivity rate in males was found to be significant ($p < 0.05$).

DISCUSSION

HIV was identified in the mid-1980s, and more than 35 years have passed since the first case was reported in Türkiye. Within the scope of WHO and UNAIDS strategies for combatting HIV, the annual number of new cases in many countries has remained stable or tended to decrease over the last decade. However, Türkiye ranks at the top of the world in terms of the annual increase in the number of new cases alongside several Eastern European, Middle Eastern, and Asian countries (6, 7). One study that statistically examined HIV infection found that, while HIV infection was under control in Western European countries (e.g., Germany, France, England, Spain, and Italy), it had grown out of control in Central and Eastern European countries (e.g., Hungary, Poland, Türkiye, and Ukraine). Among these countries, Türkiye has been shown to have the highest incidence rate of 33 per 100,000 (8).

Türkiye has had 30,293 HIV-infected persons and 2,083 AIDS cases that were positively confirmed between 1985-December 31, 2021 (9). Of these cases 81.2% have been men and 18.8% women, with most cases occurring in the 25-29 and 30-34 age groups. According to data from the Republic of Türkiye's Ministry of Health, while the number of HIV-positive people had been 1,917 in 2014, this number was reported to be 2,922 in 2021 (9), with the infection trend being observed to have increased over the years. Once COVID-19 was declared a pandemic on March 11, 2020, the early detection process for HIV infections became disrupted as a result of the interruptions in surgery and health services, social restrictions, and other reasons. Although the number of test requests to the center under study here during the COVID-19 pandemic had decreased compared to previous periods, the positivity rate was found to be similar (10, 11).

During the 2019-2022 period, the HIV prevalence was retrospectively obtained to be 0.11%, which is a similar result compared to the 2015-2018 period at the laboratory center (10). In addition, the HIV seroprevalence was found to be 0.06 for the lab center's 2006-2009 period, which shows an almost 200% increase between 2006-2022 (11). When evaluating the HIV-1/-2 laboratory test results between 2010-2018 from Elazığ Province, 495 cases were detected to have been confirmed. However, that lab observed an increase in the mean age from 2010-2015, while a decrease was observed after 2015 (12). Another important point that draws attention during the HIV epidemic in Türkiye is that the age of newly diagnosed patients has begun to gradually decrease. This is clearly seen both in the official data from the Ministry of Health and in the real-life data.

The highest rate of new diagnoses was still seen in the 25-34 age group, with the rate of newly diagnosed persons in the 35-44 age group gradually decreasing and the rate in the 20-24 age group increasing (13, 14). One study in which 173 confirmed HIV cases were reported between January 2014-December 2018 determined the highest HIV positivity rate to be found in the 26-35 age group, with the 17-25 age group being the third highest age group (15). According to the data from the Ministry of Health regarding the cases reported in 2021, the number of new diagnoses in the 25-29 age group was reported to be greater than for any other age group. Similarly, although this study found the HIV positivity rate for persons between the ages of 18-35 to be significantly higher, positivity was more common in younger groups compared to previous periods.

When comparing our study's result with the previous results from the our and other centers that had been published in Türkiye, similar results are obtained (10-12). However, due to the restraints during the COVID-19 pandemic, limited access to healthcare services, and psychological and social problems, this study is of the opinion that more HIV-infected individuals exist than have been reported. However, Türkiye is estimated to be nearing the 90-90-90 targets of UNAIDS in terms of access to treatment and treatment success, but it still falls far behind the target regarding diagnosis (16, 17). In this context, monitoring HIV infections in populations such as Istanbul that receive immigrants and have a dense and complex urban life is thought to be able to assist in taking preventive measures and improving public health in Türkiye.

Acknowledgment: We deeply appreciate Hakan Yakar and Kenan Koç for their guidance in data retrieval.

Ethics Committee Approval: This study was approved by the Clinical Research Ethics Committee of Istanbul University-Cerrahpasa, Cerrahpasa Medical Faculty (18.11.2022-539494).

Peer-review: Externally peer-reviewed.

Author Contributions: Conception/Design of Study - H.Ö.D., B.K.; Data Acquisition - H.Ö.D., B.T.K., E.K.; Performing experiments - H.Ö.D., B.T.K., E.K.; Data Analysis/Interpretation - H.Ö.D., B.T.K., E.K.; Statistical Analyses— H.Ö.D., E.K.; Drafting Manuscript - H.Ö.D., E.K.; Critical Revision of Manuscript - H.Ö.D., E.K.; Final Approval and Accountability - H.Ö.D., B.T.K., E.K., B.K.

Conflicts of Interest: The authors declare no conflict of interest.

Financial Disclosure: The authors declare that this study has received no financial support.

REFERENCES

1. WHO. Estimated number of people (all ages) living with HIV. (cited 2022 Nov 29). Available from: <https://www.who.int/data/gho/data/indicators/indicator-details/GHO/estimated-number-of-people--living-with-hiv>.
2. WHO (2021). Research & development for HIV/AIDS. (cited 2022 Nov 29). Available from: <https://www.who.int/observatories/global-observatory-on-health-research-and-development/analyses-and-syntheses/hiv-aids/priority-setting-for-research-on-hiv-aids>
3. CDC. Moving towards the UNAIDS 90-90-90 targets. (cited 2022 Nov 29). Available from: <https://www.cdc.gov/globalhealth/stories/2019/moving-towards-un aids.html>
4. HIV and AIDS Activities: HIV Testing, US Food and Drug Administration. (cited 2022 Nov 29). Available from: <https://www.fda.gov/forpatients/illness/hiv aids/default.htm>
5. WHO and HIV/AIDS. Geneva: World Health Organization. (cited 2022 Nov 29). Available from: <http://www.who.int/hiv/en>
6. T.C. Sağlık Bakanlığı Halk Sağlığı Genel Müdürlüğü. Türkiye HIV/AIDS Kontrol Programı (2019-2024) Ankara, 2019. (cited 2022 Nov 29). Available from: https://hsgm.saglik.gov.tr/depo/birimler/Bulasici-hastaliklar-db/hastaliklar/HIV-ADS/Tani-Tedavi_Rehberi/HIV_AIDS_Kontrol_Programi.pdf
7. UNAIDS. Available from: <https://aidsinfo.unaids.org/>.
8. Toluk Ö, Ercan İ, Akalın H. Seçilmiş bazı Avrupa ülkelerindeki HIV enfeksiyonu ve tüberkülozun insidanslarının istatistiksel proses kontrol yöntemi ile izlenmesi. *J Med Sci* 2021; 41(1): 36-45. [CrossRef]
9. T.C. Sağlık Bakanlığı Halk Sağlığı Genel Müdürlüğü. HIV/AIDS istatistik. (cited 2022 Nov 29). Available from: <https://hsgm.saglik.gov.tr/tr/bulasici-hastaliklar/hiv-aids/hiv-aids-liste/hiv-aids-istatistik>.
10. Dinç HÖ, Özbey D, Sirekbasan S, Gareayaghi N, Kocazeybek B. İstanbul Üniversitesi-Cerrahpaşa Cerrahpaşa Tıp Fakültesi Hastanesi 2015-2018 dönemi HIV tarama ve doğrulama verilerinin seroepidemiolojik değerlendirilmesi. *ANKEM* 2019; 33(3): 89-94
11. Yüksel P, Ziver T, İzmirli S, Aslan M, Sarıbaş S, Güngördü Z, et al. Anti-HIV-pozitif hastalarda doğrulama testi sonuçları: Beş yıllık verilerin irdelenmesi. *Klimik* 2010; 23(2): 51-4. [CrossRef]
12. Öner P, Aytaç Ö, Ferda Şenol F, Aşçı Toraman Z, Özgüler M. Elâzığ ili dokuz yıllık HIV/AIDS sonuçlarının analizi. *Türk Mikrobiyol Cemiy Derg* 2020; 50(2): 100-7.
13. Gökengin D, Oprea C, Uysal S, Begovac J. The growing HIV epidemic in Central Europe: a neglected issue? *J Virus Erad* 2016; 2(3): 156-61. [CrossRef]
14. Erdinç FŞ, Dokuzoğuz B, Ünal S, Yıldırım T, Kömür S, Fincancı M et al. Changing trends in the epidemiology of Turkey. In: 30th IUSTI Europe Conference (15-17 September 2016, Budapest, Hungary) Abstract Book. UK: International Union Against Sexually Transmitted Infections, 2016: 115-6.
15. Toptan H, Aslan FG, Karakeçe E, Aydemir Ö, Demiray T, Köroğlu M, et al. Anti-HIV ½ reaktif saptanan hastaların doğrulama test sonuçları ile birlikte değerlendirilmesi. *J Biotechnol and Strategic Health Res* 2019; 3(1): 27-32. [CrossRef]
16. Gilead, Türkiye HIV yol haritası- HIV politikalarının değerlendirilmesi ve tavsiyeler. (cited 2022 Nov 29). Available from: <https://www.gilead.com.tr/-/media/gilead-turkey/pdfs/gilead-turkey-post-covid-19-hiv-policies.pdf>
17. UNAIDS, understanding fast-track, accelerating action to end the AIDS epidemic by 2030 2015. (cited 2022 Nov 29). Available from: https://www.unaids.org/en/resources/documents/2014/JC2686_WAD2014report

Alcohol Withdrawal at Different Points in Time Distinctly Affects *Wistar* Rats' Spatial Reference Memory

Ilknur Dursun¹ , Birsen Elibol² , Ebru Haciosmanoglu³ , Ewa Jakubowska-Dogru⁴ 

¹Department of Physiology, Faculty of Medicine, Istinye University, Istanbul, Turkiye

²Department of Medical Biology, Faculty of Medicine, Istanbul Medeniyet University, Istanbul, Turkiye

³Department of Biophysics, Faculty of Medicine, Bezmialem Vakif University, Istanbul, Turkiye

⁴Department of Biological Sciences, Faculty of Science and Arts, Middle East Technical University, Ankara, Turkiye

ORCID ID: I.D. 0000-0001-7094-3336; B.E. 0000-0002-9462-0862; E.H. 0000-0001-9559-4515; E.J.D. 0000-0002-0285-2253

Cite this article as: Dursun I, Elibol B, Haciosmanoglu E, Jakubowska-Dogru E. Alcohol withdrawal at different points in time distinctly affects *wistar* rats' spatial reference memory. *Experimed* 2022; 12(3): 219-24.

ABSTRACT

Objectives: The consumption of alcohol by adults may lead to severe neurodegeneration and significant behavioral problems. An increase in the harmful effects of alcohol becomes aggravated after the development of alcohol dependence. Furthermore, the serious damage from chronic alcohol intake on the hippocampus has gained attention due to its role on learning and memory. Therefore, the study aimed to examine the retention of spatial reference memory during different points in time regarding alcohol withdrawal in *Wistar* rats.

Materials and Methods: The study has therefore administered alcohol to rats at gradually increasing doses from 4.5 to 12 g/kg/day in a binge-like manner using the intragastric intubation technique for six days followed by 24, 48, or 96 hours of alcohol withdrawal. To evaluate the effects of alcohol withdrawal, the alcohol-exposed rats have been tested regarding their spatial reference memory.

Results: An adverse effect from alcohol withdrawal on memory retention was observed in the 24-hour alcohol withdrawal group. This effect decreased at 48 hours of withdrawal, but reappeared at 96 hours.

Conclusion: The study's results suggest that alcohol withdrawal itself, even after a relatively short period of alcohol intake, may also adversely affect memory. Therefore, withdrawal therapy from alcohol should be performed in a controlled manner to protect the brain from extended alcohol withdrawal-induced spatial memory impairments.

Keywords: Alcohol withdrawal, spatial reference memory, *Wistar* rat, intragastric intubation

INTRODUCTION

Alcohol abuse is undoubtedly a major problem in human society. For several decades, chronic alcohol intake during adult life has been recognized to produce highly adverse effects on brain morphology due to severe neurodegeneration resulting in behavioral deficits. Some of these alcohol-induced adverse effects are directly related to alcohol intoxication, but some may be related with the product of the development of alcohol dependence. Alcoholics find both physical and psychological alcohol dependence to manifest itself upon withdrawing from alcohol in a form known as abstinence syndrome at different degrees of severity.

Animal studies have reported chronic alcohol consumption to damage on both the basal forebrain cholinergic system and hippocampus that structures are crucial in learning and memory (1, 2). A decrease in granule cells of the dentate gyrus, the synapses of the mossy fiber-CA3 pathway, the pyramidal neurons of the CA3 and CA1 sub-regions, and the local circuit interneurons are seen to have occurred in rodents treated with chronic alcohol consumption (3-5). Furthermore, chronic alcohol consumption has been observed to reduce the synthesis of protein in hippocampal neurons, especially in the CA3 sub-region (6). In addition, chronic alcohol treatment diminishes the intensity of the long-term potentiation (LTP) produced in the hippocampus

Corresponding Author: Birsen Elibol **E-mail:** elibolbirsen@gmail.com

Submitted: 23.10.2022 **Revision Requested:** 29.11.2022 **Last Revision Received:** 01.12.2022 **Accepted:** 08.12.2022 **Published Online:** 30.12.2022



Content of this journal is licensed under a Creative Commons Attribution-NonCommercial 4.0 International License.

(7), with a reduction in long-term depression (LTD) occurring in the hippocampal Schaffer collaterals (8).

At the behavioral level, a range of short-term memory tasks are disrupted by alcohol consumption in humans, including verbal list learning (9, 10), spatial learning, and pattern recognition (non-spatial tasks) (11, 12). Franke et al.'s study (13) used a complex elevated labyrinth and reported behavioral impairment regarding task performance in alcohol-exposed rats. As a result of chronic alcohol administration, the errors in long-term reference memory as well as the errors in trial-to-trial working memory had previously been observed as a decrease in the performance of radial maze spatial tasks (14, 15) - with working spatial memory that appearing to have been more affected than reference memory (16, 17). The effects of chronic alcohol consumption on cognitive functions and hippocampal cell loss are also exacerbated during the withdrawal phase (18, 19).

In light of these data, both chronic alcohol intake during adult life as well as alcohol withdrawal can be concluded to appear deteriorating effects on brain morphology, brain physiology, and behavior. However, some inconsistent results are found among experiments. The current studied with an animal model of human alcohol abuse to examine the effect of alcohol withdrawal at various points in time on memory retention in rats. In addition, the study aimed to dissociate the effects of early and late alcohol withdrawal with regard to testing spatial reference memory at different times in withdrawal.

MATERIALS AND METHODS

Animals

This study examined 4-month-old male *Wistar* rats provided by Ankara Serum-Production Facility (Hifzisiha, Ankara). The rats were housed at the Department of Biological Sciences at Middle East Technical University (METU). The animal room was set to a controlled 12 h light/12 h dark cycle with the temperature in the room being maintained at $22 \pm 2^\circ\text{C}$, and the tests had been conducted during the light phase of the cycle. In addition, rats had free access to laboratory chow and water throughout the applications.

The study applied to the Regulation on the Welfare and Protection of Animals Used for Experimental and Other Scientific Purposes (Official Gazette No. 28141) for all the animals during the experiments. All procedures involving animals were carried out in accordance with the ethical considerations obtained from the METU Ethics Committee (Decision No. 2009/15).

Place Learning (Acquisition Training) in the Morris Water Maze

Rodents were commonly tested for long-term spatial learning and memory using a Morris water maze (MWM). The tank was 150 cm in diameter and 60 cm high, filled with water that has been colored with food dye. The temperature of water was maintained at 23°C by an automatic heater. The animal in the MWM was recorded for measurements of distance, time, and velocity for finding the invisible platform using a computer-controlled video

system (EthoVision, Noldus Information Technology, Holland). The maze was divided into four quadrants on the computer screen through imaginary lines. A transparent Plexiglas portable platform (11×11 cm) was positioned 2 cm below the surface of the water in the center of one of the quadrants. The rats were able to swim and climb onto the platform to get out of the water. During the entire experimental period, multiple extra-maze cues remained immobile in the experimental room.

In accordance with classical MWM training (20), the study conducted six daily sessions of four trials to each animal. During the session, the rats were facing the pool wall and were placed into the MWM from one of four starting quadrants (N, S, E, W) that were pseudo-randomly selected. The trial ended once the rat climbed onto the invisible platform or spent a maximum of 60 seconds in the water. Inter-trial intervals were limited to 5 minutes. After each session, the mean latency was calculated for each rat. The learning criterium for the classical MWM training was the latency of reaching the hidden platform in 10 seconds or less. At the end of the sixth session, the rats were grouped that all three groups showed equal levels of performance at the beginning of the alcohol administration.

Alcohol Administration

To control the alcohol dosage delivered to the rats, binge drinking was applied through the intragastric intubation method. Alcohol administration started the day after the sixth session of MWM training. The alcohol was administered to the three alcohol groups (the AW24 group with a 24-hour alcohol withdrawal period ($n = 8$), the AW48 group with a 48-hour alcohol withdrawal period ($n = 7$), and the AW96 group with a 96-hour alcohol withdrawal period ($n = 8$)) by using an intragastric feeding needle (18ga, 3 in, Stoelting Co. USA) to deliver alcohol directly to each rat's stomach. The alcohol dosage was increased daily, starting with 4.5 g and going up to 12 g of alcohol per kg of body weight. The alcohol administration continued for six consecutive days. Laboratory chow and water were available *ad libitum* for these animals. The behaviors of the alcohol-treated rats were rated after each treatment in accordance with the Majchrowicz protocol (21). The maximum tolerated alcohol dosage was determined based on their ratings. To prepare the alcohol, distilled water was mixed with ethyl alcohol (99.8%, Merck) to form a 25% v/v solution. The intubation control group (IC, $n = 7$) consumed sucrose solution whose caloric value was calculated with respect to the alcohol's caloric content to observe potential intubation-related stress effects. In addition, an intact control group (C, $n = 7$) was also present that underwent no treatment whatsoever. A strict daily time schedule was followed for the rats' protocol for alcohol consumption. This schedule had allowed to the rats obtain the solutions in three equal doses at 10:00 a.m., 1:00 p.m., and 4:00 p.m. To protect the animals' stomachs, a 50 mL mixture of water and milk were given to each rat after the last alcohol dose.

Blood Alcohol Concentration (BAC)

A separate group of rats received alcohol treatment but no behavioral testing ($n = 3$) and was used for measuring BAC. Under

ether anesthesia, blood samples from the alcohol-consumed animals were collected in tubes containing EDTA through an intracardiac puncture. The blood was taken 3 h after the last intragastric intubation on the sixth day of alcohol administration (22). At room temperature, a Biolabo alcohol assay was performed to determine the BAC of the serum samples obtained by placing them in a centrifuge at 1,000 rpm for 10 minutes.

Probe Trials: A Memory Retention Test

The study used the probe trial to gain insight into the strength of rats' acquired responses as well as indirectly in regard to their spatial memory. Therefore, a 60-second probe trial was performed after completion of alcohol consumption. During the probe trial, the platform was removed from the maze, and a circle with a 40 cm diameter (annulus 40, A40) was set up on the computer monitor so it surrounded the original platform site. The total durations of time the rats spent in each quadrant as well as in the A40 circle were recorded. The probe was applied based on the groups 24, 48, or 96 hrs after the last dosage of alcohol.

Statistical Analyses

Using all variables, group means were calculated along with the standard errors for the mean (SEM). The study also used the statistical package program SPSS to conduct the repeated measures ANOVA, with the treatment being the independent variable and the sessions/trials being the repeated measures. One-way ANOVA and the post-hoc Tukey test were performed to analyze the probe data.

RESULTS

Determining BAC

The alcohol-administered rats were measured as having a BAC of 605.67 ± 36 mg/dL (range between 569-641 mg/dL) 3 hours after the last administration of alcohol (12 g/kg/day).

Classical MWM Training

According to two-way repeated measure ANOVA, the day effect ($F_{(5, 120)} = 62.70, p \leq 0.001$) was found significant regarding escape latency in the water maze. During the whole training

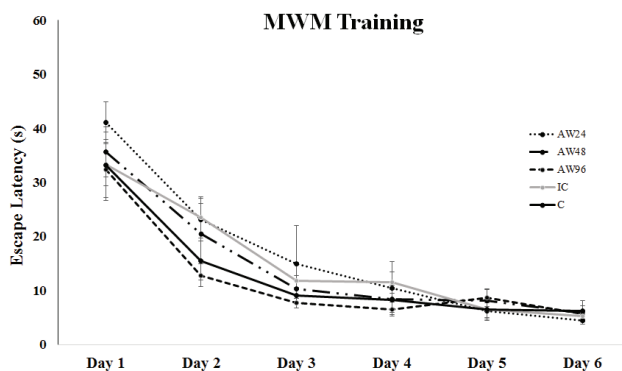


Figure 1. Comparison of the learning performance of rats by mean swim latency to reach hidden platform calculated for six days of MWM training, Error bars denote SEM.

period, the latency to get out of the water by climbing onto the invisible platform decreased for all animals. No differences were observed among the groups ($F_{(15, 120)} = 0.87, p = 0.60$). The learning criterium was achieved by all rats on the fourth day of the MWM learning period (Figure 1).

Probe Trials After Alcohol Administration

Animal performance was assessed based on the percentage of time spent in the platform quadrant. According to the one-way ANOVA, a significant difference among groups was obtained regarding the percentage of time spent in the platform quadrant ($F_{(4, 34)} = 8.135, p < 0.001$). In addition, the percentage of time spent in the platform quadrant for the AW24 and AW96 groups were significantly lower according to Tukey's test ($p = 0.024$ and $p = 0.045$, respectively) compared to the IC group. The AW48 group performed significantly better than the other AW groups ($p = 0.001$), approaching the performance of the control groups (Figure 2).

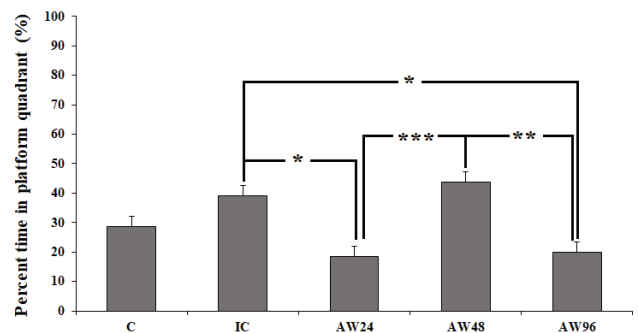


Figure 2. Percent time which was spent in the platform quadrant on the 60-s probe trials in each treatment group independently. Error bars denote SEM. The degree of significance was denoted as *for $p \leq 0.05$, ** for $p \leq 0.01$, *** for $p \leq 0.001$.

As seen in Figure 3, a significant change in the amount of time spent in the A40 circle occurred among the groups ($F_{(4, 34)} = 3.885, p = 0.012$). Compared to the control groups, the decrease in time spent in A40 was not significant for the AW24 and AW96 groups

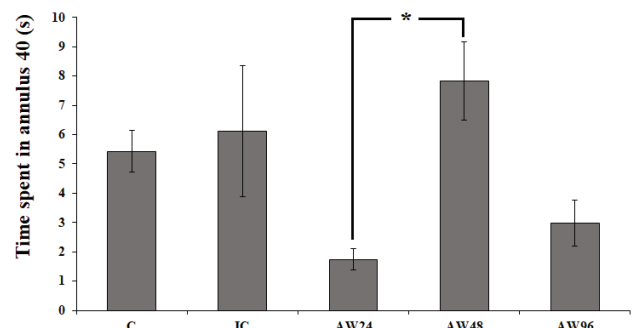


Figure 3. Time in A40 \pm SEM calculated for each treatment group independently. The degree of significance was denoted as *for $p \leq 0.05$.

according to the post-hoc comparison tests (Figure 3). However, the AW48 group was observed to have spent significantly more time than the AW24 ($p = 0.014$) and AW96 ($p = 0.063$) groups in the platform quadrant.

As seen in Figure 4, the ratio of the time spent in the platform quadrant (NE) compared to the time spent in the opposite quadrant (SW) varied significantly among the groups ($F_{(4, 34)} = 5.035, p = 0.003$), with the ratio being highest in the AW48 group ($p = 0.018$ for control; $p = 0.008$ for AW24; $p = 0.004$ for AW96).

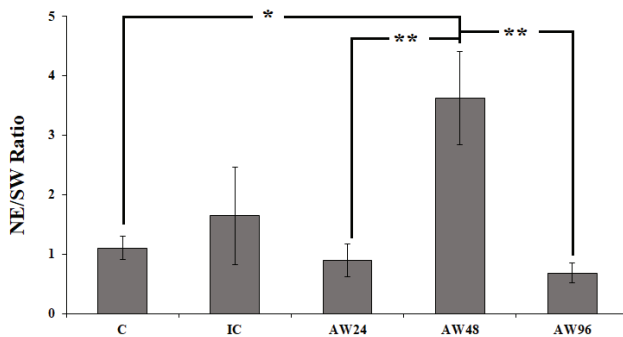


Figure 4. Total time spent ratios in the platform quadrant (NE) to the opposite quadrant (SW) for each treatment group independently. The degree of significance was denoted as *for $p \leq 0.05$ and ** for $p \leq 0.01$.

DISCUSSION

The literature has a few studies that have examined the effects of alcohol withdrawal on memory retention over different withdrawal time periods. Hence, the present study has been designed to examine whether alcohol withdrawal affects on memory retention and retrieval. According to the application of the experimental protocol (up to 12 mg/kg alcohol administration), exposing rats to binge-like alcohol dosages for 6 days produced an average BAC of 605.67 mg/dL. The memory retention was disrupted 24 hours after the last alcohol consumption, which may be indicative of an early withdrawal symptom. Interestingly, the memory performance was restored 48 hours after the last alcohol consumption, reaching the control levels. However, alcohol withdrawal dramatically deteriorated the memory performance of rats during the 96th hour of withdrawal.

The late effect of alcohol withdrawal has also been noted in previous studies. For example, researchers found remarkable alterations in memory retention tasks between alcohol and control groups when retraining was conducted a year after the learning acquisition time (16). Chronic alcohol intake has also been found to adversely affect the working spatial memory in adults more than their reference spatial memory when performing hippocampus-dependent cognitive tasks (13-15, 23). In addition, mild effects are seen to have occurred on spatial working memory after short-term alcohol intoxication

(26 days of a liquid diet containing alcohol followed by 17 days of no alcohol) (24). According to another study, all alcohol-dependent patients showed impaired free memory recall on their first day of withdrawal over a battery of behavioral tests. However, their verbal memory ameliorated on the seventh day of withdrawal, then deteriorated again on the 14th day of withdrawal (25). Accordingly, the study suggested different brain regions engaged in different memory functions to be affected at different time periods by alcohol withdrawal. The prefrontal cortex functions have been postulated as being primarily required for short-term memory while the medial temporal lobe functions are required for long-term memory. The frontal lobe is also believed to be more affected by early alcohol withdrawal than the medial temporal lobe (25, 26).

A correlation also exists between alcohol withdrawal and dysregulation of stress hormones. The level of corticosterone in rats after chronic alcohol consumption changes 24 hours after withdrawal. Animal studies have confirmed the acute rise in adrenocorticotrophic hormone (ACTH) and glucocorticoids after drinking alcohol in nonhuman primates and rodents. Neuroendocrine tolerance toward alcohol is thought to result from repeated intoxication and withdrawal cycles (27, 28). Therefore, the current study found the differences in the memory performance in the different withdrawal periods to perhaps also be related to the different levels of stress hormones.

In addition, the lack of difference at the 48-hour alcohol withdrawal group is related to the hypothesis that a compensatory process may mitigate alcohol's potential damaging effects on the brain. For instance, alcohol-exposed rats may compensate neuronal death-related functional deficits by adapting their synaptic structure to moderate alcohol doses over a relatively long period of time. This notion has been supported by the ratio of mossy fibers-CA3 synapses being shown to be maintained and the percentage of mossy fibers plasmalemma occupied by synapses to also increase while hippocampal CA3 pyramidal and granule cells gradually are lost after consuming alcohol for 6-12 months (5, 29). Interestingly, the results from these previous studies revealed the reduced formation of new contacts, suggesting a compensatory process. Moreover, the compensatory process was seen to have broken down in rats when they consumed alcohol in a liquid diet over 18 months. Another possibility is that moderate alcohol consumption might result in increased adult neurogenesis (30). Hippocampal dentate gyrus (DG) and forebrain subventricular zone (SVZ) are two important regions of the brain that undergo adult neurogenesis. Hippocampal neurogenesis also appears to be important in learning and memory development (31). While unusual adult hippocampal neurogenesis may produce negative effects on brain circuitry in a healthy brain, this may be advantageous in the alcoholic brain.

In summary, different mechanisms are suggested to be active at different points in time with regard to alcohol withdrawal. Therefore, designing a treatment for alcohol abuse and

disorders and time-dependent treatment strategies should be included in order to prevent time-dependent damages to the alcohol-addicted brain.

Ethics Committee Approval: Ethical approval was obtained from the ethical committee of the Middle East Technical University (Decision No. 2009/15).

Peer-review: Externally peer-reviewed.

Author Contributions: Conception/Design of Study – I.D., B.E., E.J.D.; Data Acquisition – I.D., E.H., B.E.; Data Analysis/Interpretation – I.D., B.E., E.J.D.; Drafting Manuscript – I.D., B.E.; Critical Revision of Manuscript – I.D., B.E., E.J.D.; Final Approval and Accountability – I.D., B.E., E.J.D.

Conflicts of Interest: The authors declare no conflict of interest.

Financial Disclosure: The authors declare that this study has received no financial support.

REFERENCES

- Connor DJ, Langlais PJ, Thal LJ. Behavioral impairments after lesions of the nucleus basalis by ibotenic acid and quisqualic acid. *Brain Res* 1991; 555(1): 84-90. [CrossRef]
- Dunnet SB, Whishaw IQ, Jones GH, Bunch ST. Behavioral, biochemical, and histochemical effects of different neurotoxic aminoacids injected into nucleus basalis magnocellularis of rats. *Neurosci* 1987; 20(2): 653-69. [CrossRef]
- Bengoechea O, Gonzalo LM. Effects of alcoholization on the rat hippocampus. *Neurosci Lett* 1991; 123(1): 112-4. [CrossRef]
- Beracochea D, Lescaudron L, Verna A, Jaffard R. Neuroanatomical effects of chronic ethanol consumption on dorsomedial and anterior thalamic nuclei and on substantia innominata in mice. *Neurosci Lett* 1987; 73(1): 81-4. [CrossRef]
- Cadete-Leite A, Tavares MA, Pacheco MM, Volk B, Paula-Barbosa MM. Hippocampal mossy fiber-CA3 synapses after chronic alcohol consumption and withdrawal. *Alcohol* 1989; 6(4): 303-10. [CrossRef]
- García-Moreno LM, Conejo NM, Pardo HG, Gómez M, Martín FR, Alonso MJ, et al. Hippocampal AgNOR activity after chronic alcohol consumption and alcohol deprivation in rats. *Physiol Behav* 2001; 72(1-2): 115-21. [CrossRef]
- Peris J, Eppler B, Hu M, Walker DW, Hunter BE, Mason K, et al. Effects of chronic ethanol exposure on GABA receptors and GABAB receptor modulation of 3H-GABA release in the hippocampus. *Alcohol Clin Exp Res* 1997; 21(6): 1047-52. [CrossRef]
- Thinschmidt JS, Walker DW, King MA. Chronic ethanol treatment reduces the magnitude of hippocampal LTD in the adult rat. *Synapse* 2003; 48(4): 189-97. [CrossRef]
- Acheson S, Stein R, Swartzwelder HS. Impairment of semantic and figural memory by acute ethanol: age-dependent effects. *Alcohol Clin Exp Res* 1998; 22(7): 1437-42. [CrossRef]
- Lister RG, Gorenstein C, Fisher-Flowers D, Weingartner HJ, Eckardt MJ. Dissociation of the acute effects of alcohol on implicit and explicit memory processes. *Neuropsychologia* 1991; 29(12): 1205-12. [CrossRef]
- Bowden SC, McCarter RJ. Spatial memory in alcohol-dependent subjects: using a push-button maze to test the principle of equiavailability. *Brain Cogn* 1993; 22(1): 51-62. [CrossRef]
- Weissenborn R, Duka T. Acute alcohol effects on cognitive function in social drinkers: Their relationship to drinking habits. *Psychopharmacol* 2003; 165(3): 306-12. [CrossRef]
- Franke H, Kittner H, Berger P, Wirkner K, Schramek J. The reaction of astrocytes and neurons in the hippocampus of adult rats during chronic ethanol treatment and correlations to behavioral impairments. *Alcohol* 1997; 14(5): 445-54. [CrossRef]
- Arendt T. Impairment in memory function and neurodegenerative changes in the cholinergic basal forebrain system induced by chronic intake of ethanol. *J Neural Transm Suppl* 1994; 44: 173-87. [CrossRef]
- Hodges H, Allen Y, Sinden J, Mitchell SN, Arendt T, Lantos PL, et al. The effects of cholinergic drugs and cholinergic-rich fetal neural transplants on alcohol-induced deficits in radial maze performance in rats. *Behav Brain Res* 1991; 43(1): 7-28. [CrossRef]
- Pereira SR, Menezes GA, Franco GC, Costa AE, Ribeiro AM. Chronic ethanol consumption impairs spatial remote memory in rats but does not affect cortical cholinergic parameters. *Pharmacol Biochem Behav* 1998; 60(2): 305-11. [CrossRef]
- White AM, Matthews DB, Best PJ. Ethanol, memory, and hippocampal function: A review of recent findings. *Hippocampus* 2000; 10(1): 88-93. [CrossRef]
- Paula-Barbosa MM, Brandao F, Madeira MD, Cadete-Leite A. Structural changes in the hippocampal formation after long-term alcohol consumption and withdrawal in the rat. *Addiction* 1993; 88(2): 237-47. [CrossRef]
- Lukoyanov NV, Pereira PA, Paula-Barbosa MM, Cadete-Leite A. Nerve growth factor improves spatial learning and restores hippocampal cholinergic fibers in rats withdrawn from chronic treatment with ethanol. *Exp Brain Res* 2003; 148(1): 88-94. [CrossRef]
- Morris R. Developments of a water-maze procedure for studying spatial learning in the rat. *J Neurosci Methods* 1984; 11: 47-60. [CrossRef]
- Majchrowicz E. Induction of physical dependence upon ethanol and the associated behavioral changes in rats. *Psychopharmacologia* 1975; 43(3): 245-54. [CrossRef]
- Tran TD, Cronise K, Marino MD, Jenkins WJ, Kelly SJ. Critical periods for the effects of alcohol exposure on brain weight, body weight, activity and investigation. *Behav Brain Res* 2000; 116: 99-110 [CrossRef]
- White AM, Simson PE, Best PJ. Comparison between the effects of ethanol and diazepam on spatial working memory in the rat. *Psychopharmacology* 1997; 133(3): 256-61. [CrossRef]
- Santucci AC, Mercado M, Bettica A, Cortes C, York D, Moody E. Residual behavioral and neuroanatomical effects of short-term chronic ethanol consumption in rats. *Brain Res Cogn Brain Res* 2004; 20(3): 449-46. [CrossRef]
- Seifert J, Seeland I, Borsutzky M, Passie T, Rollnik JD, Wiese B, et al. Effects of acute alcohol withdrawal on memory performance in alcohol-dependent patients: a pilot study. *Addict Biol* 2003; 8(1): 75-80. [CrossRef]
- Smith EE, Jonides J. Storage and executive processes in the frontal lobes. *Science* 1999; 283(5408): 1657-61. [CrossRef]
- Finn DA, Helms ML, Nipper MA, Cohen A, Jensen JP, Devaud LL. Sex differences in the synergistic effect of prior binge drinking and traumatic stress on subsequent ethanol intake and neurochemical responses in adult C57BL/6J mice. *Alcohol* 2018; 71: 33-45. [CrossRef]
- Flores-Bonilla A, Richardson HN. Sex Differences in the neurobiology of alcohol use disorder. *Alcohol Res* 2020; 40(2): 04. [CrossRef]
- Lukoyanov NV, Brandão F, Cadete-Leite AA, Madeira MD, Paula-Barbosa MM. Synaptic reorganization in the hippocampal formation of alcohol-fed rats may compensate for functional deficits related to neuronal loss. *Alcohol* 2000; 20(2): 139-48. [CrossRef]

30. Aberg E, Hofstetter CP, Olson L, Brene S. Moderate ethanol consumption increases hippocampal cell proliferation and neurogenesis in the adult mouse. *Int J Neuropsychopharmacol* 2005; 8(4): 557-67. [\[CrossRef\]](#)
31. Shors TJ, Miesegaes G, Beylin A, Zhao M, Rydel T, Gould E. Neurogenesis in the adult is involved in the formation of trace memories. *Nature* 2001; 410(6826): 372-6. [\[CrossRef\]](#)

Increased Perforin- and IL-21-Expressing NK Cells in Patients with Early-Stage Chronic Lymphocytic Leukemia

Fatih Akboga^{1,2} , Fehmi Hindilerden³ , Emine Gulturk³ , Ipek Yönel-Hindilerden⁴ , Abdullah Yilmaz¹ , Gunnur Deniz¹ , Metin Yusuf Gelmez¹ 

¹Department of Immunology, Aziz Sançar Institute of Experimental Medicine, Istanbul University, Istanbul, Türkiye

²Institute of Graduate Studies in Health Science, Istanbul University, Istanbul, Türkiye

³Hematology Clinic, Istanbul Bakirkoy Sadi Konuk Training and Research Hospital, Istanbul, Türkiye

⁴Department of Internal Medicine, Division of Hematology, Istanbul Medical Faculty, Istanbul University, Istanbul, Türkiye

ORCID ID: F.A. 0000-0002-0202-3244; F.H. 0000-0002-6297-9555; E.G. 0000-0003-2836-6162; İ.Y.H. 0000-0003-1353-2367; A.Y. 0000-0002-3003-9956; G.D. 0000-0002-0721-6213; M.Y.G. 0000-0002-5279-0855

Cite this article as: Akboga F, Hindilerden F, Gulturk E, Yönel-Hindilerden I, Yilmaz A, Deniz G, Gelmez MY. Increased perforin- and IL-21-expressing NK cells in patients with early-stage chronic lymphocytic leukemia. *Experimed* 2022; 12(3): 225-31.

ABSTRACT

Objective: CD5⁺CD19⁺ cells have a low proliferation capacity and elevated expression of anti-apoptotic protein BCL-2, mostly in the G0/G1 cell phase and accumulate in the pathogenesis of chronic lymphocytic leukemia (CLL). Natural killer (NK) cells have the ability to kill the intracellular pathogen-infected or cancer cells and secrete cytotoxic enzymes. This study evaluated the frequency, expression of cytotoxic enzymes, and intracellular cytokine levels of NK cells in CLL patients.

Materials and Methods: In this study, peripheral blood mononuclear cells were isolated from peripheral blood samples of CLL patients (n=29) and healthy controls (n=16) by density gradient centrifugation method. The frequency of the total NK cells and the intracellular levels of perforin, granzyme, interferon (IFN)- γ , interleukin (IL)-21, IL-4 and IL-17 in NK cells were investigated.

Results: Elevated total NK cell frequency were found in the CLL patients compared to the healthy controls, and negatively correlated with CD5⁺CD19⁺ malign B cell frequency. Increased perforin expression was observed in patients' total NK cells. Additionally, increased levels of IL-17 and IL-21 in total NK cell of CLL patients were obtained compared to healthy subjects.

Conclusion: The findings suggest that in the early stage of CLL, increased total NK cell frequency, and elevated perforin and IL-21 levels in NK cells might have a protective impact against the progression of the disease for CLL patients.

Keywords: Chronic lymphocytic leukemia, cytokines, natural killer cells, perforin

INTRODUCTION

The incidence of chronic lymphocytic leukemia (CLL) is high in elderly individuals, and CLL is the most common type of leukemia in Western countries (1). CLL involves an increase of CD5⁺CD19⁺ cells, which have a low proliferation capacity, increased expression of BCL-2, and accumulated in the bone marrow and peripheral blood (1, 2). Most patients are 60-65 years at the time of first diagnosed, with only 10-15% of patients being under 55 years of age (3). The

clinical outcome of CLL is variable, and treatment is delayed until the disease progresses (4). CD38 expression (30% \geq CD38 positive and 30% < CD38 negative) identifies two subgroups of CLL patients with different clinical outcomes, and CD38 positive patients have poor clinical outcome (5). Recently Rai and Binet staging systems have been used to predict progression and develop an appropriate treatment plan (4).

Natural killer (NK) cells are large granular lymphocytes and, despite being lymphoid in origin, are a member of the

Corresponding Author: Metin Yusuf Gelmez **E-mail:** yusufmetin@istanbul.edu.tr

Submitted: 20.10.2022 **Revision Requested:** 28.11.2022 **Last Revision Received:** 02.12.2022 **Accepted:** 09.12.2022 **Published Online:** 30.12.2022



Content of this journal is licensed under a Creative Commons Attribution-NonCommercial 4.0 International License.

innate immune system (6). CD3 is not expressed in NK cells, while CD16 and CD56 are expressed on the surface of NK cells (6, 7). The cells that do not express major histocompatibility complex (MHC) class I are recognized by NK cells, and cytotoxic enzymes such as perforin and granzyme are secreted by NK cells in order to target cell lysis (8). Additionally, NK cells secrete various cytokines to regulate immune responses (6) and have an important role in eliminating virus-infected cells and cancer cells. The studies have shown that individuals with low NK cell function have an increased risk of cancer early in life and that NK cells are critical in preventing tumor metastasis (9).

In this study, the total NK cell frequency and the intracellular expression of perforin, granzyme, and IFN- γ , IL-4, IL-17, IL-21 levels in NK cells were analyzed to evaluate the role of NK cells in CLL.

MATERIALS AND METHODS

Patient Groups

The study was evaluated with 9 female and 20 male CLL patients being monitored in the Hematology Department of the

Istanbul Bakirkoy Sadi Konuk Training and Research Hospital. All patients were chosen according to the International Workshop on Chronic Lymphocytic Leukemia (iwCLL) 2008 diagnostic criteria who have a lymphocyte count greater than $5 \times 10^3/\text{mm}^3$. According to the Rai/Binet staging system, CD5 and CD19 expression levels were also detected in all patients who were at an early stage and had not received any treatment yet (Table 1). The study also included 4 females and 12 males as healthy controls, matched to the patients' age and sex, without a history of cancer, autoimmunity, infection, immunosuppressive medication, or smoking. This study was approved by the Istanbul University Faculty of Medicine Local Committee with the decision number; 587348 and dated September 24, 2021.

Cell Preparation and Sorting

Peripheral blood mononuclear cells (PBMCs) were isolated using the Ficoll-Hypaque solution from peripheral blood samples obtained from the patient and healthy subjects. PBMCs were washed in a phosphate buffered saline (PBS) solution twice and suspended in the RPMI 1640 medium (Gibco, USA) which was consisted of L-glutamine (Gibco, USA) and anti-mycotic/antibiotic (Gibco USA; at respective concentrations of 10% and

Table 1. Clinical data of the patients.

	CLL	Healthy Controls	
N	29	16	
Male (n)	20	12	
Female (n)	9	4	
Age (Mean (min - max))	65 (49 - 76)	58 (50 - 78)	
WBC ($10^6/\text{mL}$) (mean (min - max))	40.34 (13 - 147)	7.18 (5.2 - 9.3)	
Lymphocytes ($10^6/\text{mL}$) (mean (min - max))	34.78 (6.9 - 140)	2.90 (2.1 - 3.6)	
CD5⁺CD19⁺% Mean (min - max)	89.10 (14.7 - 99.8)	-	
Binet Stage	A	23	-
	B	6	-
	C	-	-
Rai Stage	0	17	-
	1	5	-
	2	5	-
	3	2	-
	4	-	-
CD38	Positive	10	-
	Negative	19	-
Infection	No	No	
Treatment	No	No	

1%), PBMCs (5×10^6 cells/mL) were labeled with the anti-CD19 APC (BD-Biosciences, USA) and incubated for 20 minutes in the dark at room temperature. Lymphocytes were separated by gating on SSC versus FSC plot, and then CD19 negative cells in lymphocyte population were gated on SSC versus CD19 plot. CD19 negative cell population were sorted using the BD FACSAria II cell sorter (BD-Biosciences, USA). Sorted cells were labeled with anti-CD3 FITC, -CD56 PE and -CD16 PE monoclonal antibodies to detect the CD3 and CD19 negative cells. (All antibodies from BD-Biosciences, USA). After incubation, samples were analyzed by Novocyte flow cytometry (Agilent, USA), and CD3⁺CD19⁻ cell population considered as NK cells.

Detection of Intracellular Cytokines and Cytotoxic Enzymes in Total NK Cells

Sorted cells (1×10^6 cells) were stimulated using the cell activation cocktail with Brefeldin A (Biolegend, USA) for 5 hours. Cells were then washed and labeled with anti-CD3 FITC (BD-Biosciences, USA). Fixation and permeabilization were performed using the Fix-Perm kit according to manufacturer's instructions (Nordic MUBio, Netherlands), and the anti-IFN- γ BV510, -IL-4 PECY7, -IL-17 AlxF700, -IL-21 PE, -perforin BV510, and -granzyme AlxF700 monoclonal antibodies were added (All antibodies from BD-Biosciences, USA). Cells were then washed and analyzed by using the NovoCyte flow cytometry (Agilent, USA).

Statistical Analyses

Mann-Whitney U test was performed for the analysis of the data. Pearson's correlation test was used for the correlation analysis. GraphPad 5.3 program was used for statistical analysis and graphical designs, with $p < 0.05$ being considered statistically significant.

RESULTS

Higher Total NK Cells in CLL patients

The lymphocyte population consisted of CD3⁺ T, CD19⁺ B, NKT, and NK cells. The cells that did not express CD3 and CD19 considered as NK cells in order to evaluate NK cell functions in CLL patients in this study. To confirm this, CD19 negative cells were sorted from PBMCs and stained with anti-CD16 and -CD56. The purity of CD3⁺CD56⁺CD16⁺ NK cells were 93-96% (Figure 1A-B).

The total NK cell frequency was higher in CLL patients compared with healthy controls ($p = 0.0006$; Figure 1C). No significant differences were obtained in NK cell frequency in the patient groups according to CD38 status and Rai/Binet stages. However, the total NK cell frequency in CLL patients was negatively correlated to the CD5⁺CD19⁺ malign B cell frequency ($p = 0.03$, $R = -0.414$).

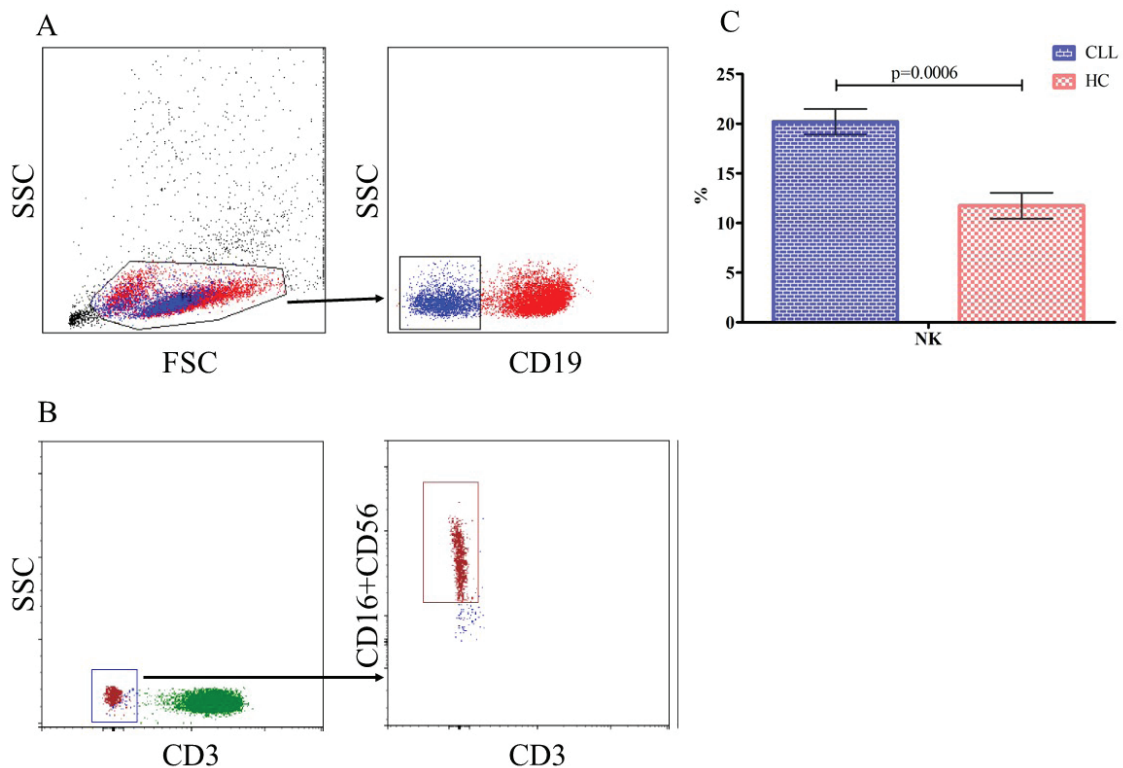


Figure 1. Gating strategy of total NK cells. CD19⁻ cells were gated in lymphocyte gate and sorted (A). NK cell purity was analyzed according to CD16 and CD56 expression of CD3⁺ cell population of sorting cells (B). Total NK cells in CLL patients (n=29) and healthy controls (n=16) was showed (C). NK: Natural killer, CLL: Chronic lymphocytic leukemia, HC: Healthy control.

Elevated Perforin Expression of NK Cells in CLL Patients

To evaluate the cytotoxic properties of the NK cells, intracellular perforin and granzyme expressions were analyzed using by flow cytometry (Figure 2A). Compared to the healthy controls, high perforin expressions were observed in NK cells of CLL patients ($p < 0.0001$), while granzyme expression was unchanged (Figure 2B). No significant differences were seen on the cytotoxic properties of NK cells in the patient groups in terms of CD38 expression and Rai/Binet stages. However, a positive correlation was found between the CD5⁺CD19⁺ malign B cell frequency and perforin expression of NK cells ($p = 0.03$, $R = 0.403$; Figure 2C).

Increased Intracellular IL-17 and IL-21 Levels in NK Cells of CLL Patients

When the intracellular cytokine levels of NK cells were analyzed, no significant difference was found between the IFN- γ and IL-4 levels of NK cells in patients and healthy controls (Figure 3A-B). On the other hand, IL-17 and IL-21 levels in total NK cells of patients were higher than healthy controls ($p < 0.0001$ and $p < 0.0001$, respectively; Figure 3B). No significant differences were found in the IFN- γ , IL-4, IL-17 and IL-21 levels of NK cells in the patient groups according to CD38 expression and Rai/Binet stages. IL-17 levels of NK cells were positively correlated with white blood cell count, lymphocyte count, and the CD5⁺CD19⁺ malign B cell frequency ($p = 0.04$, $R = 0.428$; $p = 0.02$, $R = 0.475$; $p = 0.05$, $R = 0.313$, respectively; Figure 3C).

DISCUSSION

Cancer cells can escape from adaptive immune responses through the various mechanisms they have developed (10). In particular, the most well-known mechanism is to reduce the MHC class I expression on their surface (10). NK cells recognize and lyse the non-MHC I expressing target cells. Because of these features, NK cells have a primary role in anti-tumor responses (6). Therefore, NK cell-based cancer immunotherapies have recently been designed (9).

The incidence of CLL is high in the northern hemisphere (11), with CLL patients having an accumulation of malignant cells of the CD5⁺CD19⁺CD23⁺ phenotype (12). Unlike other types of leukemia, most patients with CLL are only monitored clinically without any treatment (13). T cell frequency, especially the CD8⁺ T cell frequency, is known to increase in patients with CLL. However, data regarding the disease development and progression of increased T cell levels have been contradictory (14). Many studies regarding T cells and their role in CLL are present, but studies on NK cells and their role in CLL pathogenesis are few and conflicting (9).

In a study focused on small lymphocytic lymphoma (SLL) and CLL patients and reported the NK cell counts to have increase in CLL patients and be positively correlated with CD19 cell counts (15). On the other hand, it was detected that NK cell frequency were increased and had a negative correlation

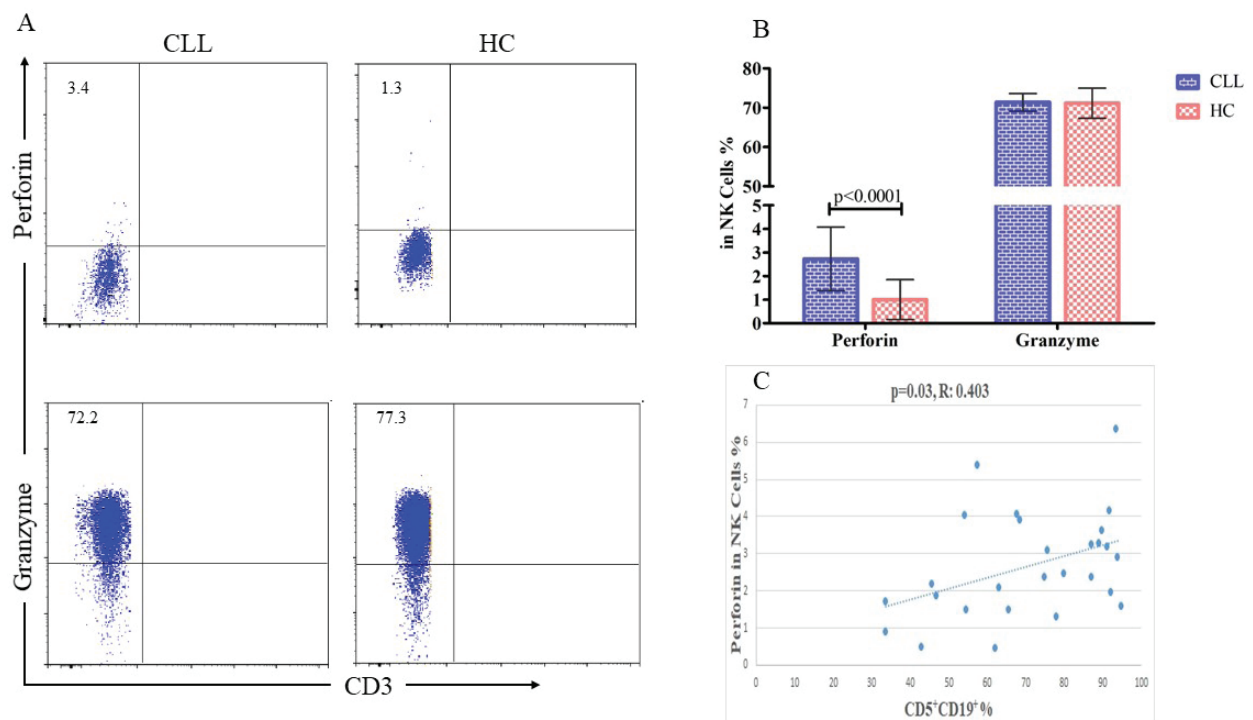


Figure 2. Representative dot-plots of perforin and granzyme expression on total NK cells in CLL patients and healthy controls (A). Perforin and granzyme expression on total NK cells in patients and healthy controls (B). Correlation graphs between perforin expression and CD5⁺CD19⁺ cell frequency (C). NK: Natural killer, CLL: Chronic lymphocytic leukemia, HC: Healthy control.

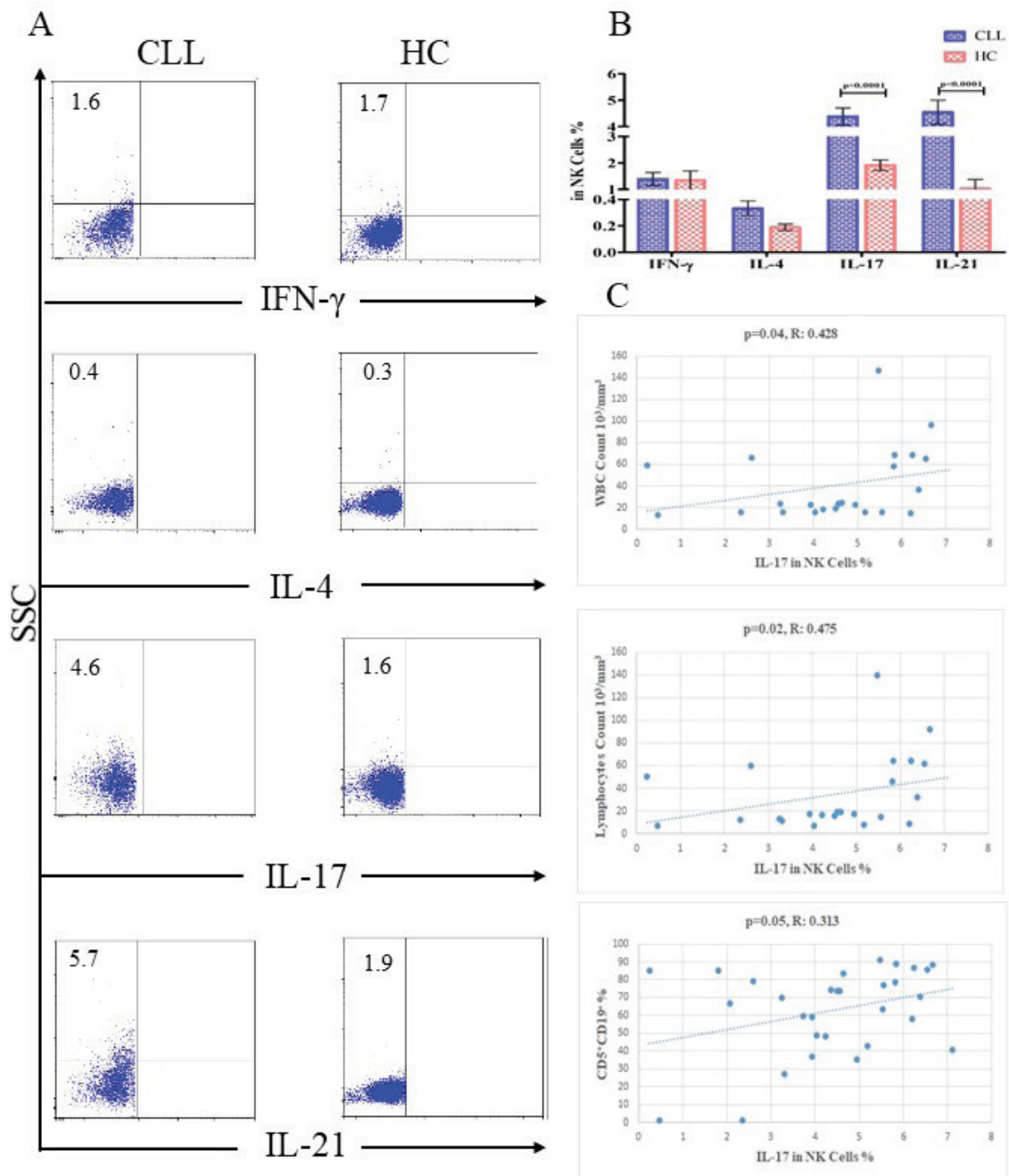


Figure 3. Representative flow graphs of IFN- γ , IL-4, IL-17 and IL-21 levels of total NK cells in patients and healthy controls (A). The statistical graph represents percentages of IFN- γ , IL-4, IL-17 and IL-21 levels of total NK cells in patients and healthy controls (B). Correlation graphs between IL-17 expression and white blood cells (WBS), lymphocytes, CD5⁺CD19⁺ cells (C). NK: Natural killer, CLL: Chronic lymphocytic leukemia, HC: Healthy control.

with the CD5⁺CD19⁺ malign B cell frequency in untreated CLL patients with the early stage. This difference might be due to the evaluation of total NK frequency in lymphocytes after CD19⁺ cells were excluded in our study. For instance, NK cell frequency was evaluated within total PBMC in MacFarlane et al. study, and NK cell dysfunction was obtained in CLL patients

(15). On the other hand, it can be thought that high NK cell frequency might be protective against the malignant B cells or disease progression.

The tumor microenvironment is very important for malignant B cells in CLL, as with many cancer types (16). Various cytokines such as IL-6 are known to be important for this tumor

environment (16), and many immune system cells, especially Th17, are known to secrete IL-17, which in turn is known to stimulate IL-6 (17, 18). Recent studies have shown CLL patients to have increased sera and plasma IL-17 levels, especially patients in the early stage (16, 19). In addition, the Th17 cell frequency has been found to be higher in patients compared to healthy controls (20). NK cells are known to mainly secrete pro-inflammatory cytokines such as IFN- γ , but recent studies have indicated IL-17 to also be secreted by NK cells (21, 22). The current study observed IL-17 expression in the total NK cell to be higher in CLL patients. According to the study's data, NK cells might contribute to possible IL-17 increases in the sera or plasma of CLL patients. Additionally, the study found a positive correlation for IL-17 expression in the total NK cell with the CD5⁺CD19⁺ cell frequency. Previous studies have shown CLL patients to have higher IL-6 levels compared to healthy subjects, as well as higher IL-6 levels to be correlated with adverse disease features and low survival (16, 23). Meanwhile, recent studies have indicated the IL-17/IL-6 axis to have an important role in CLL and to be possible therapeutic targets. When considering that IL-17 triggers IL-6 production, IL-17 expression in NK cells might be associated with a poor clinical outcome.

Recent studies have also indicated that IL-21 to be able to affect the gene expression profile of malign B cells in CLL (24). Additionally, IL-15 has been shown to increase the survival and proliferation of CLL cells, with IL-21 having the opposite effect (25). IL-21 expressing total NK cells of CLL patients were increased in our study. Furthermore, IL-21 is known to increase perforin expression, cytotoxicity, and anti-tumoral responses in NK cells (26). Consistent with this finding, the current study showed higher perforin and IL-21 levels in total NK cells. Our findings suggest that IL-21 levels of NK cells might have an autologous effect and to trigger the expression of perforin in these cells. However, these needs to be confirmed through *in vitro* studies.

NK cells are an attractive source for new immunotherapeutic strategies, including chimeric antigen receptor (CAR) therapy (9). Therefore, the role of NK cells in CLL is very important. Our findings suggest the total NK cell frequency and increased perforin and IL-21 levels of these cells might have a protective effect against the progression of early stage of CLL patients. In addition, the negative correlation observed between the malign CD5⁺CD19⁺ cell and total NK cell frequency seems to support this hypothesis. However, analyzing NK cell numbers and functions in advanced or treated CLL patients will allow us to better understand the role of NK cells have in the pathogenesis of CLL.

Ethics Committee Approval: This study was approved by the Clinical Research Ethics Committee of Istanbul University Medical Faculty (04/11/2021-587348).

Peer-review: Externally peer-reviewed.

Author Contributions: Conception/Design of Study - M.Y.G., G.D., F.A., F.H.; Data Acquisition - M.Y.G., G.D., F.A., F.H.; Performing experiments - M.Y.G., G.D., F.A., F.H.; Data Analysis/Interpretation - M.Y.G., G.D., F.A., F.H.; Statistical Analyses - M.Y.G., G.D., F.A., F.H.; Drafting Manuscript - M.Y.G., G.D., F.A., F.H.; Critical Revision of Manuscript - M.Y.G., G.D., F.A., F.H.; Final Approval and Accountability - M.Y.G., G.D., F.A., F.H.

Conflicts of Interest: The authors declare no conflict of interest.

Financial Disclosure: This study was funded by Istanbul University with the project number TYL-2022-38452.

REFERENCES

1. Yosifov DY, Wolf C, Stilgenbauer S, Mertens D. From Biology to Therapy: The CLL Success Story. *Hemasphere* 2019; 3(2): e175. [\[CrossRef\]](#)
2. Rai KR, Jain P. Chronic lymphocytic leukemia (CLL)-Then and now. *Am J Hematol* 2016; 91(3): 330-40. [\[CrossRef\]](#)
3. Kay NE, Hampel PJ, Van Dyke DL, Parikh SA. CLL update 2022: A continuing evolution in care. *Blood Rev* 2022; 54: 100930. [\[CrossRef\]](#)
4. Hallek M. Chronic lymphocytic leukemia: 2020 update on diagnosis, risk stratification and treatment. *Am J Hematol* 2019; 94(11): 1266-87. [\[CrossRef\]](#)
5. Malavasi F, Deaglio S, Damle R, Cutrona G, Ferrarini M, Chiorazzi N. CD38 and chronic lymphocytic leukemia: a decade later. *Blood* 2011; 118(13): 3470-8. [\[CrossRef\]](#)
6. Kucuksezzer UC, Aktas Cetin E, Esen F, Tahrali I, Akdeniz N, Gelmez MY, et al. The Role of natural killer cells in autoimmune diseases. *Front Immunol* 2021; 12: 622306. [\[CrossRef\]](#)
7. Gardiner CM. NK cell metabolism. *J Leukoc Biol* 2019; 105(6): 1235-42. [\[CrossRef\]](#)
8. Bi J, Tian Z. NK cell dysfunction and checkpoint immunotherapy. *Front Immunol* 2019; 10: 1999. [\[CrossRef\]](#)
9. Sportoletti P, De Falco F, Del Papa B, Baldoni S, Guarente V, Marra A, et al. NK cells in chronic lymphocytic leukemia and their therapeutic implications. *Int J Mol Sci* 2021; 22(13). [\[CrossRef\]](#)
10. Beatty GL, Gladney WL. Immune escape mechanisms as a guide for cancer immunotherapy. *Clin Cancer Res* 2015; 21(4): 687-92. [\[CrossRef\]](#)
11. Yao Y, Lin X, Li F, Jin J, Wang H. The global burden and attributable risk factors of chronic lymphocytic leukemia in 204 countries and territories from 1990 to 2019: analysis based on the global burden of disease study 2019. *Biomed Eng Online* 2022; 21(1): 4. [\[CrossRef\]](#)
12. Yoshino T, Tanaka T, Sato Y. Differential diagnosis of chronic lymphocytic leukemia/small lymphocytic lymphoma and other indolent lymphomas, including mantle cell lymphoma. *J Clin Exp Hematop* 2020; 60(4): 124-9. [\[CrossRef\]](#)
13. Chennamadhavuni A, Lyengar V, Shimanovsky A. Leukemia. In *StatPearls*. Treasure Island (FL); 2022.
14. Vlachonikola E, Stamatopoulos K, Chatzidimitriou A. T cells in chronic lymphocytic leukemia: A two-edged sword. *Front Immunol* 2020; 11: 612244. [\[CrossRef\]](#)
15. MacFarlane AWt, Jillab M, Smith MR, Alpaugh RK, Cole ME, Litwin S, et al. NK cell dysfunction in chronic lymphocytic leukemia is associated with loss of the mature cells expressing inhibitory killer cell Ig-like receptors. *Oncoimmunology* 2017; 6(7): e1330235. [\[CrossRef\]](#)
16. Zhu F, McCaw L, Spaner DE, Gorczyński RM. Targeting the IL-17/IL-6 axis can alter growth of chronic lymphocytic leukemia *in vivo*/ *in vitro*. *Leuk Res* 2018; 66: 28-38. [\[CrossRef\]](#)

17. Zhao J, Chen X, Herjan T, Li X. The role of interleukin-17 in tumor development and progression. *J Exp Med* 2020; 217(1). [\[CrossRef\]](#)
18. Chen J, Liao MY, Gao XL, Zhong Q, Tang TT, Yu X, et al. IL-17A induces pro-inflammatory cytokines production in macrophages via MAPKinases, NF-KappaB and AP-1. *Cell Physiol Biochem* 2013; 32(5): 1265-74. [\[CrossRef\]](#)
19. Bankir M, Acik DY. IL-17 and IL-23 levels in patients with early-stage chronic lymphocytic leukemia. *North Clin Istanb* 2021; 8(1): 24-30. [\[CrossRef\]](#)
20. Jain P, Javdan M, Feger FK, Chiu PY, Sison C, Damle RN, et al. Th17 and non-Th17 interleukin-17-expressing cells in chronic lymphocytic leukemia: delineation, distribution, and clinical relevance. *Haematologica* 2012; 97(4): 599-607. [\[CrossRef\]](#)
21. Martinez-Espinosa I, Serrato JA, Ortiz-Quintero B. Role of IL-10-producing natural killer cells in the regulatory mechanisms of inflammation during systemic infection. *Biomolecules* 2021; 12(1). [\[CrossRef\]](#)
22. Phoksawat W, Jumnainsong A, Leelayuwat N, Leelayuwat C. IL-17 production by NKG2D-expressing CD56+ T cells in type 2 diabetes. *Mol Immunol* 2019; 106: 22-8. [\[CrossRef\]](#)
23. Fayad L, Keating MJ, Reuben JM, O'Brien S, Lee BN, Lerner S, et al. Interleukin-6 and interleukin-10 levels in chronic lymphocytic leukemia: correlation with phenotypic characteristics and outcome. *Blood* 2001; 97(1): 256-63. [\[CrossRef\]](#)
24. De Cecco L, Capaia M, Zupo S, Cutrona G, Matis S, Brizzolara A, et al. Interleukin 21 Controls mRNA and MicroRNA expression in CD40-activated chronic lymphocytic leukemia cells. *PLoS One* 2015; 10(8): e0134706. [\[CrossRef\]](#)
25. de Toter D, Meazza R, Capaia M, Fabbi M, Azzarone B, Balleari E, et al. The opposite effects of IL-15 and IL-21 on CLL B cells correlate with differential activation of the JAK/STAT and ERK1/2 pathways. *Blood* 2008; 111(2): 517-24. [\[CrossRef\]](#)
26. Brady J, Hayakawa Y, Smyth MJ, Nutt SL. IL-21 induces the functional maturation of murine NK cells. *J Immunol* 2004; 172(4): 2048-58. [\[CrossRef\]](#)

Clues to the Harmful Effects of Aspartame on Liver Morphology and Function

E. Rumeysa Hekimoglu¹ , Birsen Elibol² , Ceyhun Toruntay³ , Seda Kirmizikan¹ ,
Ozge Pasin⁴ , Ufuk Sarikaya⁵ , Damla Alkhalidi⁶ , Mukaddes Esrefoglu¹ 

¹Department of Histology and Embryology, Faculty of Medicine, Bezmialem Vakif University, Istanbul, Turkiye

²Department of Medical Biology, Faculty of Medicine, Istanbul Medeniyet University, Istanbul, Turkiye

³Department of Molecular Biology and Genetics, Faculty of Arts and Science, Istanbul Technical University, Istanbul, Turkiye

⁴Department of Biostatistics, Faculty of Medicine, Bezmialem Vakif University, Istanbul, Turkiye

⁵Department of Medical Biochemistry, Bezmialem Vakif University, Health Cares Vocational School, Istanbul, Turkiye

⁶Faculty of Medicine, Bezmialem Vakif University, Istanbul, Turkiye

ORCID ID: E.R.H. 0000-0003-4300-7213; B.B. 0000-0002-9462-0862; C.T. 0000-0002-4743-0257; S.K. 0000-0002-5652-778X; O.P. 0000-0001-6530-0942; U.S. 0000-0003-4573-5505; D.A. 0000-0001-8553-659X; M.E. 0000-0003-3380-1480

Cite this article as: Hekimoglu ER, Elibol B, Toruntay C, Kirmizikan S, Pasin O, Sarikaya U, Alkhalidi D, Esrefoglu M. Clues to the harmful effects of aspartame on liver morphology and function. *Experimed* 2022; 12(3): 232-7.

ABSTRACT

Objective: Aspartame is a widely used artificial sweetener that was approved by the United States Food and Drug Administration (FDA) in 1996 for use as a general sweetener in all foods. Previous studies on aspartame had suggested it to be non-toxic. However, some studies have reported it to have carcinogenic, neurotoxic, apoptotic, and inflammatory effects. The knowledge obtained from previous studies has been insufficient and contradictory, thus the aim of this study was to demonstrate the harmful side effects of daily and high doses of aspartame on the rat livers.

Materials and Methods: The study separated 18 Long Evans rats weighing between 250-300g into three groups: control, low dosage, and high dosage groups ($n = 6$ in each). 50 mg/kg of aspartame was given to the low dose group and 250 mg/kg to the high dose group every day for 10 weeks. At the end of the 10th week, all groups were euthanized and their livers and blood samples collected. Liver tissues were subjected to hematoxylin-eosin and Masson's trichome staining, after which terminal deoxynucleotidyl transferase dUTP nick end labeling (TUNEL) immunohistochemistry was performed to check the serum alanine transaminase (ALT) and aspartate transaminase (AST) values. The enzyme-linked immunosorbent assay (ELISA) method was applied for analyzing superoxide dismutase (SOD) and malondialdehyde (MDA) levels.

Results: Enlargement of the bile canaliculi and dilatation of sinusoids were observed in the group that was given high doses of aspartame. At the same time, the amount of TUNEL-positive cells was higher in the high dose group. AST, ALT, and MDA values were increased while SOD values were decreased in both the low and high aspartame dosage groups.

Conclusion: This study has concluded the prolonged use of high doses of aspartame to be able to cause damage to hepatocytes by stimulating oxidative stress, hepatocyte apoptosis, and necrosis.

Keywords: Aspartame, liver, SOD, MDA, TUNEL, light microscope

INTRODUCTION

Aspartame (APM) is a widely used artificial sweetener that was discovered in 1965 by James Schlatter and has been used in foods and beverages for over 40 years (1). Phenylalanine and aspartic acid are the two amino acids that, together with a trace amount of methanol, make up aspartame. The flavoring agent in aspartame is around 180-

200 times sweeter than sugar (2). APM was approved as a food ingredient by the US Food and Drug Administration (FDA) in 1981 and then approved as a general-purpose sweetener for all foods and drinks in 1996 (3, 4). However, the FDA did not determine the maximum daily dosage for aspartame that can be taken with food and beverages to be 40 mg/kg body weight in Europe and 50 mg/kg body weight in the United States (5).

Corresponding Author: E. Rumeysa Hekimoglu **E-mail:** rumeysagurbuz@gmail.com

Submitted: 24.10.2022 **Revision Requested:** 29.11.2022 **Last Revision Received:** 30.11.2022 **Accepted:** 08.12.2022 **Published Online:** 30.12.2022



Content of this journal is licensed under a Creative Commons Attribution-NonCommercial 4.0 International License.

Among the high-intensity sweeteners, APM is a unique molecule that is metabolized into three common dietary elements (i.e., aspartic acid, phenylalanine, and methanol) by digestive esterases and peptidases (6), with the methanol portion of aspartame being released through hydrolysis of the methyl esters by the pancreatic chymotrypsin and then being immediately absorbed by the small intestine (7). While not harmful in itself, the metabolites of methanol are deleterious to cells in the body, with methanol being converted to formaldehyde, formic acid, water, and CO₂ in the liver (8, 9). These metabolites interact with the cytochrome c oxidase in mitochondria, resulting in an increase in microsomal proliferation and free oxygen radical formation (10).

Recent studies have examined the effects of aspartame and its metabolites on cellular oxidative stress state via the production of free reactive oxygen species (ROS) and modulation of the levels of antioxidant enzymes. According to previous studies, a daily dosage of 40 mg of APM was enough to cause oxidative stress in immunological organs (11, 12). Additionally, the inflammatory signaling pathways involved in the development of liver fibrosis can be altered by oxidative stress (13).

Most recent studies have shown the effects of APM using an observational approach. Because no generally observable side effect had been detected following the administration of a single high dose of APM, researchers had believed APM to be harmless for the body (5), while a few previous studies contrarily reported serious side effects, including cancer development (14-16). Decisive amounts of molecular, cellular, and histological studies have yet to accumulate regarding the adverse effects of regular and long-term usage of APM. The present study aimed to investigate the direct and indirect cellular effects of different doses of APM on rat livers.

MATERIALS AND METHODS

Animals and the Experimental Design

Ethical considerations were obtained from Bezmialem Vakif University Ethics Committee (Decision No. 2021/55). Animals had free access to food and water with controlled room temperature (22-25°C) and humidity, on a 12:12 h light/dark cycle for the duration of the study. This study uses 18 Long Evans rats weighing 250-300 g. Rats were divided into three groups: the low APM dosage (LD) group, the high APM dosage (HD) group, and the control (C) group. The aspartame dose as approved by the FDA (50 mg/kg/day) was given to the rats in the LD group in their drinking water (17). The rats in the HD group took 250 mg/kg/day of APM in their drinking water, which was determined to be an excessive APM consumption considering the metabolic rate of rats is approximately seven times higher than the human metabolic rate (18, 19). The control group drank tap water without APM. The experimental procedure continued for 10 weeks. At the end of the 10th week, blood samples were obtained from all of the rats to evaluate oxidative stress markers and to perform biochemical analysis, after which the animals were euthanized under anesthesia and their liver tissues were removed for histological analysis.

Histological Analysis

Liver tissue samples were fixed in 10% neutral-buffered formalin for one day. Using the routine light microscope tissue processing method, the fixed tissue samples were dehydrated by passing them through graded alcohols. Samples were then embedded in paraffin after being cleaned in xylol.

Sections of 3-4 µm thickness were taken from the paraffin blocks to positively charged slides using a rotary microtome. A series of decreasing alcohol concentrations was used to rehydrate these slides after they had been deparaffinized at 70°C. The slides were then subjected to hematoxylin-eosin (HE) and Masson's trichrome (MT) staining after rehydration and examined under a light microscope (Nikon Eclipse 920248, U.S.A.).

Immunohistochemical Staining

For the immunohistochemistry, the slides were stained for apoptosis with a terminal deoxynucleotidyl transferase dUTP nick end labeling (TUNEL)-based apoptosis kit (ApoTag Plus, In-Situ Apoptosis Detection Kit, S7101, Millipore). The TUNEL technique was applied according to the manufacturer's instructions on the datasheet.

Positive control slides were used with support from the manufacturer. Under a light microscope at 40X objective magnification, the apoptotic cells (brown in color) were evaluated in the liver tissue samples (Nikon Eclipse 920248, U.S.A.).

Biochemical Analysis

Blood was centrifuged at 3,000 x g for 10 min at room temperature. Serum samples were separated into a new tube and stored at -80°C. On the day of the biochemical analysis, serum samples were brought up to room temperature and then centrifuged at 12,000 x g for 10 minutes at 4°C. The supernatants were then collected into new microcentrifuge tubes.

Determining the SOD Protein Levels Using ELISA

Superoxide dismutase (SOD) protein levels were determined by the human SOD enzyme-linked immunosorbent assay (ELISA) kit (AFG Bioscience LLC, Northbrook, IL, USA). After applying the manufacturer's instructions to the serum samples, the absorbances (OD) of each sample were measured at 450 nm using the Multiskan GO ELISA reader (Thermo Fisher Scientific, Boston, MA, USA).

Determining the Oxidative Stress Marker MDA Level Using The Colorimetric Assay

Malondialdehyde (MDA) levels were determined using the thiobarbituric acid reactive substances (TBARS) microplate assay kit (Biorbyt Ltd, Cambridge, UK). After applying manufacturer's instructions to the serum samples, the ODs of each sample were measured at 535 nm using the Multiskan GO ELISA reader (Thermo Fisher Scientific, Boston, MA, USA).

Determining the ALT, AST, and Amylase Levels

Alanine aminotransferase (ALT), aspartate aminotransferase (AST), and amylase 2 (AMY 2) levels in the serum samples were measured using the Atellica Solution Immunoassay & Clinical Chemistry Analyzer (Siemens Healthineers, Germany).

Statistical Analyses

Descriptive statistics of the quantitative data in the study are given as means and standard deviations. The assumption of normally distributed data was examined using the Shapiro-Wilk test, the homogeneity of variance using Levene’s test, and comparison of the groups’ means using the one-way analysis of variance (ANOVA) test. The statistical significance level was taken as $p < 0.05$, with the study using the program SPSS (ver. 26, IBM Corp., Armonk, NY) to do the calculations.

RESULTS

Histopathological Results

When examining the sections of liver tissue, the livers from the control group were observed to show a well-defined central

vein, cord-like array of hepatic cells around the central vein, and sinusoids between the hepatic cell cords. A few hepatocytes with heterochromatic nuclei, which can also be seen in a healthy hepatic cell, were found in the C group (Figure 1A). The sinusoids and some bile canaliculus in the livers from the LD group were observed to be larger than that of the C group. Similar to the C group, a few hepatocytes with heterochromatic nuclei were also observed in the LD group (Figure 1B). The liver sections of the HD group were observed to have enlarged sinusoids, just as in the LD group (Figure 1C). However, enlarged bile canaliculi were more common in the HD group compared to those in the LD group. In contrast with the control and low dosage groups, single cell necrosis was additionally observed in some of the hepatocytes from the HD group (Figure 1D).

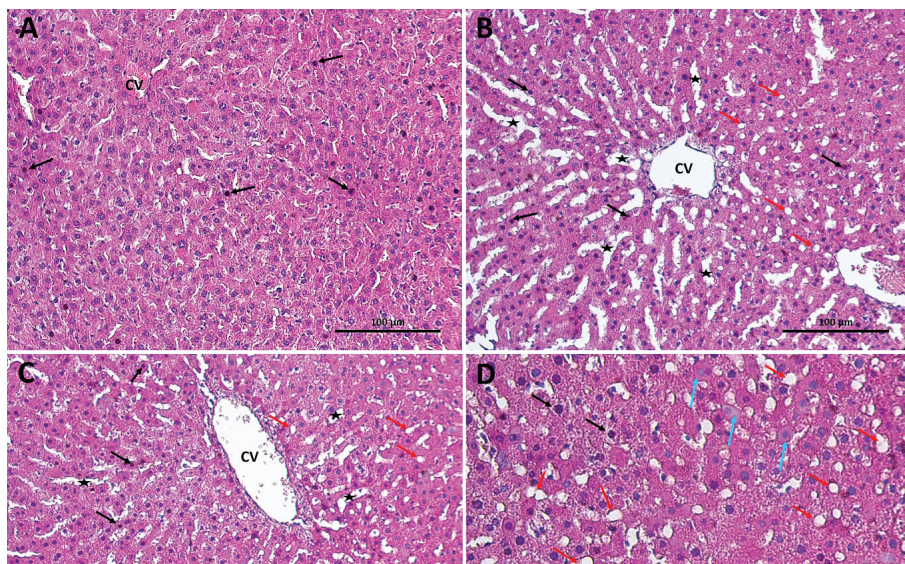


Figure 1. Photomicrographs of liver tissue stained with HE are shown. Figure 1A: Control group, Figure 1B: Low dosage group, and Figure 1C & 1D: High dosage group. Figure 1A shows radially arranged hepatocytes around the central vein (CV). Hepatocytes with heterochromatic nuclei are marked with black arrows. Figure 1B shows enlarged sinusoids (stars) and bile canaliculi (red arrows). Figure 1C & 1D show enlarged sinusoids (stars) and bile canaliculi (red arrows) to be visible in both photomicrographs. Also, the photomicrograph in 1D shows single cell necrosis (blue arrows; HE; A, B, C 20X; D 40X).

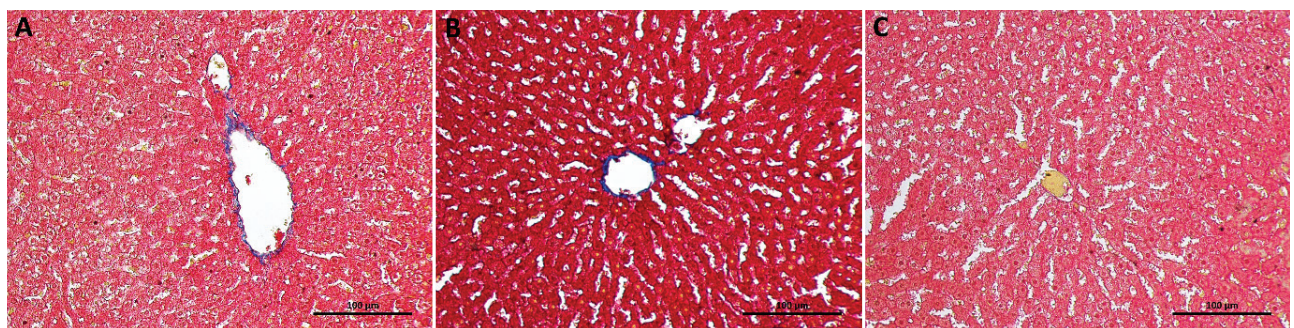


Figure 2. Photomicrographs of liver tissue with Masson’s trichome staining. A comparison of the fibrosis levels among the groups reveals no differences. 2A: Control group, 2B: Low dosage group, and 2C: High dosage group (MTX20).

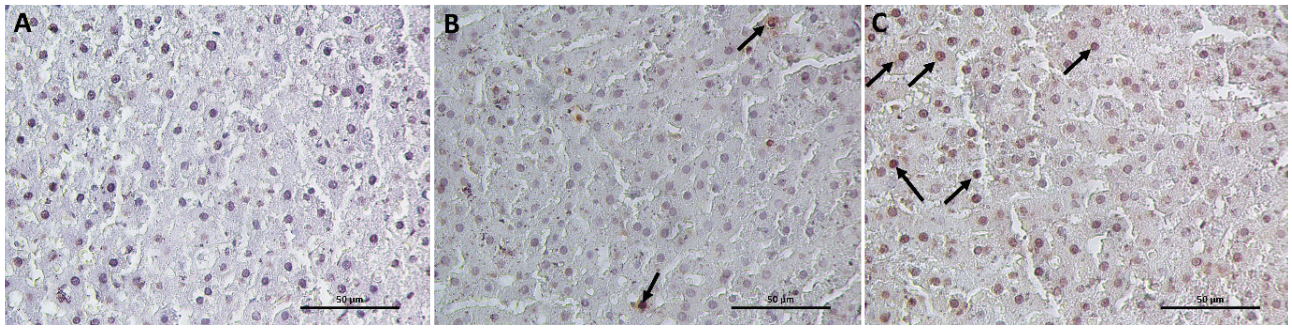


Figure 3. Photomicrograph of the TUNEL-performed liver sections. 3A: Control group, 3B: Low dosage group, and 3C: High dosage group. The distributions of the TUNEL-positive hepatocytes (black arrows) are similar in the C and low dosage groups. The TUNEL-positive hepatocytes appear much more common in the high dosage group (TUNEL X40).

The study performed Masson's trichome (MT) staining on liver tissue sections to observe collagen fibers in blue color in case of the development of hepatic fibrosis. No difference occurred in terms of collagen fiber amount and distribution among the groups regarding the MT-stained sections (Figure 2).

According to the TUNEL immunohistochemical staining, a few TUNEL-positive hepatocytes were observed in the C group (Figure 3A). As seen in Figure 3, the amounts and distributions of the TUNEL-positive hepatocytes are similar in the C and LD groups (Figure 3B). However, the TUNEL-positive hepatocytes are noted as being more common in the sections from the HD group compared to both the C and LD groups (Figure 3C).

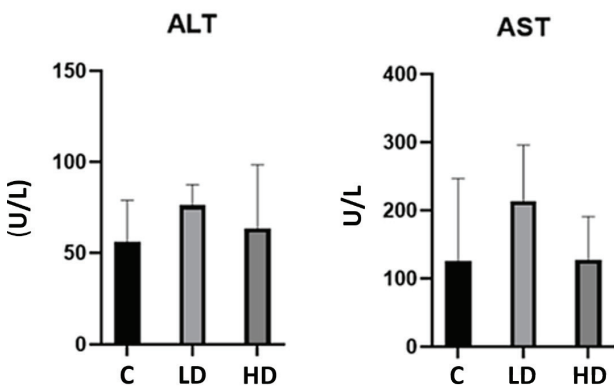


Figure 4. Activity regarding the serum ALT and AST enzymes of the rats from all groups (C: Control group, LD: Low dosage group, HD: High dosage group).

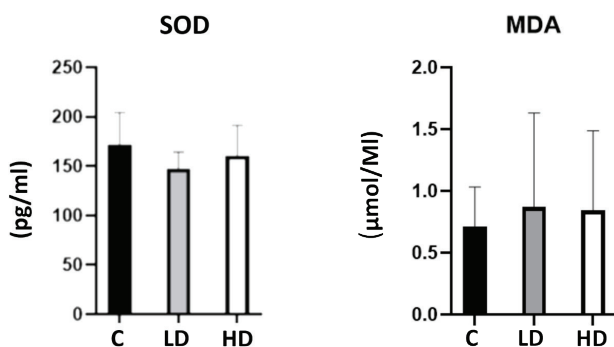


Figure 5. Aspartame's effects on SOD and MDA levels. (C: Control group, LD: Low dosage group, and HD: High dosage group).

Biochemical Results

An increase occurred in the serum ALT and AST levels of the low and high dosage groups, though not at a statistically significant level ($p = 0.388$ & $p = 0.204$, respectively; Figure 4).

Compared to the control group, a decrease is seen in the SOD-levels of both experimental groups, though more pronounced in the LD group and no statistically significant difference ($p = 0.351$). Similarly, the increase in MDA levels did not reach statistical significance ($p = 0.890$; Figure 5).

DISCUSSION

Aspartame is widely used in around 6,000 packaged foods and drinks and 500 drugs, including children's medicines (20). Instead of allowing frequent use, a daily dosage limit has been set for aspartame, with a maximum recommended daily allowance of 50 mg/kg bodyweight of aspartame according to FDA-approved studies (5).

The current study found no major histopathological changes except for enlargement of the sinusoids in the low dosage group. In the high dosage group, however, an observable change occurred in the liver morphology in the form of enlarged sinusoids and bile canaliculi. Hepatic sinusoidal dilatation refers to the expansion of the hepatic capillaries with discontinuous epithelium and discontinuous basement membrane. Although appearing unrelated, sinusoidal dilatation could relate to serious diseases including hepatic venous outflow obstruction, pericardial diseases, heart failure, compression or thrombosis of the hepatic veins or inferior vena cava, and even extrahepatic inflammatory conditions including cholecystitis, pancreatitis, and intestinal

bowel disease (21). Although appearing as a non-specific and innocent finding, bile duct dilatation has been related to both non-obstructive and obstructive cholestasis (22). The rats that were included in this study should have been examined in terms of symptoms and clues regarding these situations. A detailed examination of the body, blood and urine analysis, and molecular analysis of liver morphology using high resolution techniques may provide additional molecular knowledge about the effects of aspartame at these doses in future experiments.

Mild changes in the biochemical values related to the hepatic enzyme activities and oxidative stress markers in the low dosage group suggest that dosage to be safe with respect to liver functionality. However, Choudhary et al.'s study (11) administered 40 mg/kg/day of aspartame and found it to induce oxidative stress in the spleen, lymph nodes, bone marrow, and thymus. On the contrary, this study observed no significant changes in the lipid peroxidation status as determined by the MDA levels nor in the levels of the SOD enzyme with regard to either the low or high aspartame dosage groups. However, the current study did detect a trend toward increased lipid peroxidation and decreased antioxidant enzyme levels as clues/symptoms of increased oxidative stress.

Mohamed et al.'s high aspartame dosage (240 mg/kg) study (23) detected necrosis with an increase in the number of inflammatory cells in the liver. The current study found no inflammatory cell infiltration, even in the high dosage (250 mg/kg) group. However, the study did detect single-cell necrosis localized in single and separate places among the intact hepatocyte groups. This crucial result suggests that prolonged aspartame consumption may even cause severe cell damage, including necrosis.

In addition to the aspartame-induced cellular changes in the hepatocytes, another study reported hepatic fibrosis in mice through oxidative stress due to the long-term administration of aspartame over 12 weeks at 80mg/kg/day (24). Conversely, the current study's dosage over 10 weeks of 50-250 mg/kg/day did not result in any change being found regarding the amount or distribution of collagen in any of the groups, neither through the HE staining nor with the trichrome staining. This result parallels findings of no significant change regarding oxidative stress parameters as a result of aspartame consumption in drinking water. Previous studies have given aspartame to mice and rats using an oral gavage, which was shown to be able to cause a sudden rise in the aspartame metabolites in the circulating blood. However, the current study had rats consume the aspartame in small doses throughout the day, similar to human consumption patterns. As a result, no dramatic changes were observed in the liver tissue samples.

Apoptosis is a highly regulated programmed cell death that does not induce any inflammatory response, and the balance between pro- and anti-apoptotic proteins plays a crucial role in apoptosis. Ashok and Sheeladevi's immunohistochemical study

(25) reported long-term aspartame use to cause apoptosis due to oxidative stress. The current study found the higher number of TUNEL-positive hepatocytes in the high dosage group compared to the other groups to suggest aspartame to have deteriorating effects when consumed in high doses. One *in vitro* study (26) observed aspartame to induce apoptosis mainly through the mitochondrial pathway due to the high production of oxygen radicals.

In summary, this study can conclude long-term daily aspartame consumption in high doses to be able to damage the hepatic cells by increasing both apoptosis and necrosis. Although this study provides little hints about the harmful effects of aspartame on liver morphology and function, future experiments may perform detailed physical examinations, blood and urine analyses, and molecular and electron microscopic analyses of liver morphology, which may provide additional molecular knowledge about the side-effects of aspartame at high doses. Nevertheless, this study recommends that people avoid excessive usage of aspartame in their daily lives.

Ethics Committee Approval: Ethical considerations were obtained from Bezmialem Vakif University Ethics Committee (Decision No. 2021/55).

Peer-review: Externally peer-reviewed.

Author Contributions: Conception/Design of Study - E.R.H., B.E.; Data Acquisition - S.K., D.A., C.T., U.S.; Data Analysis/Interpretation - E.R.H., B.E., O.P.; Drafting Manuscript - M.E., B.E., S.K., D.A., C.T., U.S., O.P.; Critical Revision of Manuscript - E.R.H., M.E., B.E., S.K., D.A., C.T., U.S., O.P.; Final Approval and Accountability - R.H., M.E., B.E., S.K., D.A., C.T., U.S., O.P.

Conflicts of Interest: The authors declare no conflict of interest.

Financial Disclosure: The authors declare that this study has received no financial support.

REFERENCES

- Soffritti M, Padovani M, Tibaldi E, Fabiana L, Manservigi F, Belpoggi F. The carcinogenic effects of aspartame: The urgent need for regulatory re-evaluation. *Am J Ind Med* 2014; 57(4): 383-97. [\[CrossRef\]](#)
- "Aspartame". PubChem, National Library of Medicine, US National Institutes of Health. 17 August 2019.
- Whitehouse RC, Boullata J, McCauley AL. The potential toxicity of artificial sweeteners. *AAOHN J* 2008; 56(6): 251-9. [\[CrossRef\]](#)
- Benford D. Report of the meetings on aspartame with national experts. EFSA Supporting Publications. EFSA. Noted at the 36th Advisory Forum Meeting, 19-20 May, 2010.
- Butchko HH, Stargel WW, Comer CP, Mayhew DA, Benninger C, Blackburn GL, et.al. Aspartame: Review of safety. *Regul Toxicol Pharmacol* 2002; 35(2 Pt 2): S1-93. [\[CrossRef\]](#)
- Harriett H, Butchko and Stargely WW. Aspartame: Scientific Evaluation in the Postmarketing Period. *Regul Toxicol Pharmacol* 2001; 34, 221-233. [\[CrossRef\]](#)
- Gombos K, Varjas T, Orsós Z, Polyák E, Peredi J, Varga Z, et al. The effect of aspartame administration on oncogene and suppressor gene expressions *In Vivo*, 2007; 21(1): 89-92.

8. Ells JT, Henry MM, Lewandowski MF, Seme MT and Murray T. Development and characterization of a rodent model of methanol-induced retinal and optic nerve toxicity. *Neurotoxicology* 2000; 21(3): 321-30.
9. Prokic MD, Paunovic MG, Matic MM, Djordjevic NZ, Ognjanovic BI, Stajin AS, et al. Prooxidative effects of aspartame on antioxidant defense status in erythrocytes of rats. *J Biosci* 2014; 39(5): 859-66. [\[CrossRef\]](#)
10. Parthasarathy JN, Ramasundaram SK, Sundaramahalingam M and Pathinasamy SD. Methanol induced oxidative stress in rat lymphoid organs. *J Occup Health* 2006; 48(1): 20-7. [\[CrossRef\]](#)
11. Choudhary AK and Devi RS. Imbalance of the oxidant-antioxidant status by aspartame in the organs of immune system of Wistar albino rats. *Afr J Pharm Pharmacol* 2014; 8: 220-30. [\[CrossRef\]](#)
12. Choudhary AK, Sheela Devi R. Longer period of oral administration of aspartame on cytokine response in Wistar albino rats. *Endocrinol Nutr* 2015; 62(3): 114-22. [\[CrossRef\]](#)
13. Parola, M., and Robino, G. Oxidative stress-related molecules and liver fibrosis. *J Hepatology* 2001; 35(2): 297-306. [\[CrossRef\]](#)
14. Humphries, P, Pretorius E, Naude H. Direct and indirect cellular effects of aspartame on the brain. *Eur J Clin Nutr* 2008; 62(4): 451-62. [\[CrossRef\]](#)
15. Olney JW, Farber NB, Spitznagel E, Robins LN. Increasing brain cancer rates: is there a link to aspartame? *J. Neuropathol Exp Neurol* 1996; 55 (11): 1115-23. [\[CrossRef\]](#)
16. Schernhammer ES, Bertrand KA, Birmann BM, Sampson L, Willett WC, Feskanich D. Consumption of artificial sweetener- and sugar-containing soda and risk of lymphoma and leukemia in men and women. *Am J Clin Nutr* 2012; 96(6), 1419-28. [\[CrossRef\]](#)
17. FDA. Food additives permitted for direct addition to food for human consumption; aspartame. Food and Drug Administration. Federal Register I Vol. 48. No. 132 I Friday, July 8. 1983 I Rules and Regulations.
18. Nau H. Species differences in pharmacokinetics and drug teratogenesis. *Environ Health Perspect* 1986; 70: 113-29. [\[CrossRef\]](#)
19. Denes V, Agoston DV. How to translate time? The temporal aspect of human and rodent biology. *Front Neurol* 2017; 8: 92. [\[CrossRef\]](#)
20. Magnuson BA, Burdock GA, Doull J, Kroes RM, Marsh GM, Pariza MW, et al. Aspartame: a safety evaluation based on current use levels, regulations, and toxicological and epidemiological studies. *Crit Rev Toxicol* 2008; 629-727. [\[CrossRef\]](#)
21. Brancatelli G, Furlan A, Calandra A and Burgio MD. Hepatic sinusoidal dilatation. *Abdom Radiol (NY)* 2018; 43(8), 2011-22. [\[CrossRef\]](#)
22. Li MK, Crawford JM. The pathology of cholestasis. *Semin Liver Dis* 2004; 24(1): 21-42. [\[CrossRef\]](#)
23. Mohamed AL, Hossam GT, Yasser SS. Long-term soft drink and aspartame intake induces hepatic damage via dysregulation of adipocytokines and alteration of the lipid profile and antioxidant status. *Nutr Res* 2017; 41: 47-55. [\[CrossRef\]](#)
24. Finamor IA, Bressan CA, Torres-Cuevas I, Rius-Pérez S, Veiga M, Rocha MI, et al. Long-term aspartame administration leads to fibrosis, inflammasome activation, and gluconeogenesis impairment in the liver of mice. *Biology (Basel)* 2021; 10(2): 82. [\[CrossRef\]](#)
25. Ashok I, Sheeladevi R. Oxidant stress evoked damage in rat hepatocyte leading to triggered nitric oxide synthase (NOS) levels on long term consumption of aspartame. *J Food Drug Anal* 2015; 23(4): 679-91. [\[CrossRef\]](#)
26. Horio Y, Sun Y, Liu C, Saito T, Kurasaki M. Aspartame-induced apoptosis in PC12 cells. *Environ Toxicol Pharmacol* 2014; 37(1): 158-65. [\[CrossRef\]](#)

The Antioxidant Effects of Sesamol on Bleomycin-Induced Oral Submucous Fibrosis

Sevilay Erimsah¹ , Ayhan Cetinkaya² , Ummugul Uyeturk³ , Ugur Uyeturk⁴ , Yusufhan Yazir⁵ 

¹Department of Histology and Embryology, Faculty of Medicine, Istanbul Nisantasi University, Istanbul, Turkiye

²Department of Physiology, Faculty of Medicine, Abant Izzet Baysal University, Bolu, Turkiye

³Department of Medical Oncology, Faculty of Medicine, Abant Izzet Baysal University, Bolu, Turkiye

⁴Department of Urology, Faculty of Medicine, Abant Izzet Baysal University, Bolu, Turkiye

⁵Department of Histology and Embryology, Faculty of Medicine, Kocaeli University, Kocaeli, Turkiye

ORCID ID: S.E. 0000-0001-5400-0012; A.C. 0000-0002-8212-7149; U.U. 0000-0002-6839-2632; U.U. 0000-0002-4313-8478; Y.Y. 0000-0002-8472-0261

Cite this article as: Erimsah S, Cetinkaya A, Uyeturk U, Uyeturk U, Yazir Y. The antioxidant effects of sesamol on bleomycin-induced oral submucous fibrosis. *Experimed* 2022; 12(3): 238-42.

ABSTRACT

Objective: Oral submucous fibrosis (OSF) is a disease characterized by abnormal collagen deposition that causes inflammation and malignancy in oral mucosal tissue. Fibroblasts and myofibroblasts, are the cells that show significant activation in the development of OSF. Bleomycin (BL) is a chemotherapeutic agent commonly used in cancer treatment that also causes inflammatory changes in the oral mucosa, initiating fibrosis in the oral submucosal tissue. Sesamol (SE) has antioxidative and anti-inflammatory properties which are abundant in sesame seeds and sesame oil, and SE has a beneficial effect on the mucosal layer. This experimental study aimed to investigate SE's effects on BL-induced OSF.

Materials and Methods: The study obtained 18 healthy adult male albino rats aged 3-4 months and weighing 200-250g from Bolu Abant Izzet Baysal University's Experimental Animal Application and Research Center. The rats were divided randomly into control, BL, and BL + SE groups ($n = 6$ in each group). A model of OSF was established in the rats by administering 0.5 mg/mL of BL and 50 mg/kg of SE to the BL+SE group each day. The hematoxylin and eosin stain and Masson's trichrome stain were used to assess histopathological changes in the oral mucosa.

Results: The results revealed SE to have beneficial effects on BL-induced OSF through its antioxidant and anti-inflammatory properties. Histopathological evaluations and biochemical analysis of oral submucosal tissue samples also revealed SE to provide statistically significant protection against fibrosis in the oral mucosa ($p < 0.01$).

Conclusion: This study has demonstrated oral submucous fibrosis that develops due to BL as well as SE to have an antioxidant effect on OSF regarding BL-induced reactive oxygen species (ROS) activation and collagen synthesis.

Keywords: Oral submucous fibrosis, bleomycin, sesamol, antioxidant

INTRODUCTION

Oral submucosal fibrosis (OSF) is a disease characterized by inflammatory collagen deposition that affects human oral functionality (1). OSF is thought to be a form of collagen metabolism disorder and reduces quality of life (2). Fibroblasts and myofibroblasts are active cells that have an important role in the development of OSF (3), with the

pathogenesis of OSF having been studied in detail in recent years. Subepithelial fibrosis and hyalinization cause most of the clinical characteristic features of this condition, and while many drugs and different therapies are used to treat OSF, effective treatment is still a problem (4, 5).

Bleomycin (BL) is a chemotherapeutic agent commonly used in cancer treatment and has limited side effects

Corresponding Author: Sevilay Erimsah **E-mail:** sevilayerimsah@yahoo.com

Submitted: 27.10.2022 **Revision Requested:** 06.12.2022 **Last Revision Received:** 13.12.2022 **Accepted:** 17.12.2022 **Published Online:** 28.12.2022



Content of this journal is licensed under a Creative Commons Attribution-NonCommercial 4.0 International License.

other than pulmonary fibrosis. BL is used in studies to create an animal model of pulmonary fibrosis, scleroderma, and submucous fibrosis (6-8). In addition, BL causes inflammatory changes in tissue that result in fibrosis. Oxidative stress is also considered a cause of fibrosis through inflammatory responses and increased fibroblast activation. Oral submucous tissue is affected by chemotherapeutic agents due to rapid proliferation (5, 9). This study used BL to make an animal model for understanding the characteristics of oral submucous fibrosis.

Sesame (*Sesamum indicum* L.) has been used in Eastern countries for a long time as an anti-aging and nutritional supplement. Sesame seed oil contains sesamol, sesamin, and sesamol (SE) (10), with SE (3,4-methylenedioxyphenol) having antioxidative and anti-inflammatory effects on mucosal tissue (11, 12). SE is known to have good antioxidant activity that scavenges the hydroxyl radical due to the benzodioxol group it contains (13). A number of studies have reported SE as being a direct free radical scavenging antioxidant (14-16). SE has a protective effect on the mucosal layer in gastric ulcers caused by nonsteroidal anti-inflammatory drugs (17). SE also has antibacterial and positive antioxidant properties that reduce lipid peroxidation and free radical damage in oral tissues (12).

Studies examining quercetin, chamomile, dihydroartemisinin, leflunomide, and resveratrol for preventing fibrosis due to BL have found these substances to reduce fibrosis with their anti-inflammatory and antioxidant effects (18-21). However, the positive effect of SE on oral submucous tissue damage association with bleomycin is not yet known. The purpose of this study was to investigate SE's antioxidant effect on BL-induced oral submucous fibrosis in rats.

MATERIALS AND METHODS

The experimental study was carried out at Bolu Abant Izzet Baysal University, Experimental Animal Application and Research Center. The study used 18 healthy male Wistar albino rats aged 3-4 months and weighing 200-250g in polypropylene cages and kept them in an environment at an ambient temperature of $22\pm 2^{\circ}\text{C}$ on a 12-h light-dark cycle at a humidity level of 50-60%. Tap water was used with standard pellet feed until the day of the experiment. Rats were divided randomly into the control, BL, and BL+SE groups, ($n = 6$ in each). The control group was applied 2.5 mg/kg of saline on the first day, while the BL and BL+SE groups were applied 0.5 mg/mL of BL on the first day. For 2 h before the BL administration, saline was given to the BL group while SE (50 mg/kg/day) was given to the BL+SE group daily over a period of 10 days using an oral gavage (22). Lastly, the rats were anesthetized with ketamine (50 mg/kg), xylazine (10 mg/kg) and the blood samples were taken for biochemical parameters then rats were sacrificed by over dose anesthetics. The experimental procedures were approved by The Animal Research Ethics Committee of Bolu Abant Izzet Baysal University (Decision No. 2018/39).

For the histopathologic analysis, oral mucosal tissues from the inner surface of the lips were fixed in 10% formalin and

embedded in paraffin. Thin sections of oral tissue were taken for hematoxylin and eosin (H&E) and Masson's trichrome staining. The stained sections were assessed with a light microscope and graded histopathologically in line with the criteria from Pindborg and Sirsat's study (23): Grade 1 shows early hyalinization in the juxtaepithelial region, plump young fibroblasts, enlarged blood vessels and presence of lymphocytes (mostly mononuclear), eosinophils, and a small number of inflammatory cells in plasma cells; Grade 2 shows moderate hyalinization, less prominent fibroblasts, increased fibrocytes, narrowed vessels, and inflammatory cells; and Grade 3 shows high collagen deposition and absence of fibroblasts in the mucosal region, narrowed vessels, and inflammatory cells. A normal mucosal structure was graded as Grade 0. Histological scoring of the oral mucosa was performed by a blinded histopathologist.

For biochemical analysis, the oral mucosal tissue samples were separated into glass tubes and subsequently labeled, then the PBS-washed samples were kept at -80°C until the biochemical analysis. Next, each tissue sample was thawed and homogenized before the assay. The resulting homogenized tissues were centrifuged at 5000 g and tested for malondialdehyde (MDA) and glutathione peroxidase (GPx) concentrations as an indicator of lipid peroxidation levels. The MDA and GPx measurements were made using tissue-specific commercial kits according to protocol (Cusabio, Wuhan, China).

Statistical Analyses

The results were expressed as the mean \pm standard error of mean (SEM). The two-tailed Student's t-test was used to compare the significance of the difference between the two groups, and the one-way analysis of variance (ANOVA) test was used with Tukey's multiple comparison test to compare the data obtained from the groups. SPSS 21 was used the analysis program, with a $p < 0.05$ being considered statistically significant.

RESULTS

H&E and Masson Staining

In the histopathological examination, the epithelial layer from the control group with the normal epithelial rete ridges pattern was seen to be normal with no presence of congested or obliterated vascular changes or increased fibrosis (Figures 1A, 1D). In the BL group, the epithelial layer was thinner and the epithelial rete ridges of the oral mucosa were shorter. Also, a few inflammatory cells were found, as well as narrowing/shrinking of some vessels in the lamina propria with muscles that were atrophic in appearance. An increase of hyalinized collagen, atrophic muscle fibers, and vascular changes were also observed in the lamina propria (Figures 1B1, 1B2, 1E). In BL+SE treatment group that was applied sesamol, epithelial thinning was reduced, but inflammatory cells were still observed. A slight thin epithelial layer, mild atrophic muscle fibers, and a few vascular changes were observed in the buccal mucosa of the BL+SE group. In addition, less collagen deposition was observed in the submucosal tissue compared to the BL group (Figures 1C, 1F). The histopathologic grading

scores for the BL and BL+SE groups were assessed to be higher than in the control group ($p < 0.01$), with the BL group scores also being higher compared to the BL+SE group (Figures 1B1, 1B2, 1C, 1F). In addition, statistically significant differences were observed in all groups when compared amongst themselves ($p < 0.01$; Table 1).

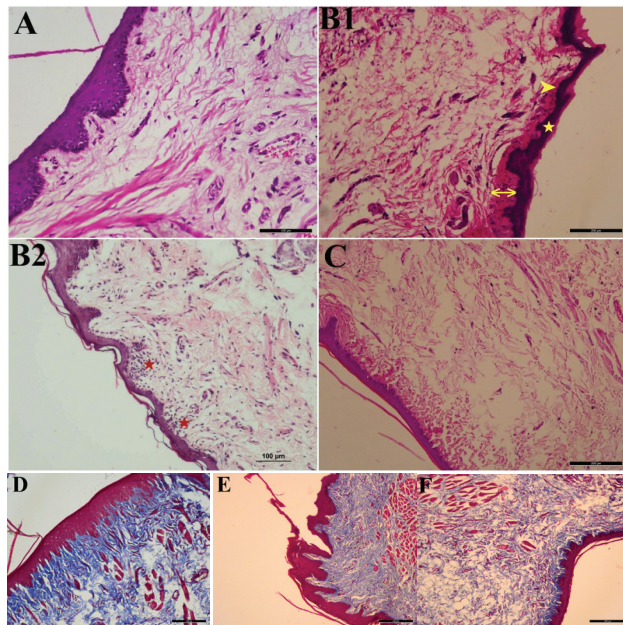


Figure 1. The oral submucosal tissues (H&E & Masson's trichrome stains). **A, D:** Control group. **B1, B2, E:** The BL group, showing a thinner epithelial layer (★), shorter epithelial rete ridges (▶), juxtaepithelial hyalinization, collagen deposition (↔), and increased inflammatory cells (★) and muscle atrophy. **C, F:** The BL+ SE group.

Table 1. Statistical analysis of the histopathologic grading scores and GPx and MDA levels of all groups.

Groups	Histopathologic Score	GPx	MDA
Control	0.264 ± 0.111	2.150 ± 0.472	0.751 ± 0.056
BL	2.564 ± 0.400*	0.393 ± 0.221*	1.523 ± 0.425*
BL+SE	1.285 ± 0.506*°	1.061 ± 0.355*°	1.043 ± 0.110*°

* $p < 0.01$ compared to the control group
° $p < 0.01$ compared to the BL group

Biochemical Analysis

Lipid peroxidation in the BL-treated rats' mucosal tissue were quantified by evaluating their MDA levels. The MDA levels of both the BL and BL+SE groups were found to be significantly

higher than the control group, which indicates increased oxidative stress in the oral mucosa ($p < 0.01$). However, when comparing the BL group to the BL+SE group, a significant difference was seen between them, with the MDA levels being found significantly lower in the SE treatment group (BL+SE; $p < 0.01$).

GPx catalyzes hydrogen peroxide and hydroperoxide reduction to form non-toxic products, and this was also measured to be higher in the control group than in the BL and BL+SE groups ($p < 0.01$). Also, GPx was found to be significantly lower in the BL group when compared to the BL+SE group ($p < 0.01$). The GPx levels from the oral submucosal tissue samples showed SE to have provided statistically significant protection against fibrosis ($p < 0.01$; Table 1; Figure 2).

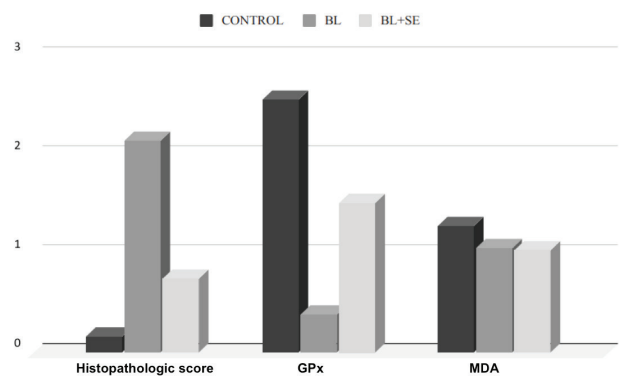


Figure 2. Histopathologic score of BL group were found to be significantly higher than the control group and BL+SE group. The MDA and GPx levels of BL, BL+SE and the control groups; the graphic indicates increased oxidative stress in the oral mucosa and also, decreased GPx level in the BL-treated group compared to other groups ($P < 0.01$). BL, Bleomycin; BL+SE, Bleomycin+Sesamol, GPx: Glutation peroxidase; MDA: Malondialdehyde.

DISCUSSION

The present study has provided data regarding SE's protective effect against BL-induced submucosal damage in rats. BL is one of the drugs used in the chemotherapy treatment of many types of tumors. In addition to complications such as immuno-suppression and hematopoietic toxicity due to BL, BL chemotherapy often causes pulmonary fibrosis (24). Therefore, BL has been widely used in developing animal models of pulmonary fibrosis (25). Repetitive administration of BL injections also induces pleural submucosal fibrosis (9). The current study created oral submucosal fibrosis to appear in BL-treated rats, similar to the human OSF pathology. This model allowed the study to examine SE's antioxidant effects on oral submucosal fibrosis. The treated rats were observed to have atrophic epithelial layers, hyalinization just below the epithelial layer, concentrations of collagen fibrils, and increased inflammatory cell counts. The increased collagen in the oral mucosa is the most distinguishing feature of OSF (26). Lamina

propria enlargement with connective tissue was also observed, similar to OSF. The rats in whose mucosal tissue the study wanted to create fibrosis were also observed to have atrophic epithelial layers, juxtaepithelial hyalinization, deposition of collagen fibrils, and some inflammatory cell infiltration (27).

This study reduced the development of fibrosis with the SE treatment, which was quantified by the histopathologic changes in the submucosal layer. The histopathologic evaluations showed the fibroblasts to have become active in the lamina propria of the oral mucosa of the BL-treated rats due to the deposition of a large amount of collagen fibers. In addition, the atrophic epithelial cells, epithelial hyalinization, and inflammatory cell infiltration in the BL-treated groups resembled OSF (26, 28). However, less atrophic epithelial cells and inflammatory cells in the lamina propria were observed in this study.

SE attenuated OSF in the BL-treated submucosa. SE was also found to be effective at reducing mucosal lipid peroxidation and hydroxyl radical levels. In addition, SE significantly maintained the reduced mucosal glutathione levels in the submucosal tissue of the BL-treated rats. Therefore, SE may be able to protect the submucosa against BL-induced injury by inhibiting lipid peroxidation (29). In the current study, SE played an excellent role in protecting the oral mucosal tissue from oxidative damage, with the histopathological results supporting with the biochemical findings.

Therefore, this study indicates SE to be able to reduce mucosal fibrosis and to ameliorate OSF with its antioxidant effects on BL-induced OSF rats.

CONCLUSION

The results showed BL to cause an increase in fibrosis in the oral submucosal tissue and SE to have potent antioxidative and anti-inflammatory properties on BL-induced apoptosis and ROS accumulation. This study has also shown SE to have an antioxidant effect on oral submucosal fibrosis and to inhibit BL-induced ROS activation and collagen synthesis. Due to the results obtained from the study on rats, SE may be an alternative approach to clinical antioxidant treatments for OSF patients.

Note: This study was presented orally at the 2nd International Health Sciences and Life Congress on April 24-27, 2019 in Istanbul.

Ethics Committee Approval: The experimental procedures were approved by The Animal Research Ethics Committee of Bolu Abant İzzet Baysal University (Decision No. 2018/39).

Peer-review: Externally peer-reviewed.

Author Contributions: Conception/Design of Study - S.E., U.U.; Data Acquisition - S.E.; Data Analysis/Interpretation - S.E.; Drafting Manuscript - Ü.U., U.U.; Critical Revision of Manuscript - S.E.; Final Approval and Accountability - A.C., Y.Y., S.E.

Conflicts of Interest: The authors declare no conflict of interest.

Financial Disclosure: The authors declare that this study has received no financial support.

REFERENCES

1. World Health Organization; International Agency for Research on Cancer. IARC monograph on the evaluation of carcinogenic risks to humans, betel-quid and areca-nut chewing and some areca-nut-derived nitrosamines. Vol. 85. Lyon, France: IARC; 2004.
2. Arakeri G, Brennan PA. Oral submucous fibrosis: An overview of the aetiology, pathogenesis, classification, and principles of management. *Br J Oral Maxillofac Surg* 2013; 51: 587-93. [\[CrossRef\]](#)
3. Angadi PV, Kale AD, Hallikerimath S. Evaluation of myofibroblasts in oral submucous fibrosis: correlation with disease severity. *J Oral Pathol Med* 2011; 40: 208-13. [\[CrossRef\]](#)
4. Kerr AR, Warnakulasuriya S, Mighell AJ, T Dietrich, M Nasser, J Rimal, et al. A systematic review of medical interventions for oral submucous fibrosis and future research opportunities. *Oral Dis* 2011; 17: 42-57. [\[CrossRef\]](#)
5. Jiang XW, Zhang Y, Yang SK, Zhang H, Lu K, Sun GL. Efficacy of salvianolic acid B combined with triamcinolone acetonide in the treatment of oral submucous fibrosis. *Oral Surg Oral Med Oral Pathol Oral Radiol* 2013; 115: 339-44. [\[CrossRef\]](#)
6. Chua F, Gauldie J, Laurent GJ. Pulmonary fibrosis: Searching for model answers. *Am J Respir Cell Mol Biol* 2005; 33: 9-13. [\[CrossRef\]](#)
7. Yamamoto T, Takagawa S, Katayama I, Yamazaki K, Hamazaki Y, Shinkai H, et al. Animal model of sclerotic skin. I: Local injections of bleomycin induce sclerotic skin mimicking scleroderma. *J Invest Dermatol* 1999; 112: 456-62. [\[CrossRef\]](#)
- 8-9. Zhang SS, Gong ZJ, Xiong W, Wang X, Min Q, Luo CD, et al. A rat model of oral submucous fibrosis induced by bleomycin. *Oral Surg Oral Med Oral Pathol Oral Radiol* 2016; 122(2): 216-23. [\[CrossRef\]](#)
- 9-10. Kabel AM, Omar MS, Elmaaboud MAA. Amelioration of bleomycin-induced lung fibrosis in rats by valproic acid and butyrate: Role of nuclear factor kappa-B, proinflammatory cytokines and oxidative stress. *Int Immunopharmacol* 2016; 39: 335-42. [\[CrossRef\]](#)
10. Jan KC, Ho CT, Hwang LS. Bioavailability and tissue distribution of sesamol in rat. *J Agric Food Chem* 2008; 56(16): 7032-7. [\[CrossRef\]](#)
11. Hsu DZ, Chen KT, Li YH, Chuang YC, Liu MY. Sesamol delays mortality and attenuates hepatic injury after cecal ligation and puncture in rats: role of oxidative stress. *Shock*. 2006; 25(5): 528-32. [\[CrossRef\]](#)
12. Hsu DZ, Chen YW, Chu PY, Periasamy S, Liu MY. Protective effect of 3,4-methylenedioxyphenol (sesamol) on stress-related mucosal disease in rats. *Biomed Res Int* 2013; 2013: 481827.
13. Kumagai Y, Lin LY, Schmitz DA, Cho AK. Hydroxyl radical mediated demethylation of (methylenedioxy) phenyl compounds. *Chem Res Toxicol* 1991; 4: 330-4. [\[CrossRef\]](#)
14. Kanimozhi P, Prasad NR. Antioxidant potential of sesamol and its role on radiation-induced DNA damage in whole-body irradiated Swiss albino mice. *Environ Toxicol Pharmacol* 2009; 28: 192-7. [\[CrossRef\]](#)
15. Prasad NR, Menon VP, Vasudev V, Pugalendi KV. Radioprotective effect of sesamol on gamma-radiation induced DNA damage, lipid peroxidation and antioxidants levels in cultured human lymphocytes. *Toxicology* 2005; 209: 225-35. [\[CrossRef\]](#)
16. Wu MS, Aquino LBB, Barbaza MYU, Hsieh CL, Castro-Cruz KA, Yang LL, et al. Anti-inflammatory and anticancer properties of bioactive compounds from *Sesamum indicum* L.-A Review. *Molecules* 2019; 24(24): 4426. [\[CrossRef\]](#)

17. Hsu D-Z, Chu P-Y, Li Y-H, Liu M-Y. Sesamol attenuates diclofenac-induced acute gastric mucosal injury via its cyclooxygenase-independent antioxidative effect in rats. *Shock* 2008; 30(4): 456-62. [\[CrossRef\]](#)
18. Zargar HR, Hemmati AA, Ghafourian M, Arzi A, Rezaie A, Javad-Moosavi SA. Long-term treatment with royal jelly improves bleomycin-induced pulmonary fibrosis in rats. *Can J Physiol Pharmacol* 2017; 95(1): 23-31. [\[CrossRef\]](#)
19. Javadi I, Emami S. The antioxidative effect of chamomile, anthocyanoside and their combination on bleomycin-induced pulmonary fibrosis in rat. *Med Arch* 2015; 69(4): 229-31. [\[CrossRef\]](#)
20. Yang D, Yuan W, Lv C, Li N, Liu T, Wang L, et al. Dihydroartemisinin suppresses inflammation and fibrosis in bleomycin-induced pulmonary fibrosis in rats. *Int J Clin Exp Pathol* 2015; 8(2): 1270-81.
21. Akgedik R, Akgedik S, Karamanli H, Uysal S, Bozkurt B, Ozol D, et al. Effect of resveratrol on treatment of bleomycin-induced pulmonary fibrosis in rats. *Inflammation* 2012; 35(5): 1732-41. [\[CrossRef\]](#)
22. Jan KC, Ho CT, Hwang LS. Elimination and metabolism of sesamol, a bioactive compound in sesame oil, in rats. *Mol Nutr Food Res* 2009; 53(1): 36-43. [\[CrossRef\]](#)
23. Shruthi P, Ajay KC, Mamta S, Mangal S, Ravi M. Correlation of histopathological diagnosis with habits and clinical findings in oral submucous fibrosis. *Head Neck Oncol* 2009; 1-10. [\[CrossRef\]](#)
24. Kawai K, Akaza H. Bleomycin-induced pulmonary toxicity in chemotherapy for testicular cancer. *Expert Opin Drug Saf* 2003; 2(6): 587-96. [\[CrossRef\]](#)
25. Lee WJ, Lee SM, Won CH, Chang SE, Lee MW, Choi JH, et al. Efficacy of intralesional bleomycin for the treatment of plantar hard corns. *Int J Dermatol* 2014; 53(12): 572-7. [\[CrossRef\]](#)
26. Utsunomiya H, Tilakaratne WM, Oshiro K, Satoshi Maruyama, Makoto Suzuki, Hiroko Ida-Yonemochi, et al. Extracellular matrix remodeling in oral submucous fibrosis: its stage-specific modes revealed by immunohistochemistry and in situ hybridization. *J Oral Pathol Med* 2005; 34: 498-507. [\[CrossRef\]](#)
27. Dai JP, Chen XX, Zhu DX, Wan QY, Chen C, Wang GF, et al. Panax notoginseng saponins inhibit areca nut extract induced oral submucous fibrosis in vitro. *J Oral Pathol Med* 2014; 43(6): 464-70. [\[CrossRef\]](#)
28. Jiang L, Deng Y, Li W, Lu Y. Arctigenin suppresses fibroblast activity and extracellular matrix deposition in hypertrophic scarring by reducing inflammation and oxidative stress. *Mol Med Rep* 2020; 22(6): 4783-91. [\[CrossRef\]](#)
29. Andargie M, Vinas M, Rathgeb A, Möller E, Karlovsky P. Lignans of Sesame (*Sesamum indicum* L.): A Comprehensive Review. *Molecules* 2021; 26(4): 883. [\[CrossRef\]](#)

EXPERIMED

AIMS AND SCOPE

Experimed is an international, scientific, open access periodical published in accordance with independent, unbiased, and double-blinded peer-review principles. The journal is the official online-only publication of Istanbul University Aziz Sancar Institute of Experimental Medicine and it is published triannually on April, August, and December. As of 2022 the publication language of the journal is only English. The manuscripts submitted for publication in the journal must be scientific work in English.

Experimed aims to contribute to the literature by publishing manuscripts at the highest scientific level on all fields of basic and clinical medical sciences. The journal publishes original articles, case reports, reviews, and letters to the editor that are prepared in accordance with ethical guidelines.

The scope of the journal includes but not limited to; experimental studies in all fields of medical sciences.

The target audience of the journal includes specialists and professionals working and interested in all disciplines of basic and clinical medical sciences.

The editorial and publication processes of the journal are shaped in accordance with the guidelines of the International Committee of Medical Journal Editors (ICMJE), World Association of Medical Editors (WAME), Council of Science Editors (CSE), Committee on Publication Ethics (COPE), European Association of Science Editors (EASE), and National Information Standards Organization (NISO). The journal is in conformity with the Principles of Transparency and Best Practice in Scholarly Publishing (doaj.org/bestpractice).

Processing and publication are free of charge with the journal. No fees are requested from the authors at any point throughout the evaluation and publication process. All manuscripts must be submitted via the online submission system, which is available at <http://experimed.istanbul.edu.tr/en/>. The journal guidelines, technical information, and the required forms are available on the journal's web page.

All expenses of the journal are covered by the Istanbul University.

Statements or opinions expressed in the manuscripts published in the journal reflect the views of the author(s) and not the opinions of the Istanbul University Aziz Sancar Institute of Experimental Medicine, editors, editorial board, and/or publisher; the editors, editorial board, and publisher disclaim any responsibility or liability for such materials.

Experimed is an open access publication and the journal's publication model is based on Budapest Open Access Initiative (BOAI) declaration. Journal's archive is available online, free of charge at <http://experimed.istanbul.edu.tr/en/>. Experimed's content is licensed under a Creative Commons Attribution-NonCommercial 4.0 International License.

Editor in Chief: Prof. Bedia Çakmakođlu

Address: Istanbul University, Aziz Sancar Institute of Experimental Medicine, Vakıf Gureba Avenue, 34093, Çapa, Fatih, Istanbul, Türkiye

Phone: +90 212 414 2000-33305

Fax: +90 212 532 4171

E-mail: bedia@istanbul.edu.tr

Publisher: Istanbul University Press

Address: Istanbul University Central Campus, 34452 Beyazit, Fatih / Istanbul - Türkiye

Phone: +90 212 440 0000

EXPERIMED

INSTRUCTIONS TO AUTHORS

Context

Experimed is an international, scientific, open access periodical published in accordance with independent, unbiased, and double-blinded peer-review principles. The journal is the official on-line-only publication of Istanbul University Aziz Sancar Institute of Experimental Medicine and it is published triannually on April, August, and December. The publication language of the journal is English.

Experimed aims to contribute to the literature by publishing manuscripts at the highest scientific level on all fields of basic and clinical medical sciences. The journal publishes original articles, case reports, reviews, and letters to the editor that are prepared in accordance with ethical guidelines.

Editorial Policy

The editorial and publication processes of the journal are shaped in accordance with the guidelines of the International Council of Medical Journal Editors (ICMJE), the World Association of Medical Editors (WAME), the Council of Science Editors (CSE), the Committee on Publication Ethics (COPE), the European Association of Science Editors (EASE), and National Information Standards Organization (NISO). The journal conforms to the Principles of Transparency and Best Practice in Scholarly Publishing (doaj.org/bestpractice).

Originality, high scientific quality, and citation potential are the most important criteria for a manuscript to be accepted for publication. Manuscripts submitted for evaluation should not have been previously presented or already published in an electronic or printed medium. The journal should be informed of manuscripts that have been submitted to another journal for evaluation and rejected for publication. The submission of previous reviewer reports will expedite the evaluation process. Manuscripts that have been presented in a meeting should be submitted with detailed information on the organization, including the name, date, and location of the organization.

Peer-Review Policy

Manuscripts submitted to Experimed will go through a double-blind peer-review process. Each submission will be reviewed by at least two external, independent peer reviewers who are experts in their fields in order to ensure an unbiased evaluation process. The editorial board will invite an external and independent editor to manage the evaluation processes of manuscripts submitted by editors or by the editorial board members of the journal. The Editor in Chief is the final authority in the decision-making process for all submissions.

Ethical Principles

An approval of research protocols by the Ethics Committee in accordance with international agreements (World Medical Association Declaration of Helsinki "Ethical Principles for Medical Research Involving Human Subjects," amended in October 2013, www.wma.net) is required for experimental, clinical, and drug studies and for some case reports. If required, ethics committee reports or an equivalent official document will be requested from the authors. For manuscripts concerning experimental research on humans, a

statement should be included that shows that written informed consent of patients and volunteers was obtained following a detailed explanation of the procedures that they may undergo. For studies carried out on animals, the measures taken to prevent pain and suffering of the animals should be stated clearly. Information on patient consent, the name of the ethics committee, and the ethics committee approval number should also be stated in the Materials and Methods section of the manuscript. It is the authors' responsibility to carefully protect the patients' anonymity. For photographs that may reveal the identity of the patients, signed releases of the patient or of their legal representative should be enclosed.

Plagiarism

Experimed is extremely sensitive about plagiarism. All submissions are screened by a similarity detection software (iThenticate by CrossCheck) at any point during the peer-review or production process. Even if you are the author of the phrases or sentences, the text should not have unacceptable similarity with the previously published data.

When you are discussing others' (or your own) previous work, please make sure that you cite the material correctly in every instance.

In the event of alleged or suspected research misconduct, e.g., plagiarism, citation manipulation, and data falsification/fabrication, the Editorial Board will follow and act in accordance with COPE guidelines.

Authorship

Each individual listed as an author should fulfill the authorship criteria recommended by the International Committee of Medical Journal Editors

(ICMJE - www.icmje.org). The ICMJE recommends that authorship be based on the following 4 criteria:

- 1 Substantial contributions to the conception or design of the work; or the acquisition, analysis, or interpretation of data for the work; AND
- 2 Drafting the work or revising it critically for important intellectual content; AND
- 3 Final approval of the version to be published; AND
- 4 Agreement to be accountable for all aspects of the work in ensuring that questions related to the accuracy or integrity of any part of the work are appropriately investigated and resolved.

In addition to being accountable for the parts of the work he/she has done, an author should be able to identify which co-authors are responsible for specific other parts of the work. In addition, authors should have confidence in the integrity of the contributions of their co-authors.

All those designated as authors should meet all four criteria for authorship, and all who meet the four criteria should be identified as authors. Those who do not meet all four criteria should be acknowledged in the title page of the manuscript.

EXPERIMED

Experimed requires corresponding authors to submit a signed and scanned version of the authorship contribution form (available for download through <http://experimed.istanbul.edu.tr/en/>) during the initial submission process in order to act appropriately on authorship rights and to prevent ghost or honorary authorship. If the editorial board suspects a case of "gift authorship," the submission will be rejected without further review. As part of the submission of the manuscript, the corresponding author should also send a short statement declaring that he/she accepts to undertake all the responsibility for authorship during the submission and review stages of the manuscript.

Conflict of Interest

The journal requires the authors and all individuals taking part in the evaluation process to disclose any existing or potential conflict of interest (such as financial ties, academic commitments, personal relationships, institutional affiliations) that could unduly influence one's responsibilities. To disclose potential conflicts of interest, the ICMJE Potential Conflict of Interest Disclosure Form should be filled in and submitted by authors as explained in the Author Form of the journal. Cases of a potential conflict of interest are resolved within the scope of COPE Conflict of Interest Flowcharts and ICMJE Conflict of Interest guidelines.

Besides conflict of interest, all financial support received to carry out research must be declared while submitting the paper.

The Editorial Board of the journal handles all appeal and complaint cases within the scope of COPE guidelines. In such cases, authors should get in direct contact with the editorial office regarding their appeals and complaints. When needed, an ombudsperson may be assigned to resolve cases that cannot be resolved internally. The Editor in Chief is the final authority in the decision-making process for all appeals and complaints.

Copyright and Licensing

Authors publishing with the journal retain the copyright to their work licensed under the Creative Commons Attribution-NonCommercial 4.0 International license ("<https://creativecommons.org/licenses/by-nc/4.0/>" CC BY-NC 4.0) which permits unrestricted, non-commercial use, distribution, and reproduction in any medium, provided the original work is properly cited.

Open Access Statement

The journal is an open access journal and all content is freely available without charge to the user or his/her institution. Except for commercial purposes, users are allowed to read, download, copy, print, search, or link to the full texts of the articles in this journal without asking prior permission from the publisher or the author. This is in accordance with the HYPERLINK "<https://www.budapestopenaccessinitiative.org/read>" BOAI definition of open access.

The open access articles in the journal are licensed under the terms of the Creative Commons Attribution-NonCommercial 4.0 International ("<https://creativecommons.org/licenses/by-nc/4.0/deed.en>" CC BY-NC 4.0) license.

Disclaimer

Statements or opinions expressed in the manuscripts published in Experimed reflect the views of the author(s) and not the opinions

of the editors, the editorial board, or the publisher; the editors, the editorial board, and the publisher disclaim any responsibility or liability for such materials. The final responsibility in regard to the published content rests with the authors.

MANUSCRIPT PREPARATION

The manuscripts should be prepared in accordance with ICMJE-Recommendations for the Conduct, Reporting, Editing, and Publication of Scholarly Work in Medical Journals (updated in December 2015 - <http://www.icmje.org/icmje-recommendations.pdf>). Authors are required to prepare manuscripts in accordance with the CONSORT guidelines for randomized research studies, STROBE guidelines for observational original research studies, STARD guidelines for studies on diagnostic accuracy, PRISMA guidelines for systematic reviews and meta-analysis, ARRIVE guidelines for experimental animal studies, and TREND guidelines for non-randomized public behavior.

Manuscripts can only be submitted through the journal's online manuscript submission and evaluation system, available at <http://experimed.istanbul.edu.tr/en/>. Manuscripts submitted via any other medium will not be evaluated.

Manuscripts submitted to the journal will first go through a technical evaluation process where the editorial office staff will ensure that the manuscript has been prepared and submitted in accordance with the journal's guidelines. Submissions that do not conform to the journal's guidelines will be returned to the submitting author with technical correction requests.

Authors are required to submit the following:

- Copyright Agreement Form,
- ICMJE Potential Conflict of Interest Disclosure Form (should be filled in by all contributing authors)

during the initial submission. These forms are available for download at <http://experimed.istanbul.edu.tr/en/>.

Preparation of the Manuscript

Title page: A separate title page should be submitted with all submissions and this page should include:

- The full title of the manuscript as well as a short title (running head) of no more than 50 characters,
- Name(s), affiliations, ORCID IDs and highest academic degree(s) of the author(s),
- Grant information and detailed information on the other sources of support,
- Name, address, telephone (including the mobile phone number) and fax numbers, and email address of the corresponding author,
- Acknowledgment of the individuals who contributed to the preparation of the manuscript but who do not fulfill the authorship criteria.

Abstract: A English abstract should be submitted with all submissions except for Letters to the Editor. The abstract of Original Articles should be structured with subheadings (Objective, Material and Method, Results, and Conclusion). Please check Table 1 below for word count specifications.

EXPERIMED

Keywords: Each submission must be accompanied by a minimum of three to a maximum of six keywords for subject indexing at the end of the abstract. The keywords should be listed in full without abbreviations. The keywords should be selected from the National Library of Medicine, Medical Subject Headings database (<https://www.nlm.nih.gov/mesh/MBrowser.html>).

Manuscript Types

Original Articles: This is the most important type of article since it provides new information based on original research. The main text of original articles should be structured with Introduction, Material and Method, Results, and Discussion subheadings. Please check Table 1 for the limitations for Original Articles.

Statistical analysis to support conclusions is usually necessary. Statistical analyses must be conducted in accordance with international statistical reporting standards (Altman DG, Gore SM, Gardner MJ, Pocock SJ. Statistical guidelines for contributors to medical journals. *Br Med J* 1983; 7; 1489-93). Information on statistical analyses should be provided with a separate subheading under the Materials and Methods section and the statistical software that was used during the process must be specified.

Units should be prepared in accordance with the International System of Units (SI).

Editorial Comments: Editorial comments aim to provide a brief critical commentary by reviewers with expertise or with high reputation in the topic of the research article published in the journal. Authors are selected and invited by the journal to provide such comments. Abstract, Keywords, and Tables, Figures, Images, and other media are not included.

Review Articles: Reviews prepared by authors who have extensive knowledge on a particular field and whose scientific background has been translated into a high volume of publications with a high citation potential are welcomed. These authors may even be invited by the journal. Reviews should describe, discuss, and evaluate the current level of knowledge of a topic in clinical practice and should guide future studies. The main text should contain Introduction, Clinical and Research Consequences, and Conclusion sections. Please check Table 1 for the limitations for Review Articles.

Case Reports: There is limited space for case reports in the journal and reports on rare cases or conditions that constitute challeng-

es in diagnosis and treatment, those offering new therapies or revealing knowledge not included in the literature, and interesting and educative case reports are accepted for publication. The text should include Introduction, Case Presentation, Discussion, and Conclusion subheadings. Please check Table 1 for the limitations for Case Reports.

Letters to the Editor: This type of manuscript discusses important parts, overlooked aspects, or lacking parts of a previously published article. Articles on subjects within the scope of the journal that might attract the readers' attention, particularly educative cases, may also be submitted in the form of a "Letter to the Editor." Readers can also present their comments on the published manuscripts in the form of a "Letter to the Editor." Abstract, Keywords, and Tables, Figures, Images, and other media should not be included. The text should be unstructured. The manuscript that is being commented on must be properly cited within this manuscript.

Tables

Tables should be included in the main document, presented after the reference list, and they should be numbered consecutively in the order they are referred to within the main text. A descriptive title must be placed above the tables. Abbreviations used in the tables should be defined below the tables by footnotes (even if they are defined within the main text). Tables should be created using the "insert table" command of the word processing software and they should be arranged clearly to provide easy reading. Data presented in the tables should not be a repetition of the data presented within the main text but should be supporting the main text.

Figures and Figure Legends

Figures, graphics, and photographs should be submitted as separate files (in TIFF or JPEG format) through the submission system. The files should not be embedded in a Word document or the main document. When there are figure subunits, the subunits should not be merged to form a single image. Each subunit should be submitted separately through the submission system. Images should not be labeled (a, b, c, etc.) to indicate figure subunits. Thick and thin arrows, arrowheads, stars, asterisks, and similar marks can be used on the images to support figure legends. Like the rest of the submission, the figures too should be blind. Any information within the images that may indicate an individual or institution should be blinded. The minimum resolution of each submitted figure should be 300 DPI. To prevent delays in the evaluation process, all submitted figures should be clear in resolution and large in size (minimum

Table 1. Limitations for each manuscript type

Type of manuscript	Word limit	Abstract word limit	Reference limit	Table limit	Figure limit
Original Article	3500	200 (Structured)	30	6	7 or total of 15 images
Review Article	5000	200	50	6	10 or total of 20 images
Case Report	1000	200	15	No tables	10 or total of 20 images
Letter to the Editor	500	No abstract	5	No tables	No media

EXPERIMED

dimensions: 100 × 100 mm). Figure legends should be listed at the end of the main document.

All acronyms and abbreviations used in the manuscript should be defined at first use, both in the abstract and in the main text. The abbreviation should be provided in parentheses following the definition.

When a drug, product, hardware, or software program is mentioned within the main text, product information, including the name of the product, the producer of the product, and city and the country of the company (including the state if in USA), should be provided in parentheses in the following format: "Discovery St PET/CT scanner (General Electric, Milwaukee, WI, USA)"

All references, tables, and figures should be referred to within the main text, and they should be numbered consecutively in the order they are referred to within the main text.

Limitations, drawbacks, and the shortcomings of original articles should be mentioned in the Discussion section before the conclusion paragraph.

References

While citing publications, preference should be given to the latest, most up-to-date publications. Authors are responsible for the accuracy of references. References should be prepared according to Vancouver reference style. If an ahead-of-print publication is cited, the DOI number should be provided. Journal titles should be abbreviated in accordance with the journal abbreviations in Index Medicus/ MEDLINE/PubMed. When there are six or fewer authors, all authors should be listed. If there are seven or more authors, the first six authors should be listed followed by "et al." In the main text of the manuscript, references should be cited using Arabic numbers in parentheses. The reference styles for different types of publications are presented in the following examples.

Journal Article: Rankovic A, Rancic N, Jovanovic M, Ivanović M, Gajović O, Lazić Z, et al. Impact of imaging diagnostics on the budget – Are we spending too much? *Vojnosanit Pregl* 2013; 70: 709-11.

Book Section: Suh KN, Keystone JS. Malaria and babesiosis. Gorbach SL, Barlett JG, Blacklow NR, editors. *Infectious Diseases*. Philadelphia: Lippincott Williams; 2004.p.2290-308.

Books with a Single Author: Sweetman SC. *Martindale the Complete Drug Reference*. 34th ed. London: Pharmaceutical Press; 2005.

Editor(s) as Author: Huizing EH, de Groot JAM, editors. *Functional reconstructive nasal surgery*. Stuttgart-New York: Thieme; 2003.

Conference Proceedings: Bengjsson S, Sothemin BG. Enforcement of data protection, privacy and security in medical informatics. In: Lun KC, Degoulet P, Piemme TE, Rienhoff O, editors. *MEDINFO 92. Proceedings of the 7th World Congress on Medical Informatics; 1992 Sept 6-10; Geneva, Switzerland*. Amsterdam: North-Holland; 1992. pp.1561-5.

Scientific or Technical Report: Cusick M, Chew EY, Hoogwerf B, Agrón E, Wu L, Lindley A, et al. Early Treatment Diabetic Retinopathy Study Research Group. Risk factors for renal replacement therapy in the Early Treatment Diabetic Retinopathy Study (ETDRS), Early Treatment Diabetic Retinopathy Study Kidney Int: 2004. Report No: 26.

Thesis: Yılmaz B. *Ankara Üniversitesindeki Öğrencilerin Beslenme Durumları, Fiziksel Aktiviteleri ve Beden Kitle İndeksleri Kan Lipidleri Arasındaki İlişkiler*. H.Ü. Sağlık Bilimleri Enstitüsü, Doktora Tezi. 2007.

Manuscripts Accepted for Publication, Not Published Yet: Slots J. The microflora of black stain on human primary teeth. *Scand J Dent Res*. 1974.

Epub Ahead of Print Articles: Cai L, Yeh BM, Westphalen AC, Roberts JP, Wang ZJ. Adult living donor liver imaging. *Diagn Interv Radiol*. 2016 Feb 24. doi: 10.5152/dir.2016.15323. [Epub ahead of print].

Manuscripts Published in Electronic Format: Morse SS. Factors in the emergence of infectious diseases. *Emerg Infect Dis* (serial online) 1995 Jan-Mar (cited 1996 June 5): 1(1): (24 screens). Available from: URL: <http://www.cdc.gov/ncidod/EID/cid.htm>.

REVISIONS

When submitting a revised version of a paper, the author must submit a detailed "Response to the reviewers" that states point by point how each issue raised by the reviewers has been covered and where it can be found (each reviewer's comment, followed by the author's reply and line numbers where the changes have been made) as well as an annotated copy of the main document. Revised manuscripts must be submitted within 30 days from the date of the decision letter. If the revised version of the manuscript is not submitted within the allocated time, the revision option may be canceled. If the submitting author(s) believe that additional time is required, they should request this extension before the initial 30-day period is over.

Accepted manuscripts are copy-edited for grammar, punctuation, and format. Once the publication process of a manuscript is completed, it is published online on the journal's webpage as an ahead-of-print publication before it is included in its scheduled issue. A PDF proof of the accepted manuscript is sent to the corresponding author and their publication approval is requested within 2 days of their receipt of the proof.

Editor in Chief: Prof. Bedia Çakmakoğlu
Address: Istanbul University, Aziz Sancar Institute of Experimental Medicine, Vakıf Gureba Avenue, 34093, Çapa, Fatih, Istanbul, Türkiye
Phone: +90 212 414 2000-33305
Fax: +90 212 532 4171
E-mail: bedia@istanbul.edu.tr

Publisher: Istanbul University Press
Address: Istanbul University Central Campus, 34452 Beyazıt, Fatih / Istanbul - Türkiye
Phone: +90 212 440 0000